

INVESTIGATION OF MULTIPLE STELLAR POPULATIONS IN GLOBULAR
CLUSTERS WITH THE SLOAN DIGITAL SKY SURVEY

By

Jason P. Smolinski

A DISSERTATION

Submitted to
Michigan State University
in partial fulfillment of the requirements
for the degree of

DOCTOR OF PHILOSOPHY

Astrophysics and Astronomy

2011

ABSTRACT

INVESTIGATION OF MULTIPLE STELLAR POPULATIONS IN GLOBULAR CLUSTERS WITH THE SLOAN DIGITAL SKY SURVEY

By

Jason P. Smolinski

This dissertation describes the study of abundance variations among stars in Galactic globular clusters using the large set of spectroscopic data collected by the Sloan Digital Sky Survey (SDSS). Globular clusters have typically been considered to be simple stellar populations – groups of stars that are coeval and chemically homogeneous. Observations within the last forty years have shed light on the possibility that they are not so simple after all by revealing the presence of star-to-star variations in light-element abundances. Additionally, several globular clusters are known to harbor multiple populations of stars by the presence of multiple sequences on a color-magnitude diagram.

In this study, the procedure for membership selection is first described. Stars are selected from the vast data set available from SDSS Data Release 7 and several cuts are made to reduce the sample down to only those stars that are members of the globular clusters in this sample. This procedure is also performed on three open clusters as well and is further used to validate the current SEGUE Stellar Parameter Pipeline.

CN and CH molecular absorption indices are then measured for all globular cluster member stars and their distributions are analyzed. Bimodal distributions in CN are seen on the red giant branch in all clusters with $[Fe/H] > -2.1$, and hints of bimodality are seen for two metal-poor clusters as well. CN-CH anticorrelations are also seen and the implications are discussed.

The observed distributions of CN absorption bandstrengths are examined and compared to theoretical predictions from two-population models. These results are combined with radial distributions and positions on the color-magnitude diagram as evidence for the presence of multiple populations of stars within the clusters in this sample.

COPYRIGHT

Copyright © by

Jason P. Smolinski

2011

DEDICATION

To Ashley,
who was there in the beginning;
to my parents,
who watched it all play out.

ACKNOWLEDGMENT

I would like to thank all those who supported me during my time in graduate school – my parents, sisters, and friends who kept me going and knew I could do it. Your encouragement was, and is still, much appreciated. I would of course like to thank my advisor, Timothy Beers, for taking a chance on me, giving constant words of affirmation, and being patient with me as I learned how to write scientific journal papers. Thanks also to Sarah Martell for the insightful and helpful discussions and collaboration. Finally, I would like to acknowledge the efforts of my little MacBook, which did far more work than it ever could have anticipated. Certainly more than any Windows machine could have done.

TABLE OF CONTENTS

List of Tables	viii
List of Figures	ix
1 Introduction	1
1.1 Overview and History of Observations	1
1.2 Proposed Explanations	3
1.3 The Sloan Digital Sky Survey	7
1.4 Summary	8
2 SDSS, the SEGUE Stellar Parameter Pipeline, and the Sample	10
2.1 Introduction	10
2.2 The Extended Validation Sample	11
2.3 Cluster Membership Selection	15
2.3.1 Likely Member Star Selection	15
2.3.2 Selection of Adopted True Members	25
2.4 Determination of Overall Metallicities and Radial Velocities of the Clusters .	26
2.5 Individual Cluster Discussion and Comparison with Previous Studies	41
2.5.1 M92 (NGC 6341)	41
2.5.2 NGC 5053	42
2.5.3 M53 (NGC 5024)	42
2.5.4 M3 (NGC 5272)	43
2.5.5 M71 (NGC 6838)	44
2.5.6 NGC 2158	44
2.5.7 M35 (NGC 2168)	45
2.5.8 NGC 6791	46
2.6 Summary	46
3 CN and CH Absorption Bandstrengths in SDSS Globular Clusters	56
3.1 Introduction	56
3.2 Observational Data	57
3.3 CN Bandstrength Distribution	60
3.3.1 CN Absorption on the Red Giant Branch	60
3.3.2 CN Absorption on the Subgiant Branch and Main Sequence	72
3.3.3 Hidden Substructure in Generalized Histograms	75
3.4 CH Bandstrength Distribution	83
3.4.1 CH Behavior at Low Metallicity	85
3.5 Correlations with Cluster Parameters	90
3.6 Summary	96

4 Evidence for Multiple Populations in SDSS Globular Clusters	99
4.1 Introduction	99
4.2 The Data Set	101
4.3 CMD distributions	103
4.4 Radial Distributions	111
4.5 Summary	118
5 Conclusions and Future Work	119
5.1 Results of this Study	119
5.2 Implications	120
5.3 Future Work	120
A Atmospheric Properties of Adopted True Member Stars	123
A.1 Atmospheric Parameters Data Table	123
A.2 Photometric Parameters Data Table	222
B CN, δCN, and CH Line Indices of True Member Stars	271
B.1 Spectroscopic Line Indices Data Table	271
Bibliography	328

LIST OF TABLES

1.1	Reaction Chains in the CNO Cycle	3
2.1	Cluster Coordinates	12
2.2	Cluster Photometric Properties	13
2.3	Cluster Spectroscopic and Physical Properties	14
2.4	Metallicities and Radial Velocities of Globular and Open Clusters	25
2.5	Residuals from Linear Regression on Metallicity	27
3.1	Individual Cluster RGB CN Number Ratios	93
3.2	Literature CN Number Ratios	96
A.1	Atmospheric Properties of Adopted True Member Stars	123
A.2	Atmospheric Uncertainties of Adopted True Member Stars	173
A.3	Photometric Properties of Adopted True Member Stars	223
B.1	Line Indices of Adopted True Member Stars	271
B.2	Line Index Uncertainties of Adopted True Member Stars	299

LIST OF FIGURES

1.1	Example Color-Magnitude Diagram, with labels	5
2.1	Stellar fields for validation clusters and first-cut radii	17
2.2	CMDs for M92 and NGC 5053 and second-cut grids	19
2.3	CMDs for M53 and M3 and second-cut grids	20
2.4	CMDs for NGC 2158 and NGC 6791 and second-cut grids	21
2.5	CMDs for M35 and M71 and second-cut fiducial sequences	22
2.6	Likely member CMDs for M92, NGC 5053, M53, and M3	23
2.7	Likely member CMDs for NGC 2158, M35, and NGC 6791	24
2.8	[Fe/H] and RV distributions for M92 and final-cut fits	28
2.9	[Fe/H] and RV distributions for NGC 5053 and final-cut fits	29
2.10	[Fe/H] and RV distributions for M53 and final-cut fits	30
2.11	[Fe/H] and RV distributions for M3 and final-cut fits	31
2.12	[Fe/H] and RV distributions for M71 and final-cut fits	32
2.13	[Fe/H] and RV distributions for NGC 2158 and final-cut fits	33
2.14	[Fe/H] and RV distributions for M35 and final-cut fits	34
2.15	[Fe/H] and RV distributions for NGC 6791 and final-cut fits	35

2.16 [Fe/H] distributions versus $(g - r)_0$ and $\langle S/N \rangle$ for true globular cluster member stars	36
2.17 [Fe/H] distributions versus $(g - r)_0$ and $\langle S/N \rangle$ for true open cluster member stars	37
2.18 [Fe/H] distributions versus $\log g$ for true globular cluster member stars	38
2.19 [Fe/H] distributions versus $\log g$ for true open cluster member stars	39
2.20 CMD for true member stars of M92	48
2.21 CMD for true member stars of NGC 5053	49
2.22 CMD for true member stars of M53	50
2.23 CMD for true member stars of M3	51
2.24 CMD for true member stars of M71	52
2.25 CMD for true member stars of NGC 2158	53
2.26 CMD for true member stars of M35	54
2.27 CMD for true member stars of NGC 6791	55
3.1 CMDs for globular clusters with $[Fe/H] < -2.0$	58
3.2 CMDs for globular clusters with $[Fe/H] > -2.0$	59
3.3 Representative spectra for CN-weak and CN-strong stars	61
3.4 Generalized histograms of δCN_N distributions of RGB stars	63
3.5 Raw CN_N values versus absolute g -magnitude, binned by $[Fe/H]$	65
3.6 Distributions of δCN_N for RGB and SGB stars in each individual cluster	66
3.7 Generalized δCN_N histogram for M53, combined with data from Martell et al. (2008b)	69
3.8 Comparison of metal-poor cluster RGB δCN_N values with a pure Gaussian	71
3.9 Distributions of δCN_H for SGB and MS stars in each individual cluster	74

3.10 Comparison of MS $\delta\text{CN}_{\text{H}}$ values with a pure Gaussian	76
3.11 Comparison of SGB $\delta\text{CN}_{\text{N}}$ values with a pure Gaussian	77
3.12 δCN values divided by CMD region for M92	79
3.13 δCN values divided by CMD region for M15	80
3.14 δCN values divided by CMD region for M2	81
3.15 δCN values divided by CMD region for M13	82
3.16 Representative RGB spectrum comparing four popular CH line index definitions	84
3.17 CN-CH anticorrelation for cluster RGB stars, plotted as CH-vs- δCN	86
3.18 CN-CH anticorrelation for cluster RGB stars, plotted as CH-vs- M_g	87
3.19 CH distribution versus luminosity for metal-poor cluster giants and subgiants	89
3.20 CH distribution versus luminosity for cluster subgiants and dwarfs	91
3.21 CN number ratio as a function of various cluster parameters	92
3.22 CN number ratio as a function of cluster mass and luminosity	95
4.1 u_0 vs. $(u - g)_0$ CMD for M92, M15, NGC 5053, and M53	102
4.2 u_0 vs. $(u - g)_0$ CMD for M2, M13, M3, and M71	104
4.3 Cumulative distributions of $(u - g)_0$ colors in CN groups in M15	106
4.4 Cumulative distributions of $(u - g)_0$ colors in CN groups in M13	107
4.5 Cumulative distributions of $(u - g)_0$ colors in CN groups in M3	108
4.6 u_0 vs. $(u - g)_0$ CMD for SGB stars in M92, M15, M2, and M13	109
4.7 CN number ratios for M13 RGB stars	110
4.8 CN number ratios for M3 RGB stars	112
4.9 RGB and SGB radial distributions	114
4.10 Cumulative radial distributions, scaled to r_t	116

CHAPTER 1:

INTRODUCTION

1.1 OVERVIEW AND HISTORY OF OBSERVATIONS

Characterized by high central stellar densities and overall spheroidal shape, globular clusters (GCs) are the most massive single collections of stars in the Galaxy. Containing $\sim 10^6$ stars, GCs have long been held up as the canonical example of a simple stellar population – a population of stars that is chemically homogeneous and coeval. Color-magnitude diagrams (CMDs) constructed from photometric data for GCs seemed to reveal populations each with a single age (e.g. Arp & Johnson, 1955). As individual objects, they are typically treated as isolated laboratories that provide ideal environments for the study of stellar dynamics and evolution. As a system, the ~ 150 known Milky Way GCs surround the Galaxy and act as a record of the chemical conditions present during its formation, while also providing a means of estimating the age of the Milky Way as well as a minimum age for the Universe.

Standard models for the formation of Galactic GCs have long held that they should display little star-to-star variation in their observed atmospheric elemental abundances. These models assume that the entire population of stars within a GC formed in one single epoch of star formation, appearing out of the collapsed remnants of an extremely massive molecular gas cloud. The gas clouds that form individual GCs are expected to be internally chemically homogeneous – and indeed, observations of iron abundances among stars within a given GC typically reveal a remarkably narrow distribution with a dispersion that is often smaller than the measurement uncertainties. When iron abundance is measured, it is typically measured with respect to that of the Sun and given the term *metallicity*.

Quantitatively, it takes the form

$$[\text{Fe}/\text{H}] = \log \left(\frac{\text{N}_{\text{Fe}}}{\text{N}_{\text{H}}} \right)_{\text{star}} - \log \left(\frac{\text{N}_{\text{Fe}}}{\text{N}_{\text{H}}} \right)_{\text{Sun}} . \quad (1.1)$$

Metallicity is a quantity of interest because it is often used as a tracer of age. As massive stars evolve, they proceed to fuse atoms heavier than hydrogen in their cores, producing increasingly heavier elements. Once these stars explode as supernovae (SNe) or, in the case of their less massive relatives, become planetary nebulae, in both cases dispersing the products of nucleosynthesis out into the interstellar medium, subsequent generations of stars may form from this chemically enriched material and contribute to further enrichment. This implies that stars that have higher metallicities are younger than more metal-poor stars. In the case of stars within a GC, their relative uniformity in [Fe/H] has significantly contributed to the idea of a single epoch of star formation producing the entire population.

While stars within a GC generally show little to no metallicity spread, with a few notable exceptions including ω Cen (e.g. Freeman & Rodgers, 1975; Butler et al., 1978; Norris & Da Costa, 1995), M54 (e.g. Carretta et al., 2010b,c), NGC 1851 (Carretta et al., 2010d) and possibly NGC 2419 (Cohen et al., 2010), observations over the past forty years (beginning with Osborn, 1971) have repeatedly shown that light elements often display a broad range of abundances. For all clusters of moderate to high metallicity ($[\text{Fe}/\text{H}] > -2.0$), significant scatter in light-element abundances has been observed on the red giant branch (RGB; e.g. Norris & Freeman, 1979; Suntzeff, 1981). Variations in carbon and nitrogen abundances are among the most commonly studied, typically through the strengths of the 3883 Å CN and 4300 Å CH molecular absorption bands.

The observed surface variations in carbon and nitrogen abundances are part of a larger light-element pattern that involves enrichment in N, Na, and Mg along with depletion in C, O, and Al, and are often studied in correlated or anticorrelated abundance pairs (C-N, O-N, Mg-Al, Na-O, etc.). These patterns seem to indicate enhancement in nuclear processing along certain chains. For example, in the CNO cycle carbon acts as a catalyst for a chain

Table 1.1. Reaction Chains in the CNO Cycle

Primary Chain		Secondary Chain	
$^{12}\text{C} + ^1\text{H}$	$\rightarrow ^{13}\text{N} + \gamma$	$^{12}\text{C} + ^1\text{H}$	$\rightarrow ^{13}\text{N} + \gamma$
^{13}N	$\rightarrow ^{13}\text{C} + e^+ + \nu$	^{13}N	$\rightarrow ^{13}\text{C} + e^+ + \nu$
$^{13}\text{C} + ^1\text{H}$	$\rightarrow ^{14}\text{N} + \gamma$	$^{13}\text{C} + ^1\text{H}$	$\rightarrow ^{14}\text{N} + \gamma$
$^{14}\text{N} + ^1\text{H}$	$\rightarrow ^{15}\text{O} + \gamma$	$^{14}\text{N} + ^1\text{H}$	$\rightarrow ^{15}\text{O} + \gamma$
^{15}O	$\rightarrow ^{15}\text{N} + e^+ + \nu$	^{15}O	$\rightarrow ^{15}\text{N} + e^+ + \nu$
$^{15}\text{N} + ^1\text{H}$	$\rightarrow ^{12}\text{C} + ^4\text{He}$	$^{15}\text{N} + ^1\text{H}$	$\rightarrow ^{16}\text{O} + \gamma$
		$^{16}\text{O} + ^1\text{H}$	$\rightarrow ^{17}\text{F} + \gamma$
		^{17}F	$\rightarrow ^{17}\text{O} + e^+ + \nu$
		$^{17}\text{O} + ^1\text{H}$	$\rightarrow ^{14}\text{N} + ^4\text{He}$

Note. — Primary and secondary reaction chains in the CNO cycle. The secondary chain occurs about 4 times in 10^3 .

of reactions that ultimately fuses four hydrogen atoms into one helium atom. Table 1.1 details the major components of the CNO cycle. When the cycle is run to equilibrium in the core, ^{14}N becomes the most abundant species, regardless of initial composition, via the $^{13}\text{C}(p, \gamma)^{14}\text{N}$ reaction. This is due to the comparatively long timescale of the subsequent proton-capture onto ^{14}N that forms ^{15}O . However, no mechanism is known that would bring this ^{14}N -enriched material from the core to the surface prior to a star’s evolution on the RGB. While these abundance variations have been observed on the RGBs of all clusters with $[\text{Fe}/\text{H}] > -2.0$, more recent observations have seen the same signatures on the subgiant branch (SGB) as well (e.g. Carretta et al., 2005; Cohen et al., 2005a), and in some cases even down to the main sequence (MS; e.g. Cannon et al., 1998; Harbeck et al., 2003a; Briley et al., 2004). Gratton et al. (2004) reviews a number of these studies, and Carretta et al. (2009b) dramatically increased the number of cluster stars surveyed for these variations.

1.2 PROPOSED EXPLANATIONS

Initial theories that were put forward to explain the observed surface enhancement in nitrogen and depletion in carbon typically involved additional mixing mechanisms that brought CNO-processed materials from the stellar interior to the surface. Meridional circulation (Sweigart & Mengel, 1979; McClure, 1979), primordial cloud inhomogeneity (Cohen, 1978; Peterson, 1980), and surface pollution (D'Antona et al., 1983) were among the original hypotheses. Currently, the progressive abundance changes on the RGB are believed to be the result of deep mixing within individual stars (Sweigart & Mengel, 1979; Charbonnel, 1994; Denissenkov & VandenBerg, 2003), beginning at the “bump” in the RGB luminosity function (Fusi Pecci et al., 1990; Shetrone, 2003). As a main sequence (see Figure 1.1) star’s core exhausts its supply of hydrogen fuel, the inert helium core begins to contract (having no radiation source to support itself against gravity) and hydrogen fusion continues in a shell surrounding the core. This fusion (via the CNO cycle) produces more energy than core fusion had, thus causing the outer stellar envelope to expand. At the same time, the initially shallow temperature gradient from the shell to the surface allows the convective envelope to penetrate deeper into the partially CNO-processed interior, driving a deep circulation referred to as *first dredge-up*, as the star moves onto and up the RGB. The precise location on the CMD where this occurs depends on the mass of the star, with more massive stars experiencing it lower on the RGB, but for a one-solar-mass star ($1 M_{\odot}$) this occurs at luminosities on the RGB slightly below the horizontal branch (HB) (Carroll & Ostlie, 1996). Eventually, the temperature gradient steepens enough that the convective envelope retreats back toward the surface.

Subsequently, the hydrogen-burning shell proceeds outward as a star evolves along the RGB, eventually (for masses up to $M \sim 2M_{\odot}$; Girardi et al., 2000; VandenBerg et al., 2006) encountering the molecular-weight discontinuity left behind by the inward reach of the convective envelope during first dredge-up (Thomas, 1967; Iben, 1968). When this occurs, the shell’s progress is delayed as its fusion rate adjusts to the new chemical abundances,

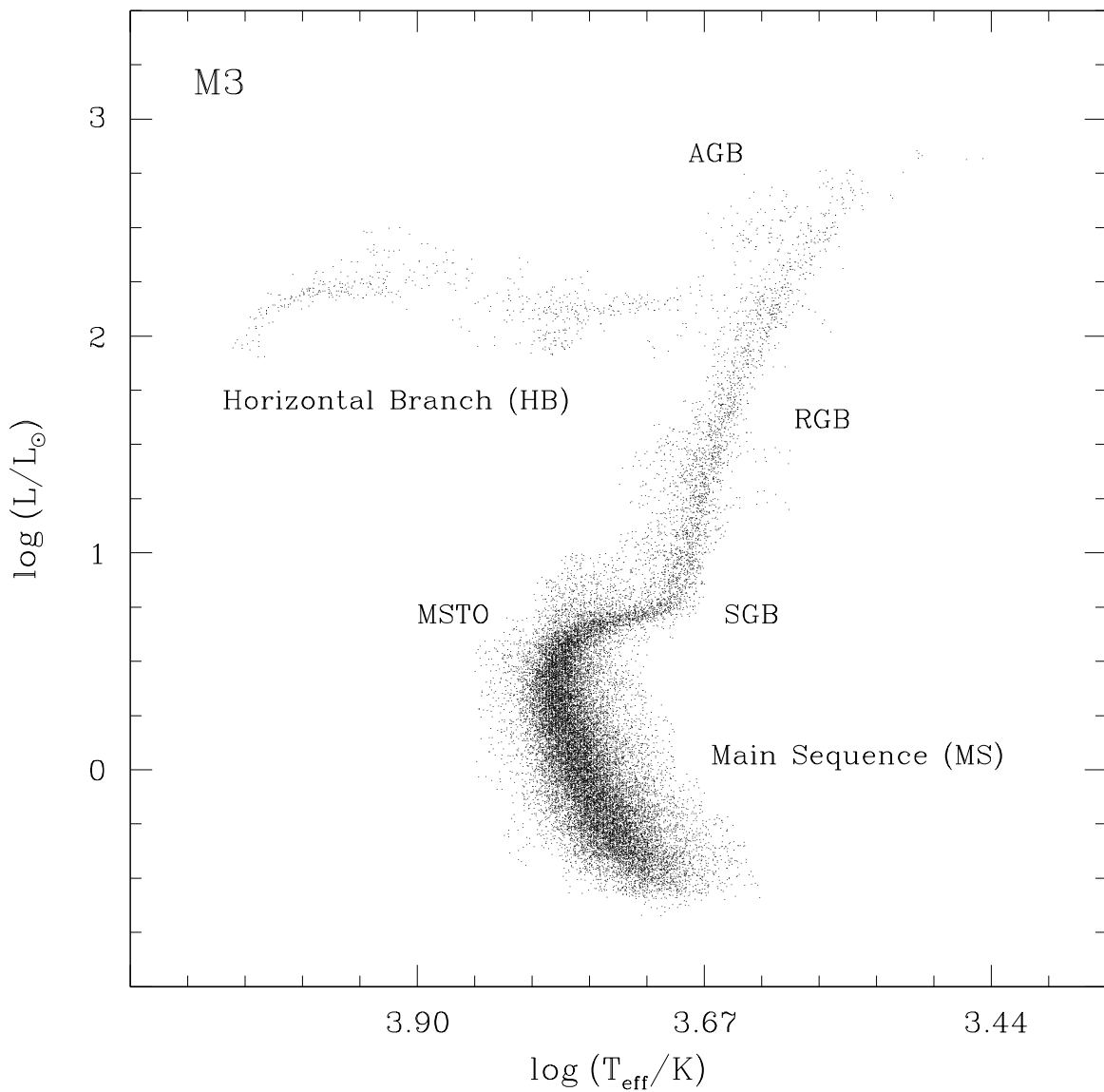


Figure 1.1 The color-magnitude diagram of M3. The main sequence and horizontal branch are labeled. Also shown are the main sequence turnoff (MSTO), the subgiant branch (SGB), the red giant branch (RGB), and the asymptotic giant branch (AGB). The temperature scale increases to the left. Axis values are approximate.

causing a concomitant small (~ 0.1 mag) decrease in the star’s luminosity as it evolves along the RGB (see, e.g., Fig. 6 of Yi et al., 2001). In a population of coeval stars, this produces an enhancement in the differential luminosity function at the point on the RGB where this loop occurs (the RGB “bump”). Once the shell begins to proceed outward again, the molecular-weight gradient it experiences is lower, and a nonconvective process of deep mixing (Denissenkov & VandenBerg, 2003) begins to operate, transporting material between the hydrogen-burning shell and the surface and continuously adjusting surface carbon and nitrogen abundances.

The notion of additional deep mixing is useful for explaining some observations of abundance variations, but not all. There are two independent modes of variation in GC light-element abundances: a steady decline in [C/Fe] and increase in [N/Fe] as stars evolve along the RGB, and star-to-star variations in the light-element abundances at a fixed luminosity, at all evolutionary phases. The presence of these abundance variations at all evolutionary phases implies some form of unexpected enrichment within individual clusters prior to, or shortly after, their formation. Some researchers have suggested that the primordial gas cloud from which a given cluster formed may have initially been chemically inhomogeneous (e.g. Cohen, 1978; Peterson, 1980). A variation on this hypothesis appeals to cluster “self-enrichment.” Rather than assuming all stars in a given cluster are co-eval, it is assumed that an additional population(s) of stars formed, with compositions affected by the gas expelled by supernovae and/or strong stellar winds from intermediate-mass asymptotic giant branch (AGB) stars. While each hypothesis has its merits and weaknesses (see Gratton et al., 2004, for a complete review), no single model accounts for the full set of observed light-element abundance variations in GCs, though it remains possible that each may play a role (e.g. Martell et al., 2008c; Decressin et al., 2009).

Early studies of star-to-star light-element abundance variations (e.g. Suntzeff, 1981; Langer, 1985) suggested that deep mixing might be responsible for the C-N variations at fixed luminosity as well as the progressive abundance changes along the RGB. However,

variations in Na, Mg and Al are difficult to explain as a result of mixing within RGB stars since they require higher temperatures than are reached in the hydrogen-burning shell. Internal mixing is also not a good explanation for light-element abundance variations in main sequence stars, since they do not have the ability to conduct high-temperature fusion, nor mass transport between their cores and surfaces.

One of the strongest constraints on the proposed scenarios is the fact that, in the majority of moderate- to high-metallicity GCs, the CN abundance distribution is bimodal. The self-enrichment scenario accommodates this observation most naturally, with the CN-weak and CN-strong groups representing the first and second populations of stars to have formed in the cluster, respectively. This idea has received increasing support recently as improved photometric measurements have revealed the presence of multiple SGBs and MSs in a few GCs (Bedin et al., 2004; Piotto et al., 2007). Spectroscopic abundance analyses have also begun to reveal distinct sequences on the RGBs of some clusters (Marino et al., 2008a). In addition, studies of the spatial distributions of stars in clusters with accurate photometry have revealed the presence of correlated differences in $U - B$ colors (Carretta et al., 2010a; Kravtsov et al., 2011), which also suggests variations in chemical composition within the cluster.

1.3 THE SLOAN DIGITAL SKY SURVEY

Whereas past studies have generally implemented a star-by-star approach to data collection, using a spectrograph targeting one star at a time, modern studies of stellar abundances in clusters typically require large sample sizes, making large survey data sets desirable. The Sloan Digital Sky Survey (SDSS; York et al., 2000) is an ambitious survey of the northern sky over southern New Mexico using the 2.5-meter telescope at Apache Point Observatory. It utilizes a 3° field of view and a drift-scan imaging camera (Gunn et al., 1998) with 30 CCD chips imaging in five u, g, r, i, z filters (Fukugita et al., 1996). In addition, it also utilizes

a pair of multi-object spectrographs, each with 640 optical fibers. The entire photometric survey, now in its eighth data release (DR8; Aihara et al., 2011) as part of SDSS-III, has covered more than $14,500 \text{ deg}^2$ on the sky, producing a catalog of nearly half a billion distinct objects, including several hundred million stars. The spectroscopic data collected in this survey constitutes approximately 1.8 million objects.

Photometric brightnesses are typically expressed in units of *magnitudes*, where the apparent magnitude (that is, how bright a star appears from Earth) in a particular filter (effectively a wavelength range) is given by $m = -2.5 \log(F) + Z$, where F is the flux in that filter and Z is a zero-point correction that depends on such things as the optical system utilized and the magnitude system used. Inspection of this equation reveals that the brighter an object appears, the lower the value of its apparent magnitude. Corrections can be made to an object’s apparent magnitude to arrive at its absolute magnitude, which is a direct indicator of luminosity. The difference between magnitudes in two different filters produces a *color index*. In the color indices used in this study, such as $(g-r)_0$, lower values indicate a bluer color, while higher values indicate a redder color. Physically, bluer colors correspond to higher temperatures, while red colors correspond to cool temperatures.

The first installation of the Sloan Extension for Galactic Understanding and Exploration (SEGUE-1; Yanny et al., 2009), one of three sub-surveys that collectively formed SDSS-II, obtained *ugriz* imaging of some 3500 deg^2 of sky outside of the SDSS-I footprint (Fukugita et al., 1996; Gunn et al., 1998, 2006; Stoughton et al., 2002; Abazajian et al., 2003, 2004, 2005, 2009; Pier et al., 2003; Adelman-McCarthy et al., 2006, 2007, 2008), with special attention being given to scans of lower Galactic latitudes ($|b| < 35^\circ$) in order to better probe the disk/halo interface of the Milky Way. SEGUE also obtained $R \simeq 2000$ spectroscopy over the wavelength range $3800\text{--}9200 \text{ \AA}$ for some 240,000 stars in 200 selected areas of the celestial sphere. When combined with stars observed during SDSS-I, and the recently completed SEGUE-2 project within SDSS-III, a total of nearly 500,000 stars exploring the thin-disk, thick-disk, and halo populations of the Galaxy now have spectroscopic data.

While SDSS is no longer the only survey instrument dedicated to gathering large amounts of data in multi-object mode (the FLAMES multi-object spectrograph at the ESO VLT being another), SDSS/SEGUE has provided one of the first large spectroscopic data sets. Combining its voluminous data acquisition with an automatic software pipeline that is capable of deriving stellar atmospheric parameters (see Section 2.1) from relatively low-resolution spectra gives us a powerful way to quickly and comprehensively study cluster abundances in revolutionary ways, and this is utilized in this Dissertation.

1.4 SUMMARY

This Dissertation is an investigation of CN and CH bandstrengths in stars at all evolutionary stages among eight GCs observed by the Sloan Digital Sky Survey. Chapter 2 describes the membership selection process used in obtaining true member stars for the clusters in this sample (Reproduced by permission of the AAS from Smolinski et al., 2011a). The procedure implements a series of cuts to pare down the full data set to only those stars one can confidently claim are true cluster members. Chapter 3 is a study of the CN and CH molecular absorption bandstrengths of those stars that passed the cuts made in Chapter 2 (Reproduced by permission of the AAS from Smolinski et al., 2011b). I demonstrate that all clusters with $[\text{Fe}/\text{H}] > -2.1$ show signs of CN variation all along the RGB, including evidence for CN variation on the SGB in several clusters. Finally, Chapter 4 examines the CN results in terms of the self-enrichment scenario, investigating evidence of multiple populations of stars in the clusters in this sample. I find evidence that corroborates previous studies, though this sample suffers from some limitations, which are discussed. The results suggest overall that light-element abundance variations within cluster stars do seem to support the hypothesis that a second generation of stars formed from enriched gas within GCs shortly after formation of the first generation. Full details of Chapter 4 will be published at a later date by J. P. Smolinski et al. (2011, in preparation).

CHAPTER 2:

SDSS, THE SEGUE STELLAR

PARAMETER PIPELINE, AND THE

SAMPLE

2.1 INTRODUCTION

The SEGUE Stellar Parameter Pipeline (SSPP; Lee et al., 2008a,b; Allende Prieto et al., 2008) processes the wavelength- and flux-calibrated spectra generated by the standard SDSS spectroscopic reduction pipeline (Stoughton et al., 2002), obtains equivalent widths and/or line indices for 85 atomic or molecular absorption lines, and estimates T_{eff} , $\log g$, and [Fe/H], along with radial velocities (RVs), through the application of a number of approaches (see Lee et al., 2008a, for a detailed discussion of the techniques employed by the SSPP).

An earlier validation paper by Lee et al. (2008b) demonstrated, on the basis of comparisons with a sample of three Galactic globular clusters (GCs) and two open clusters (OCs), that the SSPP provides sufficiently accurate estimates of stellar parameters for use in the analysis of Galactic kinematics and chemistry, at least over the ranges in parameter space covered by these clusters (in particular, for the metallicity range $-2.4 < [\text{Fe}/\text{H}] < 0.0$). However, it was noted in that paper that the largest outliers in SSPP-derived metallicities were found for clusters near the extrema of this range. The team of researchers working on the SSPP have, in the time since publication of the original validation paper, endeavored to improve the performance of the SSPP near these extremes. As part of this effort, which led to the production of a version of the SSPP suitable for application to the DR8 release

(including the \sim 120,000 stars observed during SEGUE-2), I have assembled SDSS photometry and spectroscopy for an additional sample of five GCs (including two with $[\text{Fe}/\text{H}] \sim -2.3$: M92 and NGC 5053; and one intermediate-metallicity cluster with $[\text{Fe}/\text{H}] \sim -0.7$: M71), and three OCs, one of which has been shown in the literature to exhibit a super-solar metallicity, $[\text{Fe}/\text{H}] \approx +0.3$ (NGC 6791).

2.2 THE EXTENDED VALIDATION SAMPLE

I selected five Galactic GCs (M92, NGC 5053, M53, M3, and M71) and three OCs (NGC 2158, M35, and NGC 6791) which had already been observed by SDSS and processed for further validation of the SSPP. A number of other clusters were considered but ultimately had to be rejected due to difficulties obtaining adequately reduced spectra from fields that were either too crowded or too heavily reddened. Because the default PHOTO pipeline (Lupton et al., 2001) was not designed to accurately deal with crowded fields such as those in the central regions of globular clusters, crowded-field photometric measurements were obtained using the DAOPHOT/ALLFRAME software package (Stetson, 1987, 1994) for M92, NGC 5053, M53, M3, M71, and NGC 6791 (An et al., 2008). For the remaining clusters (NGC 2158 and M35) the same procedures were followed as in An et al. (2008) to obtain crowded-field photometry. Combining the SDSS photometry of the full field with the crowded-field photometry of the inner cluster regions, corrected for reddening and extinction using values listed in Tables 2.1 and 2.2, resulted in a nearly complete catalog of *ugriz* photometry for the stars in each cluster region. Tables 2.1 – 2.3 summarize the properties of each cluster included in this study, as well as those from (Lee et al., 2008b). Metallicity values from the compilation of Harris (1996)¹ are tabulated as well as values from the recalibrated metallicity scale of Carretta et al. (2009a).

The spectroscopic data were obtained for stars targeted for spectroscopic follow-up se-

¹All references to Harris (1996) refer to the 2010 update on his web page:
<http://www.physics.mcmaster.ca/~harris/mwgc.dat>.

Table 2.1. Cluster Coordinates

Cluster		RA (J2000)	Dec (J2000)	(l, b)
NGC 6341	M92	17:17:07.39	+43:08:09.4	(68.3, +34.9)
NGC 7078	M15	21:29:58.33	+12:10:01.2	(65.0, -27.3)
NGC 5053		13:16:27.09	+17:42:00.9	(335.7, +78.9)
NGC 5024	M53	13:12:55.25	+18:10:05.4	(333.0, +79.8)
NGC 7089	M2	21:33:27.02	-00:49:23.7	(58.4, -35.8)
NGC 6205	M13	16:41:41.24	+36:27:35.5	(59.0, +40.9)
NGC 5272	M3	13:42:11.62	+28:22:38.2	(42.2, +78.7)
NGC 6838	M71	19:53:46.49	+18:46:45.1	(56.7, -4.6)
NGC 2158		06:07:25	+24:05:48	(186.6, +1.8)
NGC 2168	M35	06:08:54	+24:20:00	(186.6, +2.2)
NGC 6791		19:20:53	+37:46:18	(70.0, +10.9)

Note. — Coordinates of the clusters in our sample as drawn from the literature.

Table 2.2. Cluster Photometric Properties

Cluster	$(m - M)_0^a$	$E(B - V)^b$	r_t^a (arcmin)
M92	14.64	0.023	15.17
M15	15.37	0.110	21.50
NGC 5053	16.12	0.017	13.67
M53	16.25	0.021	21.75
M2	15.49	0.045	21.45
M13	14.48	0.017	25.18
M3	14.95	0.013	38.19
M71	12.86	0.275 ^c	8.96
NGC 2158	12.80 ^d	0.44 ^e	2.5 ^f
M35	9.80 ^g	0.20 ^g	20.0 ^f
NGC 6791	12.95 ^h	0.117 ^f	5.0 ^f

Note. — Photometric properties of the clusters in our sample as drawn from the literature. The parameter r_t is the tidal radius in arcminutes. The listed distance modulus $(m - M)_0$ is extinction corrected. Note that the Harris values (except r_t) have been drawn from the 2010 update which includes new determinations of globular cluster centers from an HST ACS survey by Goldsbury et al. (2010). Values for r_t are drawn from the 2003 update to the original 1996 catalog.

References: ^a Harris (1996); ^b Schlegel et al. (1998); ^c Grundahl et al. (2002); ^d Carraro et al. (2002); ^e Twarog et al. (1997); ^f Dias et al. (2002); ^g Kalirai et al. (2003); ^h An et al. (2009).

Table 2.3. Cluster Spectroscopic and Physical Properties

Cluster	[Fe/H] ^a	[Fe/H] _C	V _r ^a (km s ⁻¹)	log($\frac{M}{M_{\odot}}$) (dex)	R _{gc} ^a (kpc)	C ^a	σ ^a (km s ⁻¹)	ε ^a
M92	-2.31	-2.35	-120.0	5.43 ^b	9.6	1.68	6.0	0.10
M15	-2.37	-2.33	-107.0	5.84 ^c	10.4	2.28	13.5	0.05
NGC 5053	-2.27	-2.30	+44.0	4.80 ^b	17.8	0.74	1.4	0.21
M53	-2.10	-2.06	-62.9	5.65 ^b	18.4	1.72	4.4	0.01
M2	-1.65	-1.66	-5.3	5.84 ^b	10.4	1.59	8.2	0.11
M13	-1.53	-1.58	-244.2	5.57 ^b	8.4	1.53	7.1	0.11
M3	-1.50	-1.50	-147.6	5.58 ^b	12.0	1.89	5.5	0.04
M71	-0.78	-0.82	-22.8	4.29 ^c	6.7	1.15	2.3	0.00
NGC 2158	-0.25 ^d	...	+28.0 ^d					
M35	-0.16 ^d	...	-8.2 ^d					
NGC 6791	+0.30 ^e	...	-57.0 ^d					

Note. — Spectroscopic and physical properties of the clusters in our sample as drawn from the literature. The parameter [Fe/H]_C is from the recalibrated globular cluster metallicity scale of Carretta et al. (2009). Distance from Galactic center R_{gc} calculated assuming R₀ = 8.0 kpc. Central concentration C derived from a King model where $C = \log(r_t/r_c)$. Note that the Harris values have been drawn from the 2010 update at <http://www.physics.mcmaster.ca/~harris/mwgc.dat>.

References: ^a Harris (1996); ^b McLaughlin & van der Marel (2005); ^c Mandushev et al. (1991); ^d Dias et al. (2002); ^d Boesgaard et al. (2009).

lected from a photometric CMD for each cluster. Stars located on the diagram in the regions of the main sequence turn-off (MSTO) and RGB were then selected as possible cluster members. Other stars in the field of each cluster were also selected by the default SEGUE target selection algorithm to fill each plug-plate, many of which ended up being cluster members themselves. Overall, SDSS spectroscopic data were obtained for 640 targets each in the regions of NGC 5053, M53, and M3, and 1280 targets each in the regions of M92, M71, NGC 2158, M35, and NGC 6791, including sky spectra and calibration objects. Some of these targets had low average signal-to-noise spectra; for consistency with Lee et al. (2008b), only those spectra with $\langle S/N \rangle > 10$ (averaged over the entire spectrum) were considered for subsequent analysis. After processing by the SSPP some targets had no estimates for RV or [Fe/H]; these were excluded as well. After these cuts were made, there remained 775, 579, 579, 487, 1094, 495, 495, and 1087 stars considered for M92, NGC 5053, M53, M3, M71, NGC 2158, M35, and NGC 6791, respectively.

2.3 CLUSTER MEMBERSHIP SELECTION

In this section I discuss how the adopted true members for each cluster were selected, based in part on their estimated metallicities and radial velocities. Lee et al. (2008a) has shown that the stellar spectra processed through the SSPP have typical uncertainties of 141 K, 0.23 dex, and 0.23 dex for T_{eff} , $\log g$, and [Fe/H], respectively. Uncertainties in the radial velocity depends on the spectral type and apparent magnitude and fall in the range 5-20 km s^{-1} ; for most of the cluster stars the error is usually much less than 10 km s^{-1} .

2.3.1 LIKELY MEMBER STAR SELECTION

The procedure for determining the likely members of each cluster is the same as described by Lee et al. (2008b), adapted from Grillmair et al. (1995). Two procedures were designed for selecting likely true member stars, one for GCs and one for OCs. The difference is

primarily due to the lower number density of stars on the CMD of an OC compared to that of a GC. However, the techniques are sufficiently different that, due to the highly evolved nature of NGC 2158 and NGC 6791, the procedure for OCs could not be applied to these particular clusters because it relies on a function fit to the main stellar locus which, in these cases, would be double-valued around the MSTO. Hence, the procedure for GCs has been employed on the OCs NGC 2158 and NGC 6791, and specific reasons for having done so are described where applicable.

Due to the limited number of stars with spectroscopic data, it was necessary to use the photometry to produce a well-defined CMD, over which the spectroscopic data were then plotted. The stars inside each cluster's tidal radius (r_t), the point at which the cluster's gravitational influence gives way to that of the Galaxy, were selected as the first cut of likely members, indicated by the green circles in Figure 2.1. Stars inside a concentric annulus (where possible) were selected as field stars, indicated by the black circles in this figure. CMDs of both regions were obtained, then divided into sub-grids 0.2 mag wide in g_0 and 0.05 mag wide in $(g - r)_0$ color. Note that the field region of M92 is offset from the cluster center due to its proximity to the edge of the photometric scan. This was necessary because an annular field region around this location would have been inadequately populated with stars.

In each sub-grid, the signal-to-noise (s/n) was calculated using:

$$s/n(i, j) = \frac{n_c(i, j) - gn_f(i, j)}{\sqrt{n_c(i, j) + g^2n_f(i, j)}}, \quad (2.1)$$

where n_c and n_f refer to the number of stars counted in each sub-grid with color index i and magnitude index j within the cluster region and field region, respectively, and the parameter g is the ratio of the cluster area to the field area. These values were sorted in descending order in an array with index l , then star counts were obtained in increasingly larger sections of the array. The area in each section is defined as $a_k = ka_l$, where $a_l = 0.01 \text{ mag}^2$

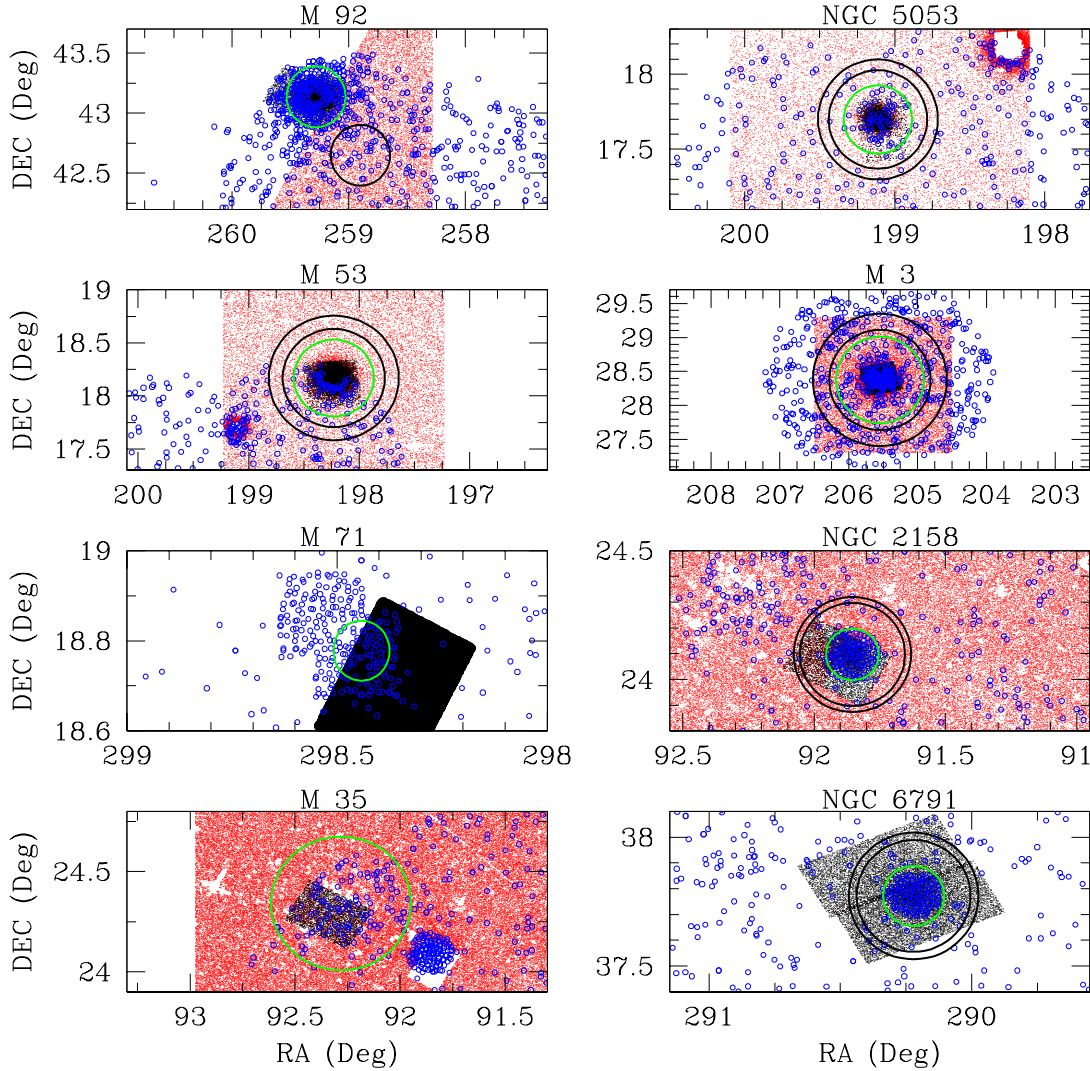


Figure 2.1 Stars with available photometry in the fields of M92, NGC 5053, M53, M3, M71, NGC 2158, M35, and NGC 6791. The black dots are stars from the crowded-field photometric analysis, the red dots are stars with photometry from the SDSS PHOTO pipeline, and the blue open circles are stars with SDSS spectroscopy. The green circle is the cluster's tidal radius (taken here as the cluster region) and the annulus between the two black circles constitutes the field region. The green circles are $15.17'$, $13.67'$, $21.75'$, $38.19'$, $4.0'$, $6.0'$, $20.0'$, and $7.0'$ in radius, respectively (Harris, 1996). In the case of M92, the cluster's proximity to the edge of the scan prevented an adequate annular field region; it was taken adjacent to the cluster region. NGC 2158 and NGC 6791 are open clusters, but due to their evolved nature, they are treated the same as globular clusters for the identification of likely true members. A larger radius was used for these clusters than those listed by Dias et al. (2002), in order to include as many member stars as possible. For interpretation of the references to color in this and all other figures, the reader is referred to the electronic version of this dissertation.

represents the area of a single sub-grid; k is the number of sub-grids in the section. Then, the cumulative signal-to-noise ratio, S/N , as a function of a_k , was calculated using:

$$S/N(a_k) = \frac{N_c(a_k) - gN_f(a_k)}{\sqrt{N_c(a_k) + g^2N_f(a_k)}}, \quad (2.2)$$

where

$$N_c(a_k) = \sum_{l=1}^k n_c(l), \quad N_f(a_k) = \sum_{l=1}^k n_f(l). \quad (2.3)$$

Here, $n_c(l)$ represents the number of cluster stars within the ordered sub-grid array element l ; $n_f(l)$ represents the same quantity for the field stars. A threshold value for s/n was adopted, based on the maximum value of $S/N(a_k)$, to identify areas of the CMD where the ratio of cluster stars to field stars was high (rejecting single-star events). These areas were taken to be sub-grids of likely cluster members, and all sub-grids with s/n greater than this threshold were identified. These sub-grids are shown as boxes in Figures 2.2 – 2.4. The left-hand panels show the stars inside the tidal radius – the sub-grids with s/n greater than the threshold value are indicated as red squares. The right-hand panels show the stars from the field region with the same sub-grids, indicated in green.

The procedures described in Lee et al. (2008b) handle OCs differently from GCs. Instead of determining sub-grid s/n ratios, a fiducial line is fit to the open cluster's MS using a robust polynomial fitting routine, then a region is picked out by eye corresponding to the MS to represent the likely member stars. The interested reader is referred to Lee et al. (2008b) for further details on the OC member selection procedure. This procedure works well on young clusters, where no significant evolution off the MS has occurred. However, NGC 2158 and NGC 6791 are evolved (older) clusters, and exhibit a distinct MSTO and RGB (see Figure 2.4). This prevents polynomial fitting of the CMD from working properly since the function would be double valued at the MSTO/SGB, so in this study NGC 2158 and NGC 6791 are processed (for the purpose of member assignment) as if they are GCs. The usual OC

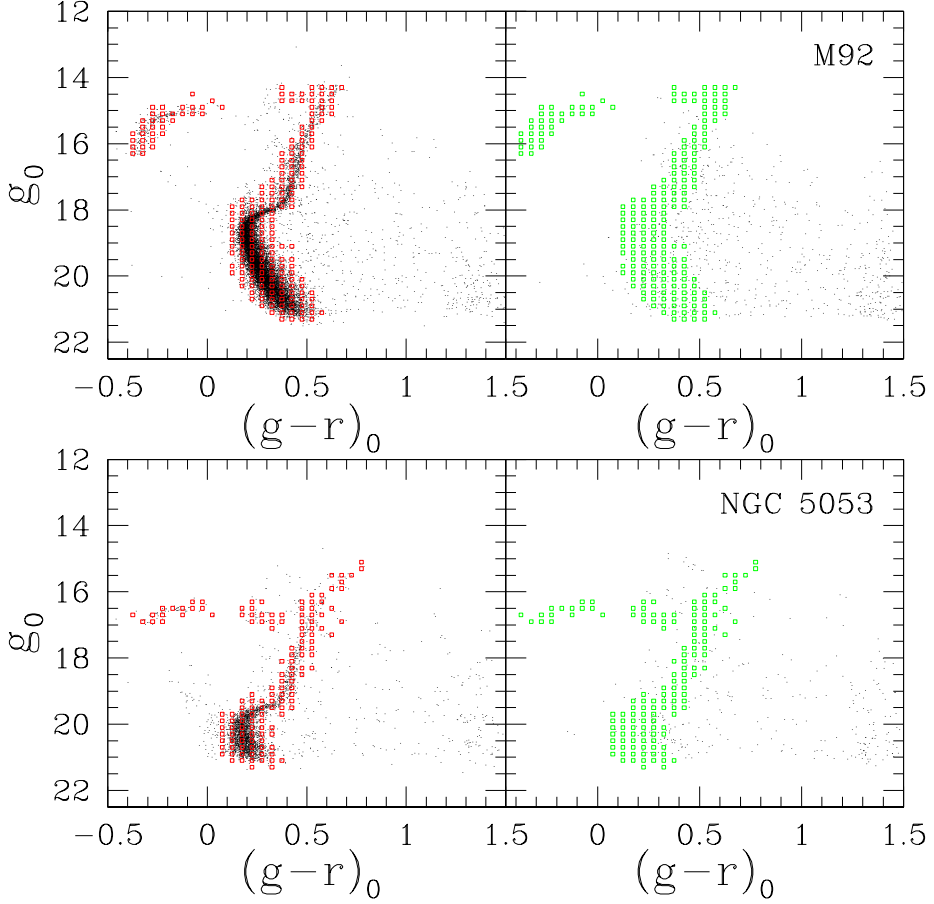


Figure 2.2 Color-Magnitude Diagrams of the stars from M92 (upper panels) and NGC 5053 (lower panels) inside the tidal radius (left-hand panels) and inside the field region (right-hand panels). The small boxes represent the sub-grids that were selected in the first cut of the CMD mask algorithm, and contain the stars used the subsequent analysis.

procedure was successfully implemented for M35 (Figure 2.5).

The cleaned CMDs for this sample are shown in Figures 2.6 and 2.7. The black points are the likely members from the photometry, while the red open circles are the likely members from the spectroscopic sample. This part of the procedure could not be carried out for M71 due to difficulties encountered with the photometry values available for this cluster at the time of this analysis (see An et al., 2008). Therefore, a first cut was made based on the tidal radius of the stars, and those stars were passed on to the final step, as outlined in the following section. Figure 2.5 shows the first-cut CMD for M71.

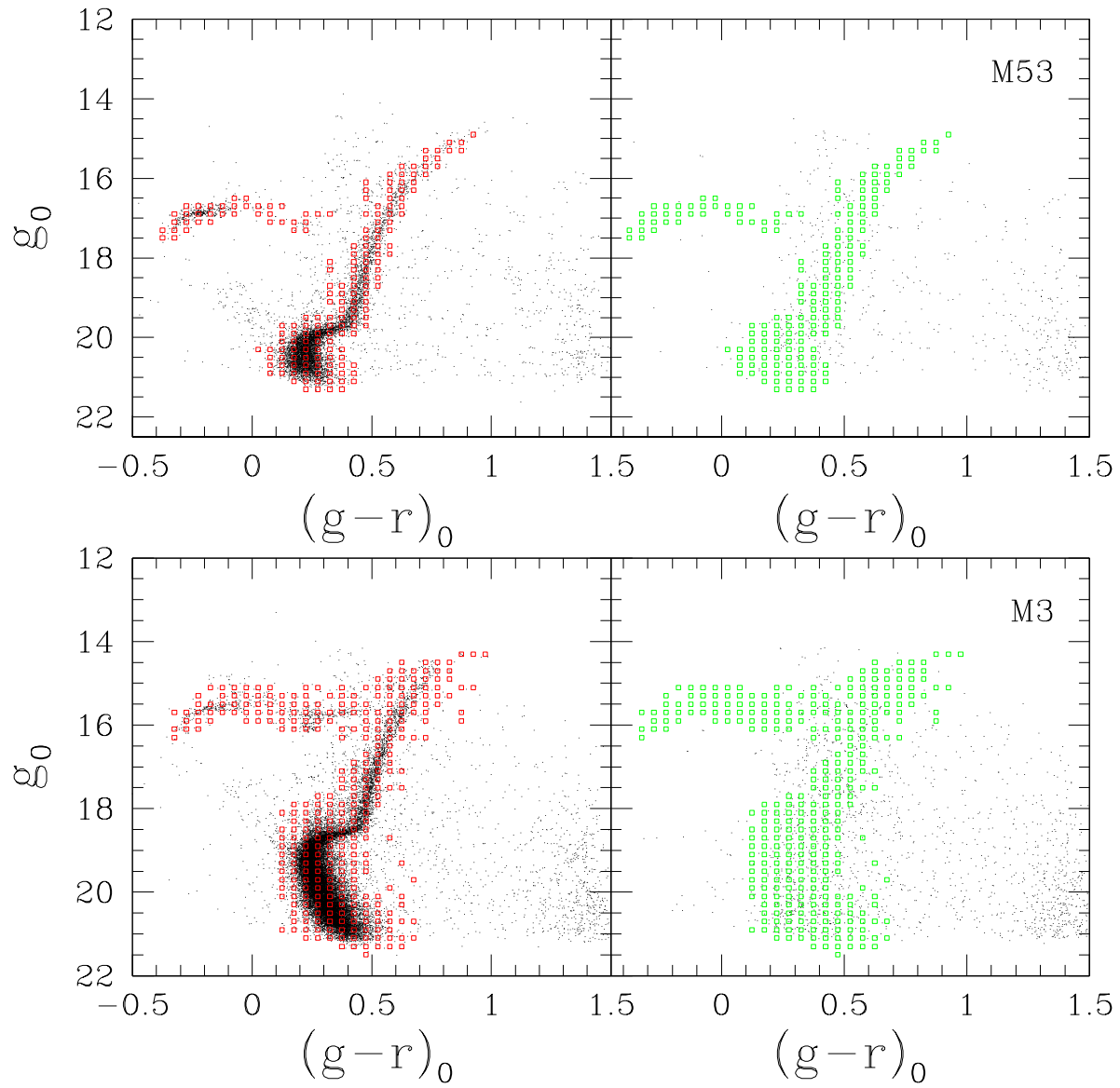


Figure 2.3 Same as Fig. 2.2, but for M53 (upper panels) and M3 (lower panels).

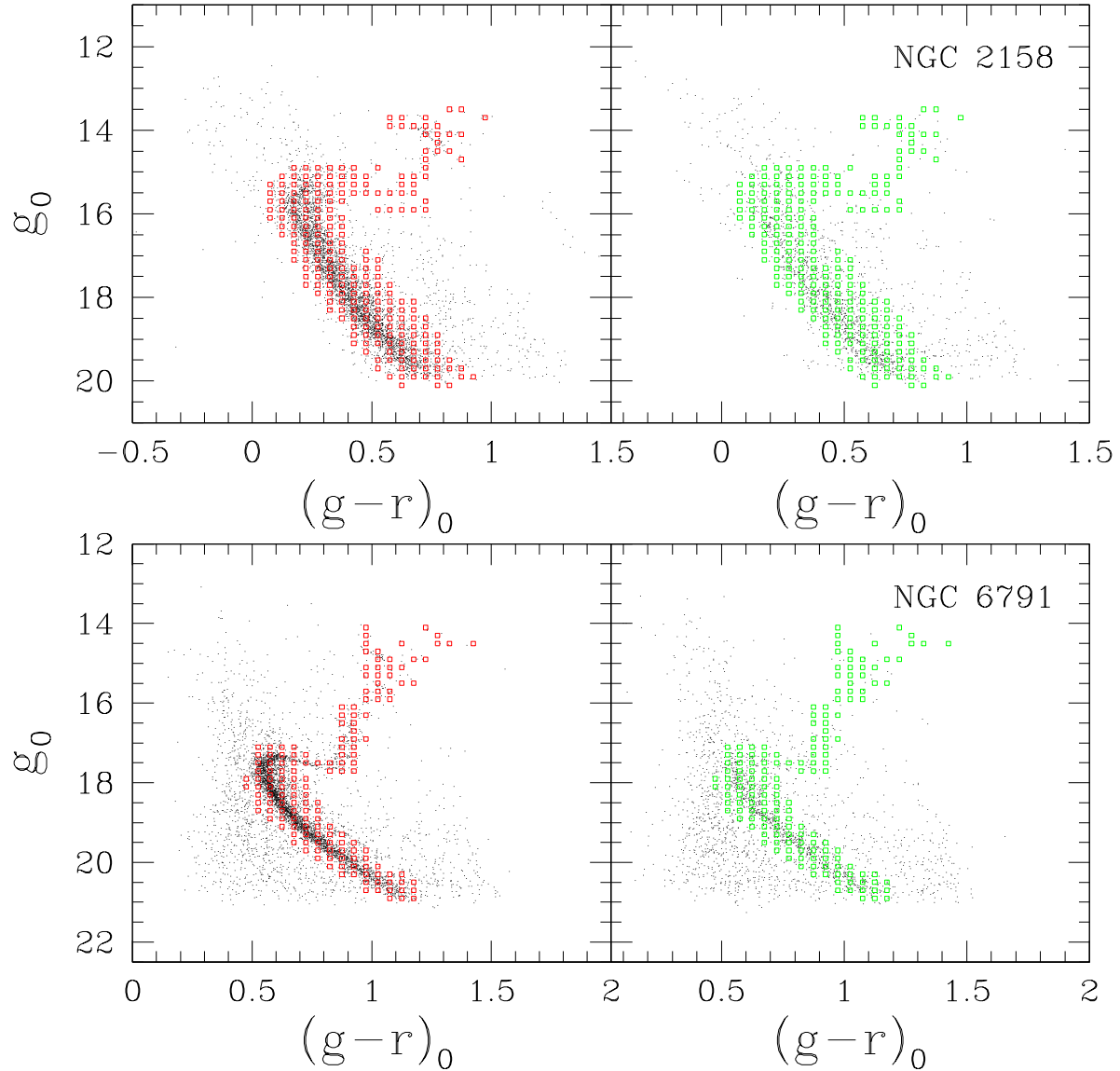


Figure 2.4 Same as Fig. 2.2, but for NGC 2158 (upper panels) and NGC 6791 (lower panels). Due to the highly-evolved nature of these open clusters, they were treated in the member selection process as if they were globular clusters.

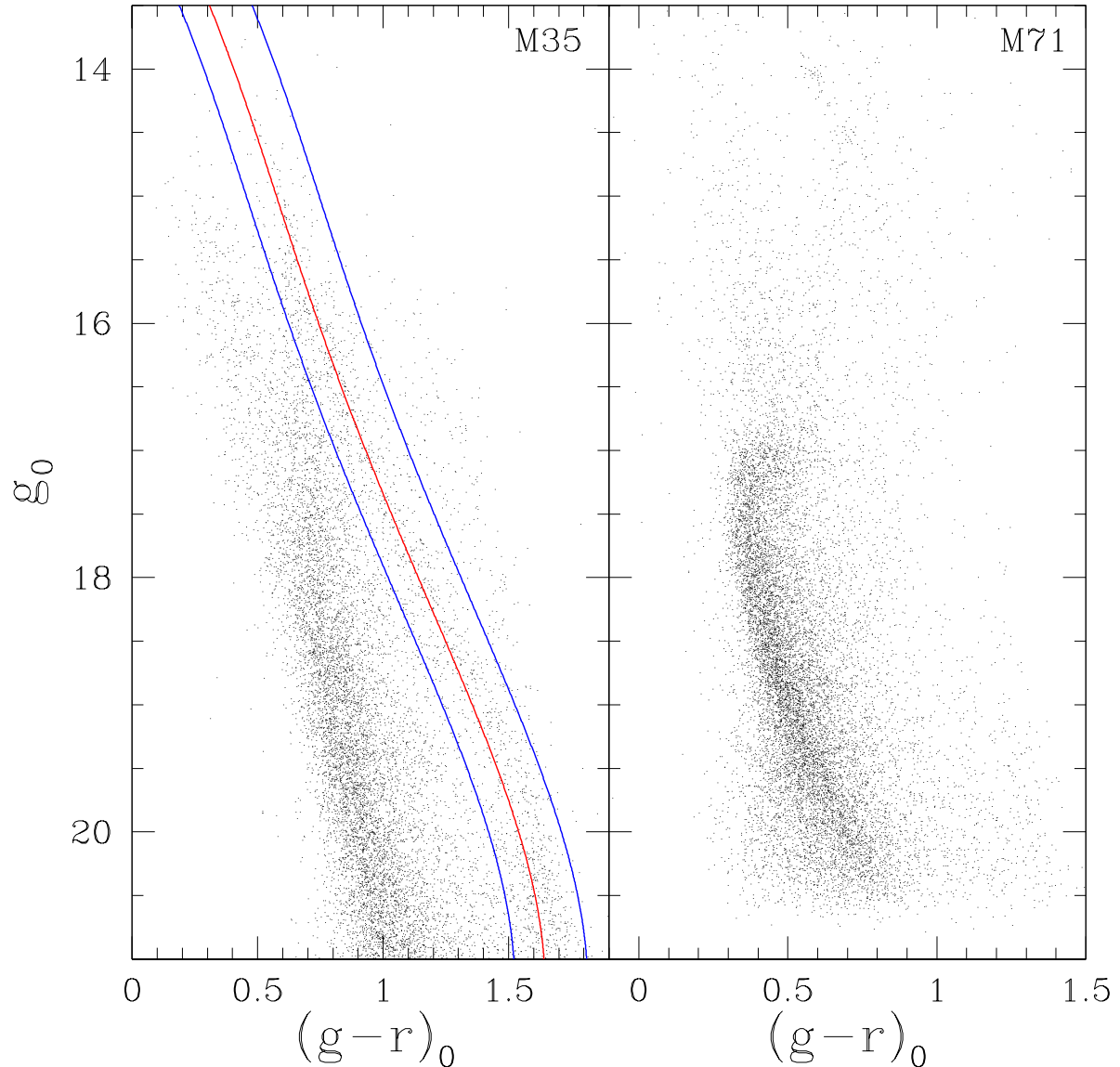


Figure 2.5 Same as Fig. 2.2, but for M35 (left-hand panel) and M71 (right-hand panel). The red line in M35 is the fiducial from a fourth-order polynomial fit, while the blue lines define the offsets of $^{+0.17}_{-0.12}$ mag inside of which were selected stars regarded as likely members from the photometric data. Because of M35's low Galactic latitude, the dense stripe of stars on the blue side of the main sequence is due to superposed disk stars. Member stars for M71 were selected strictly by radial velocity and metallicity cuts rather than by using the CMD first; no photometry was used for analysis of this cluster due to poor calibration. For this reason, the CMD for M71 is shown differently from the other globular clusters.

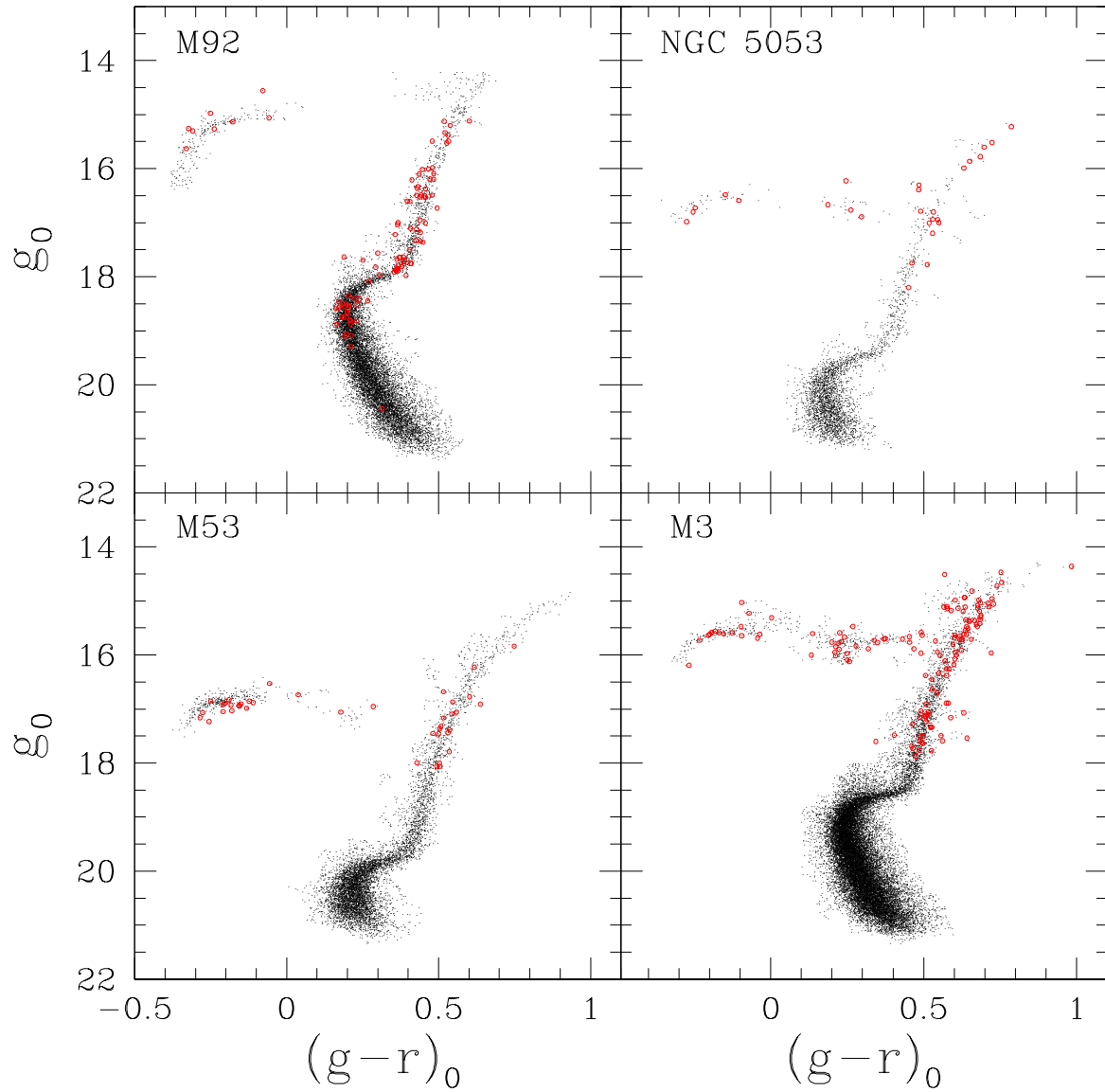


Figure 2.6 The Color-Magnitude Diagram following the second cut of likely member stars based on the sub-grid selection for M92 (upper-left panel), NGC 5053 (upper-right panel), M53 (lower-left panel), and M3 (lower-right panel). Black dots represent stars from the photometric sample, and the red open circles represent stars from the spectroscopic sample.

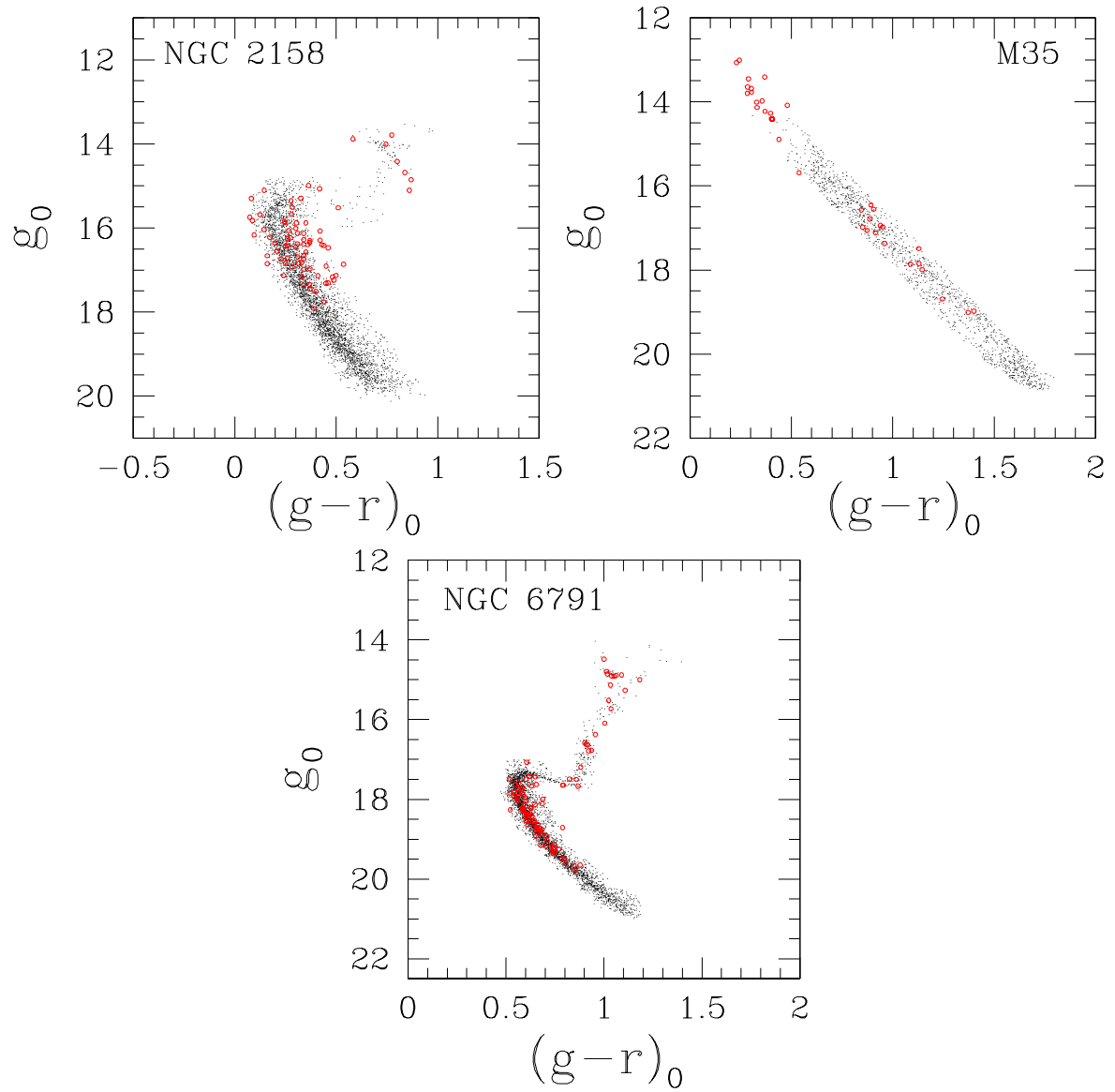


Figure 2.7 The Color-Magnitude Diagram following the second cut of likely member stars for NGC 2158 (upper-left panel), M35 (upper-right panel), and NGC 6791 (lower panel). Black dots represent stars from the photometric sample, and the red open circles represent stars from the spectroscopic sample.

Table 2.4. Metallicities and Radial Velocities of Globular and Open Clusters

Cluster	$\langle [\text{Fe}/\text{H}] \rangle$	$\sigma([\text{Fe}/\text{H}])$ (dex)	$\sigma_\mu([\text{Fe}/\text{H}])$ (dex)	$\langle \text{RV} \rangle$ (km s $^{-1}$)	$\sigma(\text{RV})$ (km s $^{-1}$)	$\sigma_\mu(\text{RV})$ (km s $^{-1}$)	N
M92	-2.25	0.17	0.02	-116.5	8.7	1.1	58
NGC 5053	-2.26	0.25	0.06	+44.0	4.9	1.2	16
M53	-2.03	0.13	0.03	-59.6	7.9	1.8	19
M3	-1.55	0.14	0.02	-141.2	5.6	0.6	77
M71	-0.79	0.06	0.01	-16.9	9.3	2.3	17
NGC 2158	-0.26	0.08	0.01	+27.8	5.9	0.7	62
M35	-0.20	0.18	0.03	-5.0	6.2	1.2	29
NGC 6791	+0.31	0.13	0.01	-47.0	6.0	0.6	90

Note. — Columns 2 and 5 list the measured mean values of [Fe/H] and RV for each cluster, while columns 3 and 6 list the 1σ spread of each value. Columns 4 and 7 are the standard errors in the mean (σ_μ) of the estimates. N lists the number of true member stars for each cluster determined by the final application of the 2σ range to the mean of the Gaussian fits on [Fe/H] and RV.

2.3.2 SELECTION OF ADOPTED TRUE MEMBERS

The true member stars were then identified as a subset of the adopted likely member stars. Figure 2.8 shows the distributions of [Fe/H] (left-hand panel) and RV (right-hand panel) for stars in the field of M92 at each culling point in the procedure. The black lines indicate all 775 stars on the original spectroscopic plate (after removing stars with no parameter estimates from the SSPP or low spectral S/N), while the red lines indicate only those stars inside r_t , and the green lines indicate those stars that passed the cut using the individual sub-grid s/n and cumulative S/N calculations. A Gaussian fit was then performed on the highest peak of the distribution of this final subset (blue line) and estimates were obtained of the mean and standard deviation of [Fe/H] and RV. Finally, outliers were rejected by applying a 2σ cut on both parameters:

$$\langle [\text{Fe}/\text{H}] \rangle - 2\sigma_{[\text{Fe}/\text{H}]} \leq [\text{Fe}/\text{H}]_\star \leq \langle [\text{Fe}/\text{H}] \rangle + 2\sigma_{[\text{Fe}/\text{H}]} \quad (2.4)$$

$$\langle \text{RV} \rangle - 2\sigma_{\text{RV}} \leq \text{RV}_\star \leq \langle \text{RV} \rangle + 2\sigma_{\text{RV}}. \quad (2.5)$$

$[\text{Fe}/\text{H}]_\star$ and RV_\star correspond to the metallicity and radial velocity of each star in question. If a star passed both cuts then it was considered a true member star. The numbers of true member stars determined by this final cut for each cluster are listed in Table 2.4.

2.4 DETERMINATION OF OVERALL METALLICITIES AND RADIAL VELOCITIES OF THE CLUSTERS

Once the true members were selected as described above, final estimates of the cluster metallicities and radial velocities were obtained. Figures 2.8–2.15 show the binned distributions of $[\text{Fe}/\text{H}]$ and RV for each cluster, as described in Section 2.3.2. The adopted cluster values are listed in Table 2.4. This table also lists the standard error of the mean (σ_μ) for the estimates of metallicity and radial velocity for each cluster; due to the large numbers of true members for each cluster, these are uniformly small.

No strong trends appear to exist in estimates of $[\text{Fe}/\text{H}]$ as a function of color or spectral quality, as shown in Figures 2.16 and 2.17. As a check, residuals of $[\text{Fe}/\text{H}]$ were calculated with respect to the values adopted for each cluster from the literature, using:

$$\text{Res}_{[\text{Fe}/\text{H}]} = [\text{Fe}/\text{H}] - [\text{Fe}/\text{H}]_{\text{lit}}, \quad (2.6)$$

and a linear regression on these values was performed as a function of $(g - r)_0$ color and $\langle \text{S/N} \rangle$ using models of the form:

Table 2.5. Residuals from Linear Regression on Metallicity

Cluster (1)	N (2)	Parameter (3)	X (4)	σ_X (5)	Y (6)	σ_Y (7)	R^2 (8)
M92	58	$(g - r)_0$	-0.347	0.145	+0.229	0.053	0.093
		S/N	-0.001	0.002	+0.135	0.051	0.004
NGC 5053	16	$(g - r)_0$	-0.585	0.164	+0.347	0.090	0.475
		S/N	-0.007	0.005	+0.333	0.182	0.133
M53	19	$(g - r)_0$	+0.166	0.138	+0.027	0.066	0.078
		S/N	-0.005	0.006	+0.192	0.132	0.048
M3	77	$(g - r)_0$	-0.219	0.056	+0.059	0.032	0.071
		S/N	+0.001	0.001	-0.085	0.044	0.022
M71	17	$(g - r)_0$	+0.017	0.177	+0.089	0.116	0.001
		S/N	-0.001	0.001	+0.140	0.078	0.018
NGC 2158	62	$(g - r)_0$	+0.017	0.047	-0.008	0.019	0.002
		S/N	+0.002	0.001	-0.099	0.036	0.110
M35	29	$(g - r)_0$	-0.289	0.062	+0.121	0.044	0.445
		S/N	+0.006	0.001	-0.451	0.084	0.468
NGC 6791	90	$(g - r)_0$	+0.276	0.077	-0.191	0.058	0.128
		S/N	+0.003	0.001	-0.110	0.040	0.103

Note. — The variables X and Y are the slope and zero-points, respectively, of a linear regression on the residuals in our measured [Fe/H] values and those adopted from the literature, along with the corresponding uncertainties from the regression. The parameter R^2 indicates the fraction of the variance accounted for by the correlations in the variables $(g - r)_0$ and S/N for each cluster.

$$\text{Res}_{\text{[Fe/H]}} = X \cdot (g - r)_0 + Y \quad (2.7)$$

$$\text{Res}_{\text{[Fe/H]}} = X \cdot \langle S/N \rangle + Y. \quad (2.8)$$

The results of the linear regressions are listed in Table 2.5. Column (2) lists the number of true member stars used in the fit, Columns (4) and (6) list the slope and zero-point of the fit, respectively, while Columns (5) and (7) list the corresponding uncertainties. Finally,

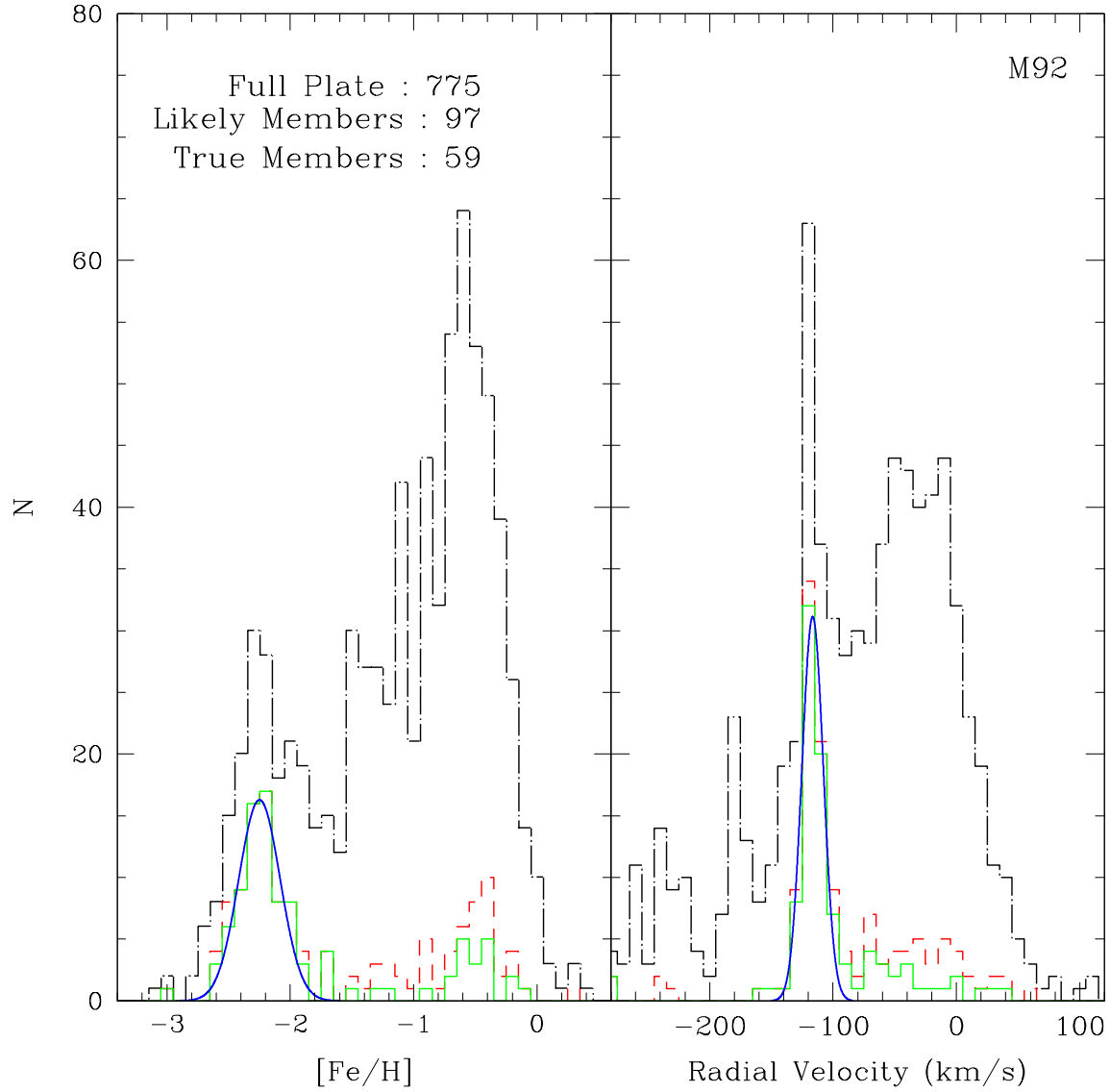


Figure 2.8 Distributions of $[\text{Fe}/\text{H}]$ and radial velocity for stars in the field of M92. The black dot-dashed line corresponds to all the stars on the plate, the red dashed line corresponds to the stars inside the tidal radius, and the green solid line corresponds to the stars that were identified as likely members by the sub-grid s/n procedure described in Section 2.3.1. The blue solid line is a Gaussian fit indicating the region of each distribution in which the true members are located, as described in Section 2.3.2.

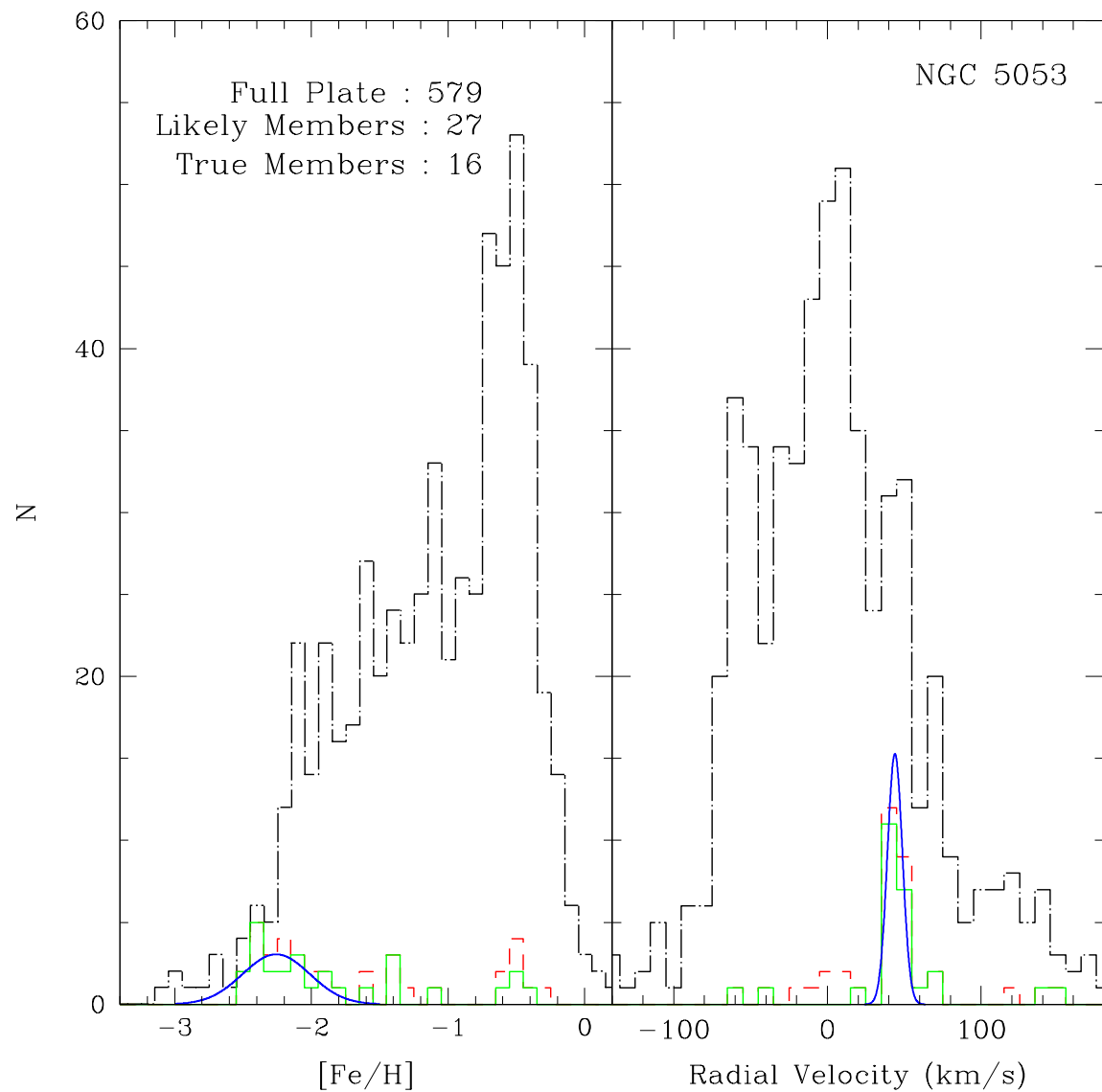


Figure 2.9 Same as Fig. 2.8, but for NGC 5053.

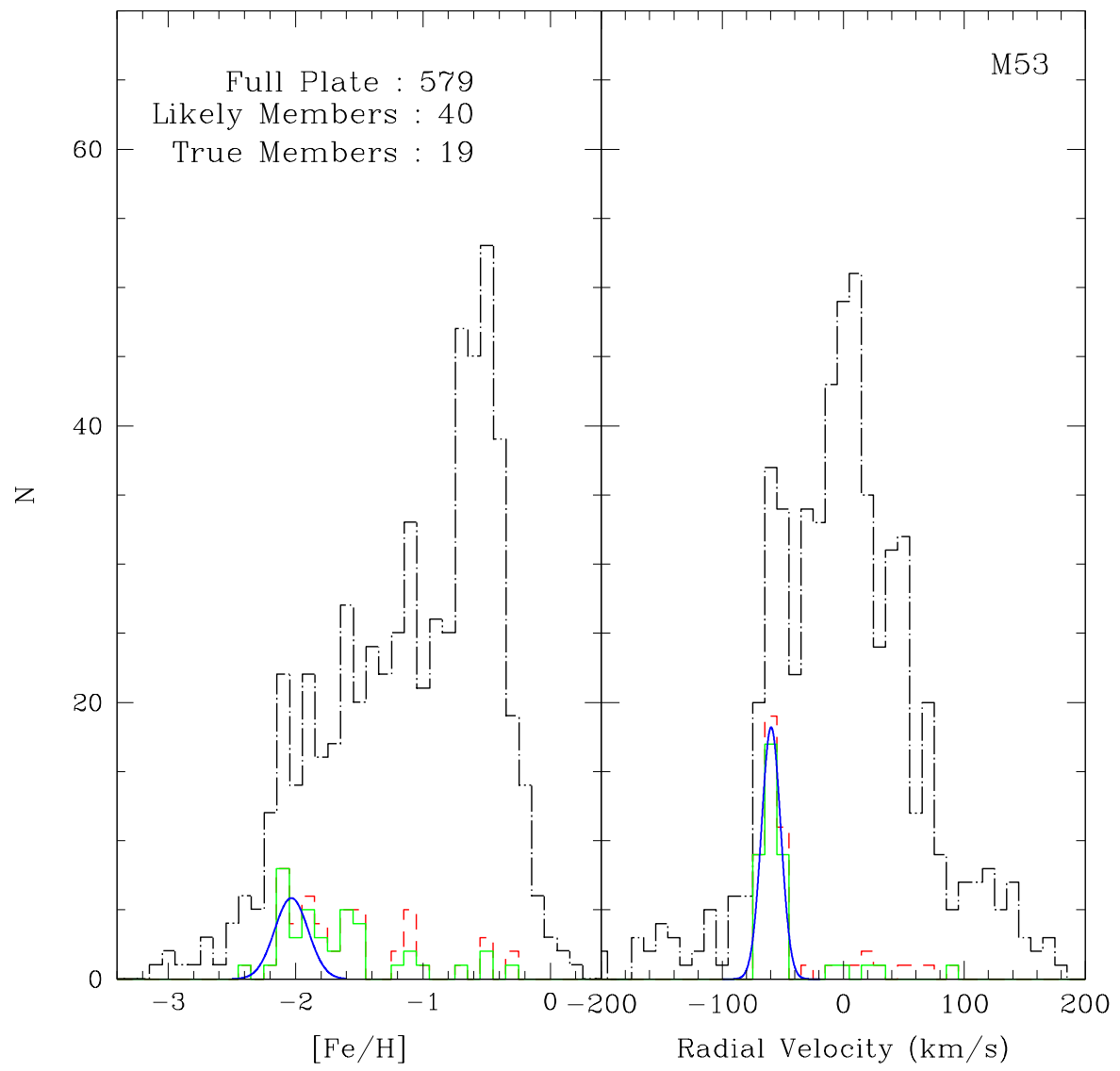


Figure 2.10 Same as Fig. 2.8, but for M53.

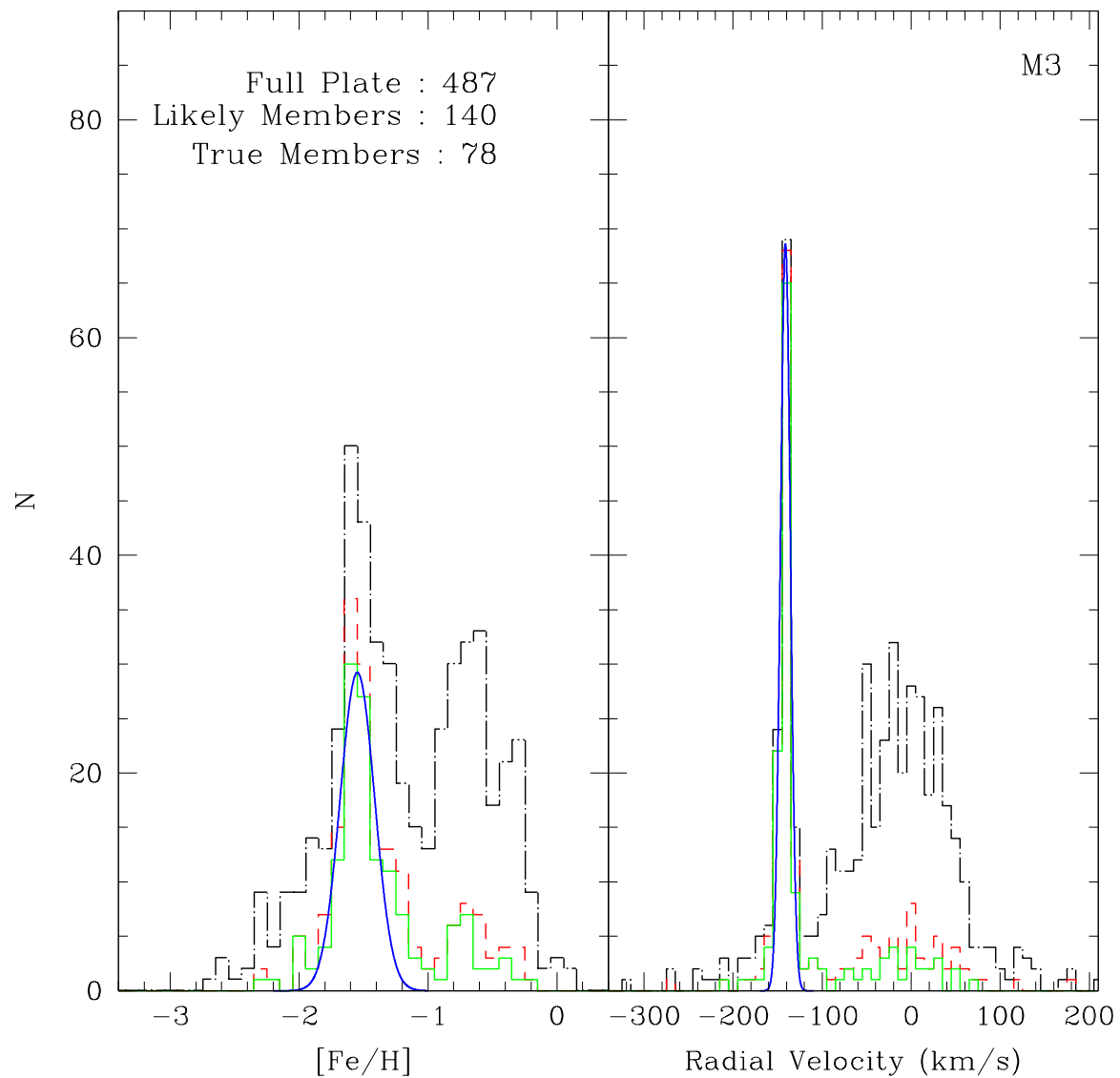


Figure 2.11 Same as Fig. 2.8, but for M3.

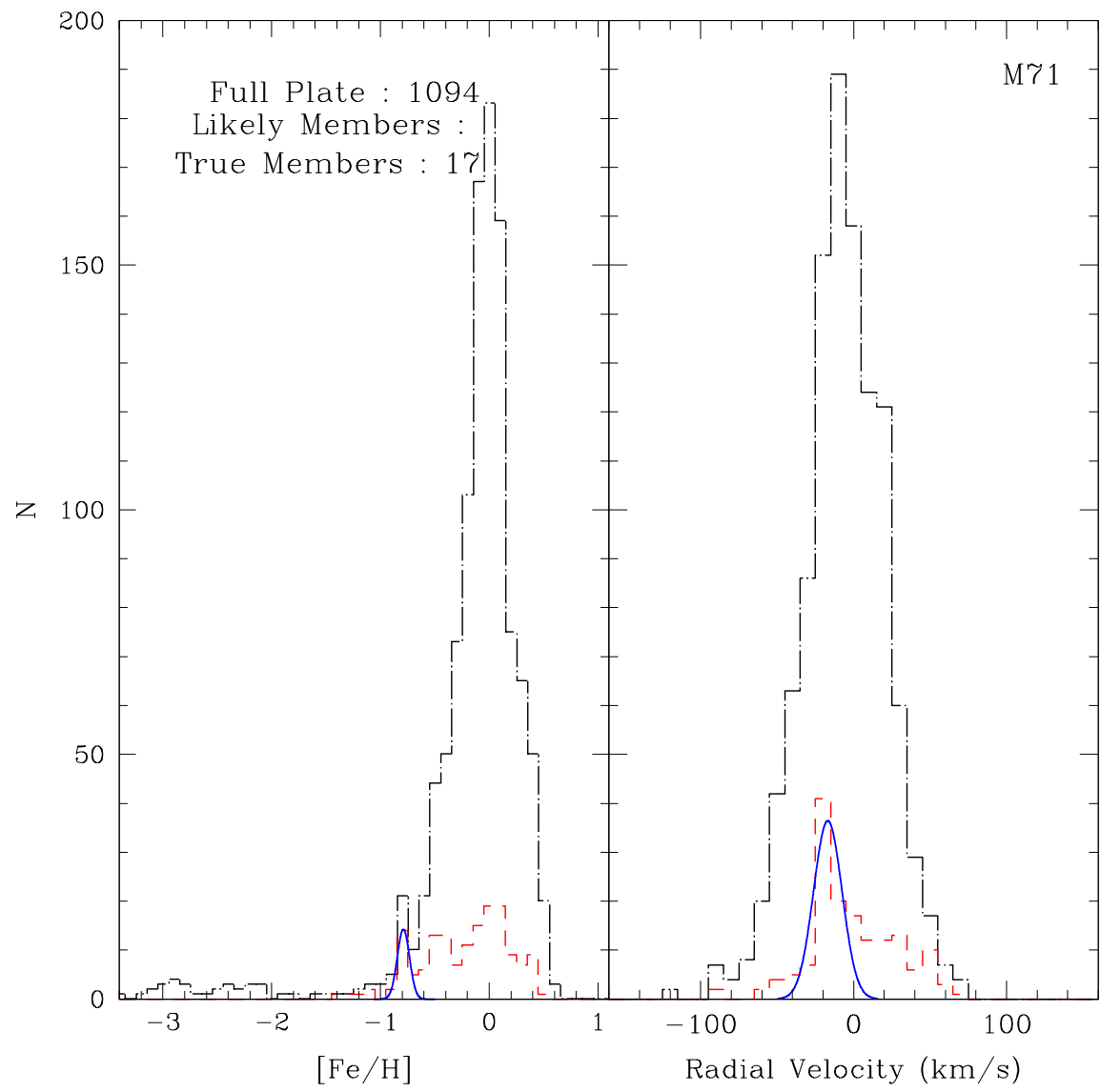


Figure 2.12 Same as Fig. 2.8, but for M71.

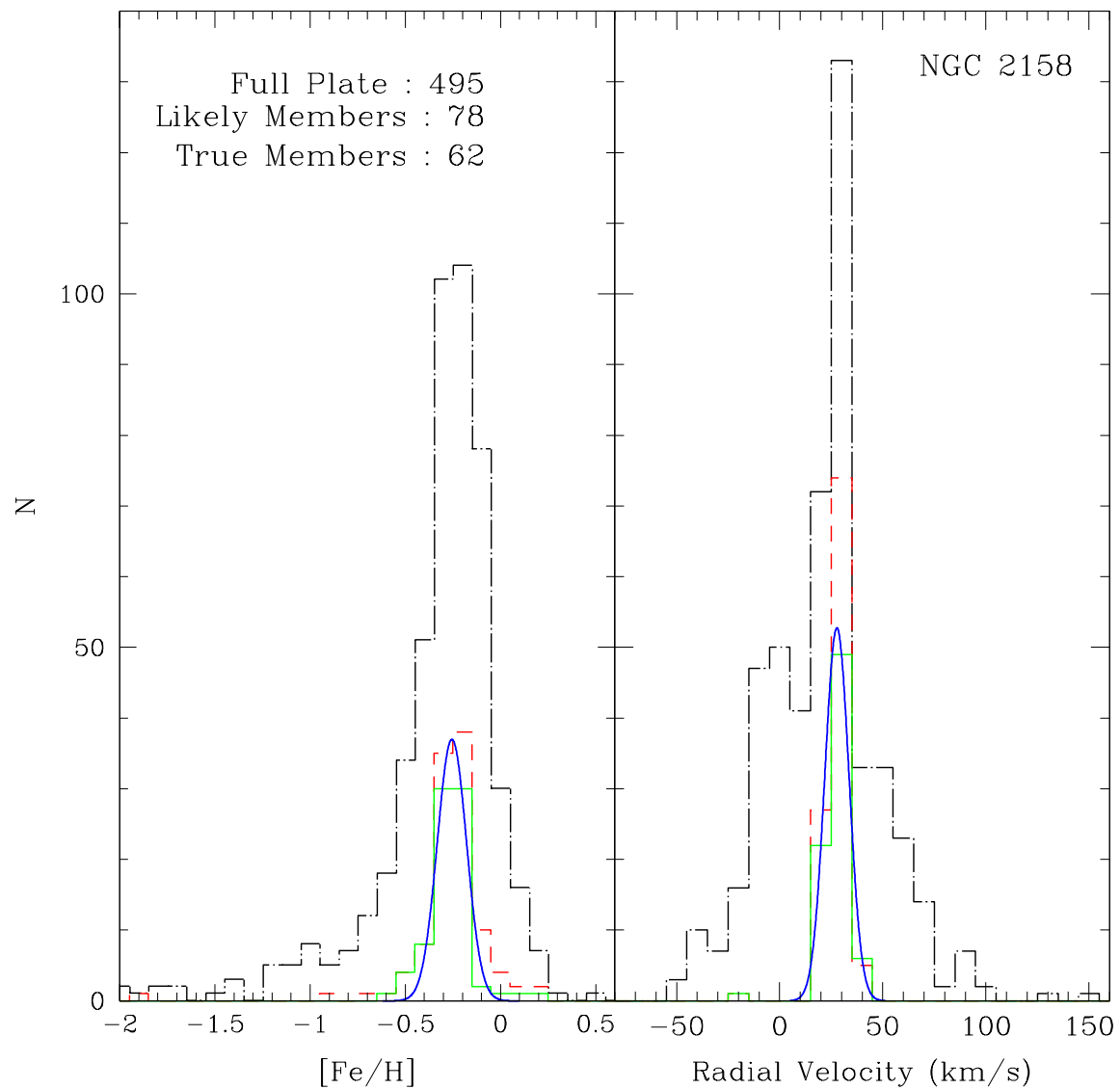


Figure 2.13 Same as Fig. 2.8, but for NGC 2158.

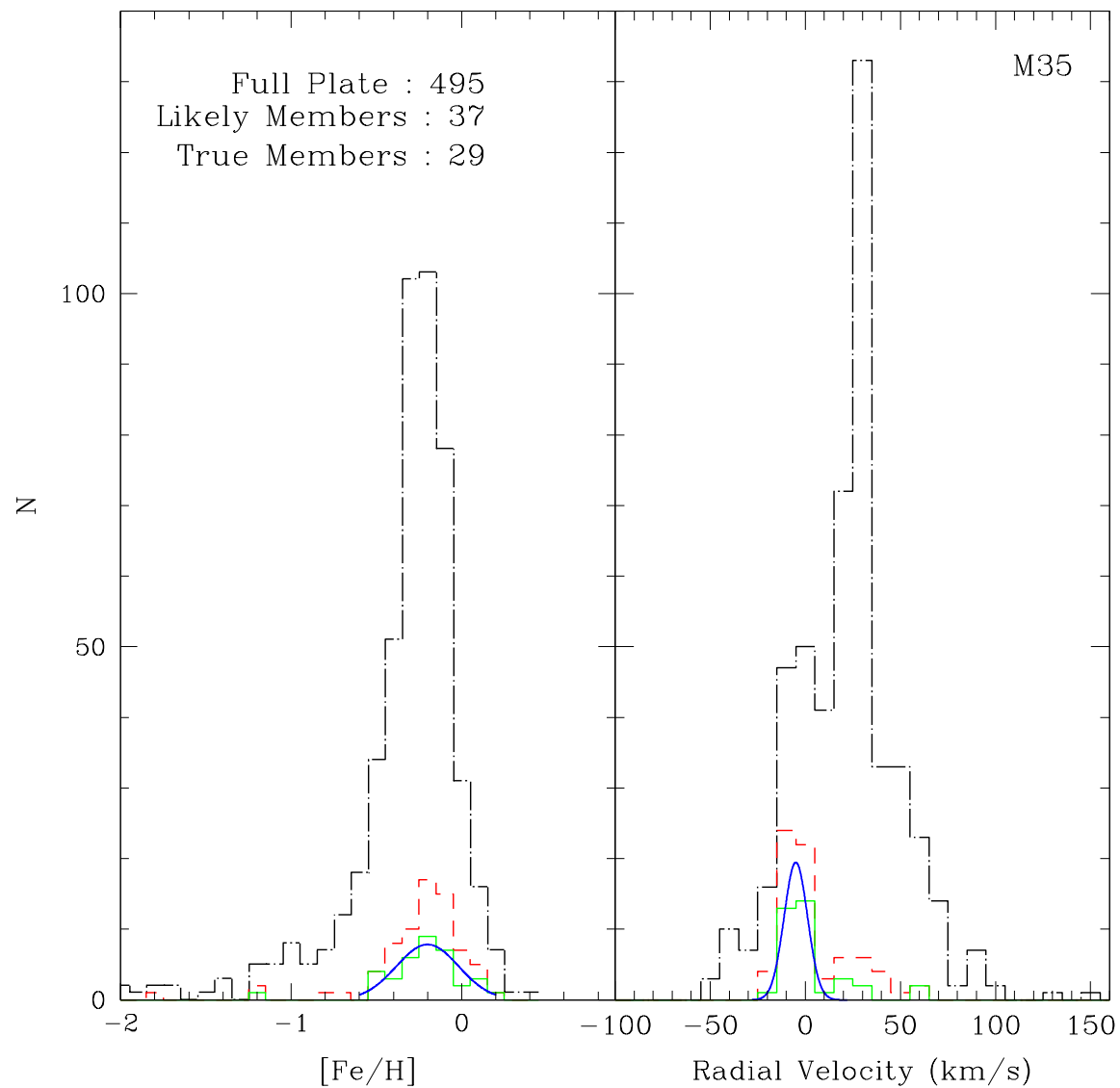


Figure 2.14 Same as Fig. 2.8, but for M35.

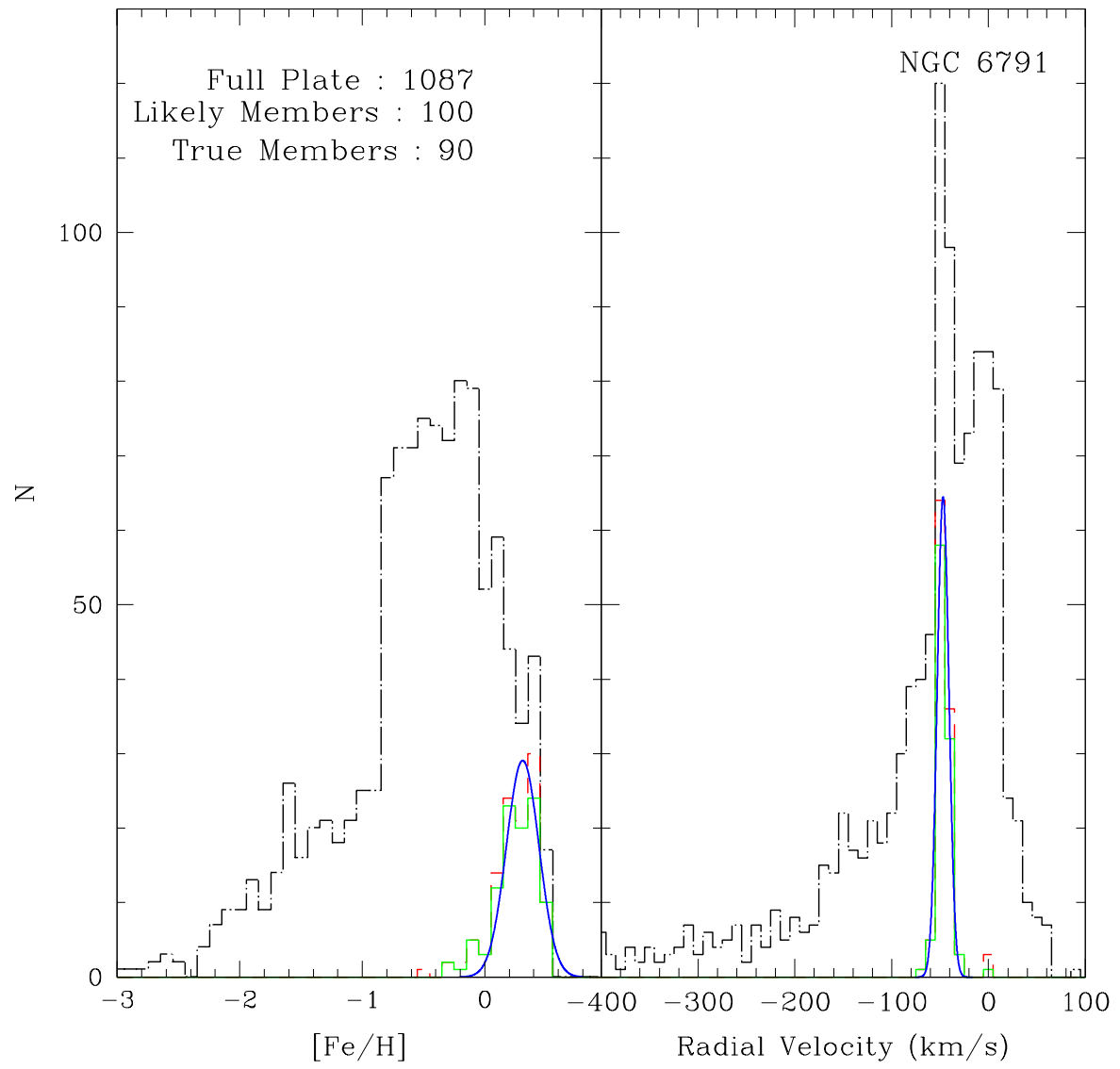


Figure 2.15 Same as Fig. 2.8, but for NGC 6791.

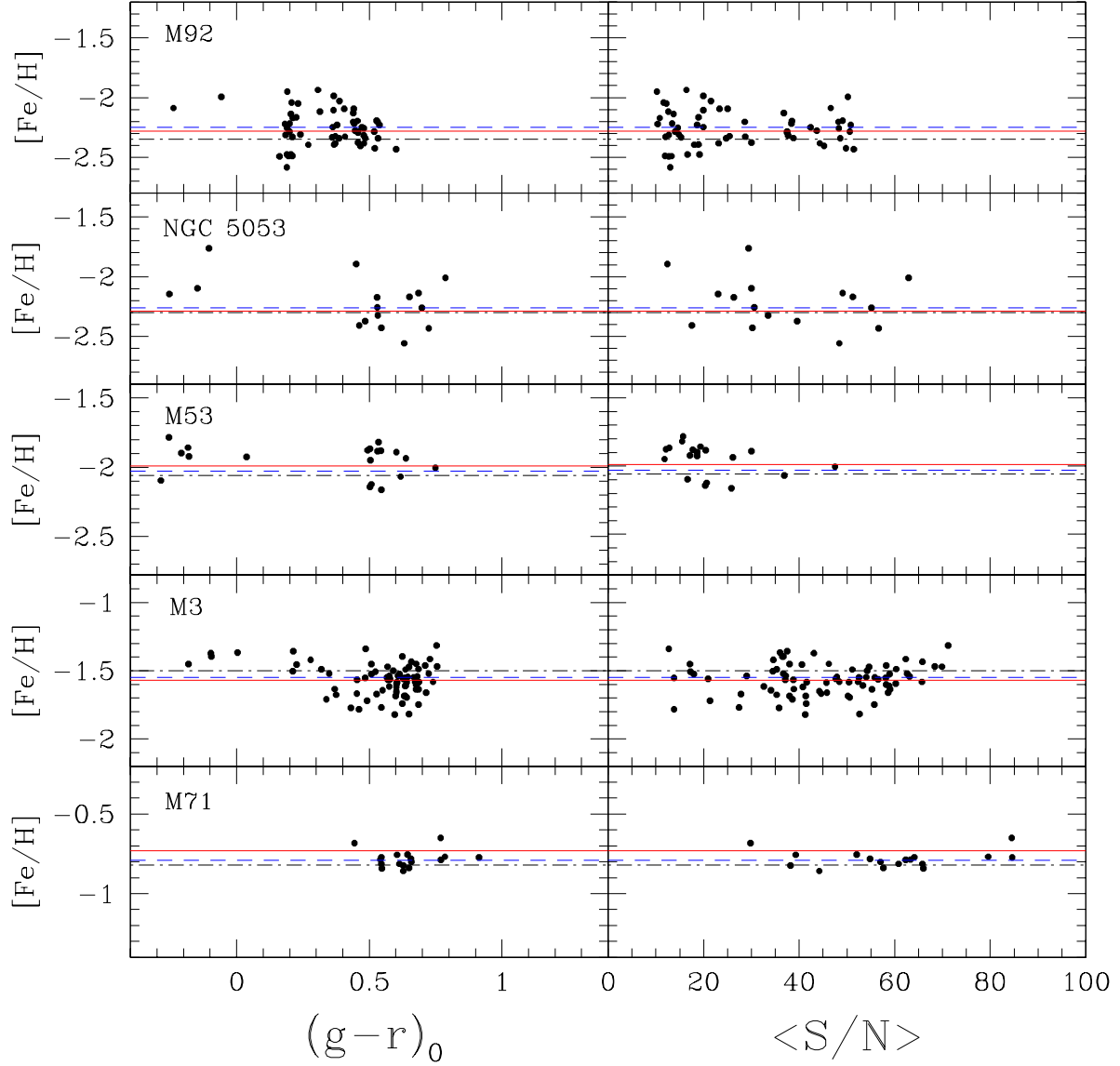


Figure 2.16 Distribution of $[\text{Fe}/\text{H}]$ as a function of $(g - r)_0$ (left-hand column) and average signal-to-noise ($\langle \text{S}/\text{N} \rangle$ right-hand column) for selected true member stars of the globular clusters M92, NGC 5053, M53, M3, and M71, ordered from top to bottom in increasing metallicity. The red solid line in each panel represents the adopted value of $[\text{Fe}/\text{H}]$ for each cluster from the Harris (1996) catalog, the black dot-dashed line is $[\text{Fe}/\text{H}]$ from the Carretta et al. (2009a) recalibration, and the dashed blue line represents the mean measured value of each cluster.

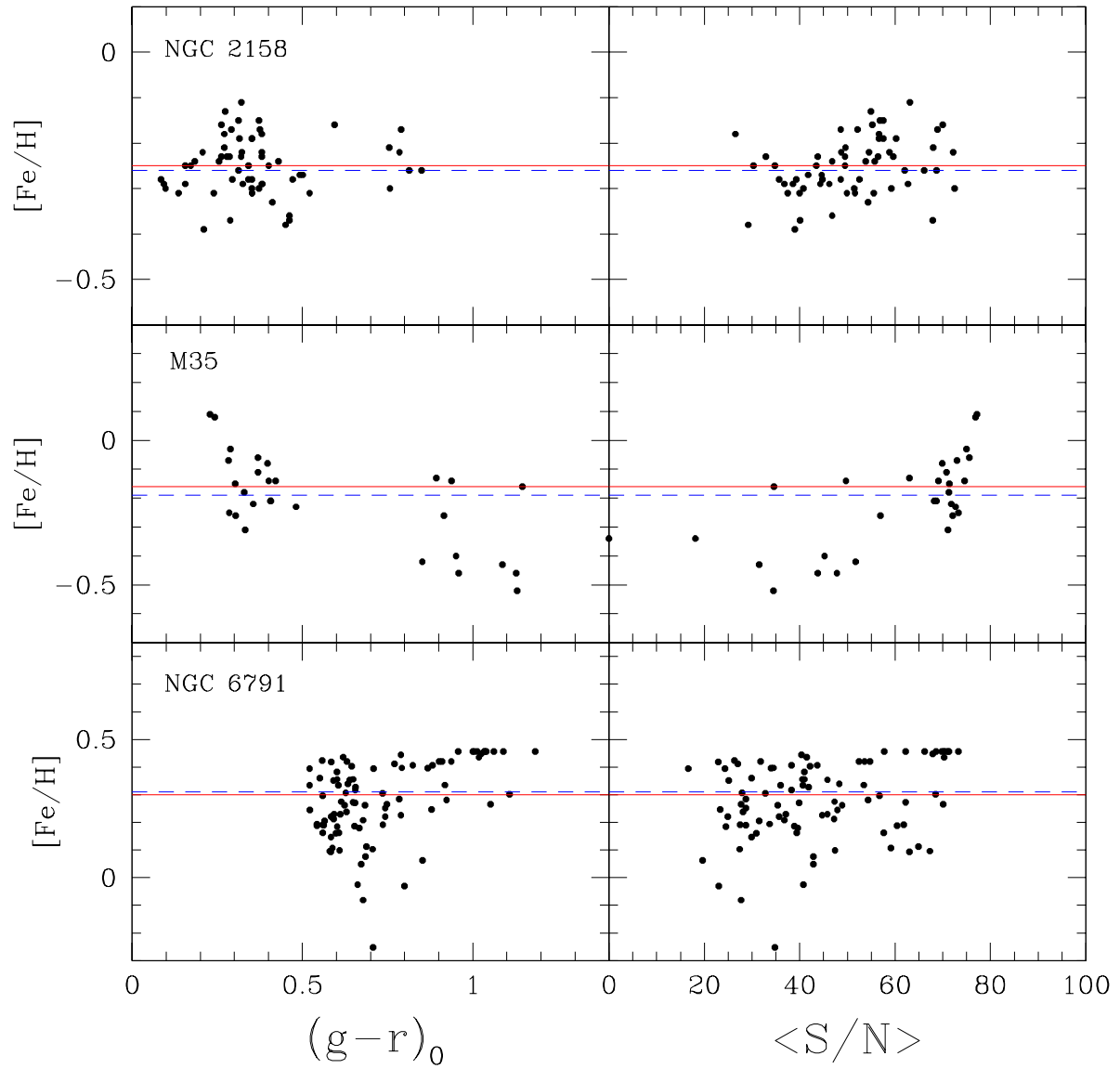


Figure 2.17 Same as Fig. 2.16, but for the open clusters NGC 2158, M35, and NGC 6791, ordered from top to bottom in increasing metallicity.

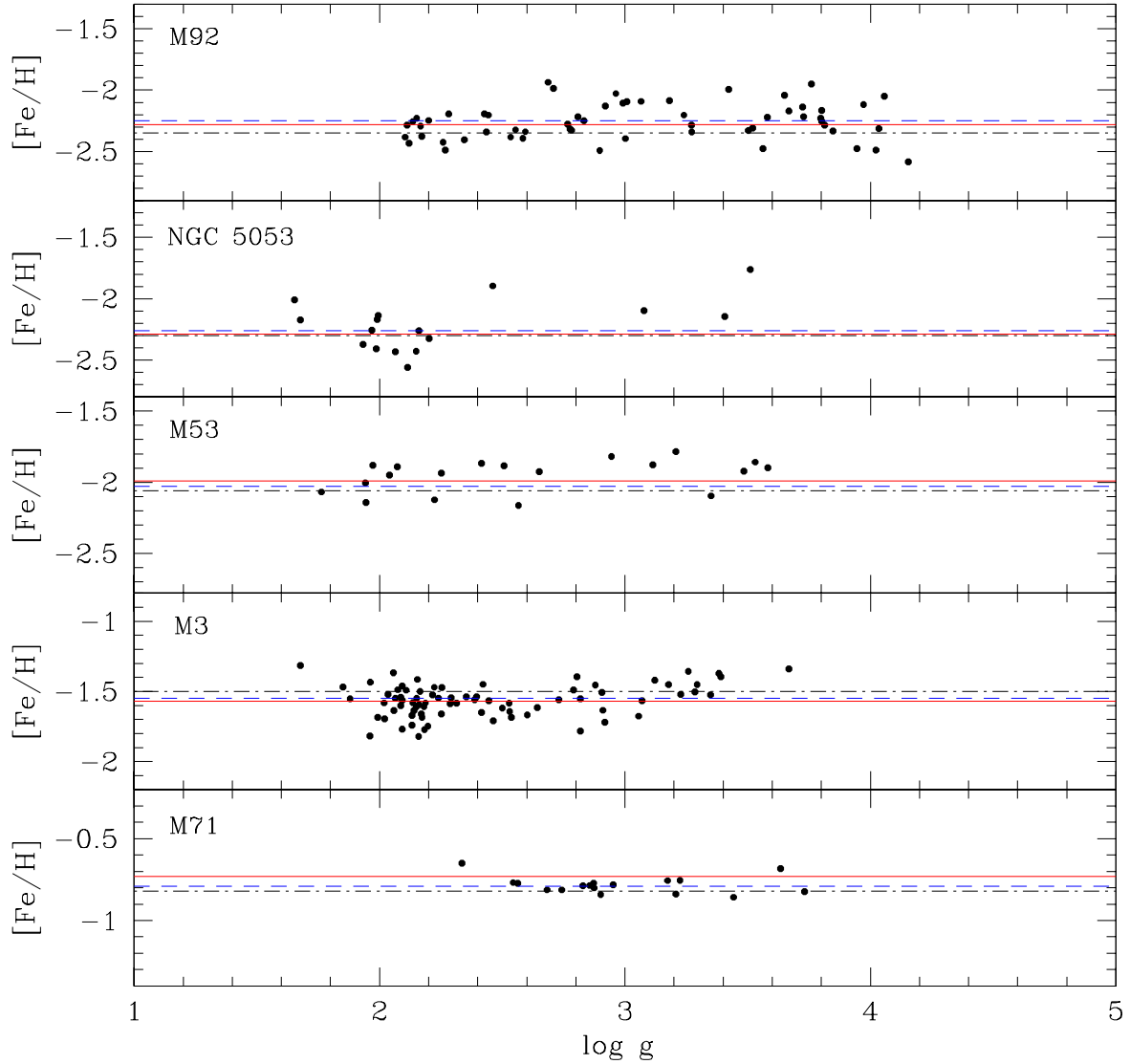


Figure 2.18 Distribution of $[Fe/H]$ as a function of estimated $\log g$ for the selected true member stars of the globular clusters M92, NGC 5053, M53, M3, and M71, ordered from top to bottom on increasing metallicity. As in Fig. 2.16, the red solid line corresponds to the adopted value for $[Fe/H]$ for each cluster from Harris (1996), the black dot-dashed is $[Fe/H]$ from the recalibrated metallicity scale of Carretta et al. (2009a), and the dashed blue is the mean measured value.

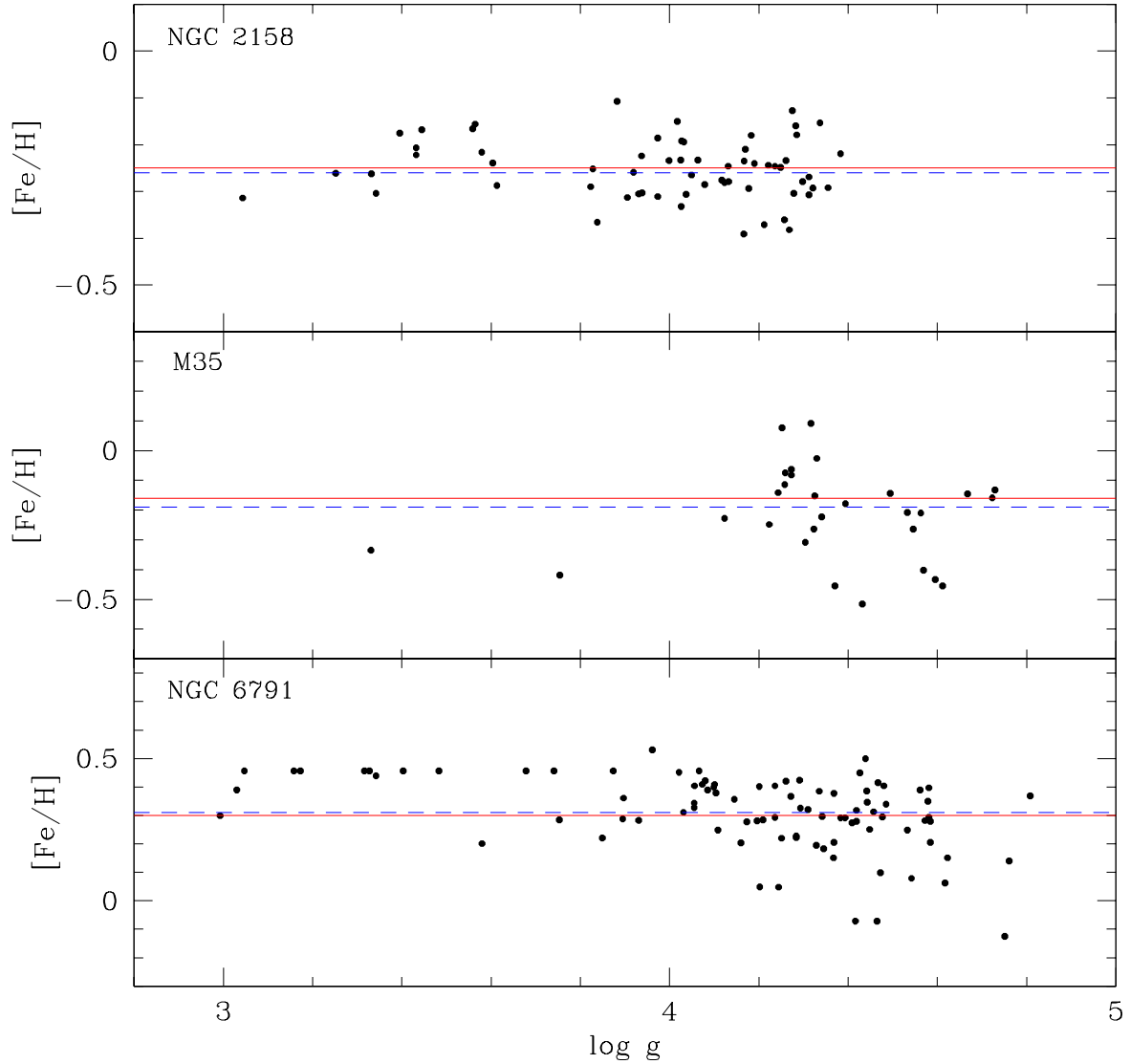


Figure 2.19 Distribution of $[Fe/H]$ as a function of estimated $\log g$ for the selected true member stars of the open clusters NGC 2158, M35, and NGC 6791, ordered from top to bottom on increasing metallicity. As in Fig. 2.16, the red solid line corresponds to the adopted literature value for $[Fe/H]$ for each cluster, while the dashed blue is the mean measured value.

Column (8) lists the R^2 value, which indicates the amount of scatter in the data that can be accommodated by the regression. Values of R^2 close to zero indicate little dependence on the independent variable (the desired goal), whereas values of R^2 close to one indicate a large dependence on the independent variable. There are two clusters (NGC 5053 and M35) for which the R^2 values are somewhat high. These appear to have been influenced by stars at the extrema of the color ranges, but still do not rise to the level of strong statistical significance. The fits for the rest of the clusters have sufficiently low values of R^2 that the correlations are not statistically significant; Figures 2.18 and 2.19 show the distribution of metallicity estimates as a function of the estimated surface gravity ($\log g$). No significant trends are observed, supporting the conclusion of Lee et al. (2008b) that the SSPP is robust and reliable over large ranges in surface gravity (luminosity) and color, even for spectra with less-than-optimal S/N.

The SSPP-estimated temperatures and surface gravities for true member stars are plotted in Figures 2.20–2.27 over the cleaned CMDs of the likely member stars from the photometric sample that passed the s/n cut. The spectroscopic data points are plotted in different colors, in temperature steps of 500 K and $\log g$ steps of 0.5 dex. Stars at the top of the MS and on the MSTO have generally lower $\langle S/N \rangle$ than those on the RGB and HB, so the fact that some non-uniformity is observed in the distribution of T_{eff} and $\log g$ in stars near the MSTO is not unexpected.

Table ?? lists the SSPP-derived properties for all stars selected as true cluster members from each cluster, and the extinction-corrected $ugriz$ magnitudes and errors for the photometry employed are given in Table A.3. These tables contain data for the clusters in this chapter as well as the clusters included in Lee et al. (2008b), in order of increasing metallicity, thus encompassing the entire sample of clusters used in validation of the SSPP.

2.5 INDIVIDUAL CLUSTER DISCUSSION AND COMPARISON WITH PREVIOUS STUDIES

Here previous studies of these clusters are examined and how well the SSPP-derived estimates for cluster metallicity and radial velocity compare with the values reported in the literature is assessed. This section is not intended to be a comprehensive review, but rather concentrates on high-resolution spectroscopic results from studies that have been published within the past decade, expected *ab initio* to produce more accurate results than our moderate-resolution spectra. Due to the relative paucity of radial velocities for some clusters, older studies are cited where needed. The globular clusters are considered first, followed by the open clusters, ordered from low metallicity to high metallicity.

2.5.1 M92 (NGC 6341)

Two spectroscopic plug-plate observations of this cluster yielded 58 true cluster members. The estimated mean metallicity, $\langle \text{[Fe/H]} \rangle = -2.25 \pm 0.17$, is within 1σ of the values given by Harris (1996, -2.28) and Carretta et al. (2009a, -2.35). While King et al. (1998) obtained a much lower metallicity estimate from only Fe I lines of 6 subgiant stars in their sample ($\text{[Fe/H]} = -2.52$), examining the 17 subgiant member stars from this cluster in this sample reveals a mean metallicity of -2.27 , in agreement with the measured overall mean metallicity as well as with the metallicities adopted by the Harris and Carretta et al. compilations. King et al. (1998) acknowledge that their low signal-to-noise spectra and limited spectral coverage, along with the metal-poor nature of M92 and an uncertain reddening correction, resulted in a degeneracy between their estimates of T_{eff} and microturbulence that may have produced a lower value for [Fe/H]. In their analysis of literature data, Kraft & Ivans (2003) report abundances from Fe I and Fe II lines of -2.50 and -2.38 , respectively; both are lower than my result but consistent with King et al. (1998).

The SSPP-derived estimate for the radial velocity, $\langle \text{RV} \rangle = -116.5 \pm 8.7 \text{ km s}^{-1}$, is

within 1σ of that provided by Harris (1996; -120.3 km s^{-1}). A recent study by Drukier et al. (2007) reported a radial velocity of $\text{RV} = -121.2 \text{ km s}^{-1}$, based on a sample of 306 cluster members, which is also in agreement with my value.

2.5.2 NGC 5053

NGC 5053 is known to be metal-poor, but has otherwise not been widely studied. One spectroscopic plug-plate observation produced only 16 true member stars, with less than optimal coverage inside r_t (see Figure 2.1). The estimate of the mean metallicity, $\langle [\text{Fe}/\text{H}] \rangle = -2.25 \pm 0.25$, is within 1σ of that reported by Harris (1996, -2.29). The recalibration by Carretta et al. (2009a) reports a value of -2.30 , with which this study is also consistent.

The mean radial velocity, $\langle \text{RV} \rangle = +44.0 \pm 4.9 \text{ km s}^{-1}$, is identical to that given by Harris (1996, $+44.0 \text{ km s}^{-1}$).

2.5.3 M53 (NGC 5024)

M53 is located at the edge of the plug-plates for observations of NGC 5053, resulting in just 50 fibers being placed inside the tidal radius. As a result, only 19 stars were selected as true members. The measured mean metallicity, $\langle [\text{Fe}/\text{H}] \rangle = -2.03 \pm 0.13$, is in agreement with Harris (1996; -1.99) and Carretta et al. (2009; -2.06), as well as with most earlier photometric and spectroscopic abundance studies that indicated a metallicity lower than -1.8 (e.g. Pilachowski et al., 1983). More recently, a moderate-resolution spectroscopic analysis of member stars from M53 by Lane et al. (2010) provided a metallicity estimate of $\langle [\text{Fe}/\text{H}] \rangle = -1.99$, with which my result agrees nicely. Although a recent photometric study by Dékány & Kovács (2009) exhibited a discrepancy in $[\text{Fe}/\text{H}]$ between HB (variable) stars and stars on the RGB, my sample shows no statistically significant difference between the mean metallicity on the HB versus the RGB for this cluster ($\langle [\text{Fe}/\text{H}] \rangle_{\text{HB}} = -2.11 \pm 0.09$; $\langle [\text{Fe}/\text{H}] \rangle_{\text{RGB}} = -1.96 \pm 0.12$). My derived mean metallicity is within 1σ of their giant branch mean metallicity of -2.12 .

Radial velocity measurements reported in the literature for this cluster are a bit more scattered. Harris (1996) reported a value of -79.1 km s^{-1} , whereas a more recent medium-resolution spectroscopic study by Lane et al. (2009), using 180 giant stars, resulted in a mean value of -62.8 km s^{-1} . My value, $\langle \text{RV} \rangle = -59.6 \pm 7.9 \text{ km s}^{-1}$, from 19 RGB and HB stars, is consistent with the Lane et al. (2009) result.

2.5.4 M3 (NGC 5272)

One spectroscopic plug-plate observation for this cluster produced 77 true member stars. My measured value of $\langle [\text{Fe}/\text{H}] \rangle = -1.55 \pm 0.13$ is well within 1σ of that reported by Harris (1996; -1.57) and the recalibrated scale by Carretta et al. (2009; -1.50). A high-resolution spectroscopic study by Cavallo & Nagar (2000) of 6 giants at the tip of the RGB produced an estimate of $[\text{Fe}/\text{H}] = -1.54$, and an analysis of literature data performed by Kraft & Ivans (2003) yielded metallicity estimates from both Fe I and Fe II lines of -1.58 and -1.50 , respectively. Furthermore, a recent study of 23 RGB stars using high-resolution spectroscopy from the Keck telescope yielded $[\text{Fe}/\text{H}] = -1.58$ from Fe II lines (Sneden et al., 2004). Finally, while my value is only barely within 1σ of the estimated iron abundance for M3 from Cohen & Meléndez (2005), who obtained a somewhat higher value of $[\text{Fe}/\text{H}] = -1.39$ based on Keck/HIRES spectroscopy, it should be kept in mind that recent results from Cohen and collaborators adopt a temperature scale that is several hundred Kelvin warmer than most other researchers, which could easily accommodate the 0.16 dex offset with respect to their reported value of metallicity. Thus, the SSPP-derived estimate for $[\text{Fe}/\text{H}]$ is in excellent agreement with all of these previous studies, while spanning the entire length of the RGB, including stars on the HB as well.

The estimate of the cluster's mean radial velocity, $\langle \text{RV} \rangle = -141.2 \pm 5.6 \text{ km s}^{-1}$, is slightly different from those of Harris (1996) and Cohen & Meléndez (2005), who both report the same value (-147.6 km s^{-1}), and Sneden et al. (2004), who reported a mean radial velocity of -149.4 km s^{-1} . However, it is only just beyond 1σ of these values; when accounting for

the uncertainty in the literature values the difference is not significant.

2.5.5 M71 (NGC 6838)

M71 is an important cluster for validation of the SSPP, due to its intermediate metallicity ($[\text{Fe}/\text{H}] \sim -0.8$), a regime that was not represented by previously considered clusters. Unfortunately, a total of 155 fibers inside the adopted radius of 4.0 arcmin resulted in just 17 true member stars. Literature values from Harris (1996, -0.73) and a Keck/HIRES study by Boesgaard et al. (2005, -0.80) are both consistent with my value of the mean metallicity, $\langle [\text{Fe}/\text{H}] \rangle = -0.79 \pm 0.06$, at the 1σ level, as is that from Carretta et al. (2009a, -0.82). In an in-depth analysis using Keck/HIRES spectroscopy of 25 stars from the turnoff to the RHB, Ramírez et al. (2001) measured iron abundances from Fe I and Fe II lines individually, and compared them against each other for various regions of the CMD. Their values range from -0.64 to -0.86 , with an error-weighted mean of -0.71 , in agreement with my value at the 1.5σ level. Finally, Kraft & Ivans (2003) also report consistent abundances from Fe I and Fe II lines of -0.82 and -0.81 , respectively.

The mean radial velocity determination, $\langle \text{RV} \rangle = -16.9 \pm 9.3 \text{ km s}^{-1}$, is within 1σ of that reported by Harris (1996, -22.8 km s^{-1}). Keck/HIRES data from Cohen et al. (2001) produced a mean radial velocity of -21.7 km s^{-1} , which is also consistent with my observation.

2.5.6 NGC 2158

A total of 109 fibers located inside the adopted radius for this open cluster (6.0 arcmin) resulted in a relatively high yield of 62 true member stars. With this sample, a mean metallicity of $\langle [\text{Fe}/\text{H}] \rangle = -0.26 \pm 0.08$ was measured. While this is in agreement with the values from Dias et al. (2002, -0.25), a high-resolution spectroscopic study of one giant star by Jacobson et al. (2009) produced a nearly solar mean metallicity of -0.03 ± 0.14 . However, a more recent follow-up study using WIYN Hydra spectroscopy at $R \sim 21,000$ for

15 stars in NGC 2158 produced a metallicity of $[\text{Fe}/\text{H}] = -0.28 \pm 0.05$ (H. Jacobson et al. 2011, in preparation), a value that is consistent not only with prior studies of this cluster, but with my study as well.

Using moderate-resolution spectroscopy, Scott et al. (1995) reported a mean radial velocity for NGC 2158 of $+28.1 \text{ km s}^{-1}$. This and the value reported by Dias et al. (2002) of $+28.0$ are both consistent with my measurement of $+27.8 \pm 5.9 \text{ km s}^{-1}$.

2.5.7 M35 (NGC 2168)

This open cluster is located at the edge of the plug-plates from the spectroscopic observations and was not heavily targeted with fibers. As a result, only 72 fibers were located inside the adopted radius, yielding 29 true members. The adopted radius is less than the tidal radius due to its proximity to NGC 2158. The field region of NGC 2158 does overlap with the tidal radius of M35, but this was not problematic for several reasons. First, stars included in a field region were never considered for membership so no M35 stars would have been picked up and included in NGC 2158 as potential members. Secondly, the rather different radial velocities of the two clusters would have ensured that even if some NGC 2158 stars were considered for membership in M35, they would have been dropped during the RV cut, if not previously. Finally, due to their differing positions on the CMD, any potential M35 stars included in the field region of NGC 2158 would only have served to reduce the s/n in those sub-grid boxes on the CMD of the cluster region of NGC 2158. These being sufficiently far from the main locus, this would not cause any complications to the member selection for NGC 2158.

The measured mean metallicity for this cluster, $\langle [\text{Fe}/\text{H}] \rangle = -0.20 \pm 0.18$, is consistent with that from Dias et al. (2002, -0.16), as well as with the study of Barrado y Navascués et al. (2001), who obtained $\langle [\text{Fe}/\text{H}] \rangle = -0.21$ from a high-resolution spectroscopic analysis of 39 probable cluster members.

Barrado y Navascués et al. (2001) measured a mean radial velocity from their sample of

$\langle RV \rangle = -8.0 \text{ km s}^{-1}$, a value consistent with my observation ($-5.0 \pm 6.2 \text{ km s}^{-1}$). While my value of $\langle RV \rangle$ is slightly higher, compared to both their sample and the value from Dias et al. (2002, -8.2), it is still within 1σ , and therefore can be considered reliable. A more recent study by Geller et al. (2010) produced a radial velocity of $\langle RV \rangle = -8.16 \text{ km s}^{-1}$ based on high-resolution spectroscopy.

2.5.8 NGC 6791

NGC 6791 is another important cluster for this validation exercise because it explores the super-solar metallicity region. This is another regime that was not considered with previously observed clusters; it is the most metal-rich cluster (to date) for which I was able to obtain successful spectroscopic reductions. There were two spectroscopic plug-plate observations for the region surrounding this cluster, which yielded a total of 90 true members. While the mean metallicity estimate, $\langle [\text{Fe}/\text{H}] \rangle = +0.31 \pm 0.13$, is statistically consistent with that given by Dias et al. (2002, $+0.11$) at the 2σ level, their reported value is significantly lower than that reported by other studies. It is known that NGC 6791 is a metal-rich open cluster, with some estimates from high-resolution spectroscopy as high as $+0.47$ (Gratton et al., 2006). A study of 24 giant stars with medium-resolution spectroscopy yielded a metallicity estimate of $[\text{Fe}/\text{H}] = +0.32$ (Worthey & Jowett, 2003), while Origlia et al. (2006) used medium-high resolution Keck/NIRSPEC spectroscopy to obtain an iron abundance of $+0.35$. Most recently, a high-resolution spectroscopic study of two MSTO stars by Boesgaard et al. (2009) yielded a value of $[\text{Fe}/\text{H}] = +0.30$. It is clear that my estimate is in better agreement with these recent high-resolution observations.

The measured value of the mean radial velocity, $\langle RV \rangle = -47.0 \pm 6.0 \text{ km s}^{-1}$, is consistent with that reported by Dias et al. (2002, -57 km s^{-1}) at the 1.5σ level, as well as with that found by Origlia et al. (2006, -52 km s^{-1}).

2.6 SUMMARY

Spectroscopic and photometric data from SDSS-I and SDSS-II/SEGUE were used to determine mean metallicities and radial velocities for five Galactic GCs, M92, NGC 5053, M53, M3, and M71, as well as for three OCs, NGC 2158, M35, and NGC 6791. The data were run through the current version of the SSPP and true member stars were selected from each cluster. The derived $\langle \text{[Fe/H]} \rangle$ and $\langle \text{RV} \rangle$ for the true members were then compared to the cluster properties reported in the literature.

The mean values of $[\text{Fe}/\text{H}]$ and RV for each cluster from the SSPP are in good agreement with those values reported in previous studies. Nearly all of the SSPP estimates are within 1σ of the adopted literature values, with nearly all exceptions falling within 2σ . The mean internal uncertainties of the SSPP-determined metallicities and radial velocities for true members in this sample are $\sigma_{[\text{Fe}/\text{H}]} = 0.05$ dex and $\sigma_{\text{RV}} = 3.0 \text{ km s}^{-1}$, respectively, while the scatter about the mean residuals compared to the adopted literature values are $\sigma_{[\text{Fe}/\text{H}]} = 0.11$ dex and $\sigma_{\text{RV}} = 5.2 \text{ km s}^{-1}$, demonstrating good internal and external consistency, and indicating that estimates of the atmospheric parameters and radial velocities for SDSS/SEGUE stellar data are sufficiently accurate for use in studies of the chemical compositions and kinematics of stellar populations in the Galaxy.

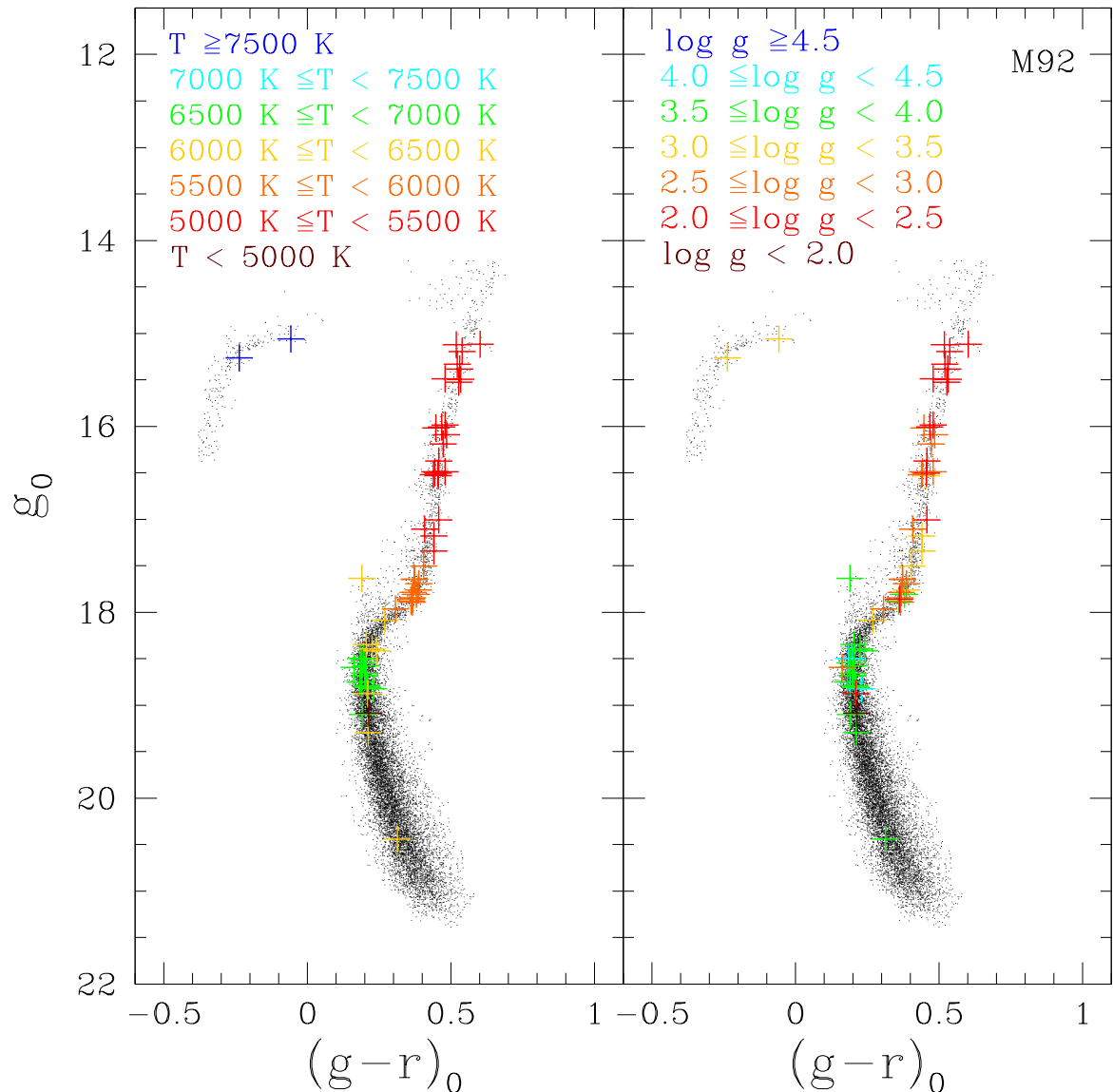


Figure 2.20 Color-Magnitude Diagram of the selected true member stars of M92. The left-hand panel shows the distribution of effective temperatures, while the right-hand panel shows the distribution of surface gravity, both based on the spectroscopic sample. The black dots are the likely member stars from the photometric sample. Each color represents a temperature step of width 500 K and a $\log g$ step of 0.5 dex, respectively.

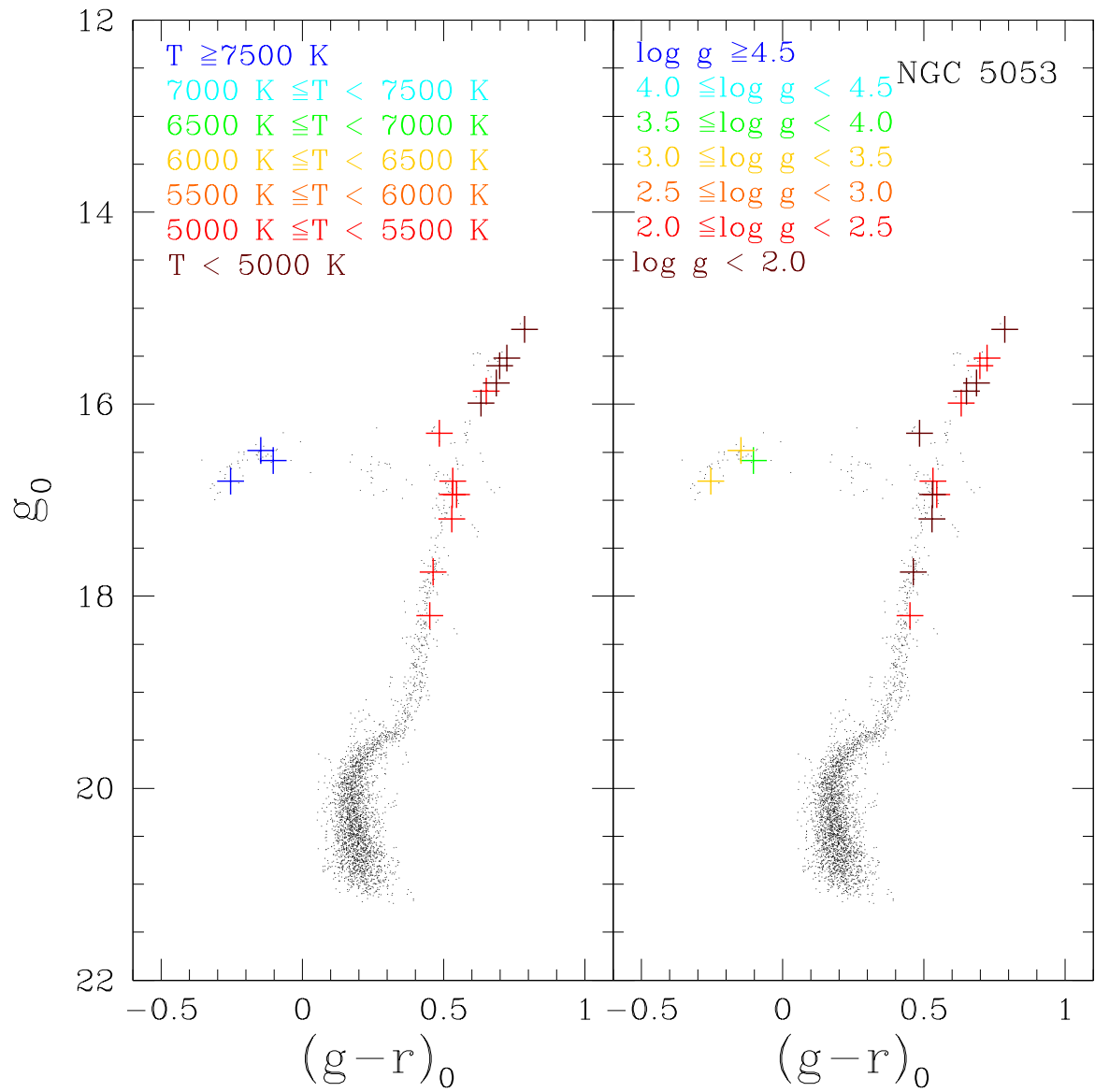


Figure 2.21 Same as Fig. 2.20, but for NGC 5053.

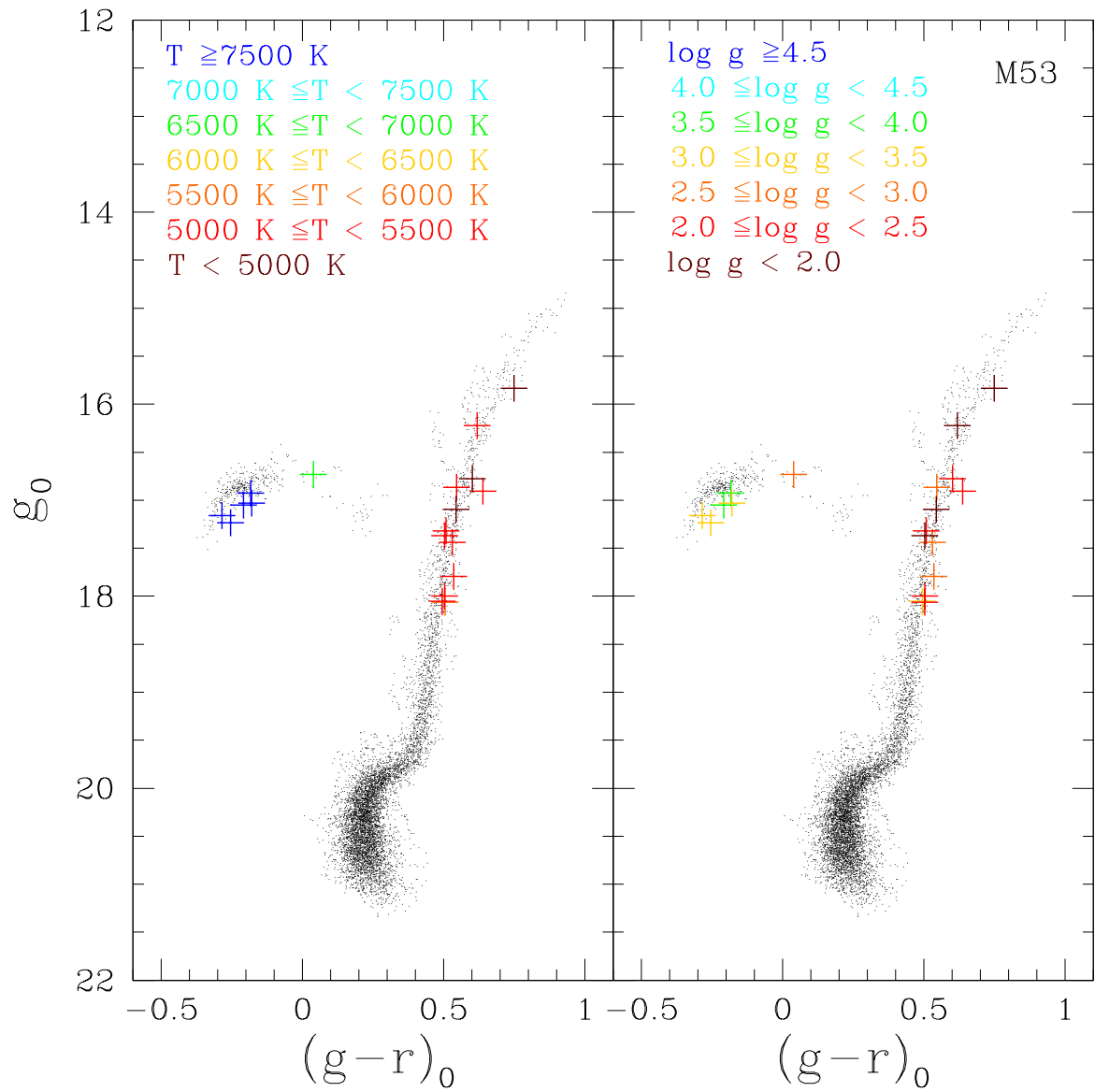


Figure 2.22 Same as Fig. 2.20, but for M53.

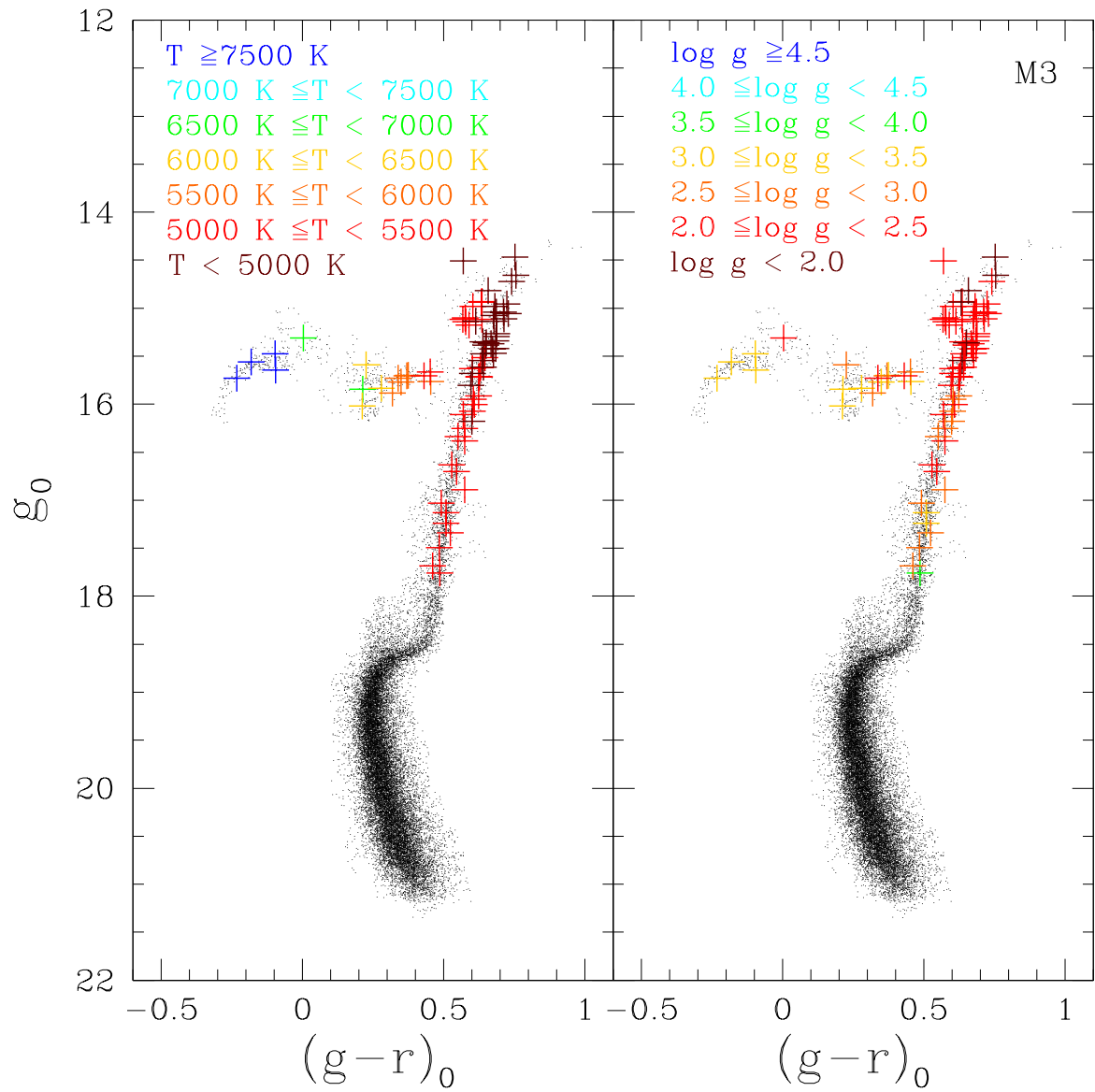


Figure 2.23 Same as Fig. 2.20, but for M3.

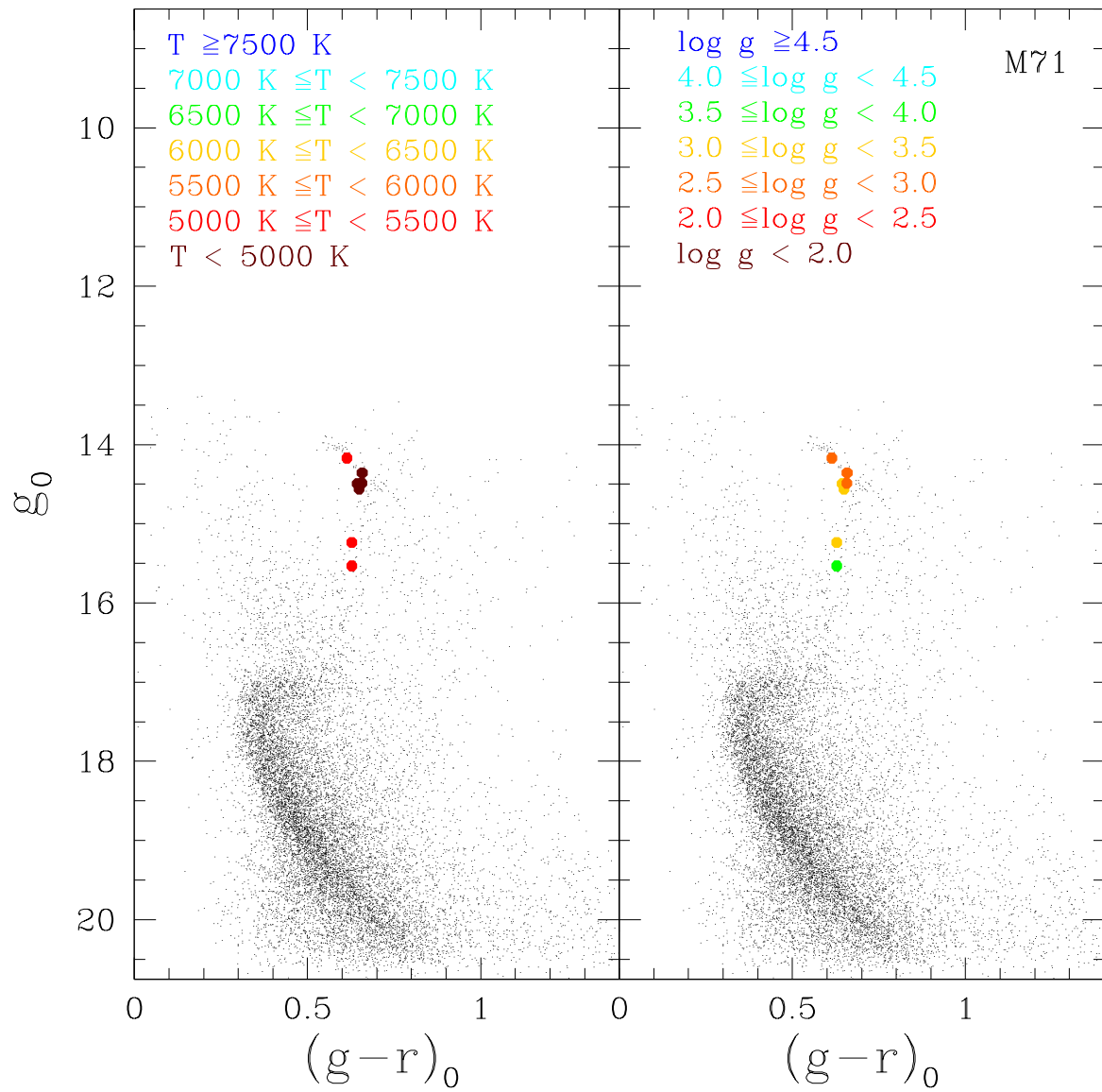


Figure 2.24 Same as Fig. 2.20, but for M71.

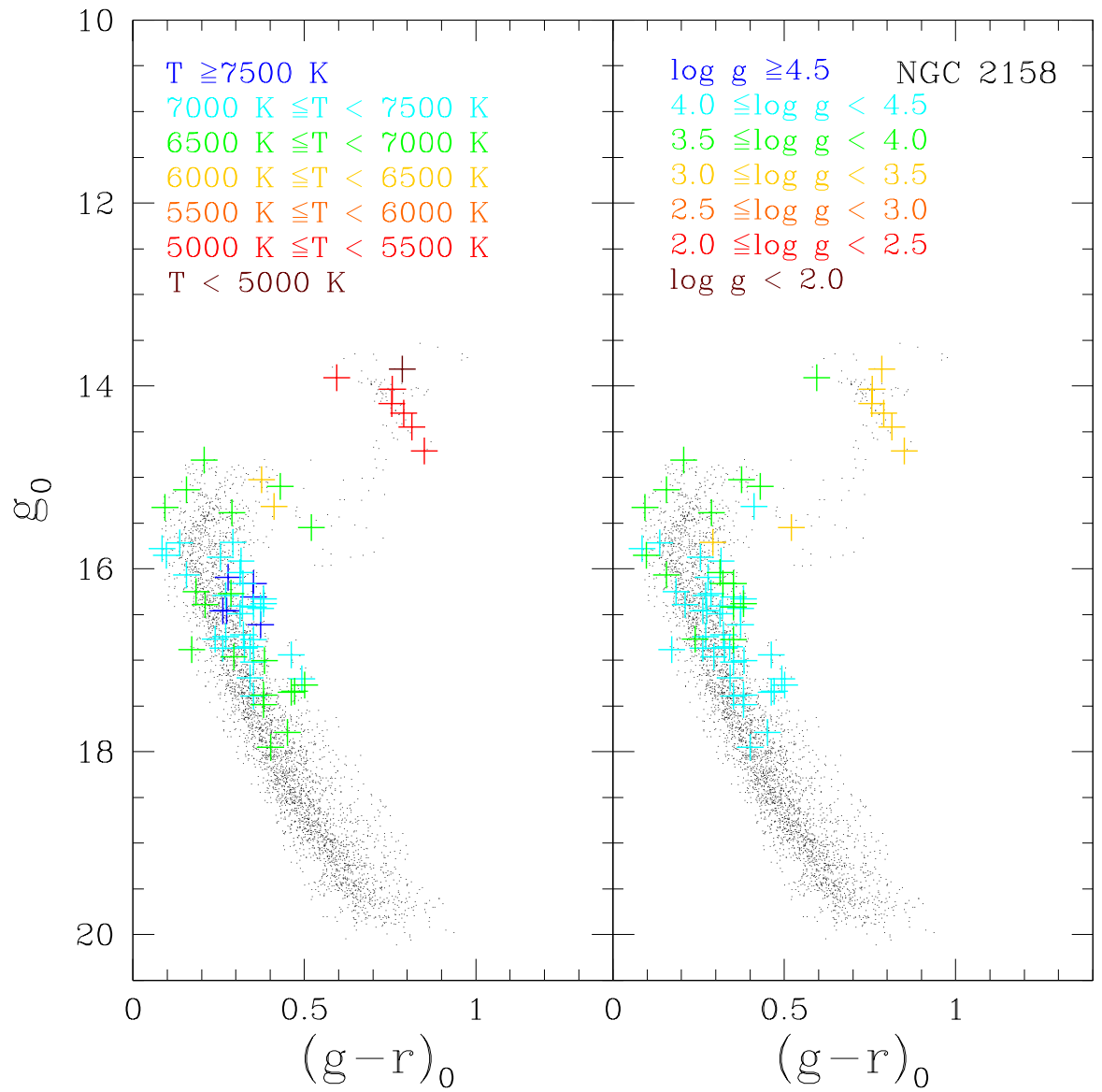


Figure 2.25 Same as Fig. 2.20, but for NGC 2158.

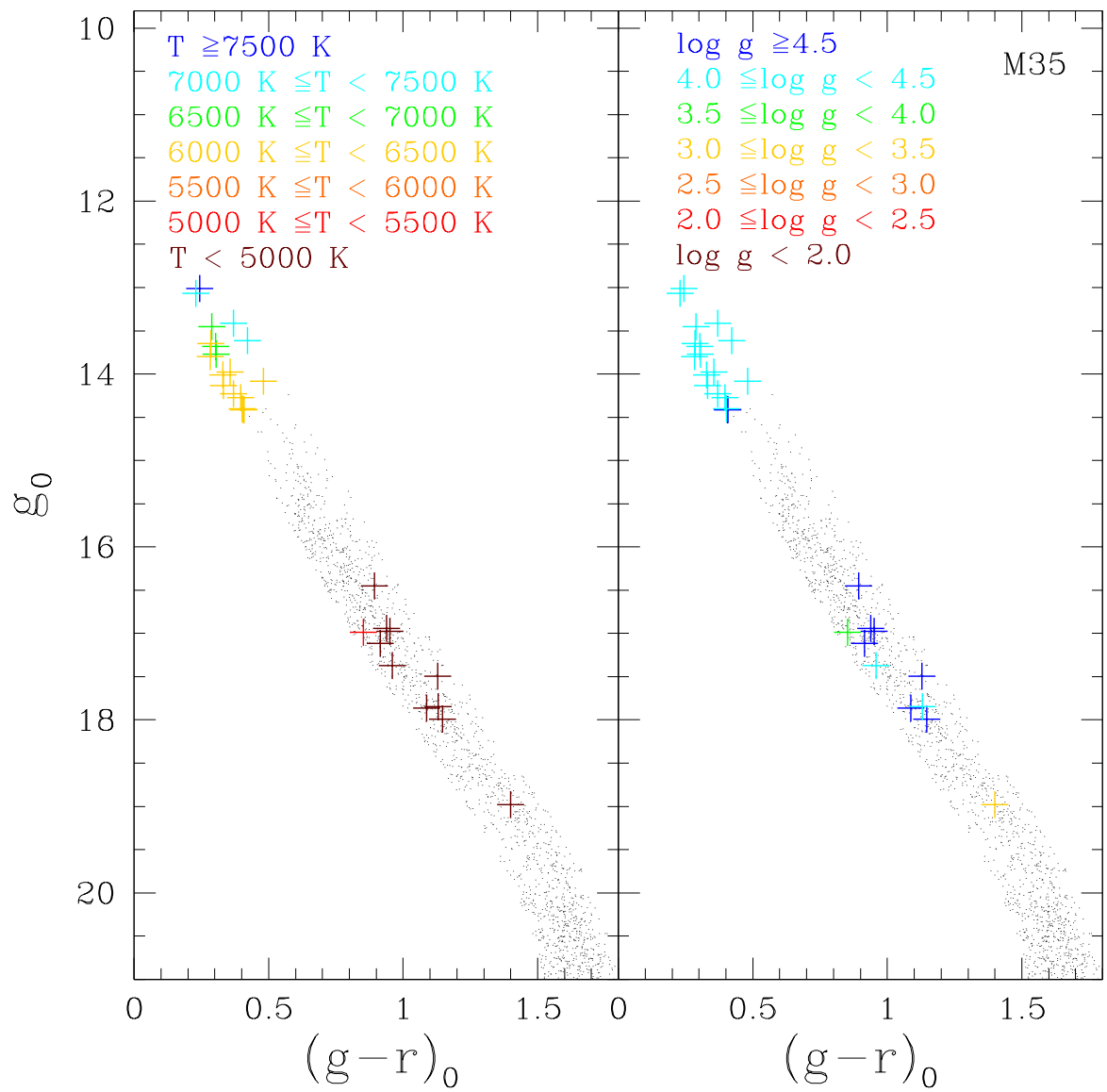


Figure 2.26 Same as Fig. 2.20, but for M35.

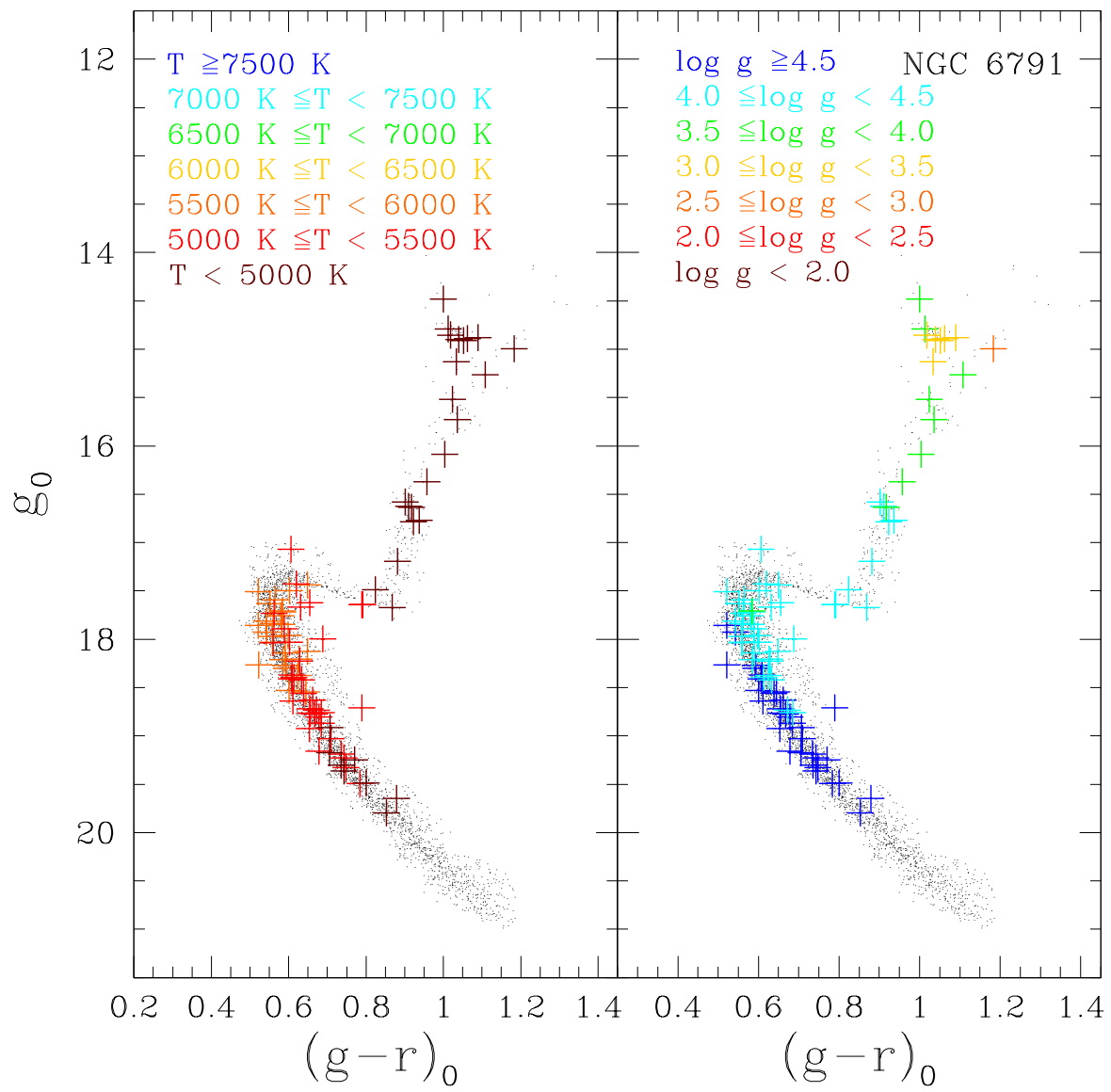


Figure 2.27 Same as Fig. 2.20, but for NGC 6791.

CHAPTER 3:

CN AND CH ABSORPTION

BANDSTRENGTHS IN SDSS

GLOBULAR CLUSTERS

3.1 INTRODUCTION

In this chapter, photometric and spectroscopic data from the member stars of GCs selected in Chapter 2 and in Lee et al. (2008b) are used to examine the CN and CH bandstrength distributions for stars in eight GCs, including stars from the upper RGB to, in some cases, 1–2 magnitudes below the main sequence turnoff (MSTO). I show that there exists a clear bimodal distribution in CN bandstrengths for clusters with $[Fe/H] \geq -2.0$. Other interesting CN bandstrength variations are suggested to exist among the three clusters in this sample with $[Fe/H] < -2.1$.

This chapter is organized as follows. Section 3.2 briefly reviews the sample. In Section 3.3 the adopted CN and CH indices are defined for stars in various stages of evolution. The derived CN and CH distributions are then compared in Section 3.4. In Section 3.5 any correlations between these distributions with the global cluster parameters are sought. Finally, the results and implications are discussed in Section 3.6.

3.2 OBSERVATIONAL DATA

Tables 2.1 – 2.3 list the photometric, spectroscopic, and physical properties of the eight GCs in this sample. The SSPP produces estimates of T_{eff} , $\log g$, [Fe/H], and radial velocities (RVs), along with the equivalent widths and/or line indices for 85 atomic and molecular absorption lines, by processing the calibrated spectra generated by the standard SDSS spectroscopic reduction pipeline (Stoughton et al., 2002). See Lee et al. (2008a) for a detailed discussion of the approaches used by the SSPP; Smolinski et al. (2011a) provides details on the most recent updates to this pipeline, along with additional validations.

Membership selection for the clusters was based on the color-magnitude diagram (CMD) mask algorithm described by Grillmair et al. (1995). Details on the application of this method to these specific clusters are described by Lee et al. (2008b) and Smolinski et al. (2011a), and will only be briefly summarized here. The procedure involved a series of cuts, reducing the overall sample to include only those stars for which one can reasonably claim true membership. First, all stars within the tidal radius of the GC were selected. Stars with available spectra but with $\langle \text{S/N} \rangle < 10$ (averaged over the entire spectrum), or that lacked estimates of [Fe/H] or RV, were excluded. A CMD was then constructed of the remaining stars, along with a CMD of stars in a concentric annulus designated to represent the field. A measure of the effective signal-to-noise in regions of the CMD was obtained, where the “signal” in this case constituted those stars within the tidal radius and the “noise” constituted those stars within the field region. Cluster-region stars within segments of the CMD above a threshold signal-to-noise were then selected. Finally, Gaussian fits to the highest peaks in the [Fe/H] and RV distributions of those stars (expected to represent the cluster) were obtained, and stars within 2σ of the mean in both [Fe/H] and RV were considered true member stars. This procedure resulted in the following numbers of true member stars: M92 (58), M15 (98), NGC 5053 (16), M53 (19), M2 (71), M13 (293), M3 (77), and M71 (8). Figures 3.1 and 3.2 show the final CMDs for these eight globular clusters.

Membership selection for M71 was complicated due to difficulties encountered with the

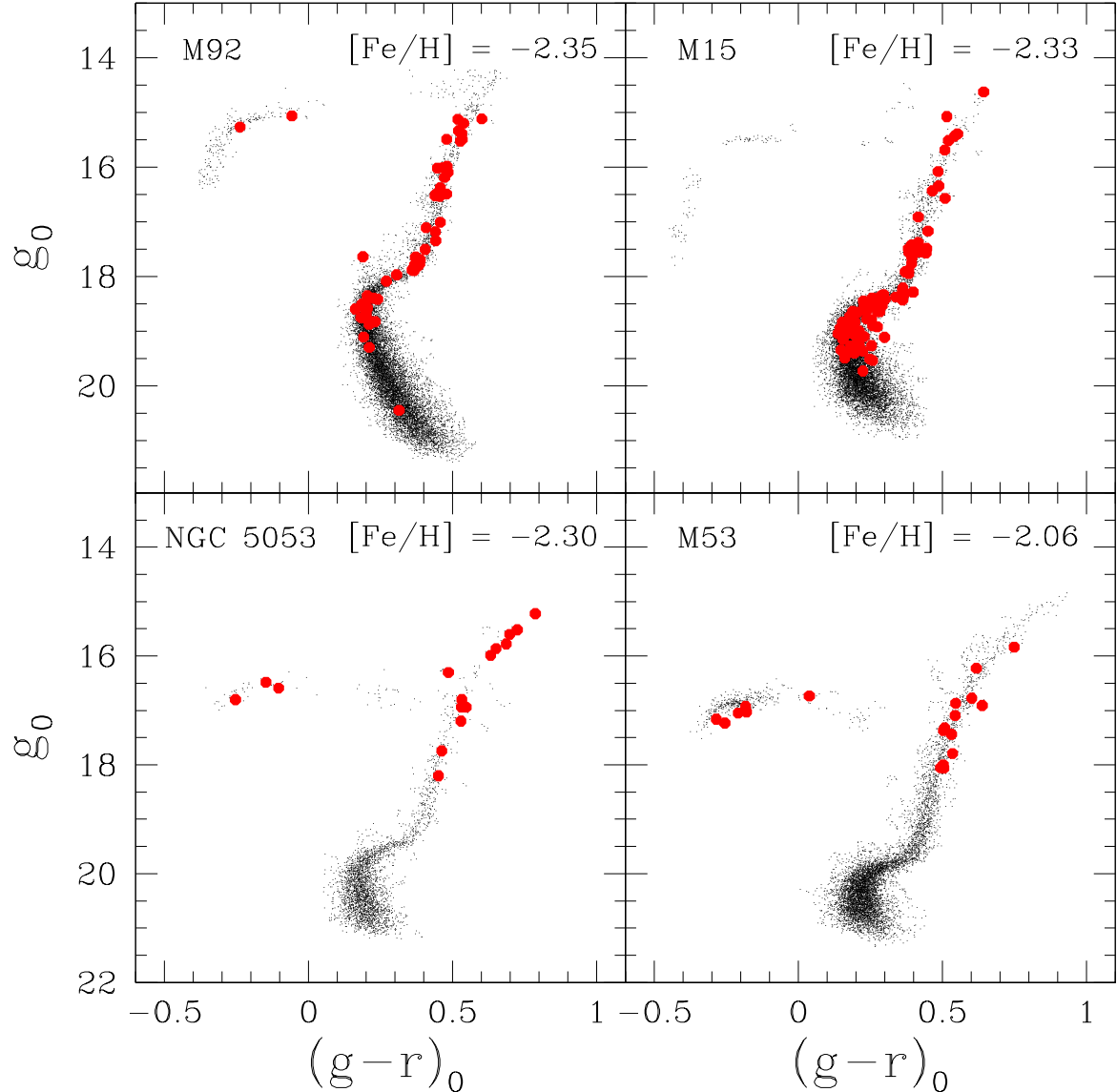


Figure 3.1 Color-magnitude diagrams for the four globular clusters in our sample with $[\text{Fe}/\text{H}] < -2.0$: M92, M15, NGC 5053, and M53. The black points represent photometric data for likely cluster members that passed the tidal radius and CMD mask algorithm cuts. The red points correspond to spectroscopic data for the selected true cluster members.

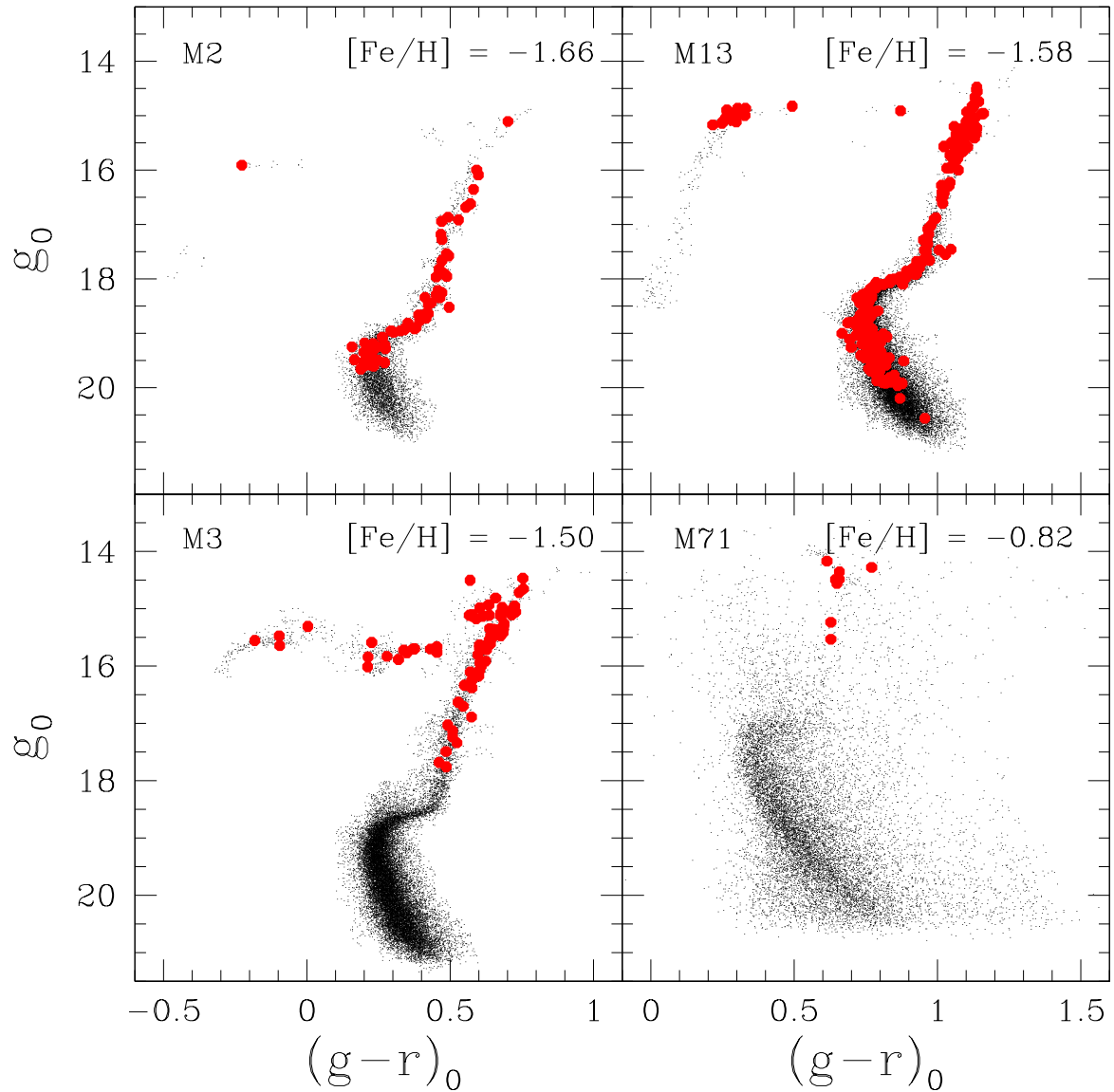


Figure 3.2 Same as Figure 3.1, but for the four globular clusters in this sample with $[Fe/H] > -2.0$: M2, M13, M3, and M71. Membership selection for M71 was slightly different, as described in Section 3.2, thus more photometric data is present in the CMD for this cluster. The black points for this cluster do not all represent likely cluster members.

photometry values available for this cluster at the time of this analysis (see An et al., 2008; Smolinski et al., 2011a). This made the CMD mask algorithm less reliable for selecting likely spectroscopic members. Therefore, stars inside the tidal radius were selected and passed on to the final [Fe/H] and RV cuts, with those stars that had questionable photometry excluded from consideration. As a result, only eight stars with available spectroscopy made it through the final cut for this cluster.

3.3 CN BANDSTRENGTH DISTRIBUTION

A common approach for investigation of the star-to-star light element abundance variations within GCs is measurement of the 3883 Å CN molecular absorption band (Norris & Freeman, 1979; Norris et al., 1981; Smith et al., 1996; Harbeck et al., 2003a,b; Pancino et al., 2010). This measurement does not require high-resolution spectroscopy, making it ideal for low-resolution spectroscopic surveys such as SDSS. The feature is typically measured using a spectral index defined as the magnitude difference between the integrated flux within a wavelength window containing the absorption band and the integrated flux within a sideband representing the continuum. However, the precise definition of this spectral index often varies according to the luminosity class of the stars under consideration due to the presence of other temperature-dependent absorption lines, such as H_ζ at 3889 Å, that can potentially interfere with the adopted continuum window. In this section, I describe the CN spectral indices used for each region of the CMD and their observed distributions.

3.3.1 CN ABSORPTION ON THE RED GIANT BRANCH

I measured the strength of the CN absorption band at 3883 Å in RGB stars using the spectral index S(3839) defined by Norris et al. (1981):

$$S(3839)_N = -2.5 \log \frac{\int_{3846}^{3883} I_\lambda d\lambda}{\int_{3916}^{3883} I_\lambda d\lambda}, \quad (3.1)$$

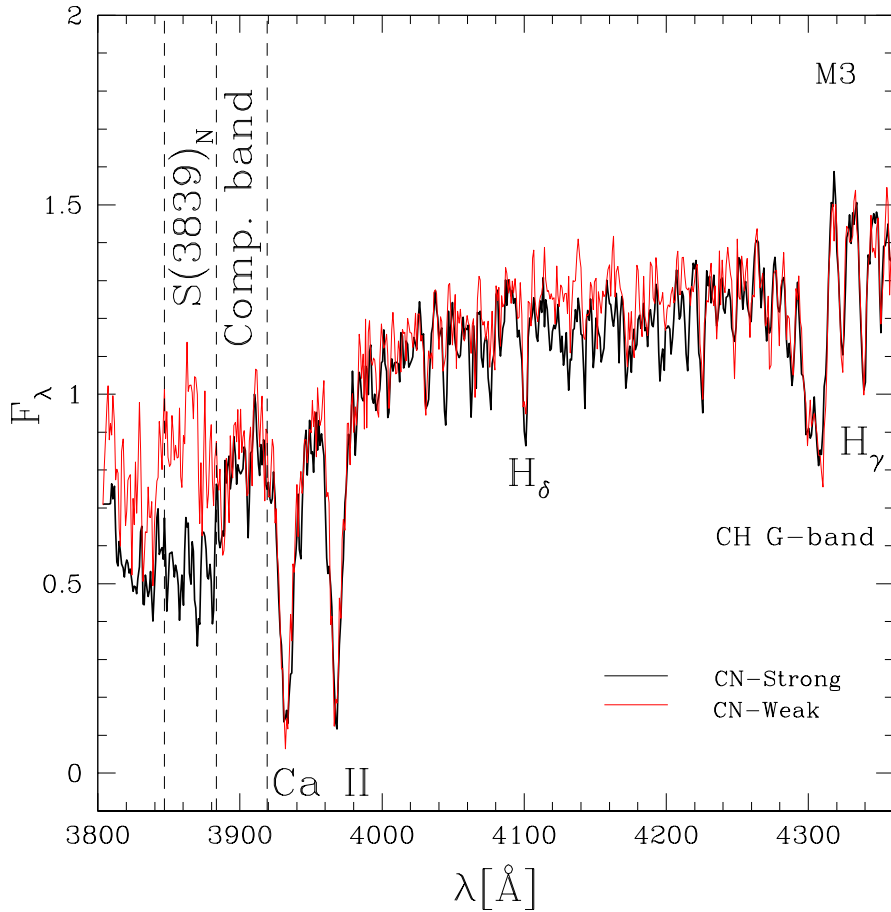


Figure 3.3 Representative blue SDSS spectra of CN-weak (red thin line; fiber 2475-53845-160) and CN-strong (black thick line; fiber 2475-53845-489) RGB stars in M3. The areas between the dashed vertical lines indicate the portions of the spectrum used in measuring $S(3839)_N$. Other prominent spectral features are labeled.

where I_λ is the measured intensity, and the subscript N indicates it is from the Norris et al. (1981) definition. Figure 3.3 shows the blue regions of SDSS spectra for two RGB stars in M3. The line-band and comparison-band windows are indicated. These two stars were selected because they have similar effective temperatures and apparent g -band magnitudes (indicating similar luminosities on the RGB), as well as nearly identical Ca II and CH G-band strengths (indicating similar metallicities and carbonicities). Despite these similarities, they exhibit clear differences in their CN 3883 Å absorption strengths.

The formation efficiency of the CN molecule is temperature dependent, where cooler

effective temperatures allow increased molecular formation. When one looks at a population of stars, one therefore sees an increased ability for molecular formation moving up the RGB. While the majority of MS stars (aside from the coolest ones) have effective temperatures too high for significant molecular formation, the ability for this molecule to form on the SGB and RGB increases with luminosity as the star expands and its surface temperature drops. As a result, one expects to see increased CN absorption on the RGB when compared to the SGB, and this effect must be accounted for in the analysis prior to inferring any abundance differences. Furthermore, for clusters of moderate metallicity, when the CN absorption strengths are plotted as a function of luminosity or temperature, two groups generally appear – one CN-weak (sometimes referred to as CN-normal), the other CN-strong (enriched). A linear relationship is then fit to the CN-weak locus, and the vertical difference in $S(3839)_N$ between each point and the baseline is measured, as illustrated for M3 in the bottom-left panel of Figure 3.4. This vertical difference is denoted as $\delta S(3839)_N$, and is taken to be a temperature-corrected measure of CN absorption. The other panels in this figure are generalized histograms of this temperature-corrected index for this sample of clusters, discussed in detail below. The raw and corrected values are listed for each cluster in Table ??.

The slope of the relationship between CN bandstrength and luminosity is metallicity dependent, so each cluster must be corrected individually prior to constructing comparisons across the sample. Figure 3.5 shows this relationship between the CN slope and $[Fe/H]$, obtained by dividing the entire sample into 0.1-dex wide metallicity bins and fitting a line to the CN-weak locus of each metallicity bin (as opposed to fitting to the blue data points, which represent stars identified as CN-weak *within their individual clusters*). Note the trend of decreasing CN slope with decreasing $[Fe/H]$, which is similar to the trend for field giants from DR7 reported by Martell & Grebel (2010). When the slope of each panel in their Figure 6 is plotted as a function of metallicity, one obtains a linear relationship for field giants:

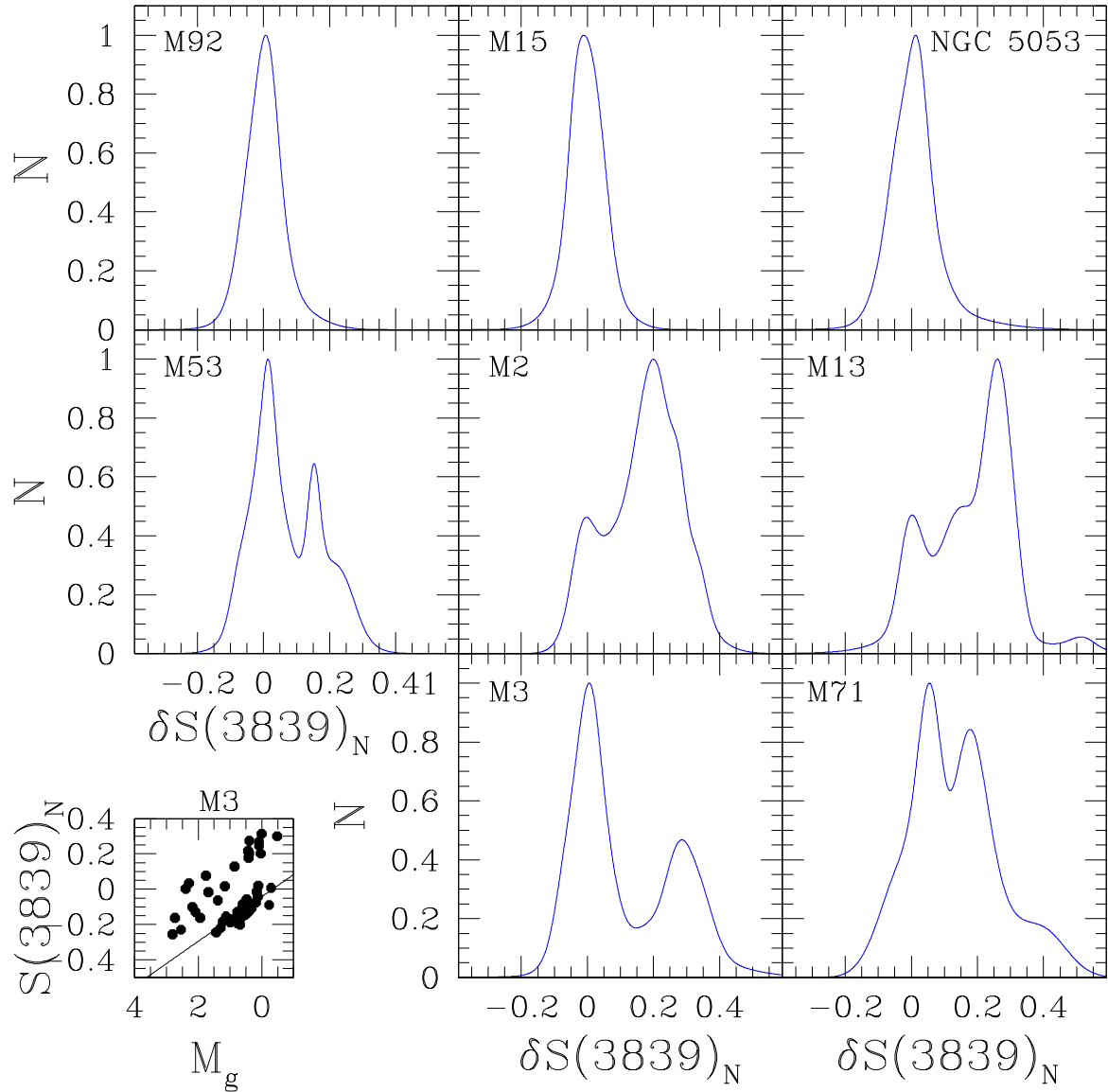


Figure 3.4 Generalized histograms of the $\delta S(3839)_N$ distributions of RGB stars within each globular cluster. The bottom-left panel shows an example of the way $\delta S(3839)_N$ was determined, as described in Section 3.3, where the baseline against which $\delta S(3839)_N$ was measured is shown as a solid line.

$$\text{CN Slope}_{\text{field}} = -0.17 - 0.08[\text{Fe}/\text{H}]. \quad (3.2)$$

The expression obtained for this sample of cluster RGB stars is:

$$\text{CN Slope}_{\text{cluster}} = -0.18 - 0.07[\text{Fe}/\text{H}], \quad (3.3)$$

and is statistically equivalent to the field giant relationship ($\sigma_{\text{slope}} = 0.04$, $\sigma_{\text{intercept}} = 0.07$). The data point corresponding to $[\text{Fe}/\text{H}] = -1.40$ has been omitted from this linear fit as an outlier.

It is difficult to draw a direct comparison between the two samples due to their differing mass functions. The cluster giants are all exclusively old and span a relatively small range in mass at any given value of M_g , whereas the field giants from the Martell & Grebel (2010) sample potentially span a much broader range of mass and age.¹ Similarities between these relationships may hint at a common origin (see Martell & Grebel, 2010, for further discussion).

Figure 3.6 shows the distribution of $\delta S(3839)_N$ as a function of absolute g -magnitude. Values for both RGB and SGB stars are shown, calculated using the CN index definition of Norris et al. (1981). Blue triangles represent SGB stars, while red circles represent RGB stars, with filled and open symbols indicating CN-strong and CN-weak stars, respectively. While a small amount of scatter exists for the most metal-poor clusters (M92, M15, and NGC 5053), no separation that would indicate a bimodal distribution is obvious, consistent with Figure 3.4. For the remaining five clusters at higher metallicity, starting with M53 at a metallicity of $[\text{Fe}/\text{H}] = -2.06$, two distinct populations of stars in $\delta S(3839)_N$ -space are apparent.

¹Figure 6 in Martell & Grebel (2010) plots CN versus absolute M_r , whereas I use absolute M_g . Because these are all RGB stars with the same $(g - r)_0 \sim 0.5$, converting M_r to M_g should only produce an essentially uniform shift of all stars in each plot, not affecting the slopes significantly.

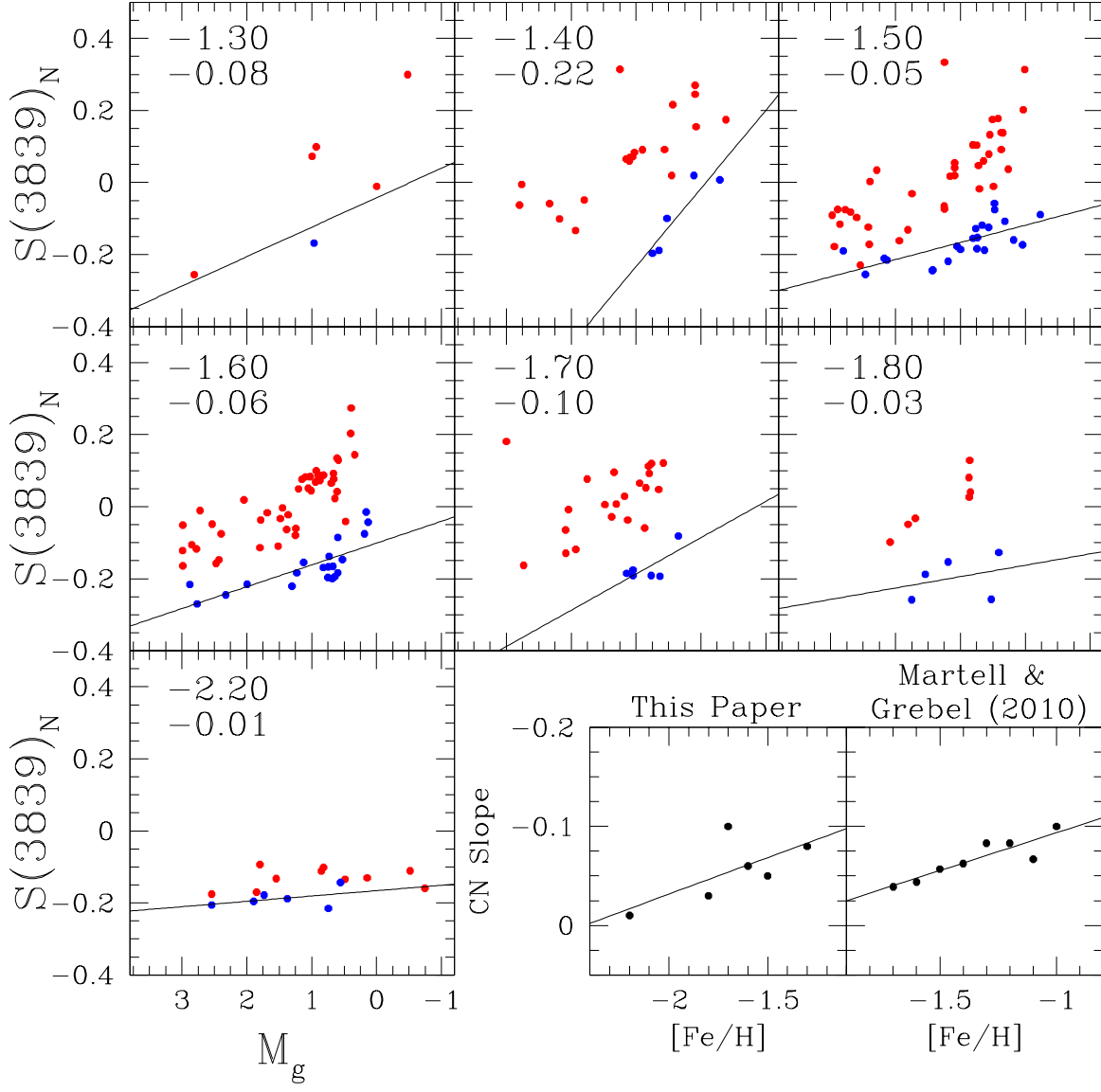


Figure 3.5 Raw $S(3839)_N$ values versus absolute g -magnitude for seven 0.1-dex-wide metallicity bins for the cluster RGB stars in this sample. The top number in the upper-left corner of each panel indicates the maximum metallicity for each bin, while the bottom number indicates the slope of the fit to the stars that appeared to be CN-weak within each $[\text{Fe}/\text{H}]$ bin (as opposed to the blue data points only, which were identified as CN-weak stars *within each cluster*). Red points indicate stars that were identified as CN-strong within their respective clusters.

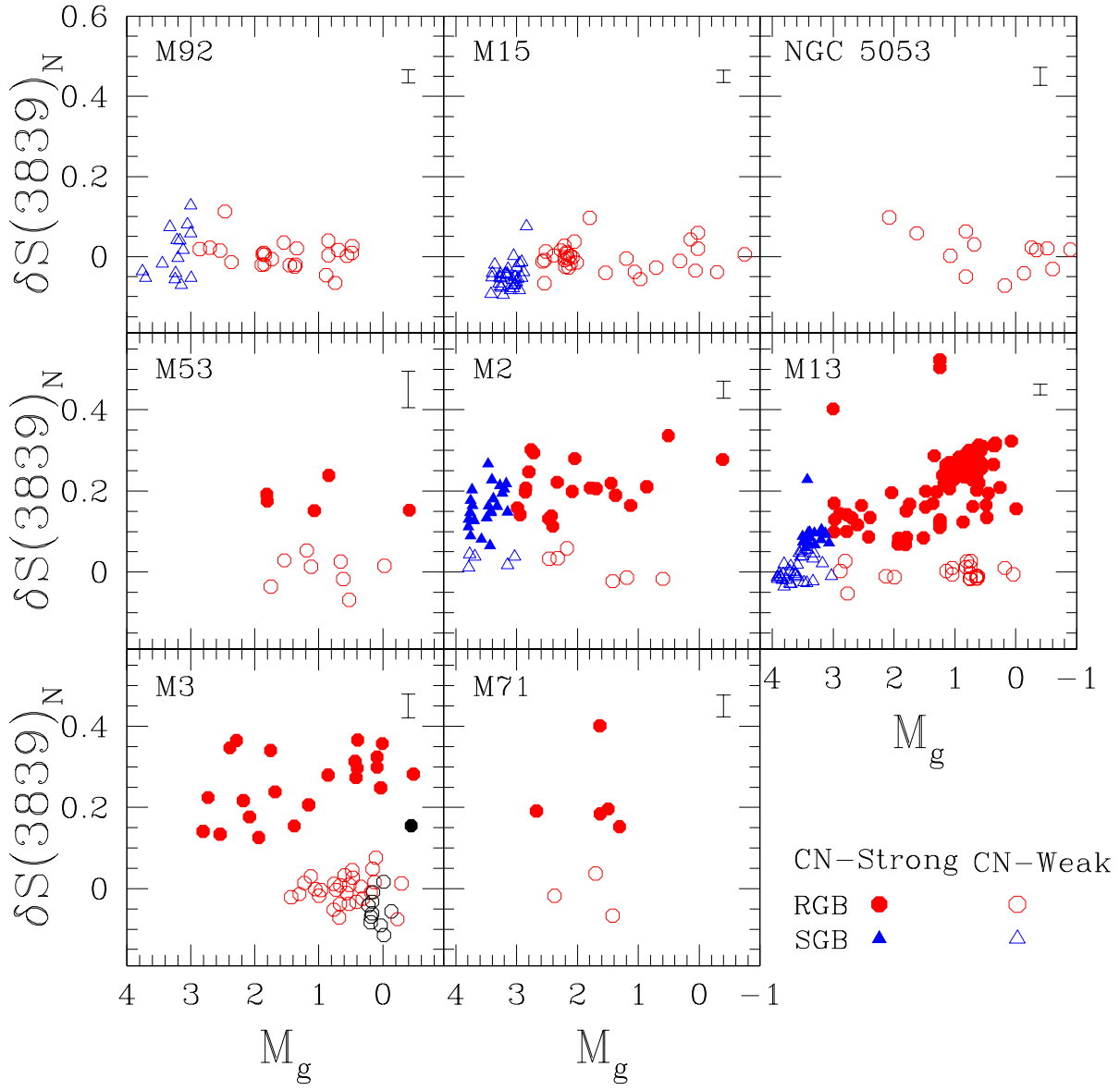


Figure 3.6 The distributions of $\delta S(3839)_N$ as a function of absolute g -magnitude for RGB and SGB stars, using the CN index definition from Norris et al. (1981). Blue triangles represent SGB stars and red circles indicate RGB stars. CN strong stars are shown using filled symbols, while the open symbols represent CN weak stars. The black points in M3 are AGB stars. Typical uncertainties are indicated by the vertical line in the upper right corner. Clusters are arranged in order of increasing [Fe/H].

For M3, a small number of possible AGB stars are noted in the figure with black symbols. The majority of these stars appear CN-weak, with only one CN-strong AGB star. This result is similar to the observations reported by Campbell et al. (2010), who found that, in a sample of nine Galactic GCs, all showed either a total lack of CN-strong AGB stars or a significant depletion of CN-strong AGB stars compared to those present on the RGB. These authors noted that no current explanation exists in standard stellar evolution theory as to why stars on the AGB should have reduced CN abundances compared to the RGB, particularly because the low effective temperatures should be suitable for similarly efficient molecular CN formation. In principle, increased mixing both on the RGB and at the beginning of AGB ascent should contribute more N (and thus stronger CN) to the stellar envelope, which should be apparent in surface abundance measurements. Such a discrepancy has been noted for a long time; two possible explanations were proposed by Norris et al. (1981). First, if two chemically distinct populations in the cluster existed after star formation ceased, one of which was helium-rich and evolved to populate the blue end of the horizontal branch (HB), but never ascended to the AGB, this might lead to the deficiency of CN-strong stars. The second explanation hypothesized that increased mixing in some stars produced increased CN abundances, but also led to increased mass loss at the RGB tip, producing stars populating the blue end of the HB that never ascended the AGB. The problem remains unsolved, and requires additional work.

Adopting the corrected values obtained from the above procedure, we produced a generalized histogram of the $\delta S(3839)_N$ distribution for each cluster, shown in Figure 3.4. This was accomplished by representing each point as a Gaussian, centered on $\delta S(3839)_N$ with a FWHM equal to the uncertainty of that particular $\delta S(3839)_N$ measurement, and then adding the individual Gaussians together. The uncertainty for each $S(3839)_N$ measurement was determined as in Martell & Grebel (2010), using a Monte Carlo approach. Each pixel in the error vector produced by the SDSS spectroscopic reduction pipeline was multiplied by a factor between 0 and 1, drawn from a normalized distribution. This new vector was then

added to the data vector and the indices were remeasured. This process was repeated 100 times and the standard deviation was taken to be the uncertainty. Naturally, the resultant uncertainties are related to the S/N of the spectra; uncertainties for the high-S/N spectra were much lower than the typical uncertainties found in the literature. For this reason, recent studies have sometimes smoothed their histograms to make them more directly comparable to past studies. Smoothing the histogram also helps eliminate any artificial substructure in the distribution created by small number statistics, while additionally accounting for unidentified sources of uncertainty.

In Figure 3.4, the clusters are arranged in order of increasing metallicity, from left to right, top to bottom, and represent the $\delta S(3839)_N$ distribution on the RGB for each cluster. Many of these clusters have been studied previously, so comparisons can be made with the present observations. Suntzeff (1981) reported a bimodal distribution in CN indices in M3 and M13 on the upper RGB (stars more luminous than the HB). This observation for M3 was confirmed on the upper RGB by Smith et al. (1996) and Lee (1999), and on the lower RGB of M3 by Norris & Smith (1984). Smith et al. (1996) also report CN bimodality among M13 RGB stars, and the proportions of CN-strong stars I observe in these two clusters agree well with those reported by Suntzeff (1981). M2 was studied by Smith & Mateo (1990) and shown to have a bimodal CN distribution, also matching in proportion to that seen in this sample.

Studies of M71 by Smith & Norris (1982), Lee (2005), and Alves-Brito et al. (2008) all report CN bimodality on the RGB. Evidence for bimodality is found in my data as well, at the same level as observed for 47 Tuc (Norris & Freeman, 1979), which is of comparable metallicity to M71. It is interesting that Alves-Brito et al. (2008) have claimed the existence of CN-strong AGB stars in their sample. As mentioned above, nearly all CN observations of AGB stars have demonstrated a depletion in CN, which makes their observation unique. It is possible that M71 is so metal-rich compared to other GCs studied to date that this encourages additional CN enrichment on the AGB, in spite of whatever mechanism might

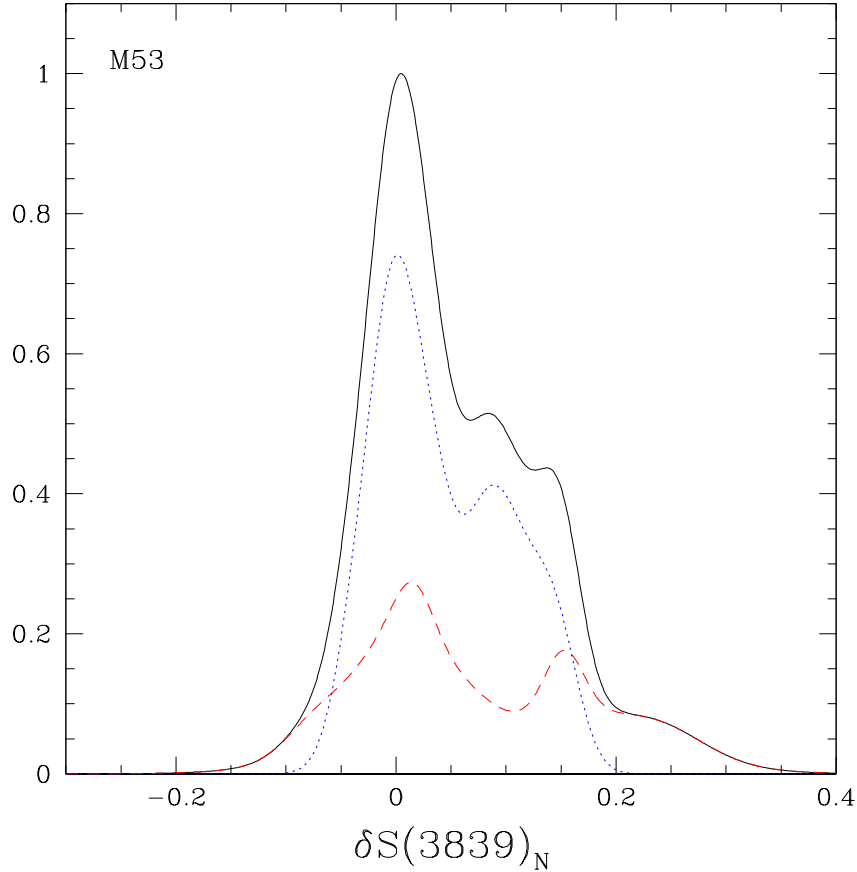


Figure 3.7 Generalized histogram for the combined (solid black line) $\delta S(3839)_N$ data sets for RGB stars in M53 from this sample (red dashed line) and that of Martell et al. (2008b) (blue dotted line). This distribution suggests that while there is a prominent CN-weak group, a group of CN-strong stars also exists in this cluster.

be causing the depletions in other cluster AGB stars. However, if this were the case, one might expect some manifestation on the RGB as well, in the form of a higher ratio of CN-strong to CN-weak stars. Yet, in the Alves-Brito et al. (2008) sample the ratio is only ~ 0.3 . Further investigation of AGB stars in M71 would be of interest to determine whether their observations are representative of the cluster. Note that Mallia (1978) reported a large fraction of CN-strong AGB stars in 47 Tuc, so one might expect to find a similar fraction in M71.

Moving to the $[\text{Fe}/\text{H}] \leq -2.0$ regime, M53 has not been extensively studied. Martell et al. (2008b) reported a broad but not strongly bimodal distribution of CN absorption

strengths in their sample of upper RGB stars (brighter than the RGB bump), where deep mixing is expected to have altered the stellar surface abundances. Their Figure 6 shows a generalized histogram for M53 that is similar to mine, shown in Figure 3.4, but theirs appears slightly narrower and smoother (though in fact my histogram has been smoothed by a larger factor than their distribution). When my $\delta S(3839)_N$ values are combined with theirs, producing a sample spanning nearly the entire RGB, a KMM test of bimodality (Ashman et al., 1994) indicates that the hypothesis that the observations are drawn from a single Gaussian parent population can be rejected at high statistical confidence ($p = 0.05$). The generalized histogram for this combined data set is shown in Figure 3.7, where the individual data sets are also indicated. The distribution clearly indicates the presence of a CN-strong component, with a ratio of CN-strong to CN-weak stars of 0.61, suggesting a population of CN-strong stars in the cluster with a range of enrichment levels.

I now consider the other very metal-poor clusters in this sample: M92, M15, and NGC 5053. Carbon abundance depletion and nitrogen enhancement have been observed before on the RGB and SGB of M92 (Carbon et al., 1982; Langer et al., 1986; Bellman et al., 2001) and RGB of M15 (Trefzger et al., 1983), with a progressive decline in [C/Fe] moving to higher luminosities. While significant CN bimodality has not been seen in either cluster, a handful of stars that exhibit CN-enhancement relative to the cluster majority have been observed (Langer et al., 1992; Lee, 2000). Additionally, indications of CN-CH anticorrelation have been observed at the base of the RGB in M15 (Cohen et al., 2005b), providing evidence that low-metallicity GCs do harbor the same light-element variations as their higher-metallicity relatives.

A recent study by Shetrone et al. (2010) of NGC 5466 ($[Fe/H] \simeq -2.2$) suggested the possible presence of two CN groups, with a small mean separation of only 0.055. They noted that the generalized histogram of their RGB stars was not well-described by a single Gaussian fit. In a similar fashion, I examined the generalized histograms for RGB stars in the very metal-poor clusters M92, M15, and NGC 5053. Figure 3.8 shows the histograms

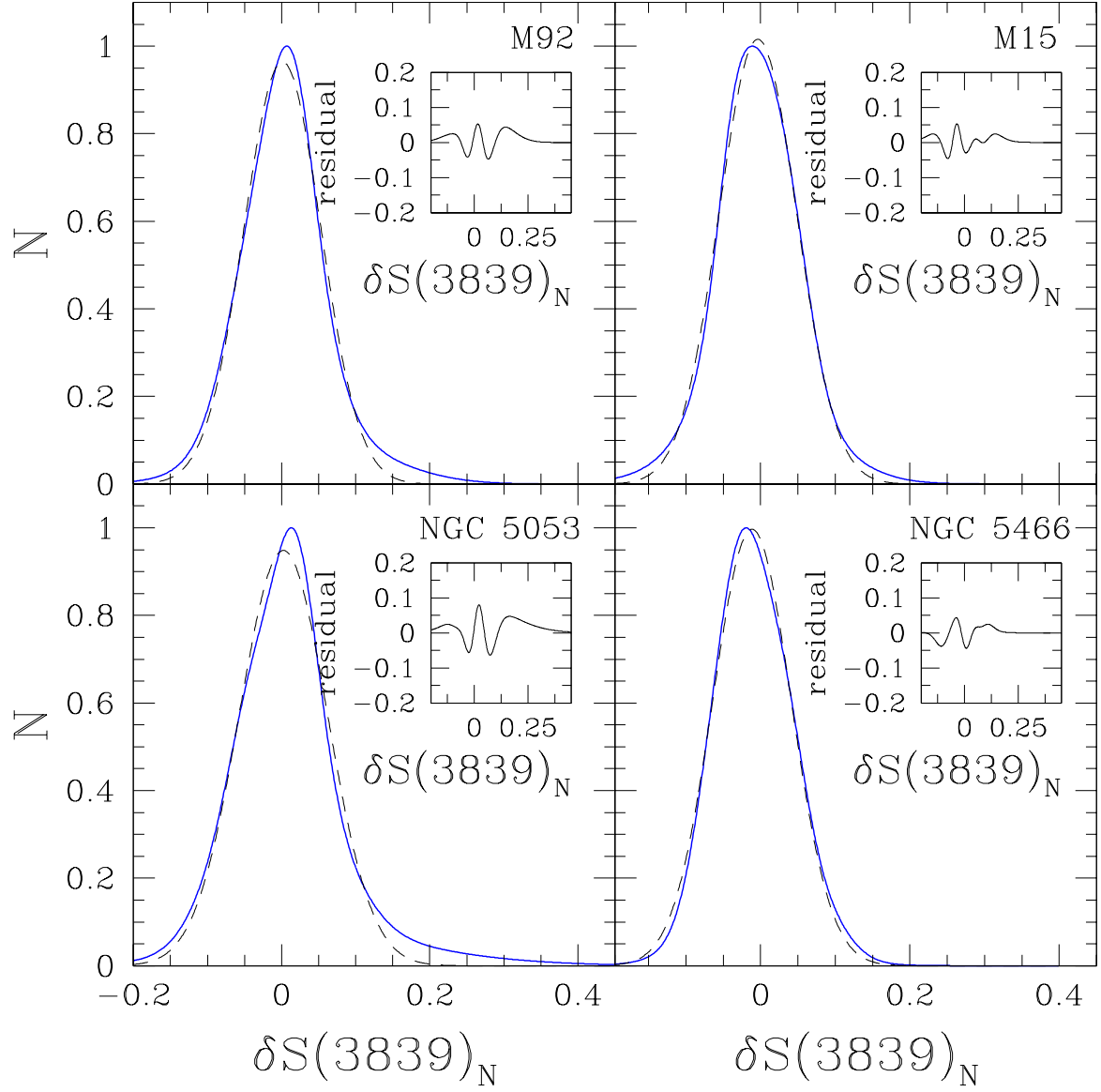


Figure 3.8 Generalized histograms for RGB stars in the very metal-poor clusters M92, M15, and NGC 5053, along with NGC 5466 ($[\text{Fe}/\text{H}] = -2.2$), taken from Shetrone et al. (2010). The blue solid line is the data, while the black dashed line represents the single Gaussian that best fit the distribution. The inset shows the residual between this best-fit curve and the data; the double-peaked nature of the residual may suggest that the data may be best represented by two overlapping Gaussian distributions.

for these clusters, as well as that of NGC 5466 from Shetrone et al. (2010), fit with a single Gaussian; residuals are plotted in the insets in each panel. The residuals from the fits to the three very metal-poor clusters are somewhat larger than those of NGC 5466, suggesting that the data also may not be well-described by a single Gaussian population. However, a KMM test for each cluster (including NGC 5466) cannot reject the null hypothesis that a single population well-describes the observed data, indicating that hints of the non-Gaussian distributions in these data may simply be due to small- n statistics. If these clusters possess multiple CN behaviors, they may not be discernible within the present measurement uncertainties. Due to the fact that double-metal molecules like CN are particularly difficult to observe at low [Fe/H], this problem could be solved by measuring individual element abundances rather than molecular bandstrengths.

3.3.2 CN ABSORPTION ON THE SUBGIANT BRANCH AND MAIN SEQUENCE

Perhaps the most intriguing observations of the CN bimodality phenomenon are to be found among stars in the relatively unevolved regions of cluster CMDs. Contrary to predictions of standard stellar evolutionary models, significant variations in CN bandstrengths have been reported for stars prior to their undergoing first dredge-up (e.g. Briley et al., 2002; Cohen et al., 2002), even down to the main sequence in 47 Tuc (Cannon et al., 1998; Harbeck et al., 2003a). However, searches within other cluster MS stars have produced mixed results. Cohen (1999a) reported no significant CN variation for MS/MSTO stars belonging to M13, although the CN features in their spectra were shown to be too weak for reliable measurement (Briley & Cohen, 2001). Carbon and nitrogen abundance analyses of these stars by Briley et al. (2004) showed that this was likely due to the fact that there is very little change in bandstrength for a given change in abundance at luminosities near the turnoff, where effective temperatures are relatively high compared to MS and giant stars (see their Figure 2). Main sequence stars in M71 have been claimed to exhibit CN

bimodality at a level larger than the measurement uncertainty, as well as an anticorrelation between CN and CH (Cohen, 1999b). Follow-up analysis of the data further showed that the variation is at the same level as that observed for RGB stars in that cluster, leading the authors to claim that no significant mixing is occurring on the RGB (although this could also simply mean that first dredge-up did not significantly affect the surface carbon and nitrogen abundances), and that the abundance variations were in place at the time the stars formed (Briley & Cohen, 2001). In their sample of eight GCs, Kayser et al. (2008) found no statistically significant variation in CN abundance for stars on the MS and SGB, but they again attributed that to low S/N spectra producing relatively large measurement uncertainties. Finally, Pancino et al. (2010) reported CN bimodality for MS stars in four of their most metal-rich clusters among a sample of 12 clusters. Clearly, minimizing measurement uncertainty plays a vital role in addressing the question of CN abundance variations on the MS, and further observations of larger samples of MS stars are needed for improved statistical certainty. In this section, I report on the MS/SGB stars observed for four clusters in our sample.

I measured the strength of the CN absorption band at 3883 Å on the main sequence using the spectral index $S(3839)$ defined by Harbeck et al. (2003a) for MS stars:

$$S(3839)_H = -2.5 \log \frac{\int_{3861}^{3884} I_\lambda d\lambda}{\int_{3910}^{3944} I_\lambda d\lambda}. \quad (3.4)$$

Uncertainties and $\delta S(3839)_H$ values were calculated the same way as described in Section 3.3.1. Figure 3.9 shows the distribution of $\delta S(3839)_H$ values for the four clusters that have SEGUE spectra for stars on the MS – M92, M15, M2, and M13 (in order of increasing [Fe/H]). A large amount of scatter is apparent, but not when compared to the typical uncertainty indicated by the error bars shown in the upper right corner of each panel. Furthermore, inset in each panel is the distribution of $\delta S(3839)_H$ as a function of $\langle S/N \rangle$, which shows that the source of this scatter may lie in the relatively low S/N of the spectra for these faint stars. The decrease in CN strength near $M_g \approx 4$ is not unexpected, since this

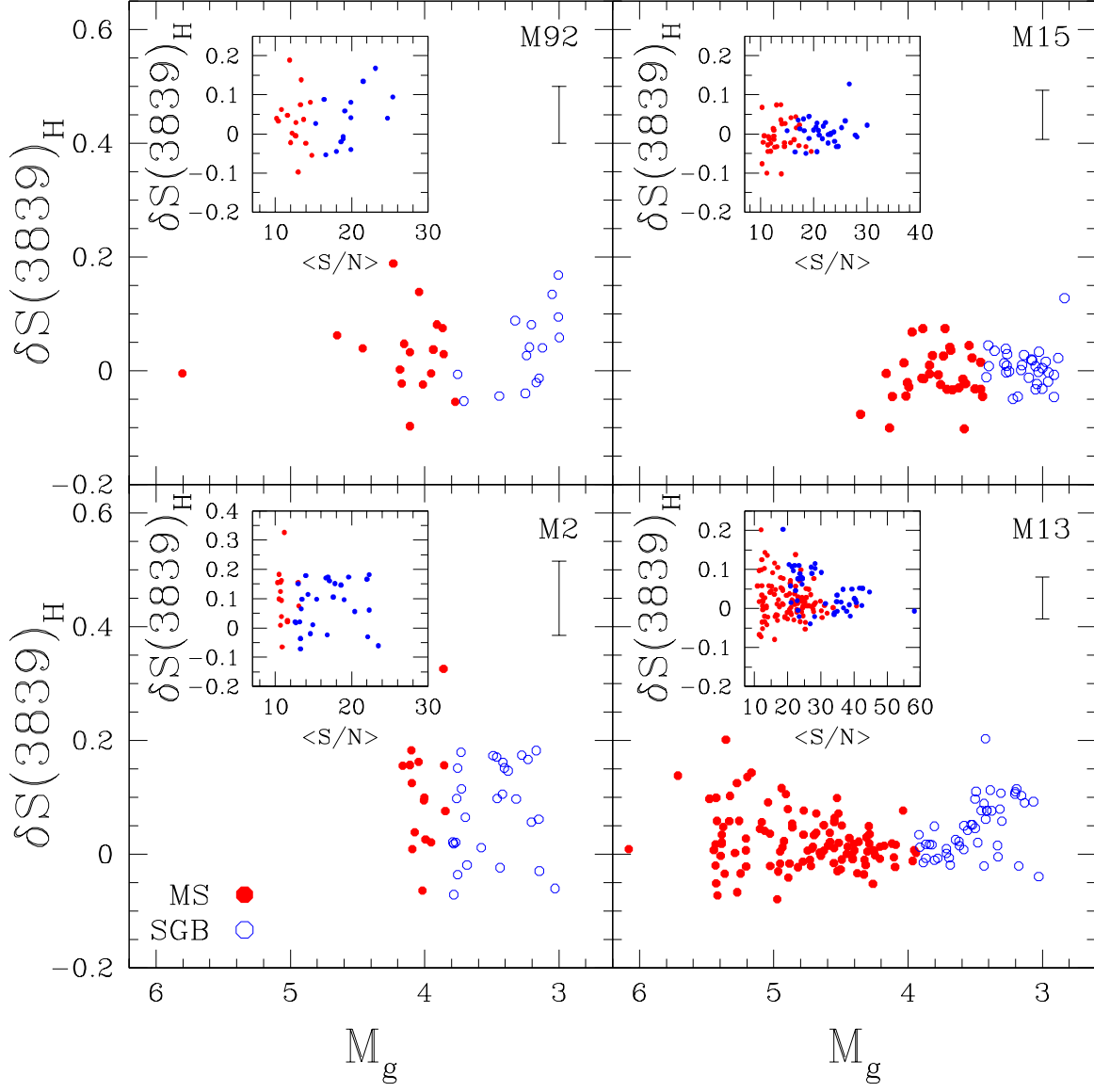


Figure 3.9 Distribution of $\delta S(3839)_H$ as a function of absolute g -magnitude for MS and SGB stars from clusters with SEGUE spectra on the MS, using the CN index definition from Harbeck et al. (2003a). Blue open circles represent SGB stars and red filled circles represent MS stars. Plotted as insets for each cluster are the distributions of $\delta S(3839)_H$ as a function of $\langle S/N \rangle$. This is done to demonstrate that the large scatter of CN absorption strength on the MS may simply be due to low S/N. Typical uncertainties are indicated by the vertical line in the upper right corner. Clusters are arranged in order of increasing [Fe/H].

corresponds to the turnoff where the effective temperatures are the highest (and thus CN molecular formation is at its lowest), but one would expect that CN bandstrengths should essentially all increase for luminosities below this point again, as it does for luminosities higher than this point, rather than simply increasing in dispersion. Generalized histograms of the $\delta S(3839)_H$ values for these four clusters are shown in Figure 3.10. No indications of bimodality are seen, suggesting that when the relatively larger uncertainties are taken into account, nothing statistically significant stands out. Although the residuals (see inset panels) are asymmetric and, in the cases of M92 and M13, double-peaked, we see nothing indicating the presence of two populations of stars. It seems more likely that the asymmetries in the figures are simply due to finite sampling from a single Gaussian distribution. A KMM test fails to reject the hypothesis that these data were drawn from a single Gaussian parent population. Further observations with smaller uncertainties are needed to determine whether the observed distributions' asymmetries are due to the presence of two distinct populations or not.

The Norris et al. (1981) definition for the CN index was used for stars located on the SGB, although the Harbeck et al. (2003a) definition could also have been used. Figure 3.11 shows the distributions of $\delta S(3839)_N$ abundances on the SGB for the same four clusters as in Figure 3.10. The histograms for M92, M2, and M13 appear to provide evidence of independent CN groups. The solid blue lines and dashed black lines are as before, while the red dotted curves provide the generalized histograms for the proposed CN groups on the SGBs of each cluster. Insets in each panel again show the differences between the data and the superposed single Gaussian curve. Cohen (1999a) looked for CN variations on the upper MS/MSTO region of M13 and reported nothing significant; however it appears that the data does indicate the presence of CN variation on the SGB of this cluster. These observations indicate that, for very metal-poor clusters such as M92, as well as for clusters with moderate metallicity such as M2 and M13, there appear to be signs of enhanced N enrichment well before the point of first dredge-up. These issues are explored further below.

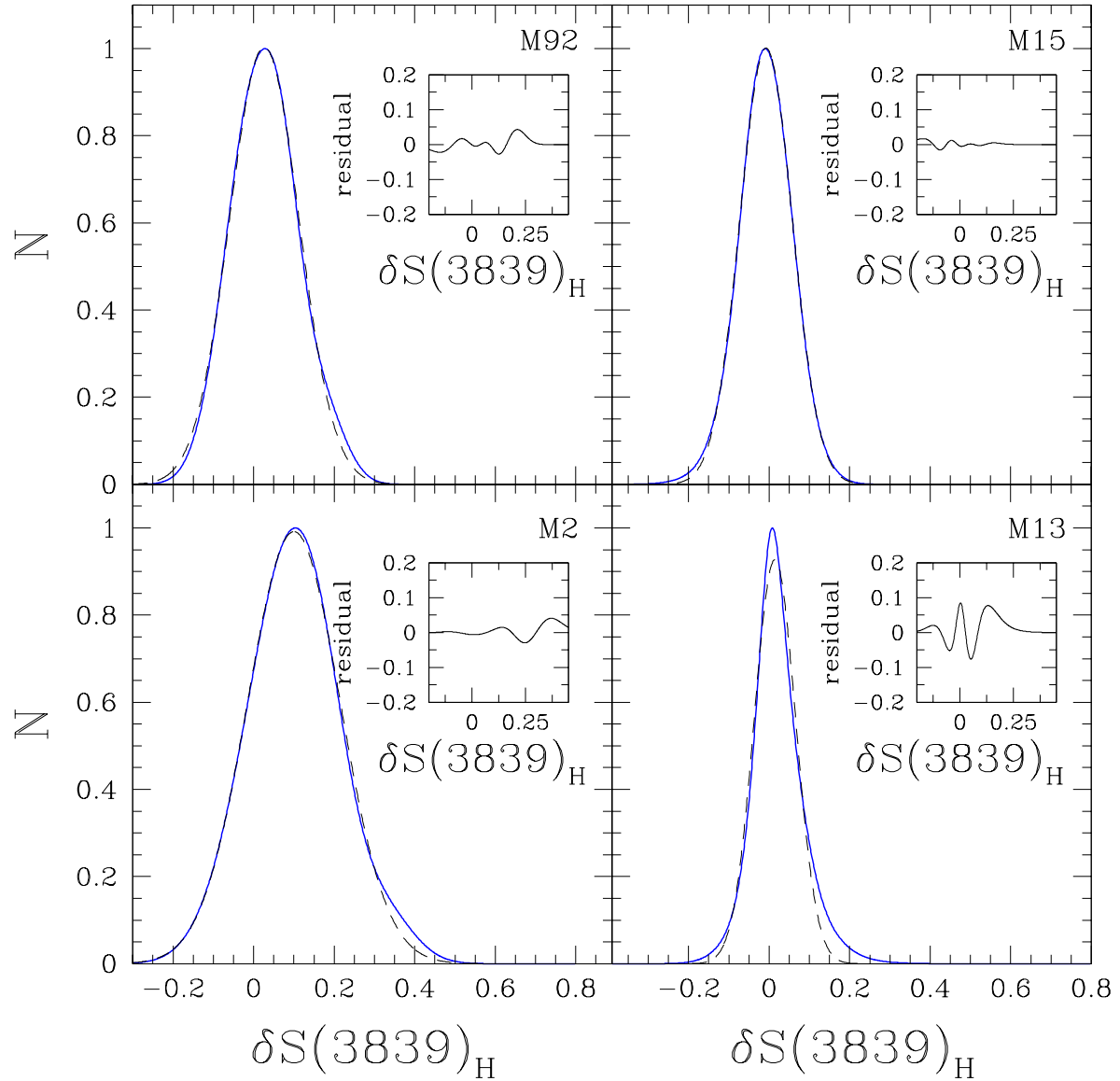


Figure 3.10 Generalized histograms for the $\delta S(3839)_H$ distributions of MS stars within each globular cluster for which SEGUE spectra exist on the MS. $\delta S(3839)_H$ on the MS is calculated in the same way as for RGB stars. No indication of bimodality is apparent.

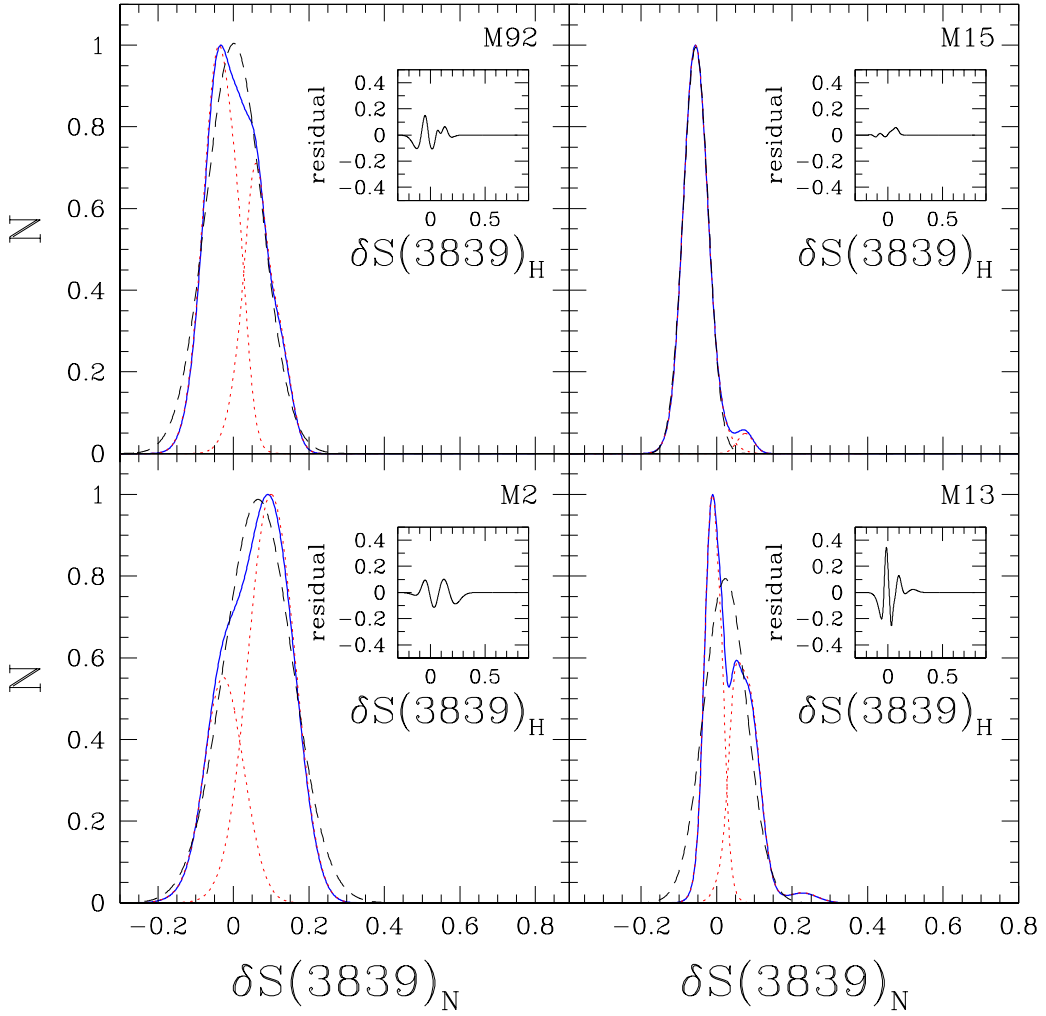


Figure 3.11 Generalized histograms for the $\delta S(3839)_N$ distributions of SGB stars within each globular cluster for which SEGUE spectra exist on the SGB. The solid blue curves are the generalized histograms for each cluster. A simple Gaussian fit to the distribution is overplotted as a dashed black line, and the red dotted curves are generalized histograms for the groups one might presume to be CN-strong and CN-weak, taken separately. The inset box shows the difference between the blue generalized histogram for the entire sample of SGB stars and the simple Gaussian fit. The small bump on the CN-strong side represents one star and cannot be confidently assigned to any presumed CN-strong group.

3.3.3 HIDDEN SUBSTRUCTURE IN GENERALIZED HISTOGRAMS

While generalized histograms are a more natural representation of the distribution of data than binned histograms, it is important to consider the impact of any adopted smoothing factors. Smoothing factors are sometimes used to produce a histogram that more closely resembles those of past studies by multiplying the uncertainties of each data point by some appropriate factor. This is also done to account for any sources of uncertainty that may have been overlooked. One may choose to adopt a smoothing factor which produces a distribution that is comparable to past studies, but choosing a smoothing factor that is too high may wash out important details in the data.

To study the potential impact of smoothing on the generalized histograms of my clusters, I divided up the CMDs for the four GCs with full CMD coverage into several regions – RGB above the bump (where the RGB bump was identified), RGB, SGB/MSTO, and MS. I then looked at the $\delta S(3839)$ indices for stars in each region and produced two generalized histograms, one smoothed to match the claimed observational uncertainties of previous studies (solid black line) and one unsmoothed (dashed red line), shown in Figures 3.12 – 3.15. Because measurement errors from previous studies are typically ~ 0.05 , when the typical Monte Carlo-calculated uncertainties were smaller than this they were amplified (smoothed) by an integer factor (shown in each panel) to approximate the errors from previous studies.

Naturally, the unsmoothed lines exhibit more potential substructure, but one must still determine what level of substructure is meaningful. This can be qualitatively estimated as a function of the number of stars in the bin and the relative peak sizes. For example, while the RGB of M92 (Figure 3.12) appears to exhibit substructure in the unsmoothed histogram, the paucity of stars in this region of the CMD obviates this claim (the CN-strong peak only has one star). As mentioned above, for very metal-poor clusters such as M92 and M15, it is expected that the difference between CN-strong and CN-weak groups should be smaller when measuring the $S(3839)$ index. At the metallicity of M92, this difference is expected

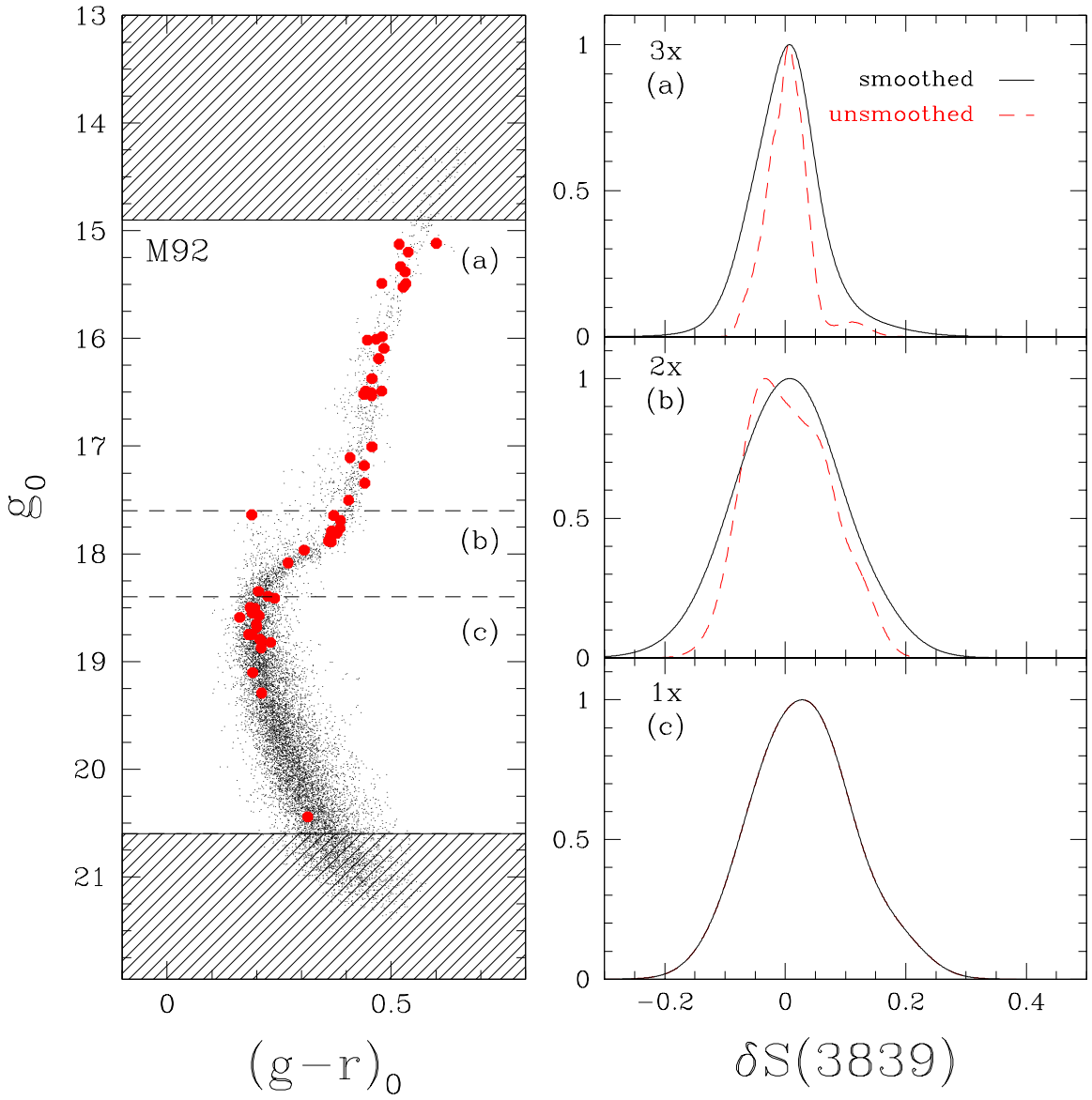


Figure 3.12 Region divisions for the color-magnitude diagram of M92 are shown in the left panel, while the right panel shows the generalized histograms of the $\delta S(3839)$ distribution within each unshaded region. The solid black lines in the histograms represent the smoothed distribution, with the smoothing factor given in the upper-left corner, while the dashed red lines represent the unsmoothed distribution. The multipliers listed in the upper left corner of the right-hand set of panels indicate the amount of smoothing employed (see text). The HB stars were not included in the analysis.

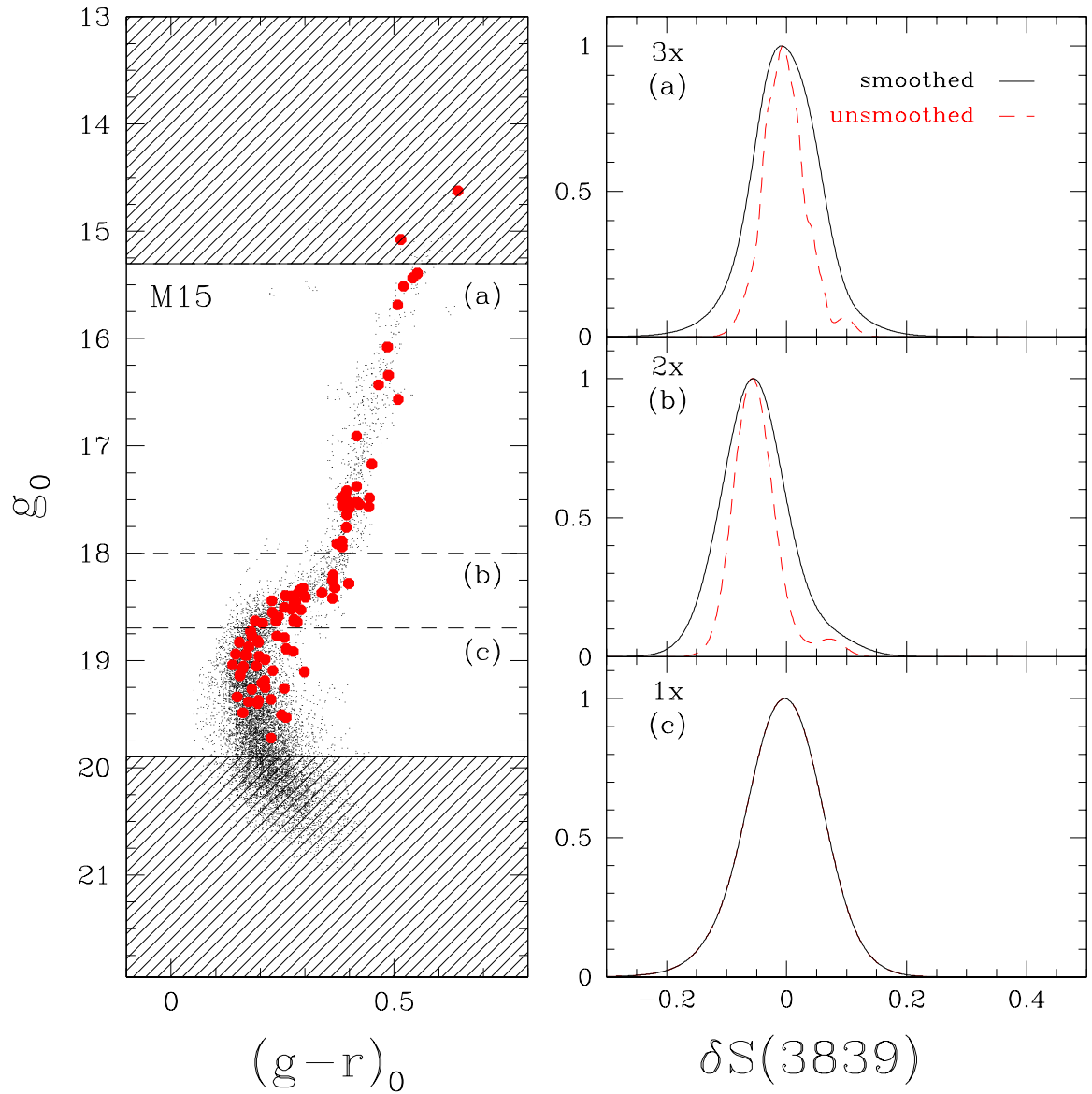


Figure 3.13 Same as Figure 3.12 but for M15.

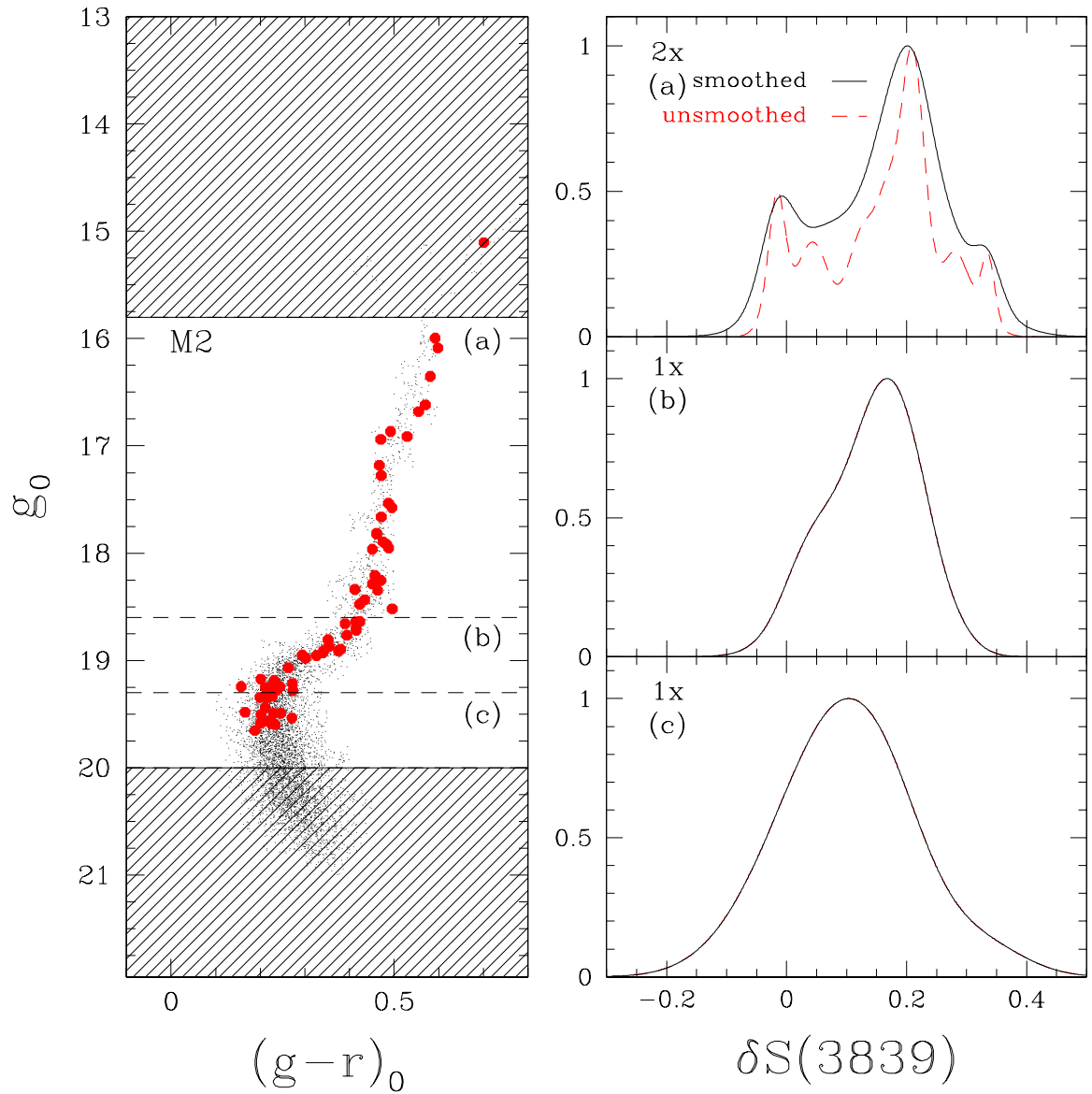


Figure 3.14 Same as Figure 3.12 but for M2.

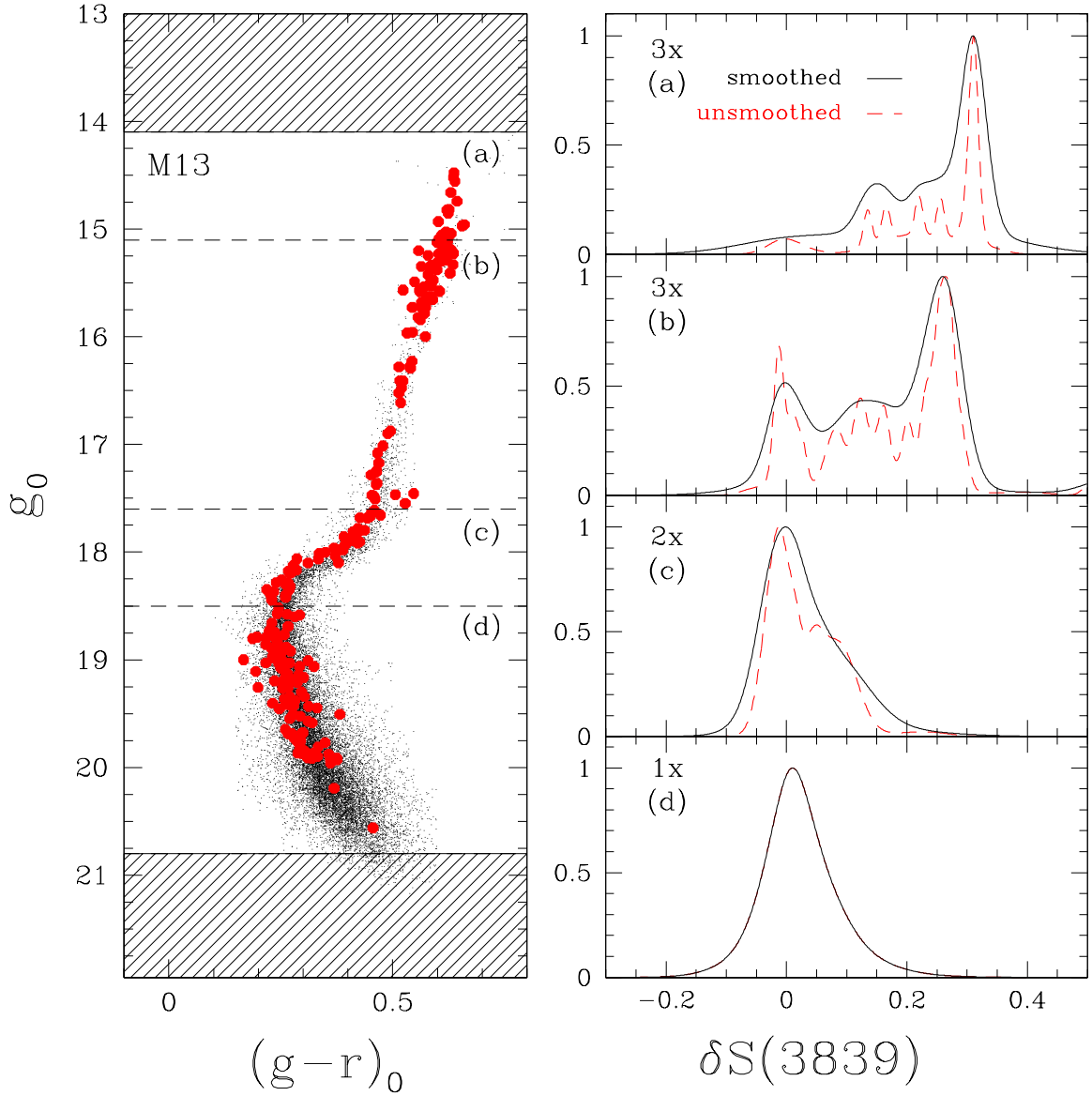


Figure 3.15 Same as Figure 3.12 but for M13. This cluster had data sampled above the RGB bump, shown in panel (a) of the right-hand set of panels. More than the other clusters, M13 shows a steady progression of increasing CN richness as one moves up the RGB. The small bump at $\delta S(3839) \approx 0.0$ in the top unsmoothed histogram corresponds to an AGB star, identified later as such by its $u - g$ color.

to be ~ 0.1 , suggesting that if more data were available one might be able to determine whether the apparent substructure is real or merely an artifact of small number statistics.

From inspection of the RGB of M15 (Figure 3.13), one again sees possible asymmetries in the upper regions that may be associated with substructure. However, a KMM test for this portion is again unable to reject a single Gaussian parent population.

At more moderate metallicities, M2 (Figure 3.14) and M13 (Figure 3.15) exhibit very clear signs of CN variation on the RGB. The uppermost region of M13 is at a luminosity above the RGB bump, suggesting that the increase in CN is likely due at least in part to the deep mixing thought to occur at that point. Figure 3.15 depicts the expected appearance of stronger CN bandstrengths as stars evolve up the RGB, although a group of CN-weak stars always remains present. It is also worth noting that initial variations first appear on the SGB, as seen in the right-hand panel (c).

3.4 CH BANDSTRENGTH DISTRIBUTION

While investigation of CN bandstrengths can provide some insight into possible chemical inhomogeneities within cluster stars, CH absorption strength is also typically considered as a means of distinguishing between nitrogen abundance behavior and carbon abundance behavior. This is generally done by measuring the absorption strength of the 4300 Å CH G-band and comparing with the CN bandstrengths. Previous studies of cluster giants have shown that, at a given luminosity, the CN-strong stars tend to have weak CH G-bands, implying nitrogen enhancement. Additionally, Gratton et al. (2000) demonstrated that the general behavior in clusters is that the CH bandstrength decreases with increasing luminosity, while the summed ratio $[(C+N+O)/Fe]$ remains constant – again indicating the presence of nitrogen enhancement as stars move up the RGB. However, these abundances are not predicted by standard stellar evolution models to change significantly along the RGB between first dredge-up and helium flash (Iben, 1964), at least without the assumption of

additional mixing.

Many definitions of indices that measure the CH G-band have been employed (Norris et al., 1981; Trefzger et al., 1983; Briley & Smith, 1993; Lee, 1999; Harbeck et al., 2003a,b; Martell et al., 2008b) and proposed (Martell et al., 2008a) in the past; these differ primarily because they were developed for use with stars of specific metallicity or luminosity ranges. Figure 3.16 shows the linebands and sidebands used by four common definitions. While the use of different CH bandstrength indices complicates quantitative comparison with literature studies, qualitative comparisons can still be useful. Inspection of Figure 3.16 reveals the presence of the H_γ and H_δ Balmer lines that can interfere with the continuum sidebands in the Norris et al. (1981) and Martell et al. (2008b) index definitions. These two definitions were developed using samples of the most luminous, and therefore the coolest, red giants in their clusters of interest, where Balmer absorption has minimal impact. Of the two that remain, the Briley & Smith (1993) definition only includes the blue side of the continuum, which can potentially cause artificially depressed values for cooler stars where the continuum is more strongly sloped. Therefore, the Lee (1999) definition was adopted for this study:

$$CH(4300)_L = -2.5 \log \frac{\int_{4270}^{4320} I_\lambda d\lambda}{\frac{1}{2} \left(\int_{4230}^{4260} I_\lambda d\lambda + \int_{4390}^{4420} I_\lambda d\lambda \right)}. \quad (3.5)$$

This definition has the advantage that it has been used for clusters covering a broad range of metallicities, from M15 (-2.33 ; Lee, 2000) to M71 (-0.82 ; Lee, 2005), and it also avoids the influence of Balmer lines that appear in hotter stars. In addition, it samples the continuum on both sides of the CH G-band, thus providing a more accurate representation of the “expected” continuum at the location of the line band, regardless of the slope of the continuum in this region. The resulting indices are also tabulated in Table ??.

Figure 3.17 shows the CH index versus $\delta S(3839)_N$ for this cluster sample, ordered from low to high metallicity. From inspection of this figure, CN-weak stars are typically also CH-strong, while those stars that are CN-strong are typically CH-weak, with a few exceptions.

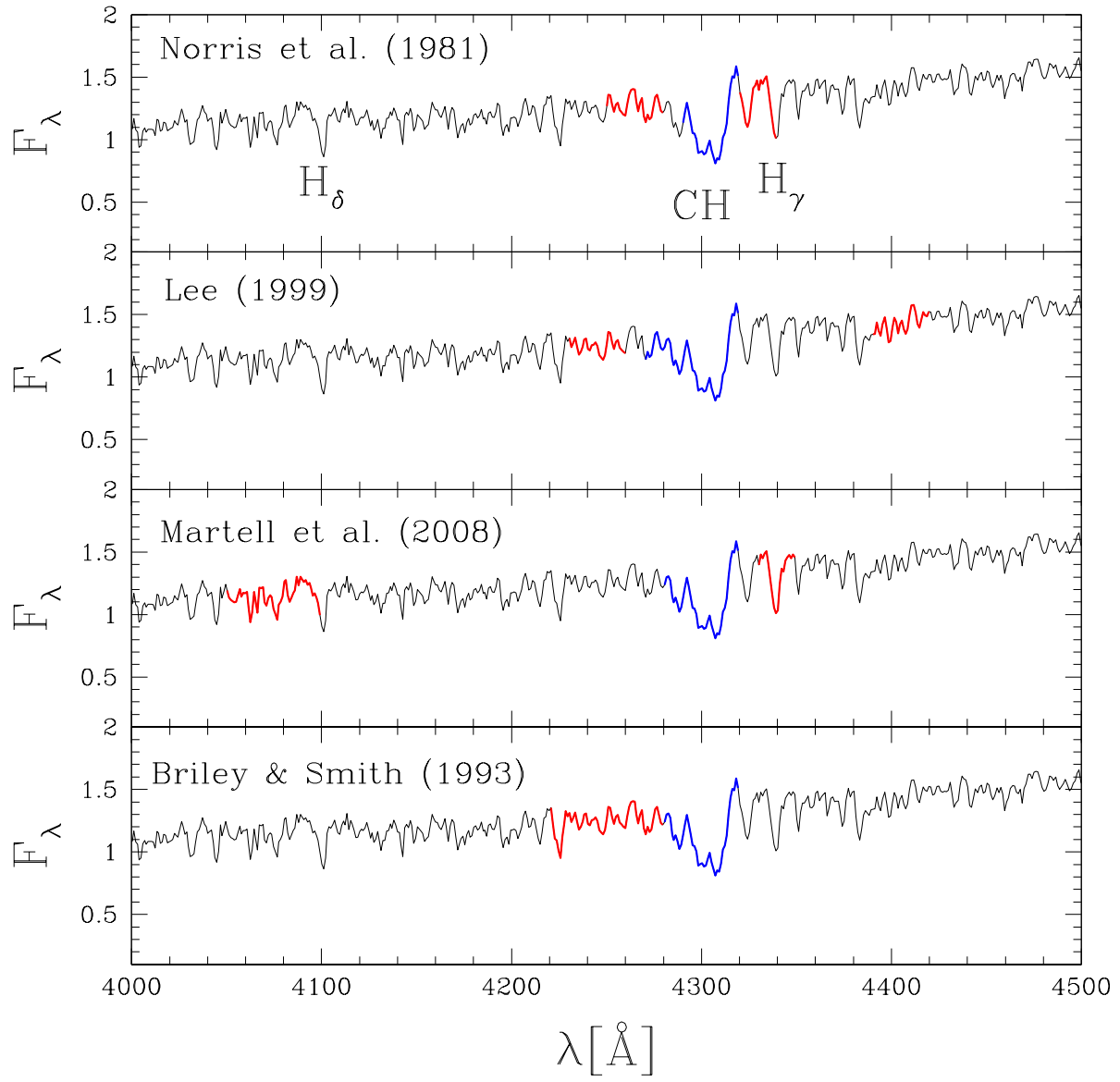


Figure 3.16 CH bandstrength measurement windows for four popular index definitions, shown for a typical M3 red giant spectrum (fiber 2475-53845-489). The blue line on each spectrum indicates the line band while the red lines indicate the continuum windows used for comparison. The CH G-band is indicated, along with two hydrogen Balmer lines for reference.

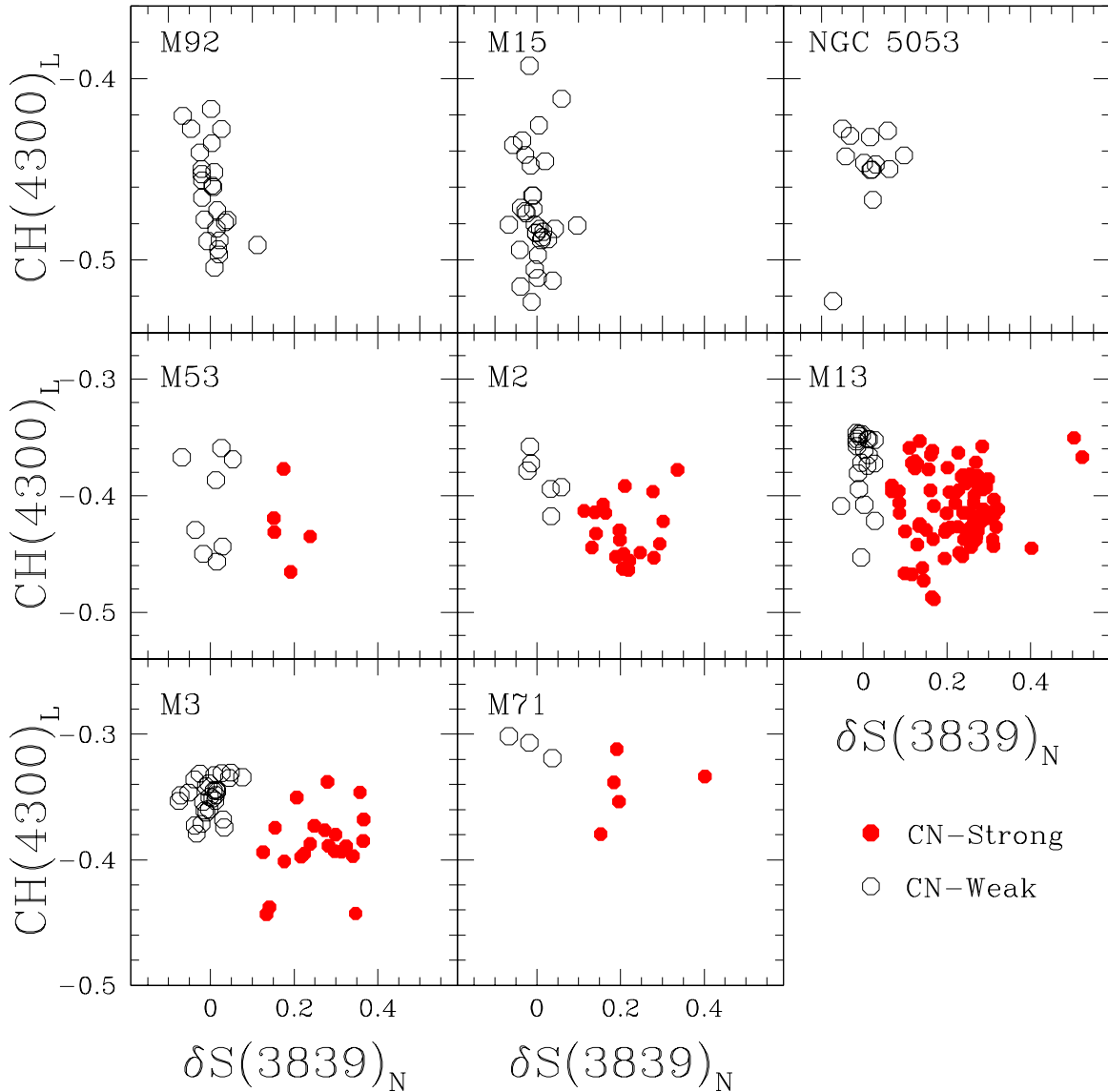


Figure 3.17 CH absorption strength versus $\delta S(3839)_N$ for RGB stars in this sample. Red filled circles are CN-strong stars and black open circles are CN-weak stars. In most clusters, a trend from CH-strong/CN-weak to CH-weak/CN-strong is seen. The subscript ‘L’ indicates the Lee (1999) definition.

Figure 3.18 is a similar set of plots, but here the CH-index is plotted against absolute g -magnitude. The RGB stars within each cluster exhibit the strongest CH absorption when they are CN-weak, and vice versa. SGB stars are included as well for the two clusters in our study where they are also available. My results are consistent with previous studies of giants in M2 (Smith & Mateo, 1990), M13 (Suntzeff, 1981; Briley & Smith, 1993; Smith et al., 1996), M3 (Suntzeff, 1981; Smith et al., 1996), and M71 (Smith & Norris, 1982; Lee, 2005; Alves-Brito et al., 2008). Interestingly, M53 does not exhibit this anticorrelation in this sample or that of Martell et al. (2008b).

3.4.1 CH BEHAVIOR AT LOW METALLICITY

Examination of the CH-CN anticorrelation for low-metallicity clusters is challenging, due in part to the decreased abundances of all metals in the stellar atmospheres. This phenomenon has been demonstrated before with synthetic spectra spanning a range of N abundances at low metallicity (Martell et al., 2008b). This suggests a possible low-metallicity observational cutoff, below which bimodality is either too difficult to detect with data of the quality SDSS was able to obtain or too difficult to measure due to the low levels of CN present.

Shetrone et al. (2010) predicted that abundance variations should exist at all metallicities, even though bandstrength variations will become impossible to see at sufficiently low values of $[\text{Fe}/\text{H}]$. To investigate this, I now consider whether the CN-CH anticorrelation is observable in the very metal-poor clusters M92, M15, and NGC 5053. Following the approach of Shetrone et al. (2010), a line was fit to the raw $S(3839)_N$ values as a function of g -magnitude, then those above the line were labeled as CN-strong and those below the line as CN-weak. The results of this exercise for M92, M15, and NGC 5053 are shown in Figure 3.19, plotted against absolute g -magnitude for direct comparison. For the remainder of this dissertation these two groups will be used to distinguish those stars with slightly higher and slightly lower CN bandstrengths. At the lowest point on the RGB (still above the SGB), there is little difference in the CH bandstrengths between the CN-strong and

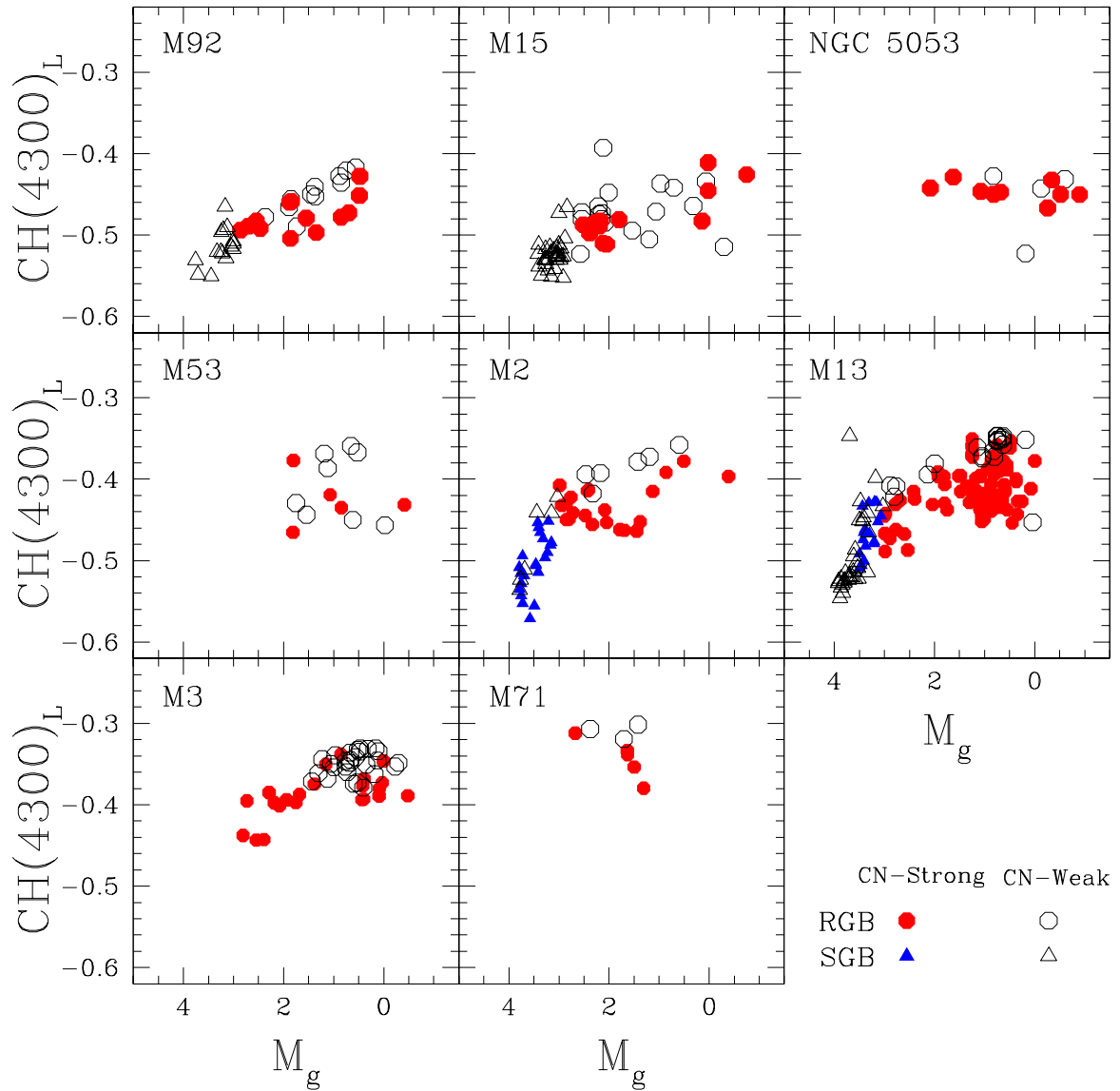


Figure 3.18 CH absorption strength as a function of luminosity, with blue triangles corresponding to SGB stars while red circles are RGB stars. Filled symbols represent CN-strong stars, while open symbols represent CN-weak stars.

CN-weak stars. However, as one moves up the RGB, an apparent anticorrelation sets in for RGB stars in M92 at $M_g \approx 1.5$. Similar behavior is not seen in M15 and NGC 5053, however.

If CN abundance variations are in place prior to a star's evolution up the RGB, one might expect to see an anticorrelation between CN and CH on the SGB and MS. Although more difficult to observe, since higher temperatures would tend to break up the molecules, such anticorrelations have been reported previously for MS stars (Cannon et al., 1998; Cohen, 1999b; Harbeck et al., 2003a; Pancino et al., 2010). Figure 3.20 shows the relationship between CH and CN indices for MS and SGB stars in M92, M15, M2, and M13, with the CN indices derived using the Harbeck et al. (2003a) definition. As in Fig. 3.9, one sees a minimum in CH bandstrength for M13 at $M_g \approx 4$, corresponding to the higher effective temperatures of the turnoff point (see Figure 2 from Briley et al., 2004). While an anticorrelation may exist on the upper SGBs of M2 and M13, which would be consistent with the signs of CN bimodality on the SGB of these clusters and consistent with Figure 3.18, no other anticorrelations are clearly seen. While further study is needed, previous studies suggest that follow-up observations of MS stars in these clusters will likely reveal the same types of bandstrength variations.

3.5 CORRELATIONS WITH CLUSTER PARAMETERS

The possibility that CN enrichment is linked in some way with various physical parameters of the parent cluster has been examined extensively in previous studies. For example, Norris (1987) identified a possible correlation between CN bandstrength and the apparent ellipticity of the cluster using data from 12 Galactic GCs. This suggested correlation was confirmed by Smith & Mateo (1990), who combined their observations of M2 with the set from Norris (1987), but was not seen by Kayser et al. (2008) using data from eight clusters (of which three were in common between the two studies). They concluded that the

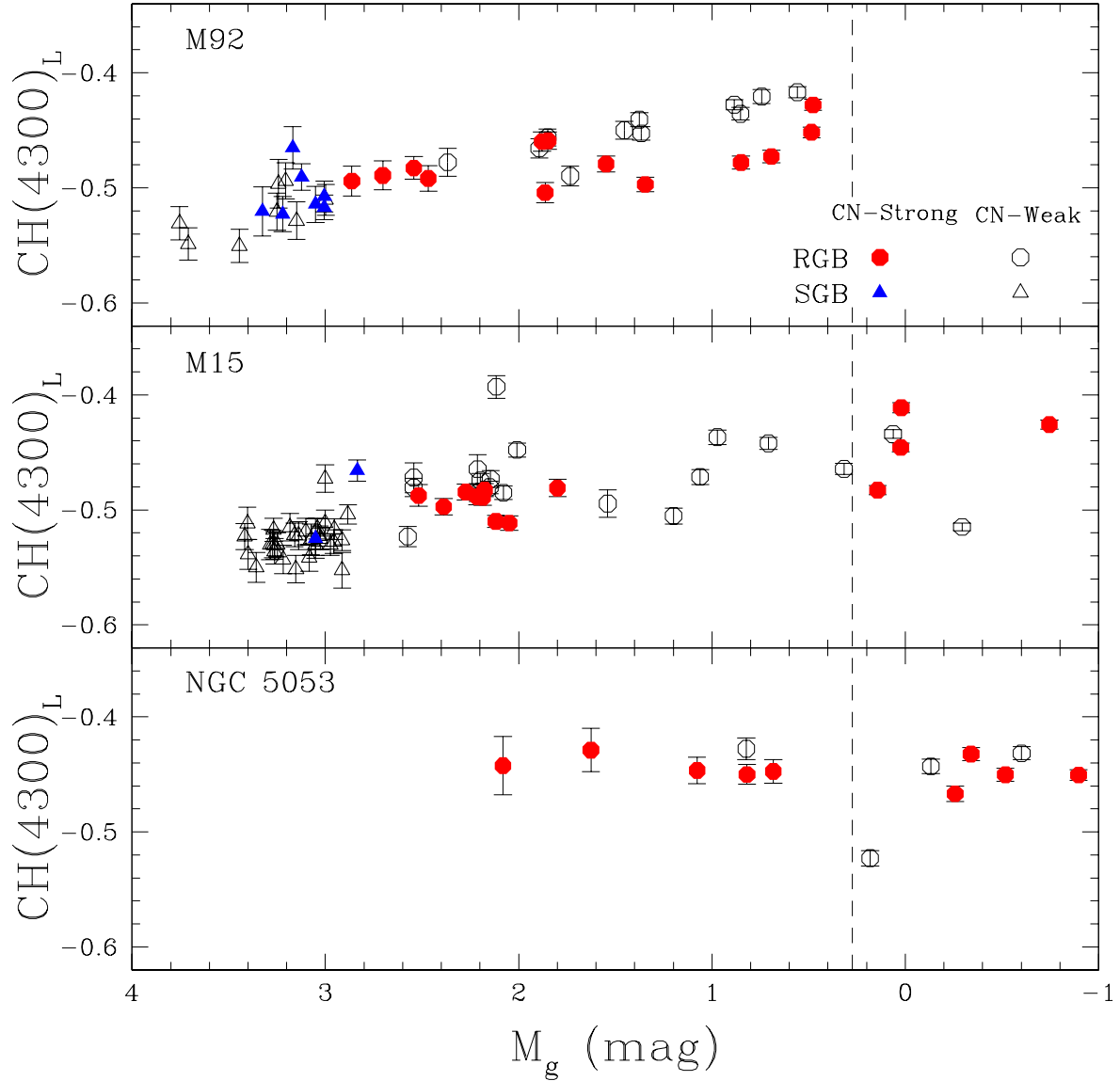


Figure 3.19 Illustration of CH scatter on the RGBs of M92 (top), M15 (middle), and NGC 5053 (bottom). I have made a proposed CN-strong/weak cut at $\delta S(3839)_N=0.0$, based on a simple linear fit to the raw RGB $S(3839)_N$ values, and have plotted the CH abundance of CN-strong (filled circles) and CN-weak (open circles) stars in each panel. The vertical dashed line is the location of the RGB bump, drawn from Fusi Pecci et al. (1990).

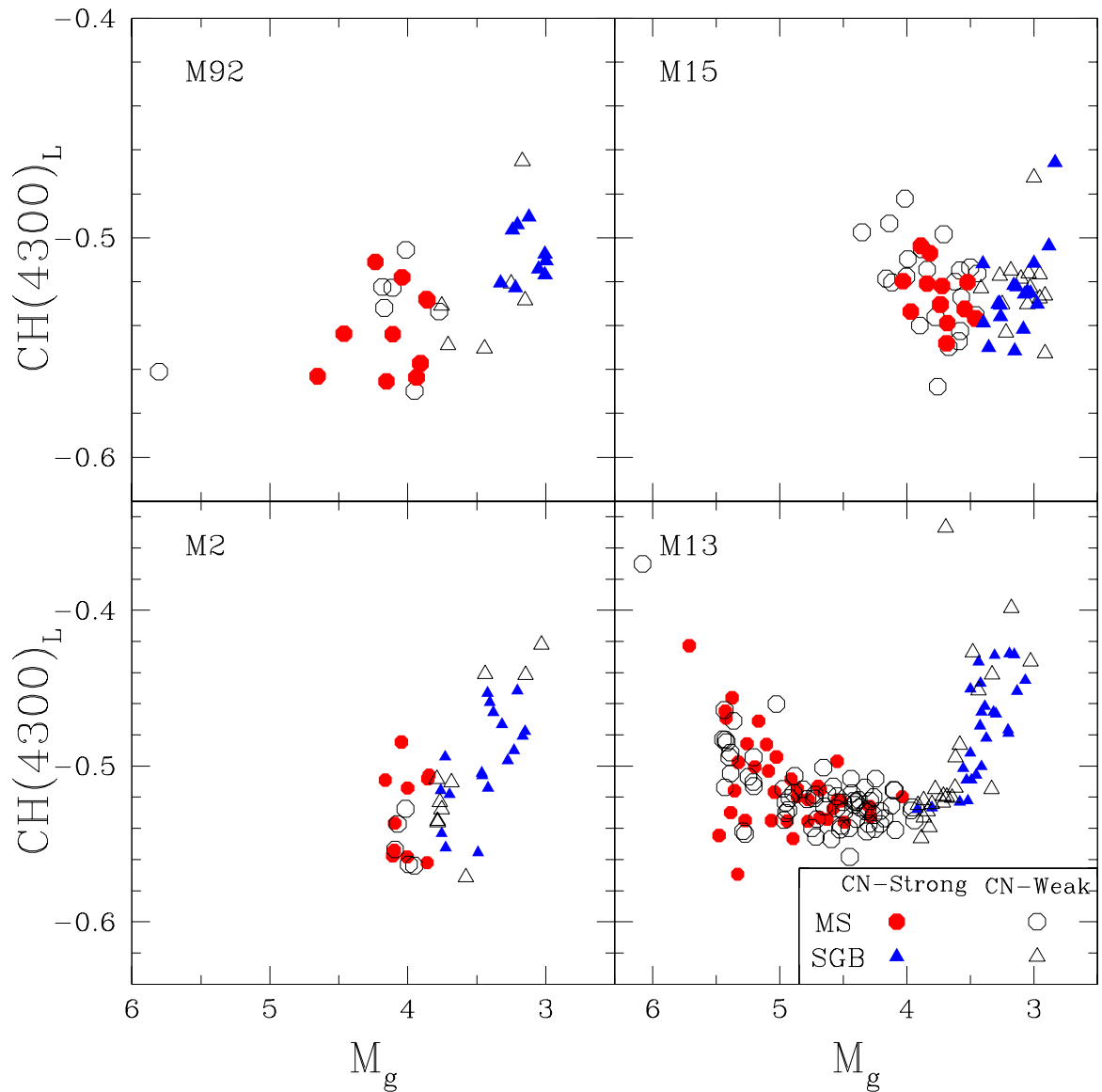


Figure 3.20 CH absorption strength versus M_g for MS and SGB stars. Approximate divisions are made to indicate those stars that are higher (filled symbols) and lower (open symbols) than the mean for CN absorption. No anticorrelation is seen.

Table 3.1. Individual Cluster RGB CN Number Ratios

Cluster	N_s	N_w	r
M92	0 (12)	24 (12)	0.00 (1.00)
M15	0 (23)	32 (9)	0.00 (2.56)
NGC 5053	0 (9)	13 (4)	0.00 (2.25)
M53	5	8	0.62
M2	21	6	3.50
M13	90	21	4.29
M3	22	28	0.79
M71	5	3	1.67

Note. — Number of CN-strong (N_s) and CN-weak (N_w) stars, and CN number ratios, for RGB stars from individual GCs in our sample. Values in parentheses for M92, M15, and NGC 5053 represent the groupings based on the proposed divisions detailed in Section 3.4.1.

correlation with ellipticity is not as significant as initially believed. Smith & Mateo (1990) also reported a correlation between CN enrichment and cluster central velocity dispersion, which was again disputed by Kayser et al. (2008). The Smith & Mateo (1990) claim of a CN enrichment correlation with integrated cluster luminosity received moderate support from the observations of Kayser et al. (2008).

Figure 3.21 shows the number ratio of CN-strong to CN-weak RGB stars for the clusters in this sample, denoted by r , plotted against various cluster parameters drawn from the Harris (1996) catalog.² These values are tabulated in Table 3.1. The number ratio is useful because it reveals the relative population sizes of the individual CN groups, and provides a constraint on the chemical evolution of the cluster.

M92, M15, and NGC 5053 were treated differently because they do not possess CN-

²All references to Harris (1996) refer to the 2010 update on his web page: <http://www.physics.mcmaster.ca/~harris/mwgc.dat>.

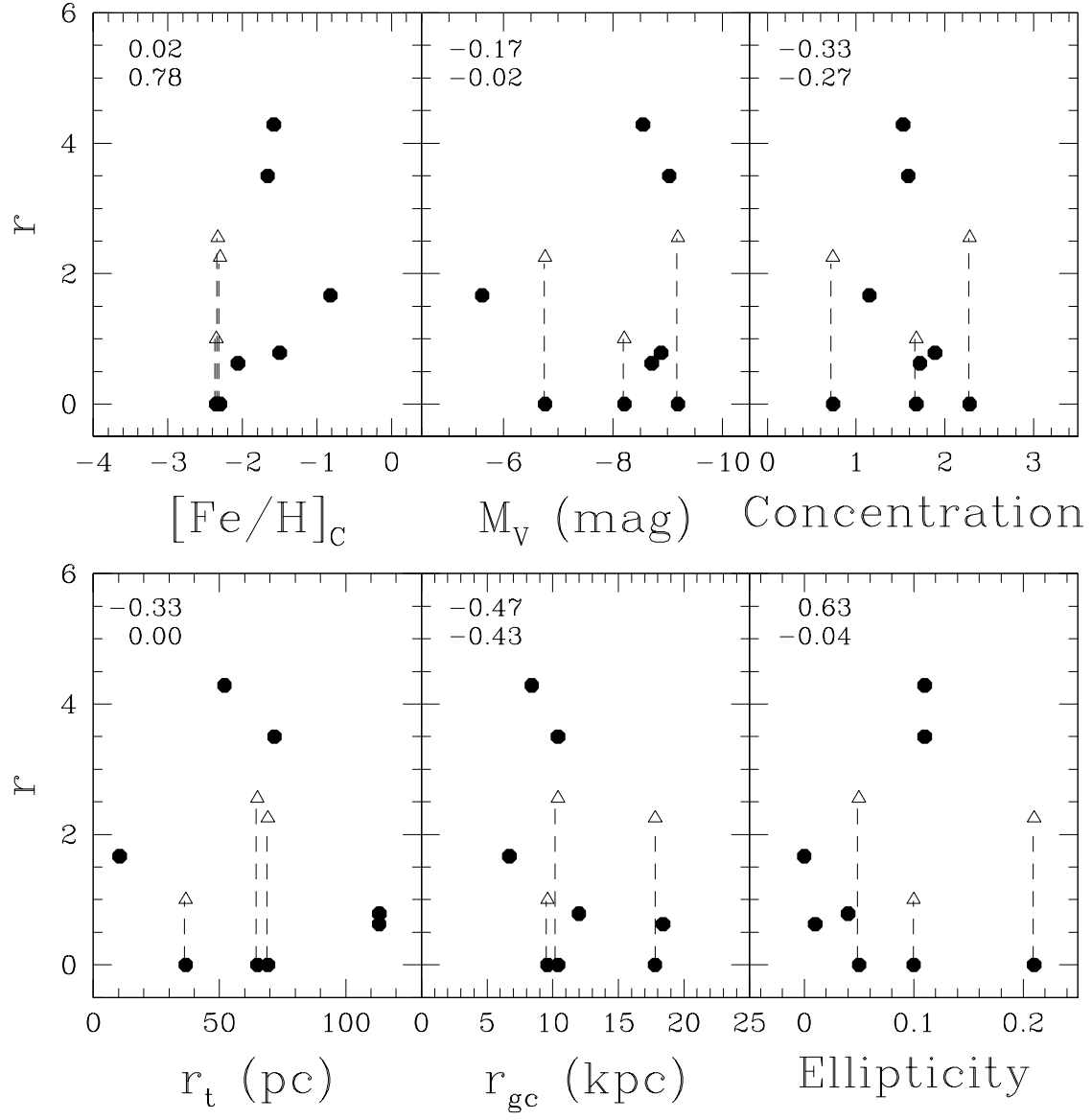


Figure 3.21 The number ratio of CN-strong to CN-weak stars (designated as r) plotted against various cluster parameters. The filled circles represent the adopted ratios for each cluster, while the open triangles representing M92 and M15 if one were to make the proposed divisions and identify relatively CN-strong and CN-weak stars in each. The Spearman rank correlation coefficients are given in the upper-left corners of each panel; the top numbers correspond to the correlation coefficient using the r values from the proposed M92 and M15 divisions (triangles), while the bottom numbers correspond to the distribution using $r = 0$ for M92 and M15.

strong stars, at least by the conventional definition, and hence would have an r value of zero. However, Figures 3.12 and 3.13 suggest the presence of stars that might be identified as CN-strong (relative to the rest of the cluster). Therefore, an alternative method for adopting relatively CN-strong and CN-weak stars was described in Section 3.4.1 for M92, M15, and NGC 5053. Using this approach, I determined alternative r values for M92, M15, and NGC 5053, which are plotted in Figure 3.21 as open triangles. Spearman rank correlation coefficients were calculated for the distributions and are provided in the upper-left corner of each panel; the top and bottom numbers correspond to the sample with and without the second r quantity included, respectively, for M92, M15, and NGC 5053.

Supporting the claims of Norris (1987) and Smith & Mateo (1990), I observe a moderate correlation between CN enrichment and cluster ellipticity. We also note a moderate correlation between CN enrichment and central velocity dispersion (Figure 3.22), in the same sense as Smith & Mateo (1990), with a Spearman coefficient of 0.52 when using the ratios for the proposed CN divisions in M92, M15, and NGC 5053, though no such correlation in these data is observed with cluster luminosity (see Figure 3.21). However, the range of cluster luminosities in this sample is not very broad. Only two clusters with absolute V -magnitude brighter than -8.0 were observed, one of which is metal-poor with no solidly identified CN-strong stars and the other having fewer than 10 stars with reliable spectroscopy. When this data set is combined with that of Kayser et al. (2008) and Smith & Mateo (1990), also shown in Figure 3.22, the overall trends become clearer; the largest fraction of CN-strong stars are found in the most luminous and massive clusters. This result is consistent with expectations from the self-enrichment scenario – the most massive clusters possess the deepest gravitational potentials, allowing them to retain the largest amount of chemically enriched gas expelled from evolving stars.

While studies to date typically quote an average value of the r parameter from the clusters in their samples, it is not clear that this quantity is meaningful. Comparing the values directly is complicated by the fact that some studies only use RGB stars, while others

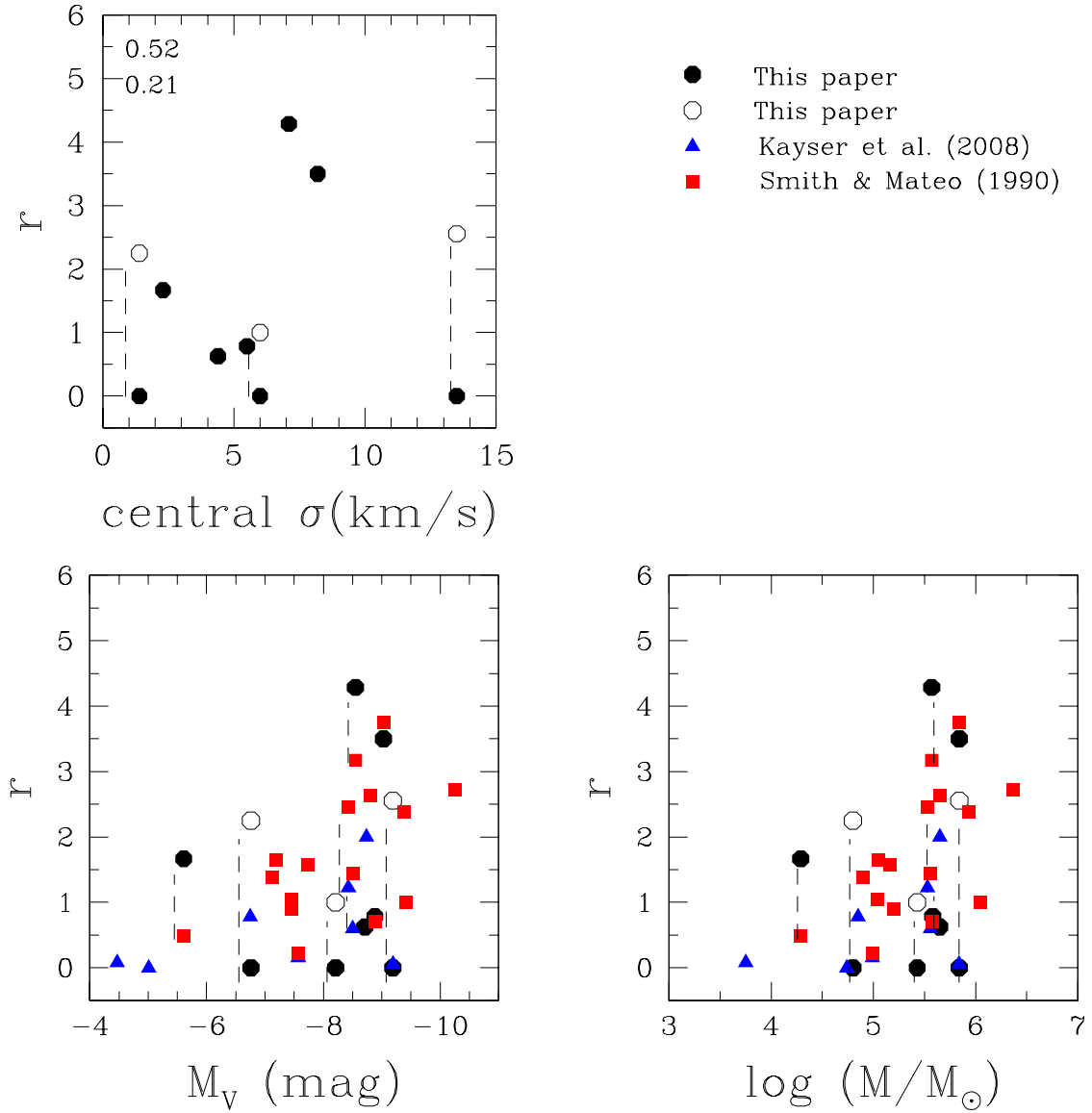


Figure 3.22 The number ratio of CN-strong to CN-weak stars plotted against central velocity dispersion, absolute V magnitude, and total cluster mass, combined with data from Kayser et al. (2008) (blue triangles) and Smith & Mateo (1990) (red squares). The Spearman rank correlation coefficients for the r - σ relation are given in the upper-left corners and correspond the same way as in Figure 3.21. A correlation is seen when using the CN division in M92 and M15. Absolute magnitudes are drawn from the 2010 revision of the Harris (1996) catalog, while masses are drawn from Mandushev et al. (1991) and McLaughlin & van der Marel (2005). Data points that correspond to the same clusters are connected with a dashed line.

Table 3.2. Literature CN Number Ratios

Sample	N	$\langle M_V \rangle$	$\langle r \rangle$
Kayser et al. (2008)	8	-6.19	0.61
Pancino et al. (2010)	12	-7.84	0.82
This study	8	-8.12	1.36
Smith & Mateo (1990)	16	-8.21	1.72

Note. — Mean CN number ratios from four samples of GCs as a function of absolute integrated magnitude. N indicates the number of clusters included in each sample.

include subgiants, dwarfs, and even AGB stars as well. Since dwarfs, with their hotter atmospheres, are less likely to show significant CN absorption, their inclusion may bias the value downward. The same holds true for the inclusion of AGB stars, since they are nearly always CN-weak (see Campbell et al., 2010, for further discussion). The study by Pancino et al. (2010), comprised entirely of MS dwarfs, reported an average of $r = 0.82 \pm 0.29$, while the average of the r values reported by Kayser et al. (2008) for the giants in their sample is 0.61. Together, these results indicate that for the clusters in their samples, both of which span a large range of [Fe/H] and luminosity, the CN-strong stars are in the minority. However, studies of Na and O abundances in cluster giants by Carretta et al. (2009c,b) suggest that the ratio is much higher, with enriched stars comprising 50–70% of the total ($r > 1$). The compilation by Smith & Mateo (1990) of giants from 16 clusters gives an average ratio of 1.72, which agrees well with Carretta et al. (2009b,c). While it is puzzling that two samples of cluster giants would yield such discrepant results, this may result from a bias toward more luminous clusters, since their inclusion would artificially inflate the fraction of CN-strong stars in the sample. Table 3.2 lists the mean r values alongside the mean M_V values for this sample and the three GCs from the literature. The increase in $\langle r \rangle$ with $\langle M_V \rangle$ is apparent, indicating that conclusions drawn based upon the CN ratio must

account for any potential biases from including or excluding massive GCs in the sample.

3.6 SUMMARY

I have used low-resolution SEGUE spectra to confirm the presence of a bimodality in the CN distributions for stars in GCs with $[\text{Fe}/\text{H}] > -2$. In addition, I extend the metallicity limit for which CN bimodality has been observed to at least $[\text{Fe}/\text{H}] \sim -2.1$, by adding M53 to the collection. Furthermore, I have presented evidence suggesting the presence of a much smaller division between CN-strong and CN-weak groups on the RGB of M92, down to luminosities corresponding to $M_V \sim 1.8$, which is in quantitative agreement with earlier studies suggesting carbon depletion setting in below the RGB bump. Evidence for two CN groups on the RGB of NGC 5053, with a similar metallicity as M92, also exists. Previous CN abundance studies of M92 have not shown strong evidence for bimodality, and NGC 5053 is reported on for the first time. I also confirm an overall anticorrelation between CN and CH bandstrengths on the RGB for M2, M13, and M3, for luminosities beyond the point of first dredge-up, while offering evidence that M92 may also display the same anticorrelation. The samples for M53 and M71 are too small to make strong claims for anticorrelations, although M53 appears to have CN and CH bandstrengths that are uncorrelated. Despite its chemical similarity to M92, no apparent CN-CH anticorrelation is present among M15 giants. Finally, NGC 5053 exhibits a remarkably uniform CH bandstrength along the RGB, in spite of the fact that this sample of stars straddles the RGB bump, where deep mixing is predicted to set in.

My observations support a scenario in which evolved stars disperse enriched gas throughout the cluster that ultimately forms a second generation of stars. This results in two chemically disparate populations of stars. Such abundance variations are not observed among even the oldest and most massive open clusters (Jacobson et al., 2008; Martell & Smith, 2009), presumably due to their significantly lower gravitational potentials preventing them

from retaining enriched gas from evolved stars. Furthermore, current theoretical models of the origin of light-element abundance variations rely heavily on the high density environments of proto-globular clusters to facilitate enrichment of subsequent stellar populations. Since these chemically enriched stellar populations appear to form preferentially in GCs, this motivates the argument that the presence of CN-strong stars in the Galactic halo may have been stripped from GCs into the field, rather than being the result of *in situ* formation (Martell & Grebel, 2010). Additional studies of halo GCs should provide an opportunity to explore and quantify this contribution directly.

CHAPTER 4:

EVIDENCE FOR MULTIPLE POPULATIONS IN SDSS GLOBULAR CLUSTERS

4.1 INTRODUCTION

Globular clusters have long been considered the canonical example of a simple stellar population – a population of stars that is chemically homogeneous and coeval. Though all stars within a single globular cluster (GC) tend to share the same Fe abundance, it has become clear in recent years that this uniformity is not observed in lighter elements. The explanation that has gained favor recently proposes the appearance of a second population of stars within the first few Myr after the cluster’s formation. The material contributing to the genesis of this second population is predicted to be ejecta from massive first generation stars, with intermediate-mass AGB stars (Ventura & D’Antona, 2008) or fast-rotating massive stars (Decressin et al., 2007b,a) as likely candidates. These have been implicated because of the required chemical makeup of the enriched gas out of which the second generation of stars is thought to have formed.

The hypothesis of an origin due to fast-rotating massive stars is relatively recent (Maeder & Meynet, 2006; Meynet et al., 2006; Decressin et al., 2007b) and as such is not without existing problems. In particular, for sufficiently deep rotational mixing to take place that brings CNO-processed material to the surface, models suggest the star must be rotating at or near the break-up velocity (Decressin et al., 2007b). Whether this is physically realistic has been drawn into question by observations of unenriched fast rotators in the Large Magellanic

Cloud by Hunter et al. (2008) which cast doubt on the efficiency of rotational mixing.

In the scenario involving asymptotic giant branch (AGB) stars, they are required to be the most massive AGB stars processing material via the hot CNO cycle through hot bottom burning at the base of the convective envelope (Ventura et al., 2001). Temperatures must be high enough that the ON cycle operates to reduce the O abundance and boost the N abundance in the envelope prior to third dredge-up, producing the observed enrichment in the second generation of stars. This envelope is then blown off the star into the intracluster medium at sufficiently low speeds as to be retained in the cluster's gravitational potential, provided that the cluster's mass is sufficiently high. One recent study by Conroy & Spergel (2011) has identified a potential lower limit of $\sim 10^4 M_\odot$, below which a cluster cannot retain gas against ram pressure from the local interstellar medium (ISM). In clusters more massive than this, modeling predicts that the gas should condense and form a cooling flow into the cluster core, where the second generation of stars is largely formed (D'Ercole et al., 2008).

As a GC ages and evolves, it initially experiences mass loss as a result of dynamical relaxation due to the loss of supernova ejecta from the first generation of stars (Chernoff & Weinberg, 1990; Fukushige & Heggie, 1995; Goodwin, 1996). As the first generation stars migrate beyond the cluster's tidal radius, they are stripped away, while the second generation stars remain roughly constant in number (D'Ercole et al., 2008). Therefore, the number ratio of enriched second generation stars to pristine first generation stars in a cluster should rise over time early in the cluster's history. In fact, D'Ercole et al. (2008) demonstrated using *N*-body simulations that the initial mass loss is so drastic that the cluster that is left behind may ultimately be dominated by second generation stars. Subsequent relaxation due to two-body interactions within the cluster then proceeds to mix the two generations of stars over timescales much longer than the dynamical timescale (see Spitzer, 1987; Meylan & Heggie, 1997, and references therein), but with the rate of further mass loss significantly reduced. Any mass loss due to two-body relaxation ought to affect both generations of stars

roughly the same.

Detections of differences in radial distributions between first and second generation stars in GCs have been reported previously for ω Cen (Pancino et al., 2003; Sollima et al., 2007; Villanova et al., 2007), NGC 1261 (Kravtsov et al., 2010b), NGC 1851 (Cassisi et al., 2008), NGC 3201 (Kravtsov et al., 2010a; Carretta et al., 2010a), NGC 6752 (Kravtsov et al., 2011), along with the collection of GCs by Lardo et al. (2011). These results were discovered using photometric data. In this chapter, evidence is investigated for multiple populations of stars within the GCs observed by the Sloan Digital Sky Survey using spectroscopic data.

4.2 THE DATA SET

I obtained photometric data from the Data Release 7 (DR7; Abazajian et al., 2009) of SDSS for the fields of eight Galactic GCs (M92, M15, NGC 5053, M53, M2, M13, M3, and M71). In addition, spectroscopic data for the fields of these clusters were obtained from the dataset produced by the Sloan Extension for Galactic Understanding and Exploration (SEGUE; Yanny et al., 2009), one of three sub-surveys that together formed SDSS-II.

True member stars were selected for these clusters using a variation of the color-magnitude diagram (CMD) mask algorithm described by Grillmair et al. (1995). Details on the application of this method to our specific clusters are described by Lee et al. (2008b) and Smolinski et al. (2011a) and will not be discussed here. The final data set of true member stars is also given in Lee et al. (2008b) and Smolinski et al. (2011a) and resulted in the following number of stars for each cluster: M92 (58), M15 (98), NGC 5053 (16), M53 (19), M2 (71), M13 (293), M3 (77), and M71 (8).

Spectroscopic line index measurements of the 3883 Å CN and 4300 Å CH molecular absorption bands were undertaken by Smolinski et al. (2011b) for these stars at all evolutionary stages using the Norris et al. (1981) S(3839) definition for RGB and SGB stars and that of Harbeck et al. (2003a) for MS stars. Smolinski et al. (2011b) identified CN bimodality

among globular cluster giants for all clusters with $[Fe/H] > -2.1$. Among the three GCs with metallicities below this (M92, M15, and NGC 5053), while it was more difficult to clearly demonstrate two distinct CN groups, suggestions of two groups did appear in M92 and NGC 5053. Figures 3.1 and 3.2 show the position of these sample stars on the reddening-corrected g_0 versus $(g - r)_0$ CMD. I make use of the photometry for these member stars from Lee et al. (2008b) and Smolinski et al. (2011a) and the line index measurements from Smolinski et al. (2011b) in this chapter.

4.3 CMD DISTRIBUTIONS

As discussed in Smolinski et al. (2011b), the CN groups in the three most metal-poor clusters (M92, M15, and NGC 5053) were difficult to distinguish and the adopted divisions on the RGB were identified by a linear fit to the total CN distribution (as done by Shetrone et al., 2010) and not via any clearly visible bimodality in a generalized histogram. However, these groups are more apparent in M15 and NGC 5053, as well as most other GCs in this sample, when one looks at the u_0 versus $(u - g)_0$ CMDs, shown in Figure 4.1 and 4.2. On the RGB, the CN-strong stars (red triangles) clearly fall on the red (right) side while the CN-weak stars (blue circles) populate the blue (left) side. While it is difficult to consider these figures beyond a visual inspection due to the relatively small sizes of one or both groups in many clusters, Figures 4.3 – 4.5 show cumulative distributions (and Kolmogorov-Smirnov (K-S) test p -values) of $(u - g)_0$ color where the sample sizes were large enough and provided sufficiently broad color coverage for M15, M13, and M3. Applying a Kolmogorov-Smirnov (K-S) test, one can reject the null hypothesis (that the two distributions are drawn from the same sample) for M15 and M13 with high probability. In the case of M3, the null hypothesis cannot be rejected but, upon inspection of Figure 4.2, this may simply be due to the non-uniform color coverage of CN-weak stars at the blue (low values of $u - g$) end. The overall observation of a color dichotomy is not unexpected, as the enhanced presence of metals in

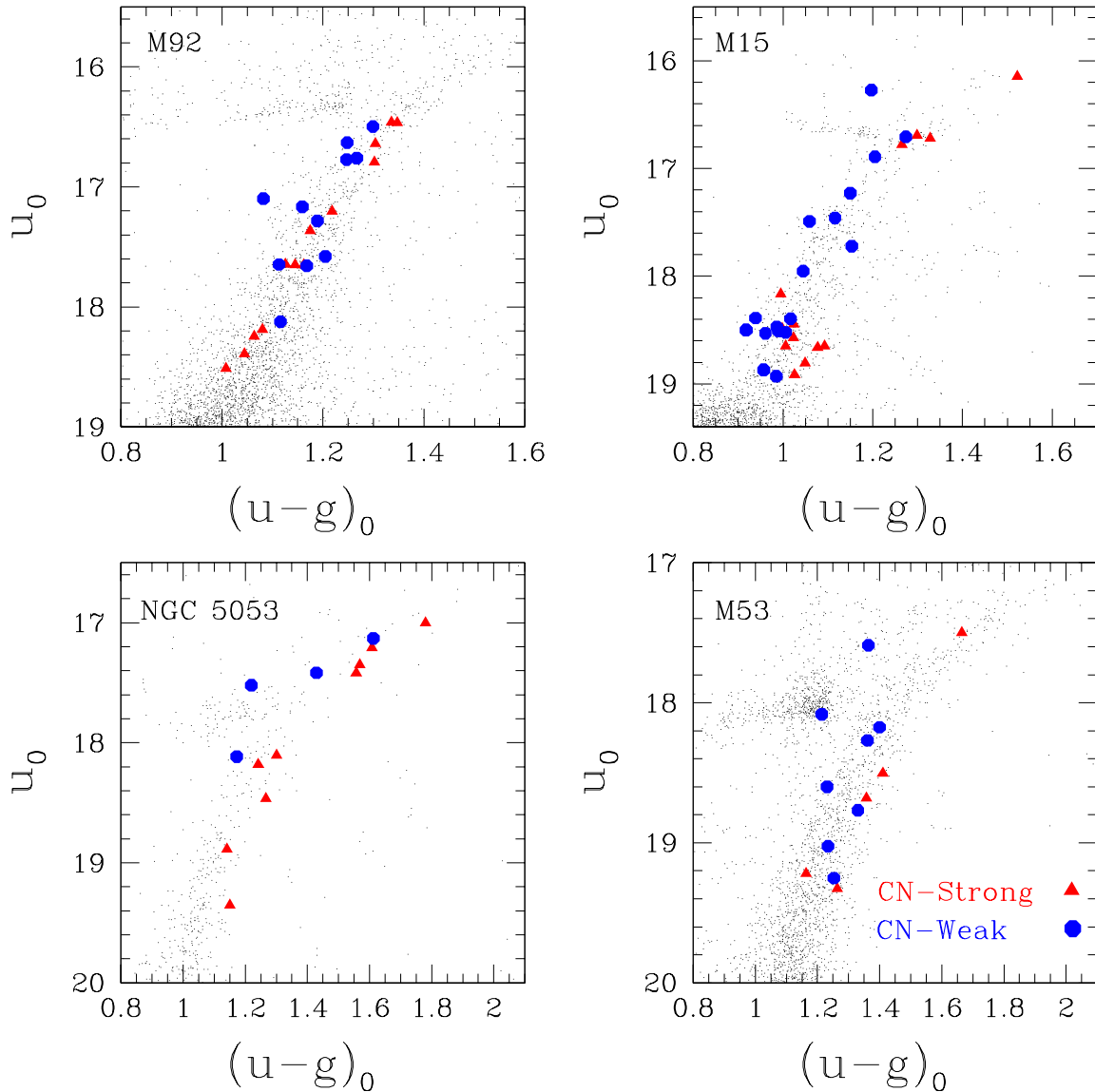


Figure 4.1 u_0 vs. $(u-g)_0$ CMDs for M92, M15, NGC 5053, and M53 from SDSS photometry. The spectroscopic data is plotted as colored points, divided by CN absorption strength where blue circles represent CN-weak stars and red triangles represent CN-strong stars. Other than M92, the two groups generally populate opposite sides of the RGB.

a stellar atmosphere is known to produce a redder spectrum due to increased absorption at blue wavelengths and has been seen before in spectroscopic analysis of elemental abundances in GC stars (e.g. Marino et al., 2008b; Milone et al., 2010). Additionally, Carretta et al. (2010a) showed a definitive spread in $U - B$ color between first and second generations in the cluster NGC 3201. In earlier studies and this study, the dichotomy is visible even down to the base of the RGB in many clusters, indicating that the two abundance groups are present well before any mixing is expected to happen. Figure 4.6 demonstrates that this bandstrength dichotomy is even present on the SGBs of M92, M2, and M13, though the color differentiation is not seen in the same manner as on the RGB.

This can also be demonstrated by examining the ratio of CN-strong stars to CN-weak stars along the length of the RGB. To do this effectively, it was necessary to have adequate sampling at all luminosities to provide for meaningful counting uncertainties. The RGBs of M13 and M3 provided ample numbers of stars for this test. Figures 4.7 and 4.8 show the results of this calculation. The stars on the RGB were divided up into bins containing equal numbers of stars (where the bin sizes are indicated by the vertical lines) and the Poisson errors were calculated for each CN ratio (indicated by the horizontal lines). Within the calculated uncertainties, there appears to be no indication that the CN ratio, and thus the chemical bimodality, is related to the evolutionary stage along the RGB. This procedure was done twice for each cluster using different numbers of bins, which produced similar results. One can therefore conclude that the distinct CN populations are present prior to any mixing that might happen and are not significantly impacted by evolution up the RGB.

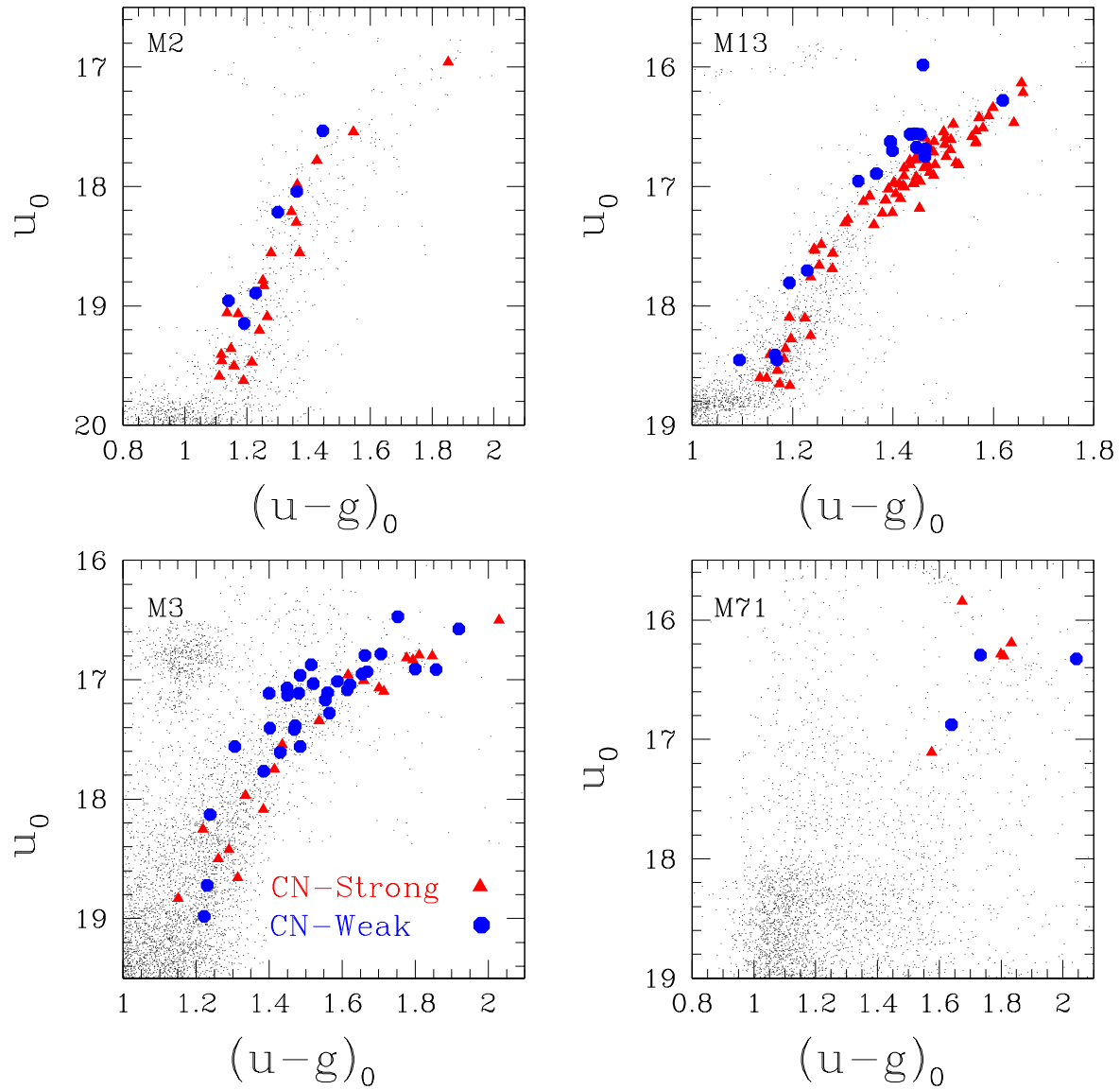


Figure 4.2 Same as Figure 4.1 but for M2, M13, M3, and M71.

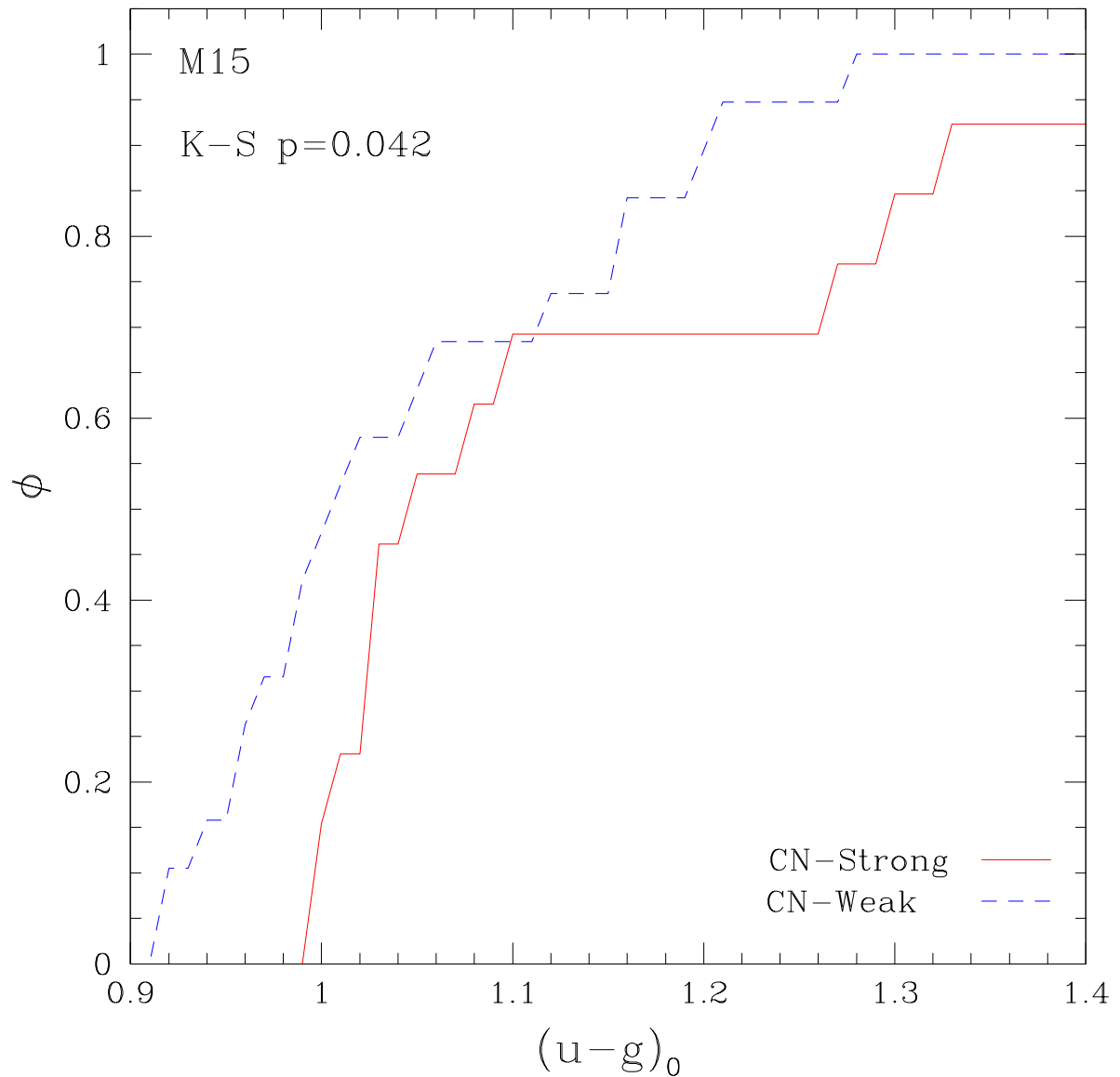


Figure 4.3 Cumulative distributions of $(u-g)_0$ colors of CN-weak (dashed blue line) and CN-strong (solid red line) populations in M15. The Kolmogorov-Smirnov p -value is shown in the upper-left corner.

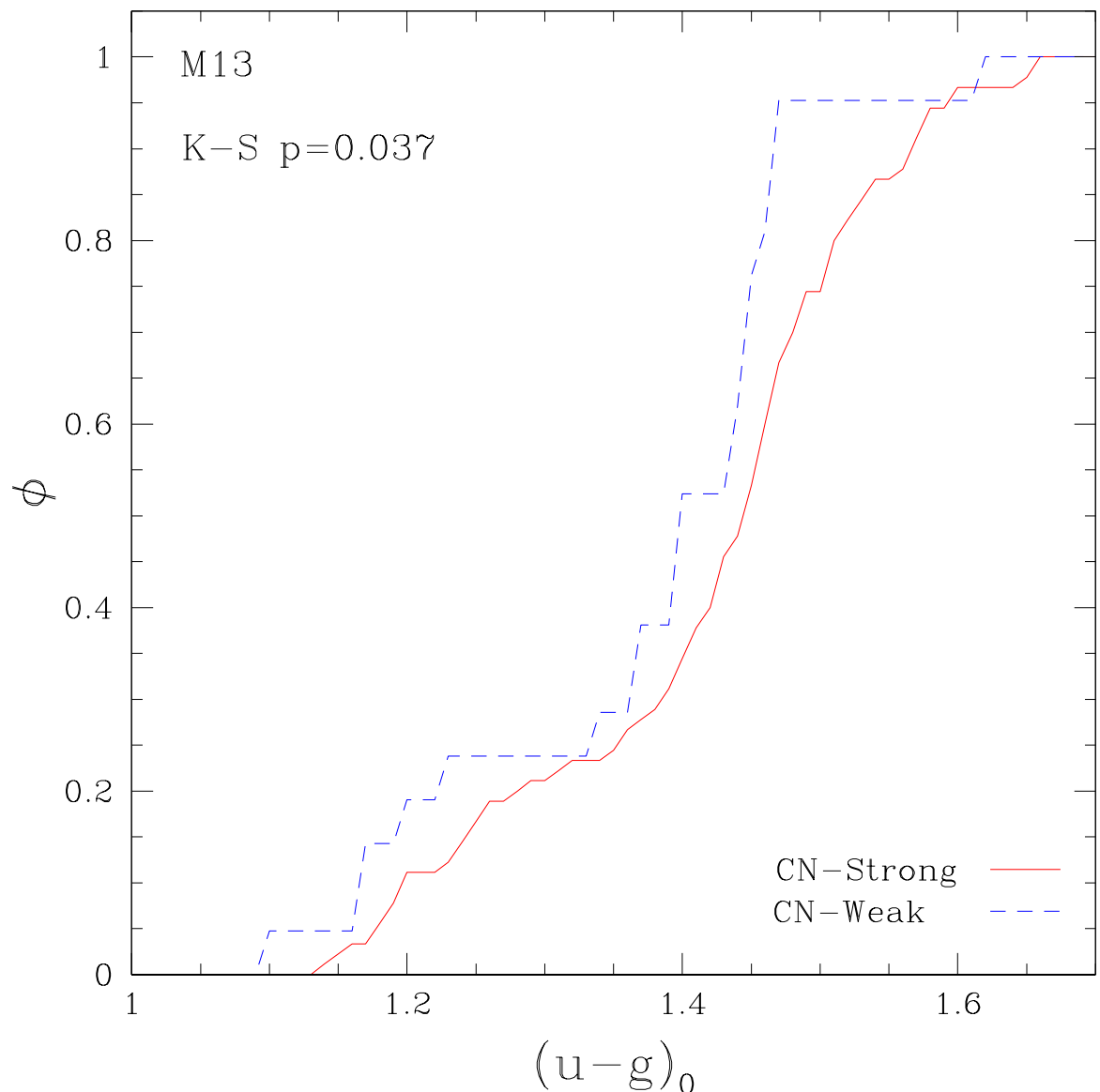


Figure 4.4 Same as Figure 4.3, but for M13.

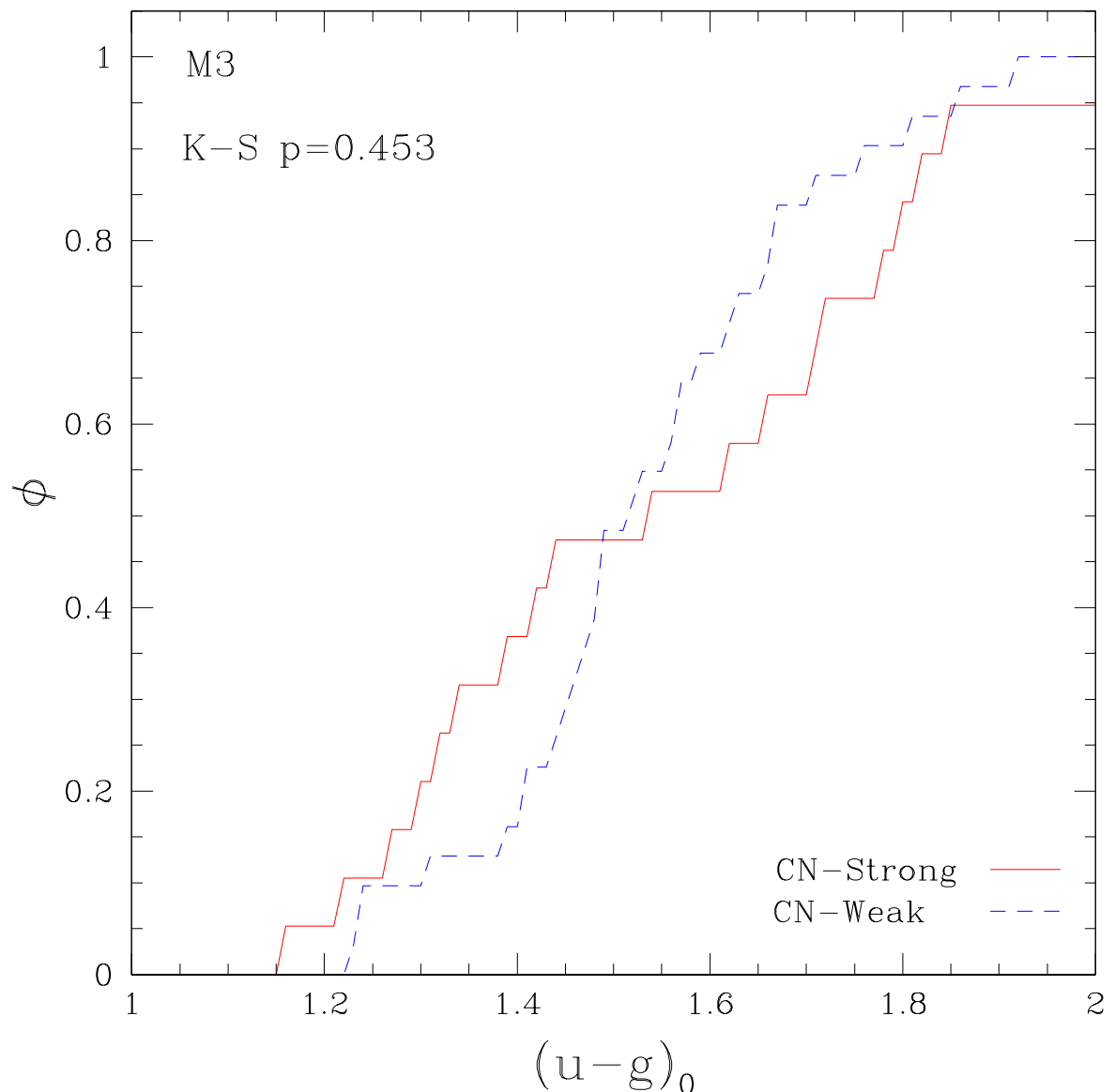


Figure 4.5 Same as Figure 4.3, but for M3.

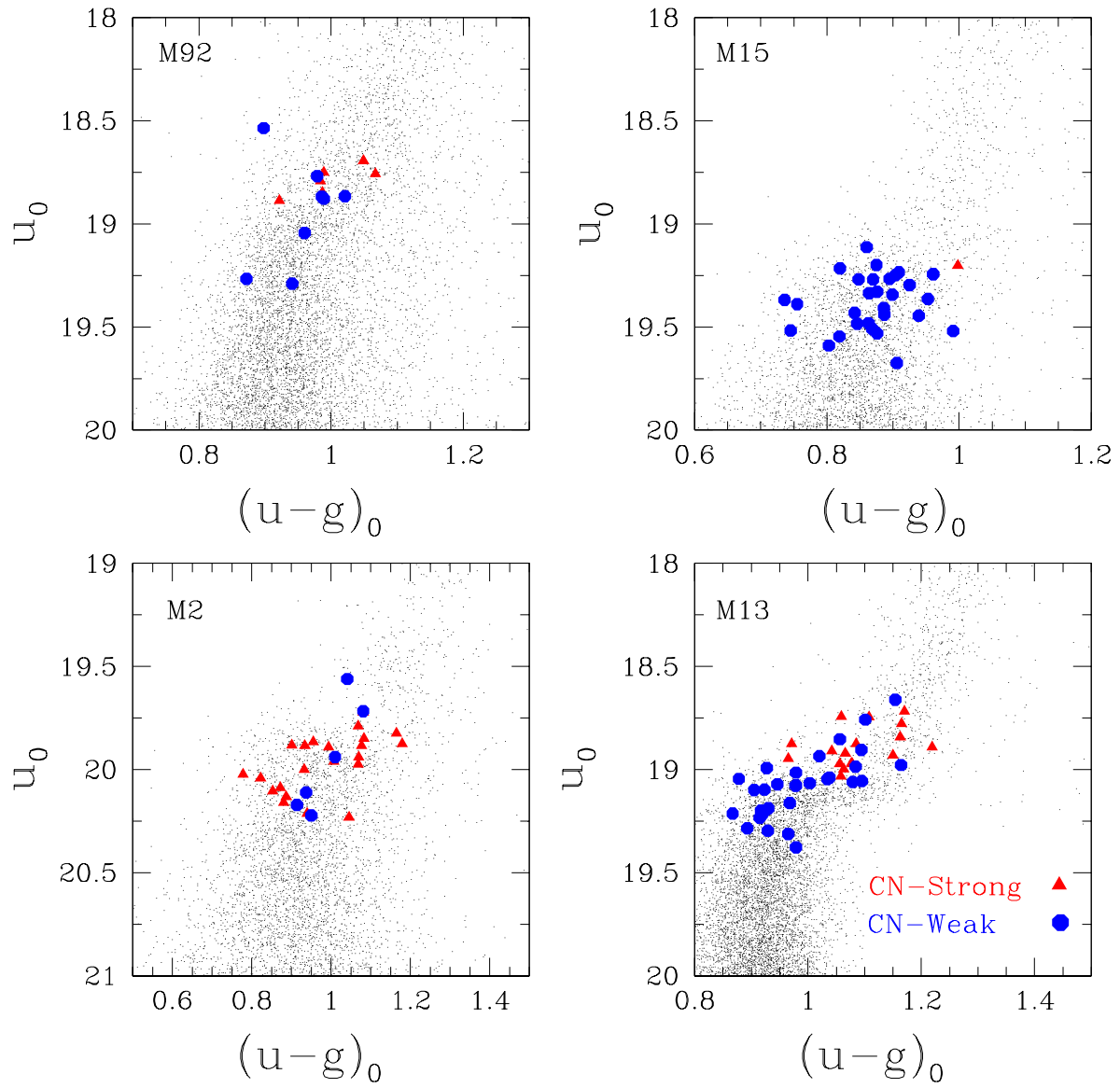


Figure 4.6 Same as Figure 4.1 but for SGB stars in M92, M15, M2, and M13. One sees indications of CN variations on the SGBs of three out of four clusters.

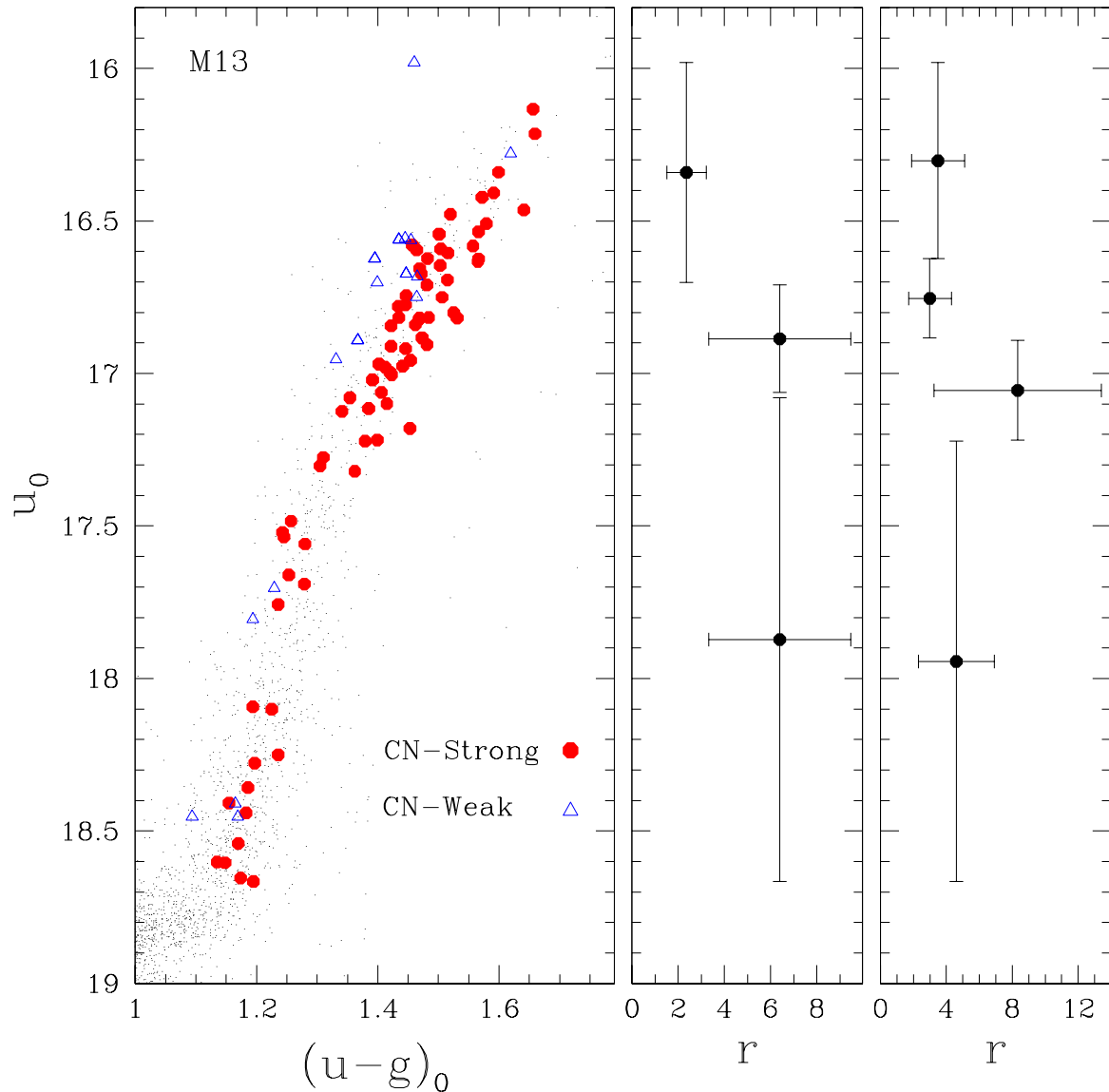


Figure 4.7 Ratio of CN-strong stars (red filled circles) to CN-weak stars (blue open triangles) along the RGB of M13. The left panel shows the distribution along the CMD, while the other panels show the CN ratio when divided into 3 (middle panel) and 4 (right panel) bins containing an equal number of stars. The vertical bars show the width of the bins, while the horizontal bars indicate the Poisson uncertainties associated with each ratio.

4.4 RADIAL DISTRIBUTIONS

Numerical simulations were done by D’Ercole et al. (2008) to study the dynamical evolution of the stellar population within a GC. The results of their simulations revealed that a substantial second generation of stars can form from gas expelled by AGB stars, forming a second generation of stars initially concentrated in the cluster core, and that the ratio of second generation to first generation stars changes over time in response to internal dynamical effects. Furthermore, they demonstrated that while two-body interactions over the course of a cluster’s lifetime do contribute to mass loss, the effect over a Hubble time is negligible and, instead, mass loss associated with supernova explosions is a significant factor in determining the initial ratio of second generation to first generation stars. This showed that the majority of stars that are lost by a cluster are first generation stars, an effect which is capable of producing a cluster that is ultimately dominated by second generation stars, and that two-body relaxation is capable of effectively mixing the two generations of stars that remain.

If these simulations are correct, then one might expect to see indications of a centrally-concentrated CN-enriched population. While dynamical studies by D’Ercole et al. (2008) and Decressin et al. (2010) demonstrate that a second generation of stars can potentially form in the cluster core, two-body relaxation is an important factor in determining what the GC will look like after $\sim 10^{10}$ years. The pertinent timescale is the two-body relaxation time, which measures the time required for deviations from a Maxwellian distribution to be significantly decreased (Spitzer, 1987). This timescale can be defined in several ways. A general definition from Spitzer (1987, Eq. 2-62) is

$$t_{relax} = \frac{0.065 \langle v_m^2 \rangle^{3/2}}{\rho \langle m \rangle G^2 \ln \Lambda}, \quad (4.1)$$

$$= 3.4 \times 10^9 \frac{[v_m(\text{km/s})]^3}{[m/M_\odot]^2 n(\text{pc}^{-3}) \ln \Lambda} \text{ years},$$

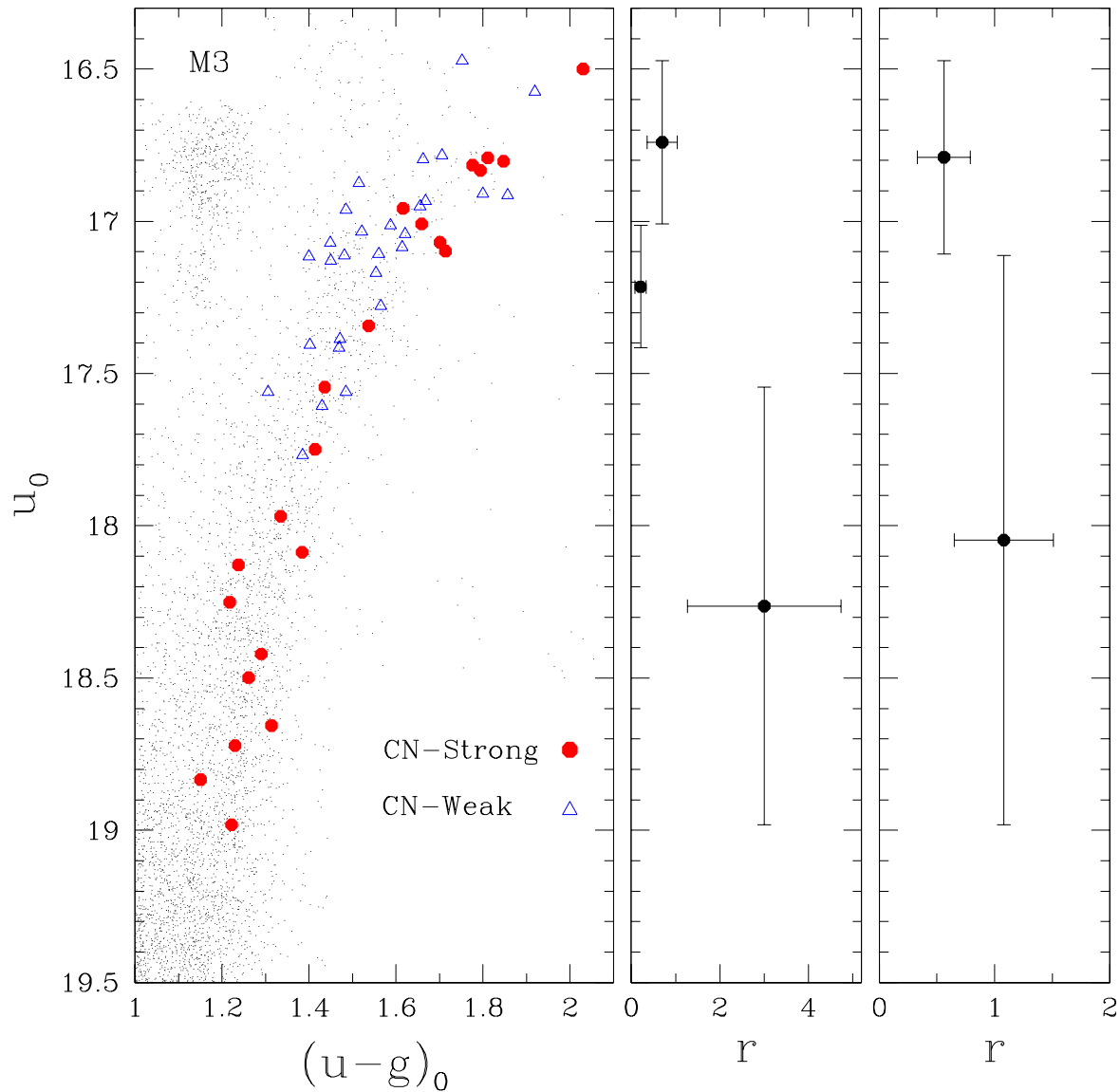


Figure 4.8 Same as Fig. 4.7 but for M3. In this case, the RGB was divided into 3 (middle panel) and 2 (right panel) bins containing an equal number of stars.

where $\langle v_m^2 \rangle$ is the mass-weighted mean square velocity of the stars, ρ is the mass density, $\langle m \rangle$ is the mean stellar mass, and $\Lambda \approx N$ (Binney & Tremaine, 1987), where N is the number of stars in the cluster.

Alternatively, theorists define a *half-mass relaxation timescale*

$$t_{relax,h} = \frac{0.138 M^{1/2} r_h^{3/2}}{\langle m \rangle G^{1/2} \ln \Lambda} \quad (4.2)$$

$$= 1.7 \times 10^5 \frac{[r_h(\text{pc})]^{3/2} N^{1/2}}{[m/M_\odot]^{1/2}} \text{ years}$$

(Spitzer, 1987; Meylan & Heggie, 1997), where typical values range from 3×10^7 to 2×10^{10} years (Djorgovski & Meylan, 1993). The half-mass relaxation timescale depends less on the evolution of the cluster and the density within the adopted radius. Comparing these timescales with the current ages of known Galactic GCs of $\sim 10^{10}$ years, one arrives at the conclusion that a GC is typically well-described as a relaxed system and two-body interactions should have effectively mixed the stars. This is confirmed by the N -body simulations of D'Ercole et al. (2008) that show a flattening radial profile of the ratio of second generation to first generation stars over time (see their Fig. 18). Nevertheless, studies by Lardo et al. (2011) and Kravtsov et al. (2011) have provided observational evidence for the existence of a radial segregation between first and second generation populations. These conclusions are drawn indirectly using photometric data, utilizing $u-g$ or $U-B$ color spreads that have been previously correlated with light-element abundance variations. They found that the stars on the red side of the color spread along the RGB (which correlate with elemental abundance enhancement) tend to be more centrally concentrated.

Using this data, one can directly probe the distributions of apparent CN abundances without requiring photometry. Figure 4.9 shows the radial distributions of CN-strong (filled symbols) and CN-weak (open symbols) RGB (red circles) and SGB (blue triangles) stars in this sample. Ideally, one would prefer uniform coverage over the full radial range with a

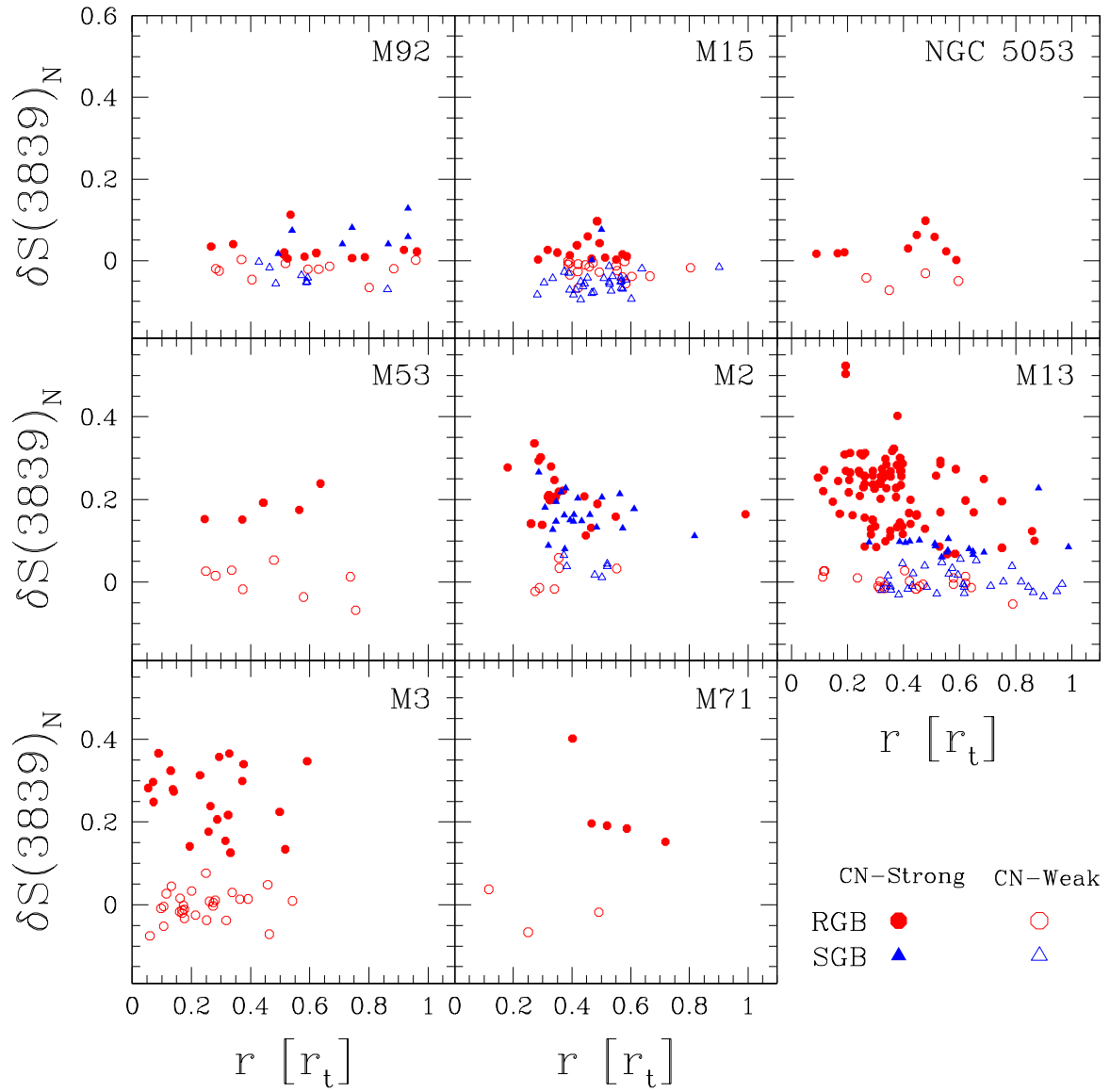


Figure 4.9 Radial distribution of RGB (red circles) and SGB (blue triangles) stars within each cluster, divided into CN-strong (filled symbols) and CN-weak (open symbols) groups.

large number of stars. For this reason, one cannot make a claim from this diagram for many of these clusters. However, M13 does appear to demonstrate a strong central concentration of CN-strong RGB stars. M2 also shows hints of a similar distribution, though the radial coverage is lacking. Unfortunately, when the radial axis is changed to units of the half-light radius r_h , shown in Figure 4.11, it is clear that the radial scales probed by the D’Ercole et al. (2008) simulations are not represented in our sample, thereby making direct comparisons with simulation results difficult.

One can gain a better sense of the statistical significance of these distributions by doing a K-S test and comparing the cumulative radial distributions, shown in Figure 4.10. For clusters such as NGC 5053, M53 and M71 where the sample sizes are small, these figures are less meaningful, but where the sample sizes are larger comparisons can be made. Shown with each pair of cumulative distributions is the K-S probability, where small values indicate that the two data sets are significantly different. The K-S probability for M13 indicates that one can reject the null hypothesis at high statistical confidence. In the cases of M92, M15, M2, and M3, one can only claim that the two groups are statistically similar.

Contrasting Figure 4.10 with Figures 4.3 – 4.5 illustrates the quandary in distinguishing individual generations of stars in GCs separated in age by a cosmologically short amount of time (D’Ercole et al., 2008). Simulations suggest that relaxation should have sufficiently mixed the stellar populations over a Hubble time such that no central concentration ought to be apparent (D’Ercole et al., 2008), as appears to be the case in Figure 4.10, implying that color and compositional differences are the only way to detect them. Yet, Lardo et al. (2011) and Kravtsov et al. (2011) demonstrate significant central concentration in their identified second-generation stars. This is particularly interesting considering that the Lardo et al. (2011) study utilized SDSS photometric data for, among others, M92, M15, M53, M2, and M13, and showed them all to have UV-red stars (interpreted to be Na-enriched and ostensibly second generation) that preferentially populate the cluster cores. The inconsistency between theory and observation, and in this specific case the inconsistency

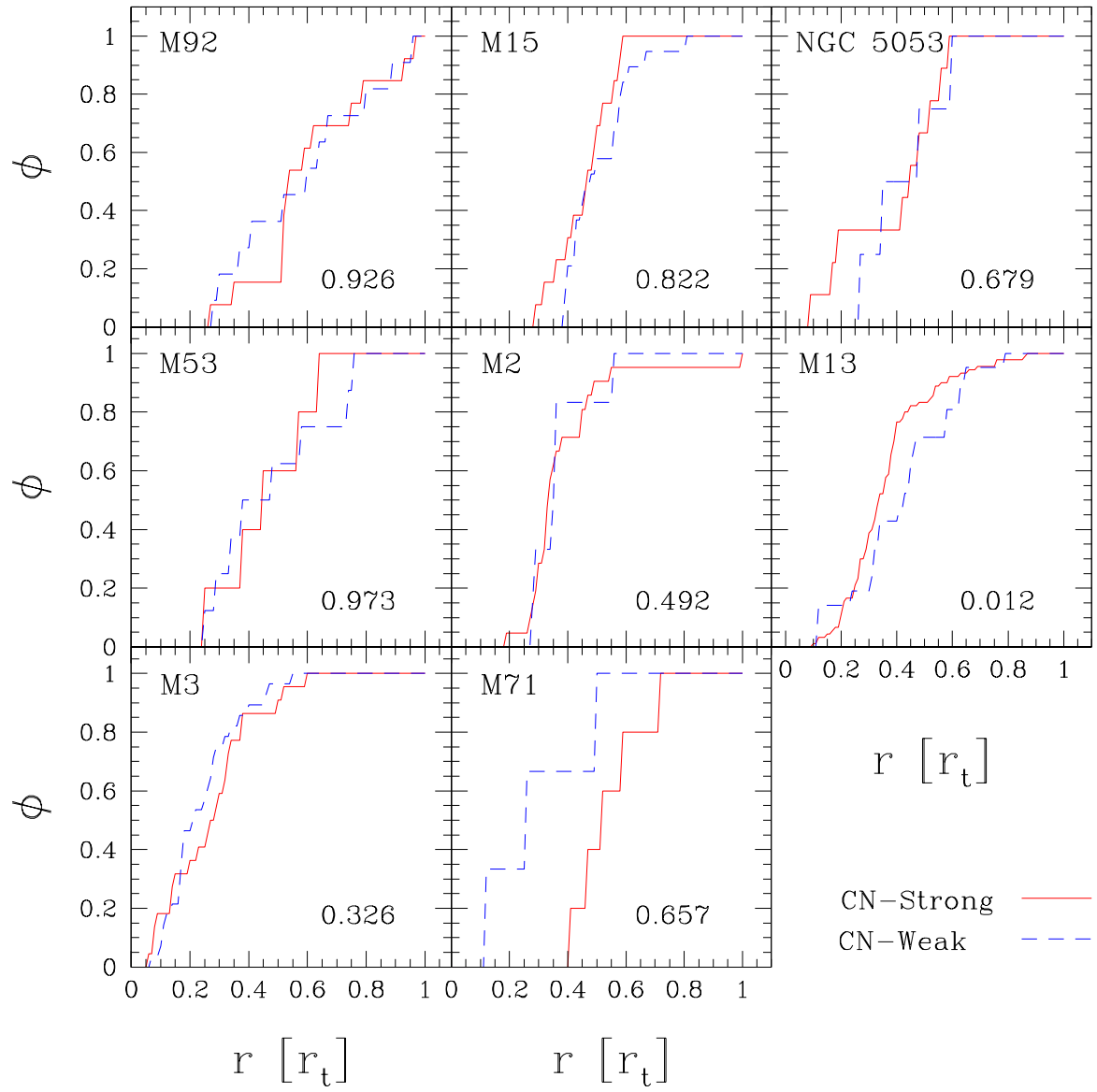


Figure 4.10 Cumulative radial distribution of CN-strong (solid red line) and CN-weak (dashed blue line) stars in each cluster, in units of the tidal radius. The K-S probability is shown in the lower-right corner of each panel.

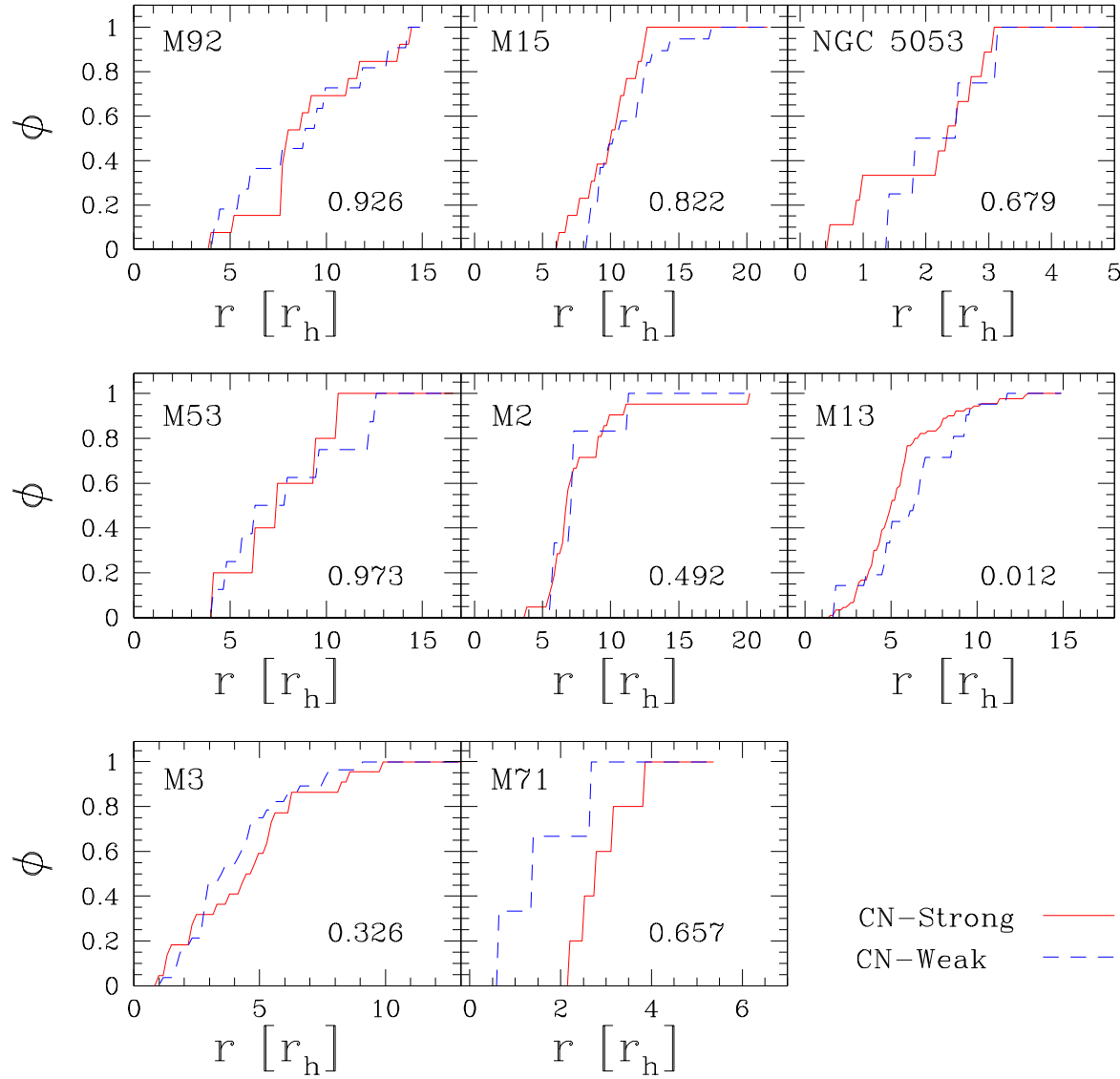


Figure 4.11 Cumulative radial distribution of CN-strong (solid red line) and CN-weak (dashed blue line) stars in each cluster, in units of the half-light radius. The K-S probability is again shown in the lower-right corner of each panel for reference.

between my spectroscopic and the Lardo et al. (2011) photometric samples, regarding radial distributions of the individual generations is currently still being debated and further study, particularly with larger spectroscopic samples providing more uniform and complete radial coverage, is needed before the question can be accurately addressed.

4.5 SUMMARY

Drawing from the work of Smolinski et al. (2011b), I have further investigated the spectroscopic and photometric analysis of member stars in my sample of eight Galactic GCs. I have demonstrated the existence of a color dichotomy related to CN bandstrength on the RGBs of every cluster except M92 and M71, and have shown that, in M13 and M3, the presence of two distinct groups is independent of evolutionary effects along the RGB.

I have also investigated the radial distributions of the CN-rich and CN-weak groups. While the spatial sampling of stars in most of these clusters limits my ability to make any definitive claims, I do see evidence suggesting a centrally concentrated population of CN-enriched stars in M13. It is worth noting, though, that the absence of central concentration is supported by the D’Ercole et al. (2008) simulations despite its incompatibility with the photometric observations of Lardo et al. (2011).

Connecting my results with those in the literature, it appears that two different stellar populations may exist in most clusters in this sample, based on radial distributions in M13 and photometric $(u - g)_0$ scatter along the RGB that is consistent with that reported previously in the literature (e.g. Marino et al., 2008b; Bragaglia et al., 2010; Carretta et al., 2010a; Lardo et al., 2011). While M71 suffers from a limited sample size and poor photometry, I am confident that further observations will reveal the same for this cluster as well. Further observations performed in a more spatially uniform manner are needed to determine whether one can use the observed radial dependence of the CN ratio to determine the mixing history of a cluster.

CHAPTER 5: CONCLUSIONS AND FUTURE WORK

5.1 RESULTS OF THIS STUDY

This Dissertation has presented the results of a spectroscopic and photometric investigation of globular cluster stars in the Sloan Digital Sky Survey. In Chapter 2, I have described the procedure used for identifying true member stars and have demonstrated that it produces [Fe/H] and RV measurements that are consistent with those published previously in the literature for these particular clusters, even at super-solar metallicities.

I have also studied 3883 Å CN and 4300 Å CH molecular line absorption in all cluster members in this sample. Since molecular absorption has been observed in the past to show star-to-star variations among cluster members, it is of particular interest to determine the fundamental cause of this phenomenon. While abundance variations have been clearly observed in clusters with moderate metallicity, it has not yet been convincingly demonstrated in low-metallicity clusters ($[{\rm Fe}/{\rm H}] < -2.1$). In Chapter 3, I confirmed the presence of CN bimodality in all clusters with $[{\rm Fe}/{\rm H}] > -2.1$, adding M53 to the list of clusters with confirmed CN bimodality, but also provided evidence for low-metallicity CN variation on the RGB of M92 and NGC 5053. In addition, I showed indications of CN variations among SGB stars in M92, M2, and M13, thus confirming that surface abundance variations are not strictly a result of evolutionary processes but must have been present at the time the enriched stars formed. CN-CH anticorrelations were also shown which demonstrate that the enrichment is related to CNO-processing, the products of which are only accessible to subsequent generations of stars if they have been brought to the surface via physical

mixing mechanisms and, most likely, blown off of their original stars prior to having been incorporated into a second generation of stars.

The observations of CN bimodality in GCs, as well as the observed light-element abundance variation patterns, are most easily explained by the formation of a second generation of stars shortly after the appearance of the first. In Chapter 4, I investigated further this hypothesis by looking for evidence that the CN-enriched group is likely to be a distinct population of stars. I showed that the spectroscopic sample does appear to be dichotomous on the u_0 vs. $(u-g)_0$ CMD, with the CN-strong stars on the red side and the CN-weak stars on the blue side. Additionally, I showed the radial distributions of the two groups in each cluster and, though my sample sizes were limited, provided evidence that the CN-enriched group in M13 appears to be centrally concentrated with respect to the CN-weak group.

5.2 IMPLICATIONS

These observations taken together support the scenario where enriched gas was ejected from an initial population of GC stars into the intracluster medium, whereupon it cooled and flowed in to the cluster core. This cooling flow then produced a second generation of stars which were enriched in light elements while maintaining typical cluster abundances in heavier elements, thus producing bimodal distributions of anticorrelated light element groups in the population as a whole. Subsequent two-body interactions allowed the cluster to relax, while mixing the two generations together, erasing much of the initial core concentration.

5.3 FUTURE WORK

While the two-generation scenario appears to elegantly answer many questions we have about GCs in the Milky Way, it will be necessary to look outside the Galaxy for confirmation since it appears that there are no concrete examples of proto-GCs “caught in the act” of forming within our own Galaxy. However, galaxies like M31 and the LMC harbor large

numbers of young and intermediate-age GCs which, given the sufficient advancement of observing resolution and instrumentation (or the development of tools that allow us to identify CN bimodality from integrated light spectra), may provide insight about whether or not current formation conditions allow the development of CN bimodality. Additionally, studying low-mass, young extragalactic GCs can provide constraints on any lower mass limit to the efficient formation of a second generation of cluster stars.

As noted in Chapter 3, measuring double-metal molecular line absorption is difficult in metal-poor clusters where the abundances of both species are significantly diminished. This makes detection of any signatures of bimodality extremely difficult. One way this problem could be alleviated is through detailed abundance analysis of stars in metal-poor GCs. Obtaining measurements of [C/Fe] and [N/Fe] for stars in metal-poor halo GCs can allow us to answer the question of whether or not there exists a low-metallicity cutoff for CN bimodality and light-element abundance variations. However, this would require a dedicated spectroscopic survey with the means of easily measuring spectra for large numbers of stars from the cluster core to the tidal radius, followed up by a software pipeline that could quickly and accurately perform detailed abundance analysis to derive the desired abundances.

Finally, while we seem to be getting an idea of what the picture looks like, there are \sim 150 GCs in the Milky Way Galaxy and these types of observations have been done for less than half, mostly in the Northern Hemisphere. Surveys of high-metallicity GCs near the Galactic bulge, additional low-metallicity GCs in the Galactic halo, and more Southern Hemisphere GCs may provide further data to help clarify the details. As for the clusters that have currently been observed, most reports of multiple generations of stars rely on photometric observations. Additional spectroscopic follow-up on larger numbers of stars (> 300) in each cluster will also help provide statistical certainty to the results they produce.

APPENDICES

APPENDIX A: ATMOSPHERIC PROPERTIES OF ADOPTED TRUE MEMBER STARS

A.1 ATMOSPHERIC PARAMETERS DATA TABLE

Based on the membership selection procedure outlined in Chapter 2, I have prepared the following tables (Tables A.1 and A.2) of SSPP-derived atmospheric parameters for the adopted true member stars of the GCs and OCs in this sample and that of Lee et al. (2008b). Column 1 lists the spSpec name, which identifies the star on the spectral plate in the form of spectroscopic plug-plate number (four digits), Modified Julian Date (five digits), and fiber used (three digits). For details on how the uncertainties in these parameters are estimated, see Lee et al. (2008a). Values with an ellipsis were problematic and have been omitted.

Table A.1: Atmospheric Properties of Adopted True Member Stars

spSpec name	α (deg)	δ (deg)	RV (km s ⁻¹)	T _{eff} (K)	$\log g$	[Fe/H]
M92						
2247-54169-361	259.05270	43.17390	-115.19037	3.18	-2.09	
2247-54169-362	259.04869	43.06008	-113.85461	3.06	-2.09	

Continued on next page...

Table A.1 – Continued

spSpec name	α (deg)	δ (deg)	RV (km s $^{-1}$)	T _{eff} (K)	$\log g$	[Fe/H]
2247-54169-364	259.08213	43.24025	-104.6	5391	3.27	-2.29
2247-54169-367	259.10185	43.19566	-112.0	5372	2.92	-2.13
2247-54169-379	259.22175	42.99835	-117.5	6474	3.56	-2.48
2247-54169-380	259.12453	43.10090	-109.5	5286	2.59	-2.34
2247-54169-404	259.14868	43.20253	-111.9	5364	2.28	-2.19
2247-54169-408	259.15160	43.11560	-120.0	5135	2.26	-2.42
2247-54169-409	259.18316	43.10430	-120.3	6301	3.97	-2.12
2247-54169-418	259.19255	43.08290	-119.6	5141	2.43	-2.19
2247-54169-444	259.17824	43.24650	-112.3	5311	2.35	-2.41
2247-54169-449	259.20122	43.17130	-116.5	5234	2.13	-2.26
2247-54169-451	259.26814	43.06960	-121.9	5355	2.83	-2.25
2247-54169-452	259.18977	43.22959	-121.4	5291	2.10	-2.38
2247-54169-458	259.20611	43.21507	-126.6	5734	2.99	-2.11
2247-54169-484	259.14905	42.94427	-115.0	5081	2.12	-2.43
2247-54169-504	259.34715	42.94880	-112.1	5124	2.11	-2.29
2247-54169-514	259.29469	42.90065	-111.3	5598	2.53	-2.38
2247-54169-516	259.32981	42.96344	-120.5	5742	2.20	-2.25
2247-54169-519	259.29888	42.91809	-120.6	5720	3.80	-2.23
2247-54169-529	259.24274	43.26023	-113.6	5445	3.24	-2.20
2247-54169-531	259.31297	43.26453	-115.2	5357	2.81	-2.22
2247-54169-538	259.34134	43.25804	-107.6	5899	2.69	-1.94
2247-54169-541	259.43884	43.03566	-129.2	5586	2.96	-2.03

Continued on next page...

Table A.1 – Continued

spSpec name	α (deg)	δ (deg)	RV (km s $^{-1}$)	T _{eff} log g	[Fe/H]
2247-54169-546	259.35424	43.02288	-117.75446	2.78	-2.33
2247-54169-561	259.34981	43.12020	-114.25354	2.78	-2.32
2247-54169-563	259.32958	43.21520	-111.75212	2.44	-2.34
2247-54169-573	259.32140	43.07420	-116.35414	2.77	-2.28
2247-54169-575	259.38118	43.24689	-111.45765	3.85	-2.33
2247-54169-581	259.39378	43.07110	-110.55357	2.17	-2.29
2247-54169-582	259.43614	43.09974	-123.27700	3.42	-1.99
2247-54169-584	259.48440	43.05953	-103.45613	2.58	-2.39
2247-54169-589	259.43215	43.06340	-114.75343	2.17	-2.38
2247-54169-608	259.45984	43.22947	-120.35150	2.44	-2.20
2247-54169-610	259.51967	43.17119	-117.25109	2.15	-2.23
2247-54169-616	259.39054	43.18959	-115.45749	2.71	-1.99
2247-54169-620	259.43737	43.13558	-103.95584	3.01	-2.10
2256-53859-411	259.06782	43.11078	-120.36407	3.52	-2.31
2256-53859-455	259.11098	43.06094	-108.66584	3.72	-2.14
2256-53859-485	259.15452	42.99086	-109.56573	3.76	-1.95
2256-53859-489	259.20858	42.99146	-128.56623	3.58	-2.22
2256-53859-501	259.37101	43.02222	-109.56623	4.16	-2.58
2256-53859-506	259.31541	43.02145	-111.16686	3.65	-2.04
2256-53859-513	259.29469	42.90065	-118.05604	2.55	-2.32
2256-53859-522	259.21141	43.23125	-116.76047	3.00	-2.40
2256-53859-530	259.36776	43.25074	-124.96550	3.73	-2.22

Continued on next page...

Table A.1 – Continued

spSpec name	α (deg)	δ (deg)	RV (km s $^{-1}$)	T _{eff} (K)	$\log g$	[Fe/H]
2256-53859-535	259.31357	43.28081	-123.1	6412	3.94	-2.48
2256-53859-536	259.28945	43.28023	-127.9	6342	3.80	-2.17
2256-53859-537	259.42460	43.12058	-112.4	6149	3.67	-2.17
2256-53859-538	259.38004	43.21048	-120.7	5567	3.27	-2.34
2256-53859-539	259.34059	43.24915	-113.1	6427	2.27	-2.49
2256-53859-546	259.48196	43.01234	-124.7	6647	4.02	-2.49
2256-53859-566	259.38565	43.03733	-115.0	6699	4.06	-2.05
2256-53859-571	259.45784	43.06219	-122.9	6528	3.81	-2.29
2256-53859-575	259.44647	43.32046	-100.6	6587	2.90	-2.49
2256-53859-576	259.43562	43.17233	-109.1	6633	3.80	-2.25
2256-53859-579	259.39772	43.05123	-112.4	6665	3.50	-2.33
2256-53859-612	259.48383	43.20252	-115.4	6654	4.03	-2.31
M15						
1960-53289-401	322.4521790	12.338844	-108.2	5227	2.36	-2.34
1960-53289-402	322.4679565	12.327691	-107.0	5050	2.06	-2.31
1960-53289-406	322.4168396	12.266688	-101.3	5059	1.71	-2.36
1960-53289-413	322.4143066	12.305798	-103.8	5160	1.98	-2.44
1960-53289-419	322.4579773	12.303373	-111.0	5064	2.23	-2.39
1960-53289-420	322.6591187	12.145007	-92.5	5961	3.57	-2.25
1960-53289-441	322.5975342	12.257596	-114.5	5427	2.42	-2.75
1960-53289-442	322.5028076	12.375646	-119.5	5170	2.32	-2.33
1960-53289-457	322.5315247	12.312680	-113.7	5568	2.47	-2.27

Continued on next page...

Table A.1 – Continued

spSpec name	α (deg)	δ (deg)	RV (km s $^{-1}$)	T _{eff} (K)	$\log g$	[Fe/H]
1960-53289-459 322.7053528	12.125361		-105.5	5222	2.12	-2.38
1960-53289-460 322.7267761	12.119604		-101.3	5343	2.62	-2.39
1960-53289-500 322.4296570	12.004886		-106.9	5457	2.64	-2.29
1960-53289-501 322.5649414	11.992488		-83.7	5732	2.61	-2.23
1960-53289-511 322.5564575	12.010468		-112.2	5364	2.24	-2.40
1960-53289-522 322.6466675	12.302749		-110.3	5387	2.01	-2.46
1960-53289-523 322.5946350	12.299892		-104.6	4930	1.93	-2.27
1960-53289-529 322.5634155	12.329430		-103.0	5110	1.91	-2.27
1960-53289-530 322.5755615	12.443088		-112.9	5351	1.96	-2.60
1962-53321-323 322.3222656	12.281335		-100.7	6024	3.19	-2.31
1962-53321-328 322.3479919	12.310190		-103.7	6482	4.04	-2.07
1962-53321-329 322.4080811	12.358446		-102.9	6244	3.58	-1.95
1962-53321-335 322.3918152	12.275231		-124.6	5898	3.41	-2.42
1962-53321-339 322.3828125	12.291987		-111.7	6673	3.38	-1.88
1962-53321-363 322.5025635	12.258308		-107.3	6555	3.62	-1.88
1962-53321-364 322.4689941	12.278071		-108.2	5476	2.95	-2.60
1962-53321-368 322.5046692	12.286249		-105.5	6132	3.08	-2.06
1962-53321-369 322.4819946	12.320425		-119.4	6191	2.76	-1.82
1962-53321-370 322.4340820	12.294349		-118.6	6141	3.71	-2.35
1962-53321-371 322.4648743	12.303191		-131.7	6075	3.52	-1.97
1962-53321-372 322.4102173	12.272476		-123.1	5885	2.99	-2.25
1962-53321-375 322.4530640	12.260857		-106.7	5508	2.77	-2.41

Continued on next page...

Table A.1 – Continued

spSpec name	α (deg)	δ (deg)	RV (km s $^{-1}$)	T _{eff} (K)	$\log g$	[Fe/H]
1962-53321-376322.4066772	12.290338		-108.35420	3.14	-2.35	
1962-53321-378322.4337463	12.256533		-123.56614	4.02	-2.39	
1962-53321-399322.2647400	12.088030		-128.76636	3.58	-2.76	
1962-53321-402322.5315247	12.312680		-103.55452	3.00	-2.44	
1962-53321-403322.5715332	12.283740		-114.75586	2.92	-2.08	
1962-53321-406322.5553284	12.353999		-104.25627	3.14	-2.19	
1962-53321-407322.5682373	12.340600		-105.26184	3.56	-2.20	
1962-53321-409322.5322266	12.338534		-112.96752	3.82	-1.86	
1962-53321-412322.5373535	12.294172		-114.96461	3.46	-2.27	
1962-53321-413322.4278564	12.366820		-110.25435	2.59	-2.34	
1962-53321-414322.5430603	12.254919		-88.05981	2.89	-2.04	
1962-53321-415322.4989014	12.316244		-106.05494	2.74	-2.19	
1962-53321-416322.5141602	12.304797		-119.86338	2.71	-2.30	
1962-53321-419322.5576782	12.301801		-130.46528	3.74	-1.96	
1962-53321-421322.3530884	12.238419		-117.95662	2.76	-2.43	
1962-53321-422322.3055115	12.095261		-126.16421	2.74	-2.11	
1962-53321-423322.3211060	12.217339		-114.55546	2.48	-2.32	
1962-53321-424322.2882080	12.088967		-117.26589	3.61	-2.37	
1962-53321-427322.3056030	12.249682		-112.05453	2.46	-2.48	
1962-53321-428322.3019104	12.225344		-125.46560	3.85	-2.16	
1962-53321-430322.3014832	12.204044		-95.66419	3.09	-2.27	
1962-53321-438322.3101501	12.185511		-111.95309	2.73	-2.46	

Continued on next page...

Table A.1 – Continued

spSpec name	α (deg)	δ (deg)	RV (km s $^{-1}$)	T _{eff} (K)	$\log g$	[Fe/H]
1962-53321-442322.6037598	12.366948		-103.66275	3.16	-2.39	
1962-53321-445322.6427917	12.275240		-93.96515	3.72	-1.88	
1962-53321-449322.6358032	12.290989		-131.86313	2.99	-2.16	
1962-53321-454322.5975342	12.257596		-116.15452	2.00	-2.37	
1962-53321-460322.6270447	12.246479		-117.96459	3.73	-2.20	
1962-53321-465322.3361511	12.095001		-132.06662	3.48	-2.37	
1962-53321-466322.3733521	12.240548		-115.55356	3.04	-2.72	
1962-53321-469322.4008179	12.225221		-132.46200	3.20	-2.52	
1962-53321-470322.3207092	12.106877		-119.26432	3.86	-2.05	
1962-53321-471322.4016724	12.009658		-102.76515	3.90	-2.21	
1962-53321-474322.3290100	12.039521		-111.85425	2.77	-2.62	
1962-53321-478322.3526611	12.008277		-126.36108	2.90	-2.41	
1962-53321-480322.3417664	12.023521		-113.76242	3.06	-2.09	
1962-53321-483322.4589844	11.991854		-83.66743	3.19	-1.87	
1962-53321-484322.5236511	12.006750		-100.66618	3.80	-2.01	
1962-53321-488322.4795532	12.013686		-100.96439	3.78	-2.08	
1962-53321-490322.4822083	11.986870		-111.26458	3.92	-2.62	
1962-53321-493322.5000610	11.843804		-107.25749	2.88	-2.35	
1962-53321-495322.4521179	11.955274		-95.06463	3.65	-1.79	
1962-53321-496322.4375000	11.972004		-83.56514	3.97	-2.19	
1962-53321-497322.4447021	12.011971		-114.36443	4.12	-2.39	
1962-53321-500322.4923096	11.963464		-111.36286	4.32	-2.39	

Continued on next page...

Table A.1 – Continued

spSpec name	α (deg)	δ (deg)	RV (km s $^{-1}$)	T _{eff} (K)	$\log g$	[Fe/H]
1962-53321-503 322.6179810	11.996145		-97.46715	3.72	-2.18	
1962-53321-505 322.6524048	12.082651		-106.06450	3.87	-2.65	
1962-53321-506 322.6019592	12.044020		-99.75420	2.74	-2.43	
1962-53321-509 322.6124878	12.028808		-104.76584	4.07	-2.06	
1962-53321-510 322.6307373	12.017861		-91.96155	3.44	-2.25	
1962-53321-512 322.5454712	12.024155		-94.76286	3.17	-2.09	
1962-53321-515 322.5826111	11.990081		-104.65466	2.74	-2.53	
1962-53321-516 322.5649414	11.992488		-97.55712	3.19	-2.41	
1962-53321-518 322.6694946	12.089317		-95.55695	3.22	-2.54	
1962-53321-519 322.5717163	12.034966		-94.56693	3.68	-2.26	
1962-53321-520 322.5625916	12.011796		-108.26234	3.47	-2.44	
1962-53321-522 322.6928101	12.298704		-120.66638	3.79	-2.09	
1962-53321-532 322.6614685	12.270009		-113.45471	2.39	-2.42	
1962-53321-533 322.6655579	12.248962		-106.26273	3.28	-2.25	
1962-53321-539 322.7539978	12.195694		-89.66595	4.01	-2.24	
1962-53321-540 322.6919556	12.215733		-88.66420	3.37	-2.48	
1962-53321-543 322.6426392	12.200052		-103.66434	3.55	-2.70	
1962-53321-545 322.6738586	12.167021		-110.06688	3.75	-2.59	
1962-53321-549 322.6310120	12.212295		-119.35904	3.36	-2.51	
1962-53321-550 322.6591187	12.145007		-105.45890	2.99	-2.26	
1962-53321-554 322.7246094	12.159374		-102.16825	3.75	-2.38	
1962-53321-555 322.6697388	12.106344		-105.56495	3.63	-2.21	

Continued on next page...

Table A.1 – Continued

spSpec name	α (deg)	δ (deg)	RV (km s $^{-1}$)	T _{eff} (K)	$\log g$	[Fe/H]
1962-53321-558322.6465759	12.128071		-108.95925	3.97	-2.32	
NGC 5053						
2476-53826-486	199.04518	17.60554	46.85287	1.99	-2.41	
2476-53826-488	199.09269	17.69851	42.54951	2.00	-2.14	
2476-53826-490	199.07441	17.62914	37.08452	3.08	-2.10	
2476-53826-497	199.08809	17.59394	36.25397	2.46	-1.90	
2476-53826-501	199.16802	17.67369	43.44973	2.11	-2.56	
2476-53826-505	199.19265	17.70156	46.85353	1.93	-2.37	
2476-53826-506	199.15790	17.64537	46.88072	3.51	-1.76	
2476-53826-507	199.18189	17.62503	37.75126	1.97	-2.26	
2476-53826-508	199.18986	17.64430	43.05125	2.20	-2.32	
2476-53826-519	199.10217	17.66400	45.64965	1.65	-2.01	
2476-53826-527	199.01911	17.78386	45.55001	1.99	-2.17	
2476-53826-531	199.06474	17.76097	46.39199	3.41	-2.15	
2476-53826-573	199.19611	17.80532	43.95267	1.68	-2.17	
2476-53826-575	199.17000	17.79282	44.34855	2.06	-2.43	
2476-53826-577	199.23569	17.75812	49.45150	2.15	-2.43	
2476-53826-578	199.14256	17.73152	42.74921	2.16	-2.26	
M53						
2476-53826-329	198.08194	18.01885	-74.35189	2.42	-1.87	
2476-53826-361	198.27909	18.09230	-59.45006	2.25	-1.94	
2476-53826-362	198.14897	18.08892	-56.16943	2.65	-1.93	

Continued on next page...

Table A.1 – Continued

spSpec name	α (deg)	δ (deg)	RV (km s $^{-1}$)	T _{eff} log g [Fe/H]
2476-53826-363	198.21748	18.06588	-58.28820	3.48 -1.92
2476-53826-369	198.17940	18.06809	-66.69007	3.58 -1.90
2476-53826-372	198.23916	18.03263	-53.55235	2.57 -2.16
2476-53826-375	198.27524	17.94161	-71.04997	1.97 -1.88
2476-53826-376	198.15708	18.05392	-48.99237	3.21 -1.78
2476-53826-378	198.19809	18.07094	-54.55069	1.76 -2.07
2476-53826-379	198.28341	17.88147	-57.59162	3.35 -2.10
2476-53826-401	198.40054	18.20061	-67.55140	2.51 -1.89
2476-53826-404	198.29193	18.10423	-64.04849	1.94 -2.00
2476-53826-405	198.43153	18.20371	-45.95297	3.11 -1.88
2476-53826-408	198.35774	18.13509	-69.58773	3.53 -1.86
2476-53826-409	198.35615	18.21558	-56.85133	2.22 -2.12
2476-53826-413	198.34337	18.12375	-69.75363	2.94 -1.82
2476-53826-418	198.39045	18.17497	-51.25511	2.04 -1.95
2476-53826-451	198.48345	18.06427	-65.04989	2.07 -1.89
2476-53826-452	198.48341	18.25271	-63.85181	1.95 -2.14
M2				
1961-53299-124323.2988892	-0.926583		-8.85063	2.38 -1.63
1961-53299-125323.3046265	-0.900651		-1.45066	2.28 -1.56
1961-53299-131323.4663696	-0.819519		6.55160	2.57 -1.58
1961-53299-134323.4247131	-0.804700		-2.24937	2.00 -1.47
1961-53299-136323.2869568	-0.885027		8.15165	2.72 -1.59

Continued on next page...

Table A.1 – Continued

spSpec name	α (deg)	δ (deg)	RV (km s $^{-1}$)	T _{eff} log g [Fe/H] (K)
1961-53299-140 323.3161316	-0.936875		-5.0	5312 2.73 -1.61
1961-53299-144 323.4824524	-0.780800		6.8	5293 2.48 -1.64
1961-53299-152 323.5119629	-0.501376		3.4	5150 2.18 -1.76
1961-53299-159 323.5318298	-0.781852		3.1	5178 2.55 -1.72
1961-53299-194 323.1741943	-0.712977		-6.8	8973 3.22 -1.62
1961-53299-213 323.2510986	-0.805550		-6.4	5226 2.00 -1.81
1961-53299-215 323.2557068	-0.864036		3.6	5076 2.20 -1.84
1963-54331-041 323.5323486	-0.898565		-4.0	6214 3.34 -1.34
1963-54331-043 323.5525513	-0.890733		8.6	5594 3.13 -1.52
1963-54331-045 323.5656433	-0.907277		12.1	6325 2.84 -1.31
1963-54331-082 323.5061035	-0.865724		-22.2	6002 2.55 -1.68
1963-54331-083 323.5080261	-0.824424		-9.3	5612 2.97 -1.66
1963-54331-090 323.4566040	-0.765115		-8.8	5721 3.56 -1.66
1963-54331-091 323.4995117	-0.948989		9.6	5396 3.33 -1.64
1963-54331-096 323.4652710	-0.816831		-6.5	5914 3.47 -1.52
1963-54331-098 323.4837952	-0.832883		-5.1	5291 2.60 -1.75
1963-54331-100 323.4888306	-0.866385		-10.0	5928 3.78 -1.55
1963-54331-102 323.5220337	-0.778994		-11.4	6062 3.35 -1.60
1963-54331-114 323.5265503	-0.677912		1.4	6287 3.48 -1.88
1963-54331-121 323.2814026	-0.907666		0.5	5356 2.98 -1.61
1963-54331-123 323.3062134	-0.993524		1.9	5480 2.93 -1.56
1963-54331-124 323.2615051	-0.910594		-4.3	6127 3.05 -1.78

Continued on next page...

Table A.1 – Continued

spSpec name	α (deg)	δ (deg)	RV (km s $^{-1}$)	T _{eff} log g [Fe/H]
1963-54331-126 323.3119507	-0.933239		-1.8 5498	3.29 -1.49
1963-54331-128 323.2590942	-0.836635		-8.3 5412	3.27 -1.45
1963-54331-131 323.3119507	-0.911349		-1.7 5330	2.68 -1.65
1963-54331-137 323.3194885	-0.976572		-2.3 5389	3.19 -1.54
1963-54331-139 323.2646790	-0.864309		-5.7 5328	3.32 -1.61
1963-54331-143 323.4908142	-0.783230		2.3 5734	3.72 -1.46
1963-54331-144 323.4483032	-0.729351		-0.4 5341	3.04 -1.53
1963-54331-145 323.4632263	-0.724424		0.6 5761	4.05 -1.52
1963-54331-146 323.4815979	-0.809713		5.4 6374	4.20 -1.60
1963-54331-147 323.4628601	-0.750568		-23.8 6287	3.62 -1.54
1963-54331-148 323.4973755	-0.808784		-8.1 5725	3.50 -1.67
1963-54331-150 323.4602051	-0.679670		-6.4 5884	3.95 -1.61
1963-54331-154 323.4409485	-0.625550		10.4 6411	3.96 -1.47
1963-54331-156 323.4447327	-0.651404		-3.2 6456	3.40 -1.59
1963-54331-162 323.2671814	-0.670811		4.1 6257	3.62 -1.81
1963-54331-164 323.4361267	-0.765563		2.1 5404	2.96 -1.58
1963-54331-169 323.4208374	-0.698915		17.7 6141	2.18 -1.68
1963-54331-170 323.4298401	-0.733806		-10.4 6427	3.74 -1.34
1963-54331-178 323.4222717	-0.635959		-8.8 5310	3.17 -1.69
1963-54331-179 323.2658691	-0.708226		11.0 6335	3.06 -1.67
1963-54331-180 323.4226990	-0.714586		-1.9 5507	3.42 -1.68
1963-54331-181 323.2662964	-0.726436		0.2 6411	3.68 -1.33

Continued on next page...

Table A.1 – Continued

spSpec name	α (deg)	δ (deg)	RV (km s $^{-1}$)	T _{eff} log g [Fe/H]
1963-54331-184 323.2333374	–0.738061		–4.8 5592	3.30 –1.76
1963-54331-185 323.2148438	–0.726361		–3.7 6453	3.47 –1.74
1963-54331-186 323.2448730	–0.776209		–23.0 6325	3.08 –1.86
1963-54331-189 323.2506104	–0.651933		11.0 6381	3.24 –1.48
1963-54331-194 323.2321777	–0.758979		–3.5 6283	3.43 –1.61
1963-54331-196 323.2610779	–0.770765		–10.8 6284	3.84 –1.69
1963-54331-197 323.1915894	–0.710805		–14.1 6388	3.00 –1.63
1963-54331-200 323.2678223	–0.754401		–10.4 6448	3.46 –1.61
1963-54331-201 323.2361145	–0.796597		–16.9 5586	3.20 –1.46
1963-54331-204 323.2236633	–0.962825		–0.9 5351	2.96 –1.58
1963-54331-206 323.2539062	–0.973936		–17.2 6339	3.56 –1.49
1963-54331-207 323.2109985	–0.851545		15.2 6582	4.08 –1.54
1963-54331-208 323.2533569	–0.887787		–5.2 5337	2.95 –1.68
1963-54331-209 323.2061462	–0.803604		5.0 5476	3.33 –1.60
1963-54331-211 323.2515259	–0.853978		–11.8 5373	3.14 –1.55
1963-54331-212 323.1940918	–0.849611		8.5 5494	3.56 –1.55
1963-54331-217 323.2306213	–0.819139		–1.2 5423	3.10 –1.47
1963-54331-218 323.2166138	–0.902027		–8.3 5399	3.20 –1.63
1963-54331-220 323.1990967	–0.894439		7.5 6438	4.00 –1.77
1963-54331-222 323.2009888	–0.778871		–2.1 6343	3.24 –1.48
1963-54331-223 323.1011353	–0.693063		6.0 6302	3.59 –1.59
1963-54331-254 323.1844177	–0.806918		–1.8 6679	3.87 –1.72

Continued on next page...

Table A.1 – Continued

spSpec name	α (deg)	δ (deg)	RV (km s $^{-1}$)	T _{eff} (K)	$\log g$	[Fe/H]
M13						
2174-53521-054	250.8113861	36.380367	-238.45637	3.25	-1.59	
2174-53521-082	250.6566925	36.292824	-241.35083	2.39	-1.70	
2174-53521-087	250.5986176	36.141987	-232.75480	3.22	-1.65	
2174-53521-093	250.6486664	36.331833	-242.75048	2.32	-1.62	
2174-53521-094	250.6187286	36.193378	-235.25432	3.31	-1.60	
2174-53521-098	250.6272430	36.330879	-250.75062	2.39	-1.79	
2174-53521-121	250.5334473	36.323925	-249.45298	2.62	-1.59	
2174-53521-126	250.4946899	36.287205	-232.95336	2.95	-1.64	
2174-53521-128	250.4741516	36.309807	-249.05374	3.24	-1.72	
2174-53521-131	250.4893646	36.332115	-243.05059	3.37	-1.45	
2174-53521-133	250.5125122	36.321091	-242.65338	3.10	-1.60	
2174-53521-134	250.5464020	36.344273	-242.65472	3.31	-1.52	
2174-53521-136	250.4905701	36.363522	-242.99332	3.20	-1.58	
2174-53521-137	250.5240936	36.376110	-251.95240	2.44	-1.54	
2174-53521-145	250.4505157	36.393330	-246.45036	2.15	-1.59	
2174-53521-146	250.3612061	36.200855	-247.15562	3.09	-1.58	
2174-53521-149	250.3400269	36.200890	-243.55560	3.42	-1.56	
2174-53521-152	250.3966980	36.394932	-246.88934	3.23	-1.68	
2174-53521-153	250.4664001	36.409313	-247.88477	3.25	-1.65	
2174-53521-154	250.4661713	36.326332	-249.95041	2.26	-1.72	
2174-53521-155	250.3851166	36.147091	-240.15279	2.82	-1.73	

Continued on next page...

Table A.1 – Continued

spSpec name	α (deg)	δ (deg)	RV (km s $^{-1}$)	T _{eff} (K)	$\log g$	[Fe/H]
2174-53521-156	250.3521576	36.409504	-239.7	5121	2.35	-1.76
2174-53521-157	250.4519958	36.301846	-247.2	9099	3.38	-1.64
2174-53521-158	250.4085236	36.303894	-243.9	5190	2.44	-1.58
2174-53521-159	250.3711243	36.398438	-237.3	5075	2.05	-1.54
2174-53521-160	250.3690338	36.363808	-255.3	5097	1.85	-1.64
2174-53521-166	250.2722931	36.365372	-237.3	5120	2.43	-1.72
2174-53521-167	250.2756042	36.422920	-246.5	5028	1.81	-1.60
2174-53521-168	250.2608337	36.437668	-244.0	5074	2.06	-1.70
2174-53521-171	250.3128967	36.398254	-247.0	4997	2.09	-1.66
2174-53521-172	250.3078461	36.417362	-247.8	5074	2.25	-1.67
2174-53521-174	250.1682281	36.190548	-250.9	5506	3.15	-1.86
2174-53521-175	250.3200226	36.326923	-235.7	8675	3.30	-1.43
2174-53521-176	250.3260651	36.347130	-240.3	5149	2.53	-1.64
2174-53521-215	250.0930939	36.313175	-242.3	5121	2.36	-1.77
2174-53521-368	250.1569672	36.596581	-254.1	5371	3.18	-1.56
2174-53521-376	250.1804047	36.558369	-247.4	5134	2.45	-1.76
2174-53521-402	250.2494965	36.627911	-252.8	5452	3.34	-1.58
2174-53521-403	250.2917633	36.632149	-258.6	5735	3.72	-1.57
2174-53521-406	250.2974548	36.656551	-249.8	5371	3.23	-1.83
2174-53521-407	250.2983246	36.606567	-251.3	5256	2.96	-1.53
2174-53521-410	250.2953033	36.564213	-237.8	5061	2.36	-1.74
2174-53521-412	250.2389069	36.587105	-242.8	5399	2.57	-1.62

Continued on next page...

Table A.1 – Continued

spSpec name	α (deg)	δ (deg)	RV (km s $^{-1}$)	T _{eff} (K)	$\log g$	[Fe/H]
2174-53521-413	250.3145905	36.517387	-237.6	5107	2.20	-1.65
2174-53521-414	250.2673035	36.586380	-241.9	5349	2.71	-1.58
2174-53521-442	250.3338928	36.614479	-249.2	8514	3.24	-1.58
2174-53521-443	250.3404846	36.465477	-255.4	5109	2.19	-1.68
2174-53521-445	250.3153534	36.581833	-247.6	5629	3.18	-1.60
2174-53521-447	250.3488159	36.637089	-246.1	5545	3.15	-1.56
2174-53521-449	250.3311310	36.507713	-244.1	5069	2.36	-1.80
2174-53521-451	250.4059753	36.421410	-245.1	8466	3.22	-1.66
2174-53521-452	250.2902679	36.445755	-256.6	4997	2.45	-1.70
2174-53521-453	250.3791046	36.437355	-238.2	5107	2.47	-1.57
2174-53521-455	250.3236237	36.436779	-251.3	5053	2.34	-1.68
2174-53521-456	250.3559265	36.608372	-248.2	5402	3.01	-1.56
2174-53521-457	250.3617706	36.424606	-244.6	5062	2.27	-1.63
2174-53521-458	250.3153839	36.463863	-245.9	5069	2.32	-1.65
2174-53521-459	250.3159637	36.554893	-245.0	5118	2.52	-1.50
2174-53521-460	250.3238525	36.491585	-238.9	5030	1.96	-1.59
2174-53521-461	250.4161987	36.592712	-245.1	5415	3.30	-1.62
2174-53521-462	250.3755035	36.591190	-245.5	5006	2.41	-1.65
2174-53521-463	250.4506531	36.594818	-243.8	5102	2.38	-1.67
2174-53521-464	250.3977661	36.604618	-239.1	8616	3.21	-1.60
2174-53521-470	250.3885956	36.541203	-241.2	4991	2.13	-1.59
2174-53521-471	250.4050598	36.680744	-248.8	5166	2.75	-1.64

Continued on next page...

Table A.1 – Continued

spSpec name	α (deg)	δ (deg)	RV (km s $^{-1}$)	T _{eff} (K)	$\log g$	[Fe/H]
2174-53521-472	250.4392548	36.430611	-243.1	7622	3.26	-1.34
2174-53521-474	250.4210815	36.630798	-237.7	5421	3.21	-1.77
2174-53521-475	250.4187622	36.526752	-239.4	5164	3.56	-1.86
2174-53521-476	250.4537811	36.534679	-249.7	5111	2.66	-1.55
2174-53521-477	250.4329834	36.411579	-240.9	5051	2.38	-1.51
2174-53521-478	250.4082642	36.497627	-234.4	5115	2.31	-1.62
2174-53521-480	250.3775940	36.560562	-244.9	5274	2.90	-1.52
2174-53521-481	250.4867401	36.625168	-246.3	5633	3.31	-1.54
2174-53521-483	250.5531464	36.489174	-254.5	5042	2.29	-1.65
2174-53521-484	250.5136871	36.465294	-255.2	5043	2.30	-1.51
2174-53521-485	250.5274811	36.482922	-251.1	5148	2.24	-1.65
2174-53521-488	250.5207062	36.526783	-246.1	5096	2.48	-1.61
2174-53521-489	250.5569153	36.554108	-246.5	5077	2.36	-1.64
2174-53521-490	250.4679413	36.425194	-234.5	8782	3.29	-1.71
2174-53521-491	250.5045319	36.562569	-249.7	9192	3.40	-1.73
2174-53521-493	250.4687042	36.450375	-247.9	5118	2.38	-1.65
2174-53521-494	250.4691467	36.473980	-234.9	5052	2.19	-1.65
2174-53521-495	250.5358582	36.516228	-250.3	5123	2.54	-1.62
2174-53521-497	250.5392151	36.566429	-240.3	5037	2.23	-1.65
2174-53521-498	250.5455017	36.409168	-240.7	5026	2.27	-1.68
2174-53521-499	250.5073700	36.389557	-242.0	5062	2.13	-1.69
2174-53521-500	250.4441376	36.501335	-249.6	5048	2.29	-1.62

Continued on next page...

Table A.1 – Continued

spSpec name	α (deg)	δ (deg)	RV (km s $^{-1}$)	T _{eff} (K)	$\log g$	[Fe/H]
2174-53521-522	250.5714569	36.525883	-244.9	5095	2.42	-1.61
2174-53521-529	250.6122742	36.650723	-245.6	5277	2.98	-1.65
2174-53521-530	250.5795441	36.617588	-246.8	5048	2.34	-1.79
2174-53521-531	250.6083527	36.451302	-243.9	4992	2.34	-1.63
2174-53521-532	250.5847015	36.450947	-245.9	8734	3.29	-1.49
2174-53521-533	250.5825653	36.416344	-248.1	5424	2.71	-1.74
2174-53521-537	250.6071167	36.431816	-252.4	5158	2.61	-1.61
2174-53521-538	250.5686798	36.437107	-252.4	5008	2.25	-1.57
2174-53521-539	250.6033020	36.480679	-251.9	5293	3.11	-1.63
2174-53521-540	250.5608978	36.462700	-253.8	9017	3.33	-1.44
2174-53521-542	250.4867096	36.697521	-248.1	5050	2.36	-1.75
2174-53521-554	250.4524536	36.731075	-248.1	5148	2.40	-1.65
2174-53521-560	250.4494934	36.746979	-246.5	5282	2.80	-1.70
2174-53521-563	250.7275696	36.537083	-245.3	5213	2.82	-1.72
2174-53521-565	250.6674805	36.541718	-248.8	5582	3.06	-1.79
2174-53521-573	250.7793579	36.401161	-245.6	5545	3.54	-1.44
2174-53521-576	250.6557617	36.483734	-244.3	5466	3.28	-1.65
2174-53521-577	250.6542358	36.559769	-250.8	5474	2.86	-1.56
2185-53532-106	250.6608429	36.252338	-246.5	6083	4.08	-1.66
2185-53532-111	250.6518555	36.315819	-247.2	6306	3.42	-1.67
2185-53532-113	250.6327362	36.302673	-259.6	5995	3.31	-1.51
2185-53532-116	250.6650848	36.212494	-254.9	6198	3.59	-1.82

Continued on next page...

Table A.1 – Continued

spSpec name	α (deg)	δ (deg)	RV (km s $^{-1}$)	T _{eff} (K)	$\log g$	[Fe/H]
2185-53532-120	250.6814728	36.301613	-232.7	6232	4.32	-1.52
2185-53532-141	250.5120239	36.217281	-239.5	6279	3.40	-1.71
2185-53532-143	250.5701752	36.201962	-233.4	6280	2.99	-1.65
2185-53532-146	250.5652161	36.224529	-236.1	6107	2.55	-1.58
2185-53532-148	250.6033325	36.234558	-245.2	6275	3.54	-1.85
2185-53532-150	250.6054077	36.200813	-242.3	6252	3.46	-1.70
2185-53532-151	250.5511475	36.331841	-227.3	6101	3.73	-1.75
2185-53532-152	250.6186066	36.331161	-237.1	6320	3.54	-1.82
2185-53532-153	250.5179138	36.306831	-244.2	5774	3.45	-1.73
2185-53532-154	250.5811462	36.316139	-234.2	6151	3.16	-1.77
2185-53532-156	250.5538483	36.304375	-242.3	6300	3.71	-1.66
2185-53532-158	250.5086365	36.321423	-243.9	6274	4.11	-1.71
2185-53532-160	250.5746155	36.340302	-239.3	6175	3.88	-1.82
2185-53532-161	250.4026489	36.216274	-240.0	6036	4.37	-1.68
2185-53532-167	250.3744202	36.210903	-249.9	6221	3.66	-1.78
2185-53532-169	250.3382111	36.202835	-237.3	6210	3.31	-1.55
2185-53532-171	250.4276733	36.282719	-243.5	6139	3.72	-1.53
2185-53532-172	250.4851227	36.205223	-248.2	6304	3.90	-1.50
2185-53532-175	250.4423218	36.258049	-253.5	6445	3.87	-1.54
2185-53532-176	250.4879761	36.319519	-238.0	6239	4.04	-1.62
2185-53532-177	250.4530029	36.298698	-249.3	6378	3.40	-1.66
2185-53532-178	250.4822845	36.300014	-245.6	6216	3.91	-1.70

Continued on next page...

Table A.1 – Continued

spSpec name	α (deg)	δ (deg)	RV (km s $^{-1}$)	T _{eff} (K)	$\log g$	[Fe/H]
2185-53532-179	250.4799957	36.221458	-242.5	6268	3.39	-1.72
2185-53532-181	250.2265778	36.218925	-247.5	6293	3.23	-1.70
2185-53532-196	250.1731720	36.201431	-248.0	6261	3.98	-1.60
2185-53532-197	250.1752930	36.316170	-241.0	6253	3.12	-1.62
2185-53532-198	250.2095490	36.280247	-244.3	6257	4.13	-1.65
2185-53532-200	250.1689453	36.354950	-246.5	6108	3.54	-1.71
2185-53532-237	250.1001129	36.310001	-239.1	5920	3.23	-1.72
2185-53532-388	250.0598145	36.565910	-250.6	6251	3.64	-1.58
2185-53532-390	250.0875244	36.539959	-249.3	6173	4.51	-1.58
2185-53532-393	250.0617828	36.626545	-255.3	6119	3.49	-1.48
2185-53532-423	250.1191559	36.614777	-249.4	6330	3.72	-1.73
2185-53532-424	250.1623840	36.546970	-243.4	6202	4.12	-1.80
2185-53532-425	250.1024933	36.708916	-250.0	6206	3.78	-1.74
2185-53532-426	250.1142273	36.579521	-244.8	5792	3.51	-1.73
2185-53532-427	250.1687622	36.572681	-245.7	5791	3.54	-1.70
2185-53532-428	250.2005005	36.620838	-246.8	6120	4.18	-1.64
2185-53532-430	250.1428375	36.630520	-254.5	6135	3.65	-1.71
2185-53532-431	250.1810608	36.514454	-238.9	6053	3.98	-1.54
2185-53532-433	250.0788116	36.418709	-255.3	5716	3.23	-1.76
2185-53532-435	250.1384125	36.391571	-240.0	6248	3.80	-1.61
2185-53532-439	250.0806732	36.503437	-240.7	6065	3.44	-1.72
2185-53532-440	250.1068573	36.427521	-232.5	6083	3.88	-1.60

Continued on next page...

Table A.1 – Continued

spSpec name	α (deg)	δ (deg)	RV (km s $^{-1}$)	T _{eff} (K)	$\log g$	[Fe/H]
2185-53532-461	250.3284149	36.700005	-241.4	6241	3.78	-1.65
2185-53532-462	250.2369232	36.717884	-248.1	6131	3.60	-1.72
2185-53532-464	250.2901764	36.685863	-236.5	6169	3.82	-1.63
2185-53532-466	250.2878876	36.725266	-245.5	6329	3.73	-1.48
2185-53532-469	250.2945404	36.606640	-246.2	6244	3.33	-1.71
2185-53532-473	250.2791901	36.576611	-238.6	6264	4.21	-1.54
2185-53532-475	250.2398529	36.588871	-249.1	6249	3.61	-1.69
2185-53532-476	250.2485657	36.574799	-244.4	6187	3.56	-1.77
2185-53532-477	250.2305450	36.610828	-244.1	6064	4.19	-1.72
2185-53532-478	250.2751617	36.618698	-243.6	6143	3.91	-1.73
2185-53532-479	250.2099609	36.532490	-251.3	6060	3.94	-1.71
2185-53532-480	250.2232056	36.626942	-243.0	6244	3.57	-1.64
2185-53532-481	250.3259277	36.655441	-244.6	6170	3.59	-1.62
2185-53532-482	250.4379120	36.601913	-233.6	5952	3.48	-1.75
2185-53532-483	250.4119263	36.610191	-252.1	6296	3.71	-1.50
2185-53532-485	250.3427429	36.637764	-248.3	6323	3.90	-1.77
2185-53532-486	250.3913116	36.619122	-259.7	6235	4.27	-1.68
2185-53532-487	250.3905029	36.591457	-242.1	6295	3.60	-1.60
2185-53532-488	250.3802643	36.661861	-239.6	6428	4.06	-1.78
2185-53532-489	250.3863983	36.711922	-244.6	6258	3.68	-1.64
2185-53532-490	250.4195862	36.592098	-242.2	6127	4.31	-1.58
2185-53532-492	250.3582611	36.607357	-240.5	6125	3.49	-1.70

Continued on next page...

Table A.1 – Continued

spSpec name	α (deg)	δ (deg)	RV (km s $^{-1}$)	T _{eff} (K)	$\log g$	[Fe/H]
2185-53532-493	250.3370056	36.581230	-238.1	6245	3.84	-1.77
2185-53532-494	250.4333649	36.619698	-243.8	6144	3.44	-1.67
2185-53532-495	250.3131714	36.642708	-242.4	6284	3.47	-1.71
2185-53532-496	250.3283539	36.603851	-245.6	5989	3.64	-1.44
2185-53532-497	250.3796539	36.606239	-237.6	5952	4.07	-1.76
2185-53532-498	250.4183960	36.693439	-235.1	6306	3.72	-1.80
2185-53532-499	250.3423157	36.618721	-230.3	6278	3.73	-1.66
2185-53532-500	250.3634491	36.578873	-245.5	6318	4.25	-1.72
2185-53532-504	250.5587463	36.680569	-250.2	6325	3.75	-1.85
2185-53532-506	250.5240936	36.660801	-245.8	5845	3.47	-1.71
2185-53532-507	250.4723969	36.677731	-243.3	6098	3.32	-1.76
2185-53532-508	250.4435272	36.712978	-249.1	6463	3.95	-1.66
2185-53532-511	250.5202179	36.342960	-246.4	6106	4.44	-1.59
2185-53532-512	250.5370789	36.365250	-250.5	6233	3.70	-1.67
2185-53532-513	250.5628357	36.372688	-246.0	6231	3.49	-1.69
2185-53532-514	250.5161896	36.359978	-237.8	6252	3.82	-1.56
2185-53532-515	250.5661469	36.400230	-246.4	6288	3.79	-1.66
2185-53532-516	250.4558868	36.613400	-239.8	5977	3.73	-1.47
2185-53532-517	250.4772949	36.625591	-258.4	6020	3.73	-1.38
2185-53532-519	250.5725555	36.425186	-246.3	6300	4.20	-1.74
2185-53532-520	250.5612183	36.355461	-249.8	6245	3.14	-1.84
2185-53532-534	250.3009644	36.802814	-252.8	6281	3.65	-1.84

Continued on next page...

Table A.1 – Continued

spSpec name	α (deg)	δ (deg)	RV (km s $^{-1}$)	T _{eff} (K)	$\log g$	[Fe/H]
2185-53532-537	250.4304962	36.822891	-241.4	6308	3.82	-1.69
2185-53532-539	250.3805847	36.807693	-250.8	6095	4.13	-1.90
2185-53532-540	250.3366394	36.751308	-232.9	6323	4.28	-1.74
2185-53532-541	250.6444855	36.637691	-226.9	5839	4.26	-1.62
2185-53532-542	250.6344757	36.460258	-237.9	5962	3.85	-1.91
2185-53532-543	250.6009674	36.613602	-252.6	6161	3.43	-1.69
2185-53532-544	250.6094360	36.447392	-247.7	6269	3.51	-1.55
2185-53532-545	250.6271667	36.714451	-242.1	6326	4.05	-1.55
2185-53532-546	250.6421814	36.477982	-255.6	5739	4.18	-1.65
2185-53532-547	250.6228180	36.621357	-256.3	5914	2.91	-1.78
2185-53532-548	250.6524048	36.419621	-253.1	6012	3.96	-1.52
2185-53532-549	250.5913239	36.461399	-235.9	5839	4.16	-1.47
2185-53532-550	250.6149445	36.501305	-236.0	6162	4.44	-1.87
2185-53532-551	250.5914764	36.413662	-233.6	5810	4.09	-1.62
2185-53532-552	250.6224670	36.431900	-257.2	6376	4.01	-1.79
2185-53532-553	250.6461029	36.350220	-246.2	5795	3.74	-1.76
2185-53532-554	250.6182556	36.410843	-246.9	6223	3.99	-1.77
2185-53532-555	250.6027374	36.400173	-244.6	6037	3.75	-1.74
2185-53532-556	250.6363068	36.383652	-246.2	6149	4.16	-1.70
2185-53532-557	250.6013031	36.364738	-244.7	6351	3.37	-1.91
2185-53532-558	250.5827942	36.475479	-250.0	6244	3.77	-1.61
2185-53532-559	250.6181030	36.472069	-243.7	6356	4.12	-1.60

Continued on next page...

Table A.1 – Continued

spSpec name	α (deg)	δ (deg)	RV (km s $^{-1}$)	T _{eff} (K)	$\log g$	[Fe/H]
2185-53532-560	250.5843353	36.379768	-239.9	6282	3.61	-1.71
2185-53532-575	250.6388245	36.796120	-234.8	6018	2.70	-1.57
2185-53532-577	250.5796356	36.790611	-258.5	6206	3.87	-1.74
2185-53532-581	250.7305756	36.608727	-244.4	6173	4.14	-1.55
2185-53532-584	250.6747742	36.539852	-253.1	6195	3.21	-1.70
2185-53532-585	250.6607666	36.504436	-234.5	6115	3.84	-1.76
2185-53532-587	250.7492065	36.463837	-241.4	6054	4.29	-1.78
2185-53532-589	250.7702637	36.421120	-243.9	6281	3.32	-1.59
2185-53532-591	250.6871948	36.405094	-251.7	6362	3.58	-1.65
2185-53532-592	250.7585297	36.405731	-239.1	6131	2.60	-1.66
2185-53532-593	250.6662598	36.387859	-243.3	6312	4.10	-1.47
2185-53532-594	250.6430359	36.701591	-234.3	6109	3.92	-1.42
2185-53532-596	250.6537323	36.525860	-238.8	5816	3.16	-1.55
2185-53532-598	250.7378235	36.401535	-250.2	6239	4.30	-1.45
2185-53532-599	250.6560211	36.458805	-245.4	6211	3.96	-1.66
2185-53532-600	250.7173309	36.396912	-237.5	6022	3.94	-1.51
2255-53565-103	250.6466827	36.307610	-247.7	5747	3.32	-1.58
2255-53565-112	250.6490173	36.331844	-239.9	5005	2.35	-1.54
2255-53565-114	250.5359039	36.338322	-242.7	5421	3.17	-1.58
2255-53565-115	250.6161957	36.345905	-243.4	5729	3.33	-1.56
2255-53565-116	250.5545197	36.267830	-249.5	5268	2.85	-1.56
2255-53565-120	250.6273346	36.330883	-252.1	5115	2.45	-1.70

Continued on next page...

Table A.1 – Continued

spSpec name	α (deg)	δ (deg)	RV (km s $^{-1}$)	T _{eff} (K)	$\log g$	[Fe/H]
2255-53565-143	250.5123444	36.306122	-229.45205	2.41	-1.70	
2255-53565-144	250.4085236	36.303902	-246.95190	2.34	-1.56	
2255-53565-147	250.4520111	36.301800	-249.19173	3.39	-1.53	
2255-53565-148	250.4909821	36.308311	-241.85150	2.30	-1.73	
2255-53565-153	250.4041443	36.351501	-249.15172	2.40	-1.68	
2255-53565-157	250.4288635	36.330101	-245.45054	2.33	-1.56	
2255-53565-171	250.3690338	36.363800	-255.45126	2.10	-1.61	
2255-53565-173	250.3810425	36.249397	-236.25392	3.57	-1.73	
2255-53565-174	250.3135834	36.387798	-246.18548	3.30	-1.62	
2255-53565-175	250.3260651	36.347099	-242.65159	2.55	-1.50	
2255-53565-177	250.3200226	36.326900	-236.28661	3.28	-1.60	
2255-53565-192	250.1939392	36.281242	-240.18931	3.43	-1.74	
2255-53565-423	250.1767273	36.542747	-249.48897	3.56	-1.63	
2255-53565-424	250.3054199	36.463902	-251.15622	3.45	-1.57	
2255-53565-425	250.2703552	36.638271	-256.35733	3.50	-1.39	
2255-53565-426	250.3145905	36.517399	-244.45268	2.41	-1.42	
2255-53565-432	250.2229156	36.471901	-251.65731	3.33	-1.57	
2255-53565-436	250.3080750	36.417400	-241.85342	3.58	-1.52	
2255-53565-437	250.2912445	36.512798	-253.35559	3.22	-1.64	
2255-53565-443	250.2730255	36.837120	-254.79071	3.38	-1.47	
2255-53565-465	250.4421692	36.429199	-245.78937	3.34	-1.47	
2255-53565-466	250.8296051	36.382706	-257.75580	3.20	-1.57	

Continued on next page...

Table A.1 – Continued

spSpec name	α (deg)	δ (deg)	RV (km s $^{-1}$)	T _{eff} (K)	$\log g$	[Fe/H]
2255-53565-476	250.5411072	36.356194	-243.8	5476	3.15	-1.52
2255-53565-482	250.3339233	36.614510	-250.0	8553	3.30	-1.42
2255-53565-483	250.3755646	36.591225	-252.2	5186	2.56	-1.49
2255-53565-485	250.3701477	36.529301	-255.1	5251	2.42	-1.48
2255-53565-486	250.3162231	36.554901	-243.1	5199	2.29	-1.53
2255-53565-490	250.3626251	36.566055	-244.7	5463	3.10	-1.48
2255-53565-492	250.3980865	36.604641	-238.0	8615	3.39	-1.49
2255-53565-495	250.4893951	36.387501	-235.2	4948	1.97	-1.50
2255-53565-496	250.3888550	36.541199	-248.9	5092	2.43	-1.52
2255-53565-504	250.4202271	36.569801	-248.5	5035	2.35	-1.36
2255-53565-510	250.4507599	36.594837	-248.2	5276	2.43	-1.45
2255-53565-512	250.5457611	36.409199	-234.9	5225	2.54	-1.54
2255-53565-515	250.4537811	36.534698	-252.9	5280	2.68	-1.47
2255-53565-518	250.4944153	36.462898	-235.9	5228	2.80	-1.45
2255-53565-520	250.4719238	36.423100	-241.2	5268	2.42	-1.47
2255-53565-542	250.5714569	36.525902	-246.9	5273	2.37	-1.40
2255-53565-543	250.5569153	36.554100	-251.1	5248	2.47	-1.48
2255-53565-544	250.5413818	36.495499	-249.4	5008	2.13	-1.73
2255-53565-545	250.6348267	36.499401	-242.7	5328	2.36	-1.39
2255-53565-548	250.5392151	36.566399	-245.2	5240	2.50	-1.38
2255-53565-550	250.5207062	36.526798	-246.5	5252	2.61	-1.50
2255-53565-551	250.6084442	36.451298	-243.3	5170	2.59	-1.46

Continued on next page...

Table A.1 – Continued

spSpec name	α (deg)	δ (deg)	RV (km s $^{-1}$)	T _{eff} (K)	$\log g$	[Fe/H]
2255-53565-552	250.5690155	36.416199	-241.4	5040	1.84	-1.42
2255-53565-553	250.5565186	36.476799	-239.5	5251	2.45	-1.44
2255-53565-556	250.5987854	36.482475	-247.3	5571	3.08	-1.51
2255-53565-557	250.5689240	36.437099	-239.6	5227	2.50	-1.44
2255-53565-559	250.5143433	36.505001	-258.8	5158	1.85	-1.54
2255-53565-586	250.5887756	36.564800	-237.3	5215	1.75	-1.56
2255-53565-589	250.5795441	36.617599	-245.9	5188	2.29	-1.53
2255-53565-597	250.6601868	36.517498	-253.1	5399	2.85	-1.45
M3						
2475-53845-105	205.65282	28.32783	-145.0	6149	3.12	-1.42
2475-53845-114	205.73204	28.36875	-137.2	5457	2.18	-1.77
2475-53845-116	205.78650	28.20934	-140.9	4846	2.17	-1.66
2475-53845-118	205.86803	28.29956	-136.0	5455	2.82	-1.55
2475-53845-119	205.63819	28.31352	-145.2	5022	2.40	-1.54
2475-53845-120	205.65500	28.36429	-140.5	5110	2.64	-1.61
2475-53845-141	205.37022	28.08121	-137.0	4961	2.42	-1.45
2475-53845-142	205.53038	28.29455	-132.0	4946	2.13	-1.58
2475-53845-143	205.67828	28.22223	-141.6	5046	2.17	-1.69
2475-53845-144	205.59709	28.33082	-139.8	5047	2.81	-1.39
2475-53845-145	205.60485	28.35609	-143.5	5240	2.15	-1.55
2475-53845-150	205.60948	28.31341	-139.8	5007	2.15	-1.61
2475-53845-160	205.60966	28.08865	-140.9	5003	2.42	-1.65

Continued on next page...

Table A.1 – Continued

spSpec name	α (deg)	δ (deg)	RV (km s $^{-1}$)	T _{eff} (K)	$\log g$	[Fe/H]
2475-53845-162	205.33562	28.19703	-139.75066	2.17	-1.50	
2475-53845-166	205.53993	28.34023	-130.56927	3.26	-1.36	
2475-53845-171	205.56812	28.30619	-141.74929	2.29	-1.59	
2475-53845-173	205.58101	28.35808	-134.05110	2.11	-1.49	
2475-53845-174	205.54022	28.30869	-142.75653	3.06	-1.68	
2475-53845-176	205.56639	28.34351	-144.24853	2.02	-1.58	
2475-53845-177	205.59311	28.30183	-142.04996	2.16	-1.82	
2475-53845-178	205.49657	28.33273	-143.95004	2.13	-1.74	
2475-53845-180	205.47751	28.33410	-141.45864	2.46	-1.71	
2475-53845-183	205.49975	28.28083	-147.15084	2.35	-1.54	
2475-53845-185	205.35177	28.31312	-141.85254	3.18	-1.45	
2475-53845-186	205.51608	28.24446	-141.84912	2.19	-1.58	
2475-53845-187	205.56002	28.16144	-144.68172	3.39	-1.40	
2475-53845-190	205.39697	28.33059	-144.45533	3.07	-1.57	
2475-53845-192	205.53319	28.16607	-138.15198	2.73	-1.56	
2475-53845-193	205.36685	28.33505	-142.75716	2.91	-1.63	
2475-53845-194	205.51430	28.30106	-130.86440	3.29	-1.50	
2475-53845-196	205.52200	28.26799	-150.75039	2.29	-1.54	
2475-53845-198	205.49830	28.31073	-145.04941	2.09	-1.46	
2475-53845-199	205.45296	28.33409	-145.95051	1.88	-1.55	
2475-53845-200	205.35902	28.28852	-136.95421	3.35	-1.52	
2475-53845-421	205.34831	28.49451	-142.64771	1.85	-1.47	

Continued on next page...

Table A.1 – Continued

spSpec name	α (deg)	δ (deg)	RV (km s $^{-1}$)	T _{eff} (K)	$\log g$	[Fe/H]
2475-53845-430	205.20487	28.53187	-131.15244	2.91	-1.51	
2475-53845-436	205.36178	28.39571	-142.64866	2.03	-1.52	
2475-53845-440	205.31259	28.40336	-139.14921	2.08	-1.49	
2475-53845-461	205.38832	28.38585	-142.64936	2.02	-1.70	
2475-53845-462	205.42846	28.40494	-135.46229	2.88	-1.45	
2475-53845-463	205.45607	28.35685	-143.85123	2.09	-1.56	
2475-53845-466	205.43604	28.38609	-147.54898	1.96	-1.82	
2475-53845-469	205.40194	28.46030	-137.05071	2.13	-1.67	
2475-53845-471	205.53495	28.43178	-149.35203	2.06	-1.55	
2475-53845-473	205.54987	28.42257	-141.74928	2.09	-1.54	
2475-53845-475	205.43603	28.43912	-139.74921	1.99	-1.68	
2475-53845-476	205.46535	28.43283	-144.75418	2.60	-1.67	
2475-53845-479	205.48329	28.39330	-136.05053	2.16	-1.59	
2475-53845-480	205.51179	28.40376	-140.84963	2.18	-1.61	
2475-53845-481	205.56280	28.45170	-139.75813	2.79	-1.49	
2475-53845-483	205.58224	28.37896	-138.74806	1.68	-1.32	
2475-53845-485	205.40959	28.49847	-147.18511	3.29	-1.45	
2475-53845-486	205.44677	28.49691	-145.84929	2.22	-1.47	
2475-53845-487	205.47013	28.47360	-147.65200	3.67	-1.34	
2475-53845-488	205.45635	28.52500	-146.44987	2.25	-1.66	
2475-53845-489	205.60288	28.39129	-142.74955	2.06	-1.64	
2475-53845-492	205.63534	28.39326	-147.25768	3.23	-1.52	

Continued on next page...

Table A.1 – Continued

spSpec name	α (deg)	δ (deg)	RV (km s $^{-1}$)	T _{eff} log g	[Fe/H]
2475-53845-496	205.59949	28.41169	-138.7	4903	2.09 -1.60
2475-53845-497	205.64308	28.41689	-139.2	4892	2.14 -1.64
2475-53845-498	205.61218	28.43980	-142.7	4906	2.24 -1.55
2475-53845-501	205.74192	28.42850	-146.3	5063	2.53 -1.64
2475-53845-505	205.68053	28.47108	-142.8	8080	3.38 -1.37
2475-53845-506	205.71187	28.46612	-143.6	4915	1.96 -1.44
2475-53845-507	205.66435	28.49271	-139.4	5184	2.92 -1.72
2475-53845-509	205.63571	28.51821	-144.9	4957	2.31 -1.58
2475-53845-510	205.60747	28.47946	-142.6	6956	2.06 -1.37
2475-53845-511	205.64513	28.43755	-144.6	4995	2.22 -1.52
2475-53845-514	205.73093	28.38494	-143.4	5074	2.44 -1.57
2475-53845-515	205.68951	28.41266	-139.7	4955	2.25 -1.47
2475-53845-518	205.70525	28.39799	-143.8	4870	2.15 -1.41
2475-53845-519	205.60952	28.45819	-143.6	5003	2.53 -1.58
2475-53845-520	205.79730	28.38930	-138.1	4980	2.54 -1.69
2475-53845-550	205.54473	28.69427	-149.4	5043	2.82 -1.78
2475-53845-551	205.53566	28.55088	-138.2	4873	2.20 -1.75
2475-53845-557	205.46425	28.60144	-148.4	5075	2.09 -1.77
2475-53845-558	205.69384	28.53518	-150.7	5005	2.50 -1.62
2475-53845-559	205.60380	28.54704	-140.7	5002	2.39 -1.56
M71					
2333-53682-077	298.59664	18.78314	-18.0	4643	2.54 -0.77

Continued on next page...

Table A.1 – Continued

spSpec name	α (deg)	δ (deg)	RV (km s $^{-1}$)	T _{eff} log g [Fe/H]
2333-53682-105	298.56809	18.84816	-22.15214	2.86 -0.79
2333-53682-144	298.45706	18.84689	-16.84798	2.33 -0.65
2333-53682-153	298.48777	18.86018	-24.25233	3.63 -0.68
2333-53682-167	298.46309	18.76964	-23.25122	2.74 -0.81
2333-53682-176	298.51460	18.78293	-20.15227	2.90 -0.84
2333-53682-178	298.52807	18.76042	-22.05216	2.87 -0.77
2333-53682-183	298.43222	18.79267	-11.04676	2.56 -0.77
2333-53682-191	298.42406	18.81066	-22.84878	2.83 -0.79
2333-53682-193	298.35753	18.84261	-19.25198	2.68 -0.81
2333-53682-198	298.45609	18.72024	-19.74963	3.22 -0.75
2333-53682-228	298.43161	18.71046	-25.04982	2.87 -0.80
2333-53682-229	298.41520	18.69626	-21.04914	2.95 -0.78
2338-53683-142	298.51727	18.80103	-27.75131	3.17 -0.76
2338-53683-186	298.44616	18.70557	-23.15144	3.44 -0.86
2338-53683-199	298.36670	18.78481	-22.35260	3.73 -0.82
2338-53683-200	298.44854	18.76227	-20.74993	3.21 -0.84
NGC 2420				
2078-53378-111114.7337700	21.533043		77.45815	4.41 -0.36
2078-53378-114114.7632300	21.450647		76.45976	4.22 -0.37
2078-53378-116114.7709500	21.494594		79.64988	4.62 -0.51
2078-53378-118114.7213000	21.550411		76.15230	4.70 -0.45
2078-53378-142114.6714600	21.474437		73.95725	4.41 -0.40

Continued on next page...

Table A.1 – Continued

spSpec name	α (deg)	δ (deg)	RV (km s $^{-1}$)	T _{eff} log g [Fe/H]
2078-53378-149	114.6430600	21.448729	74.16700	3.95 -0.35
2078-53378-150	114.6955000	21.390019	76.95836	4.37 -0.41
2078-53378-151	114.6724100	21.539542	76.96027	4.36 -0.34
2078-53378-152	114.6924200	21.552748	76.55161	4.51 -0.32
2078-53378-154	114.6604000	21.508270	74.15341	4.62 -0.32
2078-53378-156	114.7031100	21.515936	78.16005	4.36 -0.25
2078-53378-157	114.6541400	21.529307	73.95792	4.42 -0.27
2078-53378-158	114.6927300	21.469569	78.35210	4.62 -0.38
2078-53378-159	114.6708200	21.450686	75.66778	4.01 -0.31
2078-53378-161	114.5712400	21.543399	78.86759	3.88 -0.34
2078-53378-165	114.6024300	21.426910	76.35111	4.60 -0.43
2078-53378-166	114.5820400	21.519642	73.96561	4.27 -0.30
2078-53378-167	114.6017500	21.449791	73.45776	4.40 -0.38
2078-53378-168	114.6115600	21.318135	73.96512	4.12 -0.38
2078-53378-169	114.5819600	21.280654	78.66706	3.90 -0.29
2078-53378-170	114.6131300	21.505038	74.44963	4.35 -0.34
2078-53378-171	114.6198000	21.561135	75.25624	4.51 -0.38
2078-53378-172	114.5688700	21.504909	74.25664	4.49 -0.21
2078-53378-173	114.6418000	21.560445	80.05146	4.74 -0.23
2078-53378-174	114.6008000	21.527756	75.45450	4.59 -0.26
2078-53378-175	114.6295500	21.542134	78.55296	4.46 -0.28
2078-53378-176	114.6416800	21.603818	74.86735	4.23 -0.38

Continued on next page...

Table A.1 – Continued

spSpec name	α (deg)	δ (deg)	RV (km s $^{-1}$)	T _{eff} log g [Fe/H]
2078-53378-177114.6228200	21.586616		76.95399	4.60 -0.42
2078-53378-178114.6506600	21.588241		78.65138	4.60 -0.46
2078-53378-179114.5720900	21.569319		71.66756	4.04 -0.37
2078-53378-182114.5458400	21.481654		78.06775	4.07 -0.33
2078-53378-186114.5329300	21.496721		73.16866	3.94 -0.30
2078-53378-192114.5202700	21.508390		73.95822	4.45 -0.31
2078-53378-194114.4920900	21.528856		77.65462	4.47 -0.32
2078-53378-195114.5080200	21.480667		73.36716	3.98 -0.29
2078-53378-197114.5511100	21.571731		75.05783	4.44 -0.30
2078-53378-199114.5634600	21.418985		75.16434	4.23 -0.31
2078-53378-200114.5385000	21.543732		75.65307	4.59 -0.40
2078-53378-223114.3904500	21.523255		71.46435	4.30 -0.31
2078-53378-224114.4638600	21.543933		78.46775	3.92 -0.36
2078-53378-227114.4512700	21.468901		74.75910	4.40 -0.22
2078-53378-232114.4003400	21.434925		76.26762	3.99 -0.27
2078-53378-233114.3611500	21.547221		78.75952	4.36 -0.36
2078-53378-235114.4902200	21.548446		78.15731	4.20 -0.38
2078-53378-273114.3406700	21.562316		76.35969	4.39 -0.38
2078-53378-422114.4277900	21.642904		72.45450	4.53 -0.12
2078-53378-427114.4302700	21.777520		73.95877	4.43 -0.18
2078-53378-431114.4749200	21.663054		71.56748	3.92 -0.18
2078-53378-435114.4620100	21.588031		74.05435	4.45 -0.24

Continued on next page...

Table A.1 – Continued

spSpec name	α (deg)	δ (deg)	RV (km s $^{-1}$)	T _{eff} log g [Fe/H]
2078-53378-440	114.4428000	21.680481	73.5	5685 4.59 -0.14
2078-53378-462	114.5509900	21.740853	71.2	6316 4.38 -0.34
2078-53378-463	114.5498300	21.721819	72.4	6673 4.20 -0.17
2078-53378-464	114.5741000	21.872315	73.5	5811 4.10 -0.46
2078-53378-465	114.5717800	21.840559	74.4	5594 4.58 -0.28
2078-53378-466	114.5513800	21.821870	72.0	6779 4.14 -0.30
2078-53378-468	114.5113100	21.658002	74.2	5673 4.49 -0.26
2078-53378-469	114.5523900	21.648226	73.4	6639 3.73 -0.30
2078-53378-470	114.5214000	21.710367	73.8	5857 4.43 -0.36
2078-53378-471	114.5303200	21.614900	76.3	6321 4.37 -0.33
2078-53378-472	114.5822100	21.598426	74.8	6745 3.90 -0.33
2078-53378-473	114.5220800	21.600907	72.8	6191 4.33 -0.23
2078-53378-475	114.4970800	21.644300	72.3	5223 4.62 -0.34
2078-53378-476	114.5061000	21.610610	75.5	5397 4.55 -0.19
2078-53378-477	114.5529400	21.628851	76.6	5856 4.51 -0.19
2078-53378-478	114.5313000	21.647832	80.1	5602 4.65 -0.23
2078-53378-480	114.5518000	21.664013	74.1	5770 4.58 -0.36
2078-53378-481	114.5914200	21.674248	69.7	6411 4.31 -0.20
2078-53378-485	114.6053800	21.694122	79.0	5909 4.48 -0.29
2078-53378-491	114.6300500	21.615073	75.1	6706 4.18 -0.49
2078-53378-492	114.6291800	21.672440	74.5	5952 4.34 -0.19
2078-53378-493	114.5901700	21.628422	77.1	5457 4.65 -0.37

Continued on next page...

Table A.1 – Continued

spSpec name	α (deg)	δ (deg)	RV (km s $^{-1}$)	T _{eff} log g [Fe/H]
2078-53378-496	114.6028900	21.614570	73.0 5954	4.47 -0.27
2078-53378-499	114.5844700	21.697393	76.4 5792	4.39 -0.22
2078-53378-503	114.6589000	21.779420	71.9 6767	3.98 -0.30
2078-53378-510	114.7120300	21.617662	64.1 5754	4.42 -0.42
2078-53378-511	114.6601500	21.613201	73.4 6838	4.21 -0.27
2078-53378-512	114.6719800	21.630064	72.4 6642	4.24 -0.36
2078-53378-513	114.6427400	21.634517	75.4 6089	4.52 -0.23
2078-53378-514	114.7189500	21.580207	72.9 5982	4.49 -0.33
2078-53378-515	114.7006500	21.605630	73.4 6105	4.26 -0.28
2078-53378-516	114.6420300	21.651564	72.1 6362	4.33 -0.27
2078-53378-517	114.6432900	21.728846	76.7 5631	4.48 -0.24
2078-53378-518	114.6788700	21.703910	67.3 6624	4.14 -0.23
2078-53378-519	114.7201400	21.600649	74.3 5726	4.49 -0.32
2078-53378-520	114.6900700	21.580940	74.5 6186	4.33 -0.38
2078-53378-548	114.7715200	21.684803	74.0 6851	4.03 -0.32
2078-53378-552	114.7907100	21.658454	81.6 5047	4.48 -0.33
2078-53378-553	114.7563200	21.637694	79.7 5289	4.54 -0.30
2078-53378-554	114.7373500	21.682465	71.5 6798	4.13 -0.30
2078-53378-557	114.7612200	21.602289	73.8 6443	4.29 -0.24
2078-53378-560	114.7902800	21.615337	76.7 5771	4.48 -0.25
2079-53379-071	114.8473500	21.432501	79.2 4885	4.56 -0.39
2079-53379-076	114.8654000	21.591274	77.7 4910	4.58 -0.35

Continued on next page...

Table A.1 – Continued

spSpec name	α (deg)	δ (deg)	RV (km s $^{-1}$)	T _{eff} log g [Fe/H]
2079-53379-101	114.7611100	21.490309	73.94400	4.45 -0.26
2079-53379-102	114.7788500	21.400061	79.84442	4.32 -0.34
2079-53379-108	114.7754900	21.503532	78.24302	4.49 -0.31
2079-53379-113	114.7522800	21.451730	83.04297	4.46 -0.46
2079-53379-114	114.8108100	21.427293	62.04626	4.69 -0.21
2079-53379-119	114.7431700	21.578207	74.14389	4.22 -0.22
2079-53379-141	114.7252900	21.498738	75.34559	4.49 -0.24
2079-53379-148	114.6623700	21.491985	75.14577	4.47 -0.22
2079-53379-149	114.7246300	21.518278	76.64732	4.48 -0.41
2079-53379-152	114.7128300	21.469206	77.44561	4.54 -0.37
2079-53379-153	114.6333400	21.580304	68.54394	4.50 -0.21
2079-53379-156	114.7116500	21.534131	73.74857	4.55 -0.32
2079-53379-157	114.6400200	21.563115	74.34432	4.31 -0.24
2079-53379-158	114.6514700	21.519801	77.24506	4.53 -0.30
2079-53379-159	114.6842700	21.541289	80.44554	4.45 -0.32
2079-53379-160	114.6688400	21.578449	75.64678	4.52 -0.32
2079-53379-161	114.6037900	21.466938	75.24411	4.55 -0.09
2079-53379-162	114.6411300	21.466083	77.64905	4.59 -0.18
2079-53379-163	114.6339800	21.310769	71.74569	4.48 -0.53
2079-53379-164	114.5535900	21.543980	78.84719	4.37 -0.45
2079-53379-165	114.5703200	21.534152	73.34421	4.64 -0.31
2079-53379-166	114.5640000	21.557892	76.74922	4.65 -0.31

Continued on next page...

Table A.1 – Continued

spSpec name	α (deg)	δ (deg)	RV (km s $^{-1}$)	T _{eff} (K)	log g [Fe/H]
2079-53379-167	114.6235500	21.455992	77.9	4280	4.06 -0.21
2079-53379-168	114.6708300	21.438009	76.0	4475	4.90 -0.09
2079-53379-169	114.5825700	21.549603	76.4	4911	4.60 -0.33
2079-53379-178	114.5719400	21.445641	76.6	4987	4.58 -0.21
2079-53379-181	114.5458400	21.481654	73.0	6765	4.01 -0.33
2079-53379-182	114.5021800	21.350065	79.8	4530	4.49 -0.25
2079-53379-185	114.5404100	21.421194	66.5	4249	4.25 -0.22
2079-53379-191	114.5309900	21.548797	81.0	4718	4.59 -0.47
2079-53379-192	114.5139700	21.403902	76.9	4884	4.49 -0.29
2079-53379-194	114.5345700	21.444081	75.2	4985	4.61 -0.37
2079-53379-195	114.5383800	21.459230	77.6	4777	4.57 -0.36
2079-53379-196	114.4932800	21.577397	74.7	4460	4.41 -0.09
2079-53379-198	114.5100600	21.580111	76.4	4947	4.61 -0.19
2079-53379-199	114.5401500	21.574061	76.7	4373	4.74 -0.32
2079-53379-200	114.5501800	21.515901	78.2	4719	4.60 -0.43
2079-53379-234	114.4902800	21.529356	73.3	4473	4.37 -0.10
2079-53379-237	114.3715100	21.576729	74.9	4618	4.58 -0.25
2079-53379-238	114.4818700	21.496135	74.3	4777	4.60 -0.22
2079-53379-270	114.3305500	21.473141	78.9	4690	4.43 -0.28
2079-53379-431	114.3533000	21.674222	72.5	4812	4.67 -0.15
2079-53379-434	114.3718200	21.656651	86.9	4687	4.40 -0.47
2079-53379-440	114.3739700	21.682238	78.6	4449	4.30 -0.14

Continued on next page...

Table A.1 – Continued

spSpec name	α (deg)	δ (deg)	RV (km s $^{-1}$)	T _{eff} log g [Fe/H]
2079-53379-463	114.4646500	21.774120	80.8	4280 4.34 -0.16
2079-53379-466	114.4836000	21.728158	77.3	4508 4.71 -0.47
2079-53379-467	114.5359200	21.782800	78.4	4833 4.58 -0.22
2079-53379-474	114.4939800	21.612208	76.6	4419 4.38 -0.19
2079-53379-476	114.4833500	21.630688	73.9	4441 4.70 -0.24
2079-53379-477	114.5016300	21.681392	75.4	4835 4.62 -0.17
2079-53379-480	114.5439600	21.591729	72.2	4624 4.65 -0.45
2079-53379-482	114.6128000	21.662743	77.1	4420 4.38 -0.33
2079-53379-483	114.5822100	21.598426	68.3	6755 3.92 -0.34
2079-53379-487	114.6304000	21.655710	78.7	4492 4.59 -0.26
2079-53379-488	114.5538100	21.617337	77.3	4274 4.16 -0.43
2079-53379-490	114.5893300	21.713299	79.5	4398 4.27 -0.33
2079-53379-493	114.5601200	21.648805	76.3	4343 4.56 -0.18
2079-53379-495	114.5839200	21.631277	78.3	4811 4.58 -0.21
2079-53379-496	114.6000900	21.607352	78.2	4919 4.57 -0.21
2079-53379-498	114.6408400	21.609080	79.4	4795 4.68 -0.30
2079-53379-500	114.5563800	21.802400	78.5	4628 4.64 -0.26
2079-53379-502	114.6971800	21.661120	76.2	4703 4.62 -0.24
2079-53379-507	114.7510500	21.611731	81.5	4510 4.46 -0.48
2079-53379-510	114.7320600	21.659275	82.6	4296 3.93 -0.22
2079-53379-511	114.7137100	21.664611	76.6	4773 4.57 -0.36
2079-53379-512	114.6809200	21.718416	74.5	5044 4.56 -0.21

Continued on next page...

Table A.1 – Continued

spSpec name	α (deg)	δ (deg)	RV (km s $^{-1}$)	T _{eff} log g [Fe/H]
2079-53379-514	114.6947400	21.611378	79.6	4353 4.41 -0.30
2079-53379-516	114.6617100	21.614836	74.9	4814 4.68 -0.19
2079-53379-519	114.6623800	21.765588	79.1	4609 4.46 -0.37
2079-53379-552	114.8454600	21.609291	61.9	4537 4.48 -0.39
2079-53379-558	114.7901800	21.681409	76.0	4947 4.63 -0.26
NGC 2158				
2887-54521-416	91.77971	24.14997	27.1	5131 3.44 -0.17
2887-54521-442	91.89992	24.10639	28.7	6497 3.56 -0.17
2887-54521-445	91.85167	24.13172	25.8	6250 4.03 -0.33
2887-54521-446	91.85258	24.15344	25.2	6568 3.61 -0.29
2887-54521-447	91.87250	24.14558	25.4	5190 3.43 -0.21
2887-54521-451	91.88104	24.13031	25.8	6907 3.58 -0.22
2887-54521-452	91.92525	24.07644	26.7	6652 3.60 -0.24
2887-54521-460	91.88954	24.06314	25.8	7095 3.40 -0.17
2887-54521-511	91.83700	24.00167	25.6	6592 3.04 -0.31
2887-54521-531	91.88554	24.17808	20.1	5187 3.56 -0.16
2887-54521-532	91.91121	24.16419	27.3	4965 3.43 -0.22
2887-54521-547	91.92800	24.04764	26.7	5164 3.34 -0.30
2887-54521-552	91.92346	24.09833	27.7	5072 3.25 -0.26
2887-54521-559	91.94121	24.08608	29.1	5068 3.33 -0.26
2912-54499-409	91.79567	24.15931	30.6	7650 4.17 -0.23
2912-54499-416	91.80908	24.13578	28.3	7071 3.83 -0.25

Continued on next page...

Table A.1 – Continued

spSpec name	α (deg)	δ (deg)	RV (km s $^{-1}$)	T _{eff} log g [Fe/H]
2912-54499-417	91.80938	24.17028	30.6 6912	4.17 -0.39
2912-54499-442	91.87000	24.15608	25.4 7467	4.19 -0.24
2912-54499-444	91.88554	24.16933	29.6 7167	4.12 -0.28
2912-54499-445	91.88062	24.18756	25.1 7100	3.94 -0.30
2912-54499-446	91.89346	24.15556	19.8 7116	4.26 -0.23
2912-54499-450	91.86475	24.17319	36.9 6915	3.82 -0.29
2912-54499-453	91.85146	24.14342	22.9 7099	4.38 -0.22
2912-54499-458	91.89862	24.17961	26.1 7093	4.04 -0.31
2912-54499-459	91.81154	24.15192	16.3 6656	4.24 -0.25
2912-54499-461	91.75933	24.10450	18.5 7595	4.28 -0.30
2912-54499-462	91.77433	24.04967	26.3 7298	4.31 -0.27
2912-54499-483	91.82025	24.05197	25.1 7558	3.97 -0.19
2912-54499-484	91.81408	24.06819	26.2 7532	4.03 -0.19
2912-54499-488	91.78896	24.14458	19.7 6799	4.00 -0.23
2912-54499-489	91.79008	24.11892	27.2 7341	3.94 -0.22
2912-54499-499	91.79063	24.03228	28.6 7343	4.26 -0.36
2912-54499-501	91.84150	24.10564	20.1 7218	4.31 -0.31
2912-54499-502	91.85879	24.11939	25.2 7498	4.17 -0.21
2912-54499-503	91.82617	24.11897	19.4 7442	4.03 -0.23
2912-54499-505	91.86846	24.13533	26.0 7567	4.28 -0.16
2912-54499-506	91.84617	24.08989	23.9 6525	4.13 -0.25
2912-54499-507	91.81417	24.10178	26.7 7963	4.28 -0.13

Continued on next page...

Table A.1 – Continued

spSpec name	α (deg)	δ (deg)	RV (km s $^{-1}$)	T _{eff} log g [Fe/H]
2912-54499-509	91.82708	24.13514	31.1 7146	3.93 -0.30
2912-54499-510	91.88258	24.01472	27.7 6868	4.21 -0.37
2912-54499-511	91.86654	24.00914	32.5 6954	4.05 -0.27
2912-54499-514	91.83721	24.05189	30.6 7214	4.06 -0.23
2912-54499-515	91.83862	24.07103	30.0 7317	3.90 -0.31
2912-54499-516	91.82779	24.09117	24.5 7276	4.02 -0.15
2912-54499-518	91.85975	24.05356	30.8 7287	4.30 -0.28
2912-54499-519	91.85563	24.07247	26.8 7205	4.25 -0.25
2912-54499-531	91.93679	24.14572	28.8 6885	4.22 -0.24
2912-54499-534	91.93967	24.10997	34.4 6550	4.18 -0.18
2912-54499-539	91.91863	24.17281	19.1 7162	3.97 -0.31
2912-54499-540	91.91633	24.12875	32.4 6916	4.13 -0.28
2912-54499-542	91.90304	24.07997	24.6 6621	3.84 -0.37
2912-54499-543	91.89542	24.11381	26.0 6623	4.18 -0.29
2912-54499-544	91.88567	24.07508	23.4 6592	4.27 -0.38
2912-54499-545	91.88704	24.13492	30.0 7403	4.29 -0.18
2912-54499-547	91.87900	24.11878	30.3 6722	4.36 -0.29
2912-54499-549	91.88500	24.09136	24.5 7209	4.34 -0.15
2912-54499-552	91.89858	24.05819	25.7 7312	3.92 -0.26
2912-54499-553	91.89375	24.03914	26.6 7047	4.12 -0.28
2912-54499-556	91.87758	24.05083	27.8 7276	3.88 -0.11
2912-54499-558	91.92079	24.06769	25.3 7249	4.03 -0.19

Continued on next page...

Table A.1 – Continued

spSpec name	α (deg)	δ (deg)	RV (km s $^{-1}$)	T _{eff} log g [Fe/H]
2912-54499-559	91.93942	24.06436	27.17027	4.32 -0.29
2912-54499-560	91.89983	24.02447	23.46784	4.08 -0.28
		M35		
2887-54521-528	92.12229	24.48356	-11.16167	4.12 -0.23
2887-54521-534	92.11242	24.43275	-10.17898	4.25 +0.08
2887-54521-561	92.19954	24.33650	-4.77415	4.27 -0.06
2887-54521-562	92.18996	24.48508	-8.17125	4.32 +0.09
2887-54521-566	92.21008	24.37531	-7.07073	4.24 -0.14
2887-54521-571	92.17171	24.26314	1.06436	4.22 -0.25
2887-54521-574	92.24525	24.33811	-4.26173	4.49 -0.14
2887-54521-575	92.18267	24.28672	-0.16399	4.34 -0.22
2887-54521-576	92.16121	24.28150	-3.56504	4.32 -0.26
2887-54521-577	92.12313	24.23586	-4.56579	4.33 -0.15
2887-54521-580	92.22917	24.28611	-6.76213	4.56 -0.21
2887-54521-602	92.29150	24.30103	-4.56306	4.39 -0.18
2887-54521-604	92.37287	24.35117	-5.76265	4.27 -0.08
2887-54521-606	92.34713	24.32714	-6.96315	4.30 -0.31
2887-54521-608	92.34037	24.28469	-4.96414	4.26 -0.07
2887-54521-611	92.38533	24.22036	-5.86967	4.33 -0.03
2887-54521-616	92.27704	24.23072	-1.56276	4.26 -0.11
2887-54521-620	92.33058	24.31908	-8.16213	4.53 -0.21
2912-54499-524	92.04133	24.36569	-6.94478	4.43 -0.52

Continued on next page...

Table A.1 – Continued

spSpec name	α (deg)	δ (deg)	RV (km s $^{-1}$)	T _{eff} (K)	log g	[Fe/H]
2912-54499-563	92.23489	24.45188	-3.0	4695	4.55	-0.26
2912-54499-564	92.15571	24.49417	-0.6	4496	4.61	-0.46
2912-54499-575	92.18929	24.21147	-0.7	4668	4.72	-0.16
2912-54499-576	92.27554	24.45567	-16.2	5158	3.75	-0.42
2912-54499-601	92.29767	24.42347	-7.0	4577	4.37	-0.46
2912-54499-604	92.36371	24.35142	-1.7	4347	3.33	-0.34
2912-54499-605	92.42192	24.38517	-10.6	4685	4.67	-0.14
2912-54499-611	92.31054	24.23417	-11.4	4714	4.73	-0.13
2912-54499-619	92.39379	24.39831	-7.2	4537	4.57	-0.40
2912-54499-620	92.38533	24.45678	-3.7	4378	4.59	-0.43
M67						
2667-54142-361	132.6933300	11.871264	36.2	5446	4.60	+0.03
2667-54142-363	132.5890400	11.985747	33.2	5540	4.65	-0.03
2667-54142-364	132.6169200	11.913978	34.2	6004	4.47	-0.04
2667-54142-372	132.6952900	11.897903	33.5	5367	4.66	-0.04
2667-54142-378	132.6899800	11.926571	37.7	5034	4.68	+0.11
2667-54142-379	132.5899200	11.839747	36.4	5861	4.52	+0.08
2667-54142-402	132.7021700	12.014961	35.9	5525	4.66	+0.02
2667-54142-404	132.7532100	11.886464	34.6	5725	4.57	+0.03
2667-54142-406	132.7005000	11.913181	34.7	6016	4.39	+0.04
2667-54142-407	132.7347100	11.858081	36.0	6074	4.41	-0.06
2667-54142-408	132.7437500	11.994214	34.2	5927	4.50	+0.02

Continued on next page...

Table A.1 – Continued

spSpec name	α (deg)	δ (deg)	RV (km s $^{-1}$)	T _{eff} log g [Fe/H]
2667-54142-409	132.7742500	11.886261	35.6	5551 4.64 -0.06
2667-54142-410	132.7377900	11.947350	32.7	5613 4.58 -0.02
2667-54142-411	132.8010300	11.787528	28.3	5524 4.63 +0.01
2667-54142-412	132.7361200	11.831808	34.5	5771 4.56 +0.01
2667-54142-413	132.7688200	11.862833	24.7	5901 4.46 -0.01
2667-54142-414	132.7769200	11.791894	38.6	4581 4.72 -0.11
2667-54142-415	132.7000800	11.828167	35.3	5801 4.54 +0.03
2667-54142-417	132.7567100	11.937789	34.4	5590 4.62 +0.05
2667-54142-418	132.7534700	11.814725	36.4	5810 4.56 -0.07
2667-54142-419	132.7431200	11.970697	32.4	5879 4.47 -0.02
2667-54142-420	132.7914300	11.771442	34.4	5822 4.40 -0.01
2667-54142-429	132.3948800	11.788092	34.6	5945 4.57 +0.01
2667-54142-441	132.8041200	11.950172	35.8	5866 4.50 +0.05
2667-54142-444	132.8395800	11.984572	31.1	6098 4.44 +0.09
2667-54142-445	132.7831700	11.981397	34.2	5725 4.53 +0.03
2667-54142-451	132.8012500	11.906319	35.3	6031 4.43 -0.02
2667-54142-452	132.7928000	12.025431	37.4	4902 4.81 -0.06
2667-54142-453	132.8423700	11.807839	23.2	5076 4.74 -0.02
2667-54142-454	132.8407700	11.861747	36.1	5957 4.49 -0.01
2667-54142-455	132.9283300	11.991872	33.2	6067 4.35 -0.03
2667-54142-457	132.9065800	11.945644	35.9	5851 4.53 +0.06
2667-54142-458	132.8022500	12.188075	34.8	5836 4.47 +0.05

Continued on next page...

Table A.1 – Continued

spSpec name	α (deg)	δ (deg)	RV (km s $^{-1}$)	T _{eff} (K)	$\log g$	[Fe/H]
2667-54142-459	132.8128300	11.822606	33.9	6042	4.39	-0.01
2667-54142-460	132.7881300	11.950017	35.5	5805	4.56	+0.03
2667-54142-463	132.5035400	11.702733	34.9	5981	4.46	+0.04
2667-54142-466	132.6327000	11.502099	36.3	5146	4.70	-0.03
2667-54142-467	132.5376200	11.557281	36.3	6069	4.29	-0.07
2667-54142-469	132.6607100	11.776742	33.8	5290	4.72	+0.06
2667-54142-476	132.5400400	11.645006	34.8	5846	4.51	-0.01
2667-54142-477	132.7222900	11.727772	35.7	5746	4.55	+0.00
2667-54142-478	132.6963700	11.715228	33.8	6007	4.45	+0.02
2667-54142-479	132.7179200	11.750975	35.3	5810	4.58	-0.01
2667-54142-481	132.7949200	11.664139	39.4	5780	4.58	+0.02
2667-54142-485	132.7586500	11.755369	31.7	5597	4.60	+0.07
2667-54142-486	132.7528300	11.678155	36.7	5324	4.64	+0.07
2667-54142-487	132.7741000	11.729775	41.7	5741	4.59	-0.01
2667-54142-491	132.7797500	11.596875	35.4	6066	4.42	-0.13
2667-54142-492	132.7834200	11.640567	37.2	5864	4.50	-0.02
2667-54142-496	132.7887500	11.559197	35.3	5701	4.54	-0.01
2667-54142-500	132.7791300	11.697017	34.3	4987	4.62	-0.06
2667-54142-504	132.8498300	11.580686	37.3	5718	4.62	-0.06
2667-54142-505	132.8408200	11.734822	37.3	5869	4.42	-0.00
2667-54142-507	132.8529400	11.718478	35.9	5591	4.57	-0.04
2667-54142-508	132.8550400	11.637817	33.8	5441	4.67	-0.04

Continued on next page...

Table A.1 – Continued

spSpec name	α (deg)	δ (deg)	RV (km s $^{-1}$)	T _{eff} log g [Fe/H]
2667-54142-516132.8466200	11.654136		32.35635	4.66 +0.03
2667-54142-517133.0788800	11.397178		35.05525	4.60 +0.04
2667-54142-518133.0567100	11.393450		36.25805	4.57 -0.05
2667-54142-522133.0017500	11.935228		38.45904	4.48 +0.06
2667-54142-531132.9857500	11.790236		36.25836	4.52 +0.00
2667-54142-533132.9950000	11.804089		34.25155	4.77 -0.04
2667-54142-537132.9948800	11.833992		33.45881	4.49 -0.01
2667-54142-538132.9619800	11.869030		34.35013	4.77 +0.10
2667-54142-539133.0190000	11.980183		37.05075	4.74 -0.02
2667-54142-540132.9941700	11.870869		32.85428	4.67 +0.06
2667-54142-541133.1261300	11.714000		33.15904	4.40 -0.11
2667-54142-546133.0400800	11.779472		35.66078	4.33 -0.08
2667-54142-547133.1811700	11.610503		34.45487	4.70 +0.04
2667-54142-550133.0475000	11.675556		33.45971	4.48 +0.05
2667-54142-551132.9911100	11.762748		38.24958	4.63 -0.12
2667-54142-561133.0414600	12.175214		34.46026	4.52 +0.01
2667-54142-566133.2035400	12.046594		30.05586	4.55 -0.02
2667-54142-575133.0644200	11.883697		34.35901	4.54 +0.03
2667-54142-576133.0925800	11.817458		38.65569	4.55 -0.08
2667-54142-579133.0659200	11.775536		35.35598	4.63 -0.03
NGC 6791				
2800-54326-151	290.31055	37.77577	-47.74904	4.18 +0.41

Continued on next page...

Table A.1 – Continued

spSpec name	α (deg)	δ (deg)	RV (km s $^{-1}$)	T _{eff} log g [Fe/H]
2800-54326-152	290.27792	37.80231	-45.85632	4.48 +0.42
2800-54326-154	290.25604	37.80142	-47.14542	3.89 +0.46
2800-54326-155	290.29071	37.76133	-54.55623	4.22 +0.42
2800-54326-156	290.28943	37.78397	-43.94810	4.07 +0.42
2800-54326-157	290.31383	37.79217	-41.45689	4.32 +0.35
2800-54326-159	290.27624	37.74988	-45.84535	3.53 +0.46
2800-54326-160	290.30839	37.75263	-47.24883	4.07 +0.42
2800-54326-161	290.26887	37.72120	-46.55111	4.12 +0.40
2800-54326-165	290.23537	37.77058	-55.55752	3.95 +0.15
2800-54326-169	290.24479	37.72029	-45.34481	3.01 +0.27
2800-54326-171	290.25504	37.73653	-56.45464	4.25 +0.18
2800-54326-172	290.20854	37.79775	-45.35376	4.37 +0.42
2800-54326-173	290.23082	37.79705	-47.94924	4.31 +0.40
2800-54326-174	290.25360	37.75939	-46.84414	3.40 +0.46
2800-54326-175	290.25360	37.77766	-49.54476	3.10 +0.46
2800-54326-176	290.23775	37.74739	-50.15457	4.32 +0.33
2800-54326-178	290.21406	37.77513	-48.74601	3.56 +0.46
2800-54326-180	290.22034	37.75919	-45.64526	3.22 +0.43
2800-54326-181	290.18823	37.74275	-49.64369	3.55 +0.30
2800-54326-182	290.13027	37.77522	-47.45451	4.12 +0.19
2800-54326-183	290.18888	37.78830	-52.44478	3.41 +0.46
2800-54326-184	290.12773	37.75476	-50.65540	4.11 +0.36

Continued on next page...

Table A.1 – Continued

spSpec name	α (deg)	δ (deg)	RV (km s $^{-1}$)	T _{eff} log g [Fe/H]
2800-54326-185	290.16345	37.74368	-46.8 4483	3.16 +0.46
2800-54326-186	290.15705	37.72575	-49.4 44832	4.04 +0.42
2800-54326-189	290.16875	37.78517	-45.9 4930	4.23 +0.41
2800-54326-190	290.17674	37.76421	-46.4 4667	4.00 +0.46
2800-54326-194	290.17419	37.70602	-53.9 5599	4.07 +0.20
2800-54326-197	290.18075	37.72142	-46.7 4584	3.96 +0.34
2800-54326-199	290.16395	37.80132	-45.7 4280	2.77 +0.46
2800-54326-424	290.13763	37.82931	-46.4 5482	4.34 +0.24
2800-54326-462	290.18642	37.85478	-42.1 5627	4.43 +0.19
2800-54326-464	290.27438	37.82203	-43.7 5569	4.21 +0.36
2800-54326-465	290.24050	37.81700	-44.9 4481	3.82 +0.46
2800-54326-466	290.28500	37.83567	-41.7 5043	4.30 +0.44
2800-54326-469	290.23600	37.85450	-47.4 5549	4.38 +0.16
2800-54326-471	290.21029	37.83431	-46.3 5427	4.21 +0.44
2800-54326-473	290.25912	37.84825	-48.0 5592	4.08 +0.36
2800-54326-475	290.19271	37.81957	-43.2 4503	3.74 +0.45
2800-54326-476	290.18508	37.83414	-45.3 5702	4.41 +0.33
2800-54326-477	290.24383	37.83556	-44.4 4713	4.04 +0.28
2800-54326-479	290.16329	37.83461	-46.8 5513	4.46 +0.31
2800-54326-480	290.15792	37.81897	-44.4 5462	4.14 +0.32
2800-54326-497	290.30292	37.80739	-57.7 5606	4.28 +0.22
2821-54393-141	290.29286	37.73219	-46.8 5617	4.61 +0.21

Continued on next page...

Table A.1 – Continued

spSpec name	α (deg)	δ (deg)	RV (km s $^{-1}$)	T _{eff} log g [Fe/H]
2821-54393-142	290.29538	37.78913	-40.95215	4.87 -0.08
2821-54393-145	290.31488	37.78708	-44.05635	4.67 +0.23
2821-54393-146	290.28602	37.71747	-43.95524	4.59 +0.38
2821-54393-149	290.29258	37.75206	-43.25802	4.56 +0.39
2821-54393-161	290.26746	37.73246	-48.65700	4.44 +0.19
2821-54393-165	290.16959	37.70742	-48.74911	4.72 +0.10
2821-54393-166	290.21646	37.79267	-43.85392	4.66 +0.19
2821-54393-167	290.25304	37.76144	-43.95312	4.58 +0.18
2821-54393-169	290.23571	37.74950	-43.65246	4.66 +0.21
2821-54393-172	290.23312	37.77947	-48.55383	4.65 +0.35
2821-54393-173	290.23404	37.72550	-46.55415	4.52 +0.16
2821-54393-174	290.27438	37.76821	-47.05495	4.69 +0.23
2821-54393-176	290.23888	37.79792	-42.45078	4.59 +0.28
2821-54393-177	290.25525	37.78111	-44.85360	4.55 +0.27
2821-54393-178	290.27083	37.79364	-47.95279	4.63 +0.26
2821-54393-179	290.23317	37.69495	-46.45641	4.40 +0.10
2821-54393-182	290.19167	37.75022	-45.05410	4.54 +0.10
2821-54393-183	290.16181	37.72236	-48.35499	4.36 +0.16
2821-54393-184	290.21133	37.69576	-37.05060	4.70 +0.25
2821-54393-185	290.16196	37.79569	-54.95571	4.63 +0.40
2821-54393-187	290.18507	37.73330	-49.35583	4.50 +0.19
2821-54393-188	290.16150	37.74609	-43.14903	4.56 +0.41

Continued on next page...

Table A.1 – Continued

spSpec name	α (deg)	δ (deg)	RV (km s $^{-1}$)	T _{eff} log g [Fe/H]
2821-54393-190	290.21180	37.71344	-43.14830	4.67 +0.06
2821-54393-191	290.16200	37.77697	-50.55297	4.51 -0.03
2821-54393-192	290.14174	37.74134	-57.24720	4.65 -0.03
2821-54393-193	290.14857	37.75947	-44.34973	4.53 -0.25
2821-54393-194	290.18383	37.77736	-45.65451	4.40 +0.34
2821-54393-195	290.20292	37.76702	-44.64897	4.66 +0.19
2821-54393-196	290.21350	37.74117	-48.75459	4.46 +0.28
2821-54393-197	290.14430	37.78641	-46.15585	4.49 +0.30
2821-54393-199	290.19034	37.71489	-48.14838	4.75 +0.22
2821-54393-235	290.12569	37.76434	-42.15503	4.31 +0.09
2821-54393-436	290.12584	37.81327	-44.35320	4.40 +0.08
2821-54393-438	290.14612	37.83670	-49.85509	4.29 +0.27
2821-54393-439	290.11927	37.79796	-44.25497	4.27 +0.11
2821-54393-440	290.15288	37.81589	-35.25354	4.40 +0.11
2821-54393-468	290.26379	37.84733	-49.74866	4.71 +0.25
2821-54393-469	290.28646	37.80753	-41.85226	4.52 +0.30
2821-54393-472	290.26775	37.82575	-45.55302	4.54 +0.33
2821-54393-473	290.18250	37.84431	-42.45215	4.42 +0.05
2821-54393-474	290.22450	37.83158	-46.95613	4.70 +0.24
2821-54393-475	290.20554	37.84583	-40.05207	4.63 +0.27
2821-54393-478	290.24763	37.83678	-48.95531	4.32 +0.26
2821-54393-479	290.23475	37.81458	-41.35029	4.62 +0.23

Continued on next page...

Table A.1 – Continued

spSpec name	α (deg)	δ (deg)	RV (km s $^{-1}$)	T _{eff} log g	[Fe/H]
2821-54393-480	290.23092	37.84886	−44.35374	4.65	+0.39

Table A.2: Atmospheric Uncertainties of Adopted True Member Stars

spSpec name	$\sigma(\text{RV})$ (km s $^{-1}$)	$\sigma(\text{T}_{\text{eff}})$ (K)	$\sigma(\log g)$ (dex)	$\sigma([\text{Fe}/\text{H}])$ (dex)	$\langle \text{S/N} \rangle$
M92					
2247-54169-361	2.3	218	0.03	0.07	46.6
2247-54169-362	4.6	62	0.03	0.03	25.0
2247-54169-364	3.2	53	0.30	0.04	37.5
2247-54169-367	3.5	34	0.27	0.05	36.8
2247-54169-379	6.6	70	0.04	0.06	19.1
2247-54169-380	3.1	71	0.21	0.07	38.8
2247-54169-404	3.4	68	0.12	0.00	38.5
2247-54169-408	2.5	20	0.19	0.04	49.8
2247-54169-409	13.0	147	0.54	0.06	12.6
2247-54169-418	2.2	13	0.20	0.03	49.1
2247-54169-444	2.6	63	0.09	0.04	45.2
2247-54169-449	2.6	87	0.12	0.04	48.3

Continued on next page...

Table A.2 – Continued

spSpec name	$\sigma(\text{RV})$ (km s $^{-1}$)	$\sigma(\text{T}_{\text{eff}})$ (K)	$\sigma(\log g)$ (dex)	$\sigma(\text{[Fe/H]})$ (dex)	$\langle \text{S/N} \rangle$
2247-54169-451	3.0	32	0.26	0.04	42.4
2247-54169-452	2.9	36	0.07	0.03	44.3
2247-54169-458	7.1	56	0.18	0.05	19.9
2247-54169-484	2.1	94	0.22	0.04	51.4
2247-54169-504	2.2	37	0.19	0.03	50.6
2247-54169-514	5.7	69	0.29	0.06	23.1
2247-54169-516	6.8	23	0.56	0.07	19.9
2247-54169-519	6.3	22	0.27	0.01	18.6
2247-54169-529	4.1	15	0.23	0.03	28.6
2247-54169-531	3.0	59	0.17	0.04	38.4
2247-54169-538	8.0	88	0.53	0.05	16.4
2247-54169-541	6.2	31	0.22	0.04	21.5
2247-54169-546	4.3	57	0.24	0.06	28.7
2247-54169-561	3.2	55	0.18	0.04	37.7
2247-54169-563	2.3	26	0.23	0.03	48.6
2247-54169-573	3.2	34	0.23	0.04	43.7
2247-54169-575	9.1	111	0.43	0.07	15.3
2247-54169-581	3.3	67	0.26	0.03	37.5
2247-54169-582	2.1	138	0.30	0.02	50.2
2247-54169-584	6.4	155	0.61	0.05	18.9
2247-54169-589	4.5	78	0.29	0.02	30.0
2247-54169-608	2.4	19	0.18	0.04	48.2

Continued on next page...

Table A.2 – Continued

spSpec name	$\sigma(\text{RV})$ (km s $^{-1}$)	$\sigma(\text{T}_{\text{eff}})$ (K)	$\sigma(\log g)$ (dex)	$\sigma(\text{[Fe/H]})$ (dex)	$\langle \text{S/N} \rangle$
2247-54169-610	1.8	47	0.13	0.03	50.8
2247-54169-616	6.2	32	0.55	0.06	19.9
2247-54169-620	4.8	76	0.28	0.03	23.3
2256-53859-411	8.0	98	0.37	0.01	14.8
2256-53859-455	8.8	113	0.54	0.05	13.7
2256-53859-485	15.9	58	0.21	0.05	10.2
2256-53859-489	15.2	29	0.08	0.06	10.4
2256-53859-501	9.6	44	0.27	0.01	13.0
2256-53859-506	10.6	84	0.35	0.09	11.6
2256-53859-513	5.3	80	0.30	0.03	25.4
2256-53859-522	7.3	76	0.41	0.06	18.0
2256-53859-530	10.1	74	0.18	0.07	13.4
2256-53859-535	7.1	51	0.54	0.06	16.6
2256-53859-536	6.3	57	0.20	0.09	18.9
2256-53859-537	14.1	107	0.12	0.09	10.8
2256-53859-538	5.5	48	0.29	0.04	24.7
2256-53859-539	11.4	34	0.60	0.01	11.9
2256-53859-546	10.5	45	0.24	0.10	13.3
2256-53859-566	11.2	92	0.00	0.06	12.2
2256-53859-571	9.1	61	0.40	0.05	14.0
2256-53859-575	8.8	58	0.48	0.05	12.7
2256-53859-576	9.6	65	0.34	0.03	14.6

Continued on next page...

Table A.2 – Continued

spSpec name	$\sigma(\text{RV})$ (km s $^{-1}$)	$\sigma(\text{T}_{\text{eff}})$ (K)	$\sigma(\log g)$ (dex)	$\sigma(\text{[Fe/H]})$ (dex)	$\langle \text{S/N} \rangle$
2256-53859-579	10.8	50	0.52	0.07	12.0
2256-53859-612	9.9	58	0.26	0.04	12.7
M15					
1960-53289-401	2.6	15	0.16	0.05	55.9
1960-53289-402	2.4	33	0.22	0.04	62.2
1960-53289-406	2.3	15	0.14	0.02	65.1
1960-53289-413	3.0	26	0.07	0.02	57.6
1960-53289-419	2.1	17	0.26	0.02	65.1
1960-53289-420	13.9	82	0.39	0.06	15.0
1960-53289-441	6.0	97	0.45	0.02	23.7
1960-53289-442	3.5	23	0.06	0.03	46.8
1960-53289-457	9.1	68	0.39	0.06	20.3
1960-53289-459	1.9	14	0.20	0.03	68.2
1960-53289-460	3.4	68	0.24	0.03	47.8
1960-53289-500	4.5	47	0.25	0.03	35.4
1960-53289-501	10.5	123	0.46	0.04	16.5
1960-53289-511	4.0	67	0.18	0.04	43.5
1960-53289-522	5.0	73	0.29	0.06	33.6
1960-53289-523	1.7	52	0.26	0.06	70.7
1960-53289-529	2.4	20	0.15	0.04	63.7
1960-53289-530	4.9	64	0.18	0.16	29.2
1962-53321-323	6.9	79	0.31	0.08	22.7

Continued on next page...

Table A.2 – Continued

spSpec name	$\sigma(\text{RV})$ (km s $^{-1}$)	$\sigma(\text{T}_{\text{eff}})$ (K)	$\sigma(\log g)$ (dex)	$\sigma(\text{[Fe/H]})$ (dex)	$\langle \text{S/N} \rangle$
1962-53321-328	9.3	95	0.30	0.08	17.4
1962-53321-329	6.7	42	0.05	0.06	20.0
1962-53321-335	7.4	72	0.13	0.10	22.7
1962-53321-339	11.9	80	0.27	0.03	12.7
1962-53321-363	14.4	119	0.03	0.05	12.5
1962-53321-364	3.3	63	0.28	0.06	40.4
1962-53321-368	8.2	67	0.27	0.05	20.6
1962-53321-369	7.1	116	0.55	0.07	18.5
1962-53321-370	7.1	62	0.24	0.02	21.8
1962-53321-371	6.7	119	0.23	0.04	20.6
1962-53321-372	7.2	139	0.60	0.05	23.8
1962-53321-375	4.2	86	0.33	0.12	31.6
1962-53321-376	3.3	75	0.25	0.04	41.5
1962-53321-378	12.8	45	0.20	0.03	13.8
1962-53321-399	9.4	45	0.38	0.06	16.7
1962-53321-402	3.9	82	0.14	0.06	33.3
1962-53321-403	4.5	54	0.10	0.05	31.8
1962-53321-406	4.7	45	0.22	0.07	32.1
1962-53321-407	7.7	115	0.37	0.00	20.4
1962-53321-409	14.0	48	0.19	0.07	11.5
1962-53321-412	10.6	112	0.37	0.08	14.5
1962-53321-413	3.2	84	0.25	0.05	40.6

Continued on next page...

Table A.2 – Continued

spSpec name	$\sigma(\text{RV})$ (km s $^{-1}$)	$\sigma(\text{T}_{\text{eff}})$ (K)	$\sigma(\log g)$ (dex)	$\sigma(\text{[Fe/H]})$ (dex)	$\langle \text{S/N} \rangle$
1962-53321-414	6.5	96	0.57	0.06	21.6
1962-53321-415	3.5	71	0.19	0.02	42.8
1962-53321-416	11.2	88	0.52	0.05	13.1
1962-53321-419	11.3	123	0.04	0.09	11.7
1962-53321-421	5.1	102	0.44	0.04	24.6
1962-53321-422	10.2	174	0.75	0.08	13.8
1962-53321-423	5.1	110	0.03	0.01	26.7
1962-53321-424	7.9	111	0.21	0.02	13.9
1962-53321-427	3.9	94	0.28	0.06	38.5
1962-53321-428	9.8	97	0.29	0.08	14.5
1962-53321-430	9.5	241	0.91	0.10	12.5
1962-53321-438	3.2	80	0.17	0.01	42.2
1962-53321-442	8.4	122	0.50	0.15	17.1
1962-53321-445	12.4	112	0.18	0.18	10.3
1962-53321-449	13.9	165	0.70	0.05	10.5
1962-53321-454	4.0	75	0.35	0.05	37.8
1962-53321-460	14.5	72	0.20	0.01	11.4
1962-53321-465	9.4	11	0.23	0.06	15.6
1962-53321-466	3.5	80	0.31	0.04	45.1
1962-53321-469	8.2	152	0.32	0.05	20.9
1962-53321-470	6.2	77	0.22	0.05	22.2
1962-53321-471	8.0	64	0.21	0.06	18.5

Continued on next page...

Table A.2 – Continued

spSpec name	$\sigma(\text{RV})$ (km s $^{-1}$)	$\sigma(\text{T}_{\text{eff}})$ (K)	$\sigma(\log g)$ (dex)	$\sigma(\text{[Fe/H]})$ (dex)	$\langle \text{S/N} \rangle$
1962-53321-474	3.2	79	0.21	0.09	44.6
1962-53321-478	12.8	163	0.67	0.07	10.3
1962-53321-480	8.4	138	0.52	0.06	17.2
1962-53321-483	11.9	90	0.80	0.05	12.5
1962-53321-484	9.2	31	0.02	0.10	14.6
1962-53321-488	7.9	85	0.15	0.07	18.1
1962-53321-490	8.7	45	0.31	0.07	17.3
1962-53321-493	5.6	77	0.28	0.03	27.8
1962-53321-495	7.6	70	0.34	0.04	19.1
1962-53321-496	7.7	41	0.08	0.04	19.1
1962-53321-497	8.5	77	0.24	0.03	18.2
1962-53321-500	6.2	42	0.15	0.04	25.9
1962-53321-503	8.2	77	0.36	0.06	16.3
1962-53321-505	14.0	205	0.06	0.09	11.4
1962-53321-506	2.9	60	0.12	0.06	46.3
1962-53321-509	10.2	101	0.29	0.02	13.0
1962-53321-510	7.2	57	0.45	0.03	23.2
1962-53321-512	14.7	101	0.50	0.07	11.2
1962-53321-515	2.8	55	0.13	0.05	42.9
1962-53321-516	5.3	44	0.31	0.06	28.1
1962-53321-518	4.8	59	0.27	0.06	30.0
1962-53321-519	8.8	51	0.03	0.03	15.7

Continued on next page...

Table A.2 – Continued

spSpec name	$\sigma(\text{RV})$ (km s $^{-1}$)	$\sigma(\text{T}_{\text{eff}})$ (K)	$\sigma(\log g)$ (dex)	$\sigma(\text{[Fe/H]})$ (dex)	$\langle \text{S/N} \rangle$
1962-53321-520	5.8	51	0.33	0.05	23.1
1962-53321-522	12.7	92	0.04	0.03	11.9
1962-53321-532	3.4	81	0.11	0.01	43.6
1962-53321-533	7.2	54	0.38	0.11	21.0
1962-53321-539	8.8	41	0.23	0.05	19.5
1962-53321-540	12.0	148	0.33	0.08	12.4
1962-53321-543	9.1	123	0.29	0.10	16.6
1962-53321-545	8.3	209	0.42	0.09	14.0
1962-53321-549	5.6	70	0.30	0.04	23.9
1962-53321-550	6.3	56	0.18	0.01	24.2
1962-53321-554	11.9	221	0.03	0.07	11.9
1962-53321-555	12.9	95	0.20	0.09	10.7
1962-53321-558	5.6	75	0.26	0.03	25.2
NGC 5053					
2476-53826-486	6.4	101	0.47	0.04	17.5
2476-53826-488	2.2	87	0.21	0.06	49.1
2476-53826-490	4.3	171	0.28	0.03	30.0
2476-53826-497	9.8	87	0.10	0.08	12.4
2476-53826-501	2.6	52	0.25	0.07	48.4
2476-53826-505	3.3	63	0.28	0.04	39.6
2476-53826-506	5.0	116	0.23	0.08	29.4
2476-53826-507	4.2	65	0.20	0.06	30.6

Continued on next page...

Table A.2 – Continued

spSpec name	$\sigma(\text{RV})$ (km s $^{-1}$)	$\sigma(\text{T}_{\text{eff}})$ (K)	$\sigma(\log g)$ (dex)	$\sigma(\text{[Fe/H]})$ (dex)	$\langle \text{S/N} \rangle$
2476-53826-508	3.5	61	0.16	0.03	33.5
2476-53826-519	1.5	35	0.17	0.01	62.9
2476-53826-527	2.1	76	0.21	0.04	51.2
2476-53826-531	5.5	222	0.11	0.12	23.0
2476-53826-573	5.1	91	0.25	0.04	26.3
2476-53826-575	1.9	82	0.28	0.12	56.6
2476-53826-577	4.0	46	0.26	0.04	30.2
2476-53826-578	1.9	91	0.37	0.07	55.1
M53					
2476-53826-329	7.0	193	0.38	0.10	12.8
2476-53826-361	4.0	108	0.19	0.09	26.1
2476-53826-362	6.5	154	0.32	0.11	18.6
2476-53826-363	7.6	130	0.11	0.07	17.1
2476-53826-369	7.2	142	0.23	0.04	18.6
2476-53826-372	5.1	64	0.32	0.04	25.8
2476-53826-375	6.9	82	0.23	0.04	17.7
2476-53826-376	8.7	313	0.29	0.08	15.7
2476-53826-378	3.0	70	0.17	0.03	36.9
2476-53826-379	7.9	301	0.45	0.01	16.6
2476-53826-401	5.2	23	0.17	0.06	20.4
2476-53826-404	2.0	89	0.22	0.04	47.5
2476-53826-405	9.2	19	0.43	0.10	12.1

Continued on next page...

Table A.2 – Continued

spSpec name	$\sigma(\text{RV})$ (km s $^{-1}$)	$\sigma(\text{T}_{\text{eff}})$ (K)	$\sigma(\log g)$ (dex)	$\sigma(\text{[Fe/H]})$ (dex)	$\langle \text{S/N} \rangle$
2476-53826-408	6.9	96	0.10	0.12	19.3
2476-53826-409	4.9	112	0.35	0.01	20.6
2476-53826-413	7.5	141	0.35	0.05	15.5
2476-53826-418	8.4	59	0.33	0.10	11.8
2476-53826-451	3.4	40	0.16	0.05	30.0
2476-53826-452	5.9	64	0.26	0.09	20.3
M2					
1961-53299-124	1.5	60	0.01	0.13	51.9
1961-53299-125	1.6	54	0.10	0.06	52.6
1961-53299-131	1.9	46	0.19	0.02	43.6
1961-53299-134	1.1	72	0.09	0.09	60.8
1961-53299-136	2.4	4	0.06	0.05	39.1
1961-53299-140	2.9	43	0.10	0.05	34.1
1961-53299-144	2.7	69	0.28	0.05	37.5
1961-53299-152	2.0	51	0.04	0.04	44.1
1961-53299-159	2.4	2	0.20	0.06	39.5
1961-53299-194	2.4	197	0.13	0.01	46.0
1961-53299-213	3.3	114	0.36	0.06	33.2
1961-53299-215	2.0	92	0.16	0.01	48.2
1963-54331-041	16.4	77	0.39	0.11	10.5
1963-54331-043	5.9	58	0.23	0.03	19.6
1963-54331-045	12.8	25	0.26	0.05	11.2

Continued on next page...

Table A.2 – Continued

spSpec name	$\sigma(\text{RV})$ (km s $^{-1}$)	$\sigma(\text{T}_{\text{eff}})$ (K)	$\sigma(\log g)$ (dex)	$\sigma(\text{[Fe/H]})$ (dex)	$\langle \text{S/N} \rangle$
1963-54331-082	15.6	179	0.63	0.07	10.8
1963-54331-083	8.6	65	0.32	0.04	17.1
1963-54331-090	5.9	63	0.09	0.06	18.6
1963-54331-091	4.1	53	0.15	0.05	23.5
1963-54331-096	6.9	41	0.22	0.01	16.6
1963-54331-098	2.6	29	0.18	0.03	40.5
1963-54331-100	6.8	91	0.13	0.06	16.8
1963-54331-102	9.4	62	0.20	0.08	15.4
1963-54331-114	9.2	40	0.36	0.04	13.0
1963-54331-121	2.5	44	0.09	0.04	40.3
1963-54331-123	5.2	56	0.19	0.02	20.4
1963-54331-124	9.0	74	0.42	0.04	14.9
1963-54331-126	3.8	82	0.16	0.03	27.1
1963-54331-128	3.6	57	0.10	0.04	27.7
1963-54331-131	3.7	58	0.06	0.04	28.2
1963-54331-137	3.0	42	0.07	0.03	33.4
1963-54331-139	3.2	18	0.14	0.04	33.8
1963-54331-143	6.1	60	0.35	0.06	19.0
1963-54331-144	2.3	11	0.10	0.05	38.8
1963-54331-145	6.2	26	0.39	0.09	17.6
1963-54331-146	10.3	126	0.15	0.04	13.4
1963-54331-147	11.1	132	0.30	0.03	13.5

Continued on next page...

Table A.2 – Continued

spSpec name	$\sigma(\text{RV})$ (km s $^{-1}$)	$\sigma(\text{T}_{\text{eff}})$ (K)	$\sigma(\log g)$ (dex)	$\sigma(\text{[Fe/H]})$ (dex)	$\langle \text{S/N} \rangle$
1963-54331-148	7.4	61	0.05	0.03	17.8
1963-54331-150	7.7	61	0.27	0.04	16.9
1963-54331-154	10.9	58	0.24	0.09	10.5
1963-54331-156	9.8	105	0.33	0.06	11.6
1963-54331-162	12.3	96	0.20	0.00	10.7
1963-54331-164	3.6	119	0.14	0.09	26.7
1963-54331-169	10.6	112	0.70	0.04	10.7
1963-54331-170	10.8	209	0.37	0.02	11.6
1963-54331-178	4.0	5	0.19	0.06	25.0
1963-54331-179	9.2	60	0.64	0.04	14.0
1963-54331-180	4.8	52	0.03	0.05	22.0
1963-54331-181	8.5	58	0.27	0.04	14.6
1963-54331-184	4.5	67	0.13	0.06	22.3
1963-54331-185	11.6	96	0.35	0.10	10.9
1963-54331-186	13.8	155	0.31	0.18	10.3
1963-54331-189	9.3	81	0.28	0.04	12.7
1963-54331-194	8.7	55	0.28	0.04	14.3
1963-54331-196	9.8	107	0.21	0.03	13.3
1963-54331-197	10.5	130	0.75	0.09	10.7
1963-54331-200	12.8	93	0.42	0.05	10.8
1963-54331-201	5.0	41	0.13	0.05	22.3
1963-54331-204	2.7	58	0.08	0.05	34.2

Continued on next page...

Table A.2 – Continued

spSpec name	$\sigma(\text{RV})$ (km s $^{-1}$)	$\sigma(\text{T}_{\text{eff}})$ (K)	$\sigma(\log g)$ (dex)	$\sigma(\text{[Fe/H]})$ (dex)	$\langle \text{S/N} \rangle$
1963-54331-206	11.6	62	0.29	0.06	12.6
1963-54331-207	11.6	116	0.24	0.02	10.8
1963-54331-208	2.8	22	0.13	0.05	36.5
1963-54331-209	4.0	28	0.12	0.01	27.6
1963-54331-211	4.1	32	0.17	0.02	27.6
1963-54331-212	5.2	50	0.21	0.02	22.1
1963-54331-217	3.2	27	0.13	0.02	33.1
1963-54331-218	3.1	19	0.14	0.04	33.3
1963-54331-220	10.4	99	0.29	0.08	13.1
1963-54331-222	8.8	85	0.17	0.04	13.0
1963-54331-223	11.3	24	0.19	0.03	13.2
1963-54331-254	8.1	172	0.19	0.03	13.3
M13					
2174-53521-054	5.1	44	0.16	0.03	21.0
2174-53521-082	1.7	42	0.14	0.05	55.0
2174-53521-087	3.3	54	0.13	0.05	29.1
2174-53521-093	1.9	49	0.14	0.03	57.2
2174-53521-094	3.5	46	0.14	0.05	30.1
2174-53521-098	1.6	69	0.15	0.06	54.7
2174-53521-121	1.9	60	0.13	0.02	48.0
2174-53521-126	3.9	66	0.09	0.05	33.1
2174-53521-128	4.3	50	0.18	0.05	24.7

Continued on next page...

Table A.2 – Continued

spSpec name	$\sigma(\text{RV})$ (km s $^{-1}$)	$\sigma(\text{T}_{\text{eff}})$ (K)	$\sigma(\log g)$ (dex)	$\sigma(\text{[Fe/H]})$ (dex)	$\langle \text{S/N} \rangle$
2174-53521-131	2.0	39	0.47	0.08	58.2
2174-53521-133	3.4	56	0.10	0.03	37.8
2174-53521-134	3.2	64	0.10	0.04	30.0
2174-53521-136	2.0	312	0.16	0.26	54.4
2174-53521-137	1.8	64	0.13	0.06	55.6
2174-53521-145	1.6	72	0.13	0.02	60.1
2174-53521-146	4.4	33	0.23	0.04	23.4
2174-53521-149	4.8	49	0.12	0.05	20.9
2174-53521-152	1.8	202	0.12	0.11	56.1
2174-53521-153	1.8	155	0.13	0.06	56.7
2174-53521-154	1.6	50	0.09	0.07	59.1
2174-53521-155	2.4	45	0.15	0.03	41.8
2174-53521-156	1.7	54	0.15	0.04	53.6
2174-53521-157	2.1	216	0.15	0.01	53.7
2174-53521-158	1.6	49	0.14	0.05	54.1
2174-53521-159	1.4	50	0.08	0.04	58.9
2174-53521-160	1.7	59	0.19	0.07	56.9
2174-53521-166	1.9	63	0.16	0.02	54.1
2174-53521-167	1.4	52	0.15	0.07	60.1
2174-53521-168	1.4	49	0.03	0.06	57.3
2174-53521-171	1.5	72	0.12	0.04	60.2
2174-53521-172	1.5	59	0.12	0.06	57.6

Continued on next page...

Table A.2 – Continued

spSpec name	$\sigma(\text{RV})$ (km s $^{-1}$)	$\sigma(\text{T}_{\text{eff}})$ (K)	$\sigma(\log g)$ (dex)	$\sigma(\text{[Fe/H]})$ (dex)	$\langle \text{S/N} \rangle$
2174-53521-174	7.8	3	0.30	0.02	18.6
2174-53521-175	1.7	154	0.11	0.06	53.5
2174-53521-176	1.9	51	0.11	0.03	53.5
2174-53521-215	1.8	44	0.16	0.02	56.9
2174-53521-368	3.4	66	0.09	0.07	26.8
2174-53521-376	2.0	46	0.21	0.06	47.3
2174-53521-402	3.9	49	0.03	0.04	23.1
2174-53521-403	5.2	50	0.06	0.06	21.7
2174-53521-406	4.4	111	0.16	0.05	23.8
2174-53521-407	1.9	57	0.11	0.03	44.5
2174-53521-410	1.4	75	0.24	0.02	58.7
2174-53521-412	3.7	56	0.15	0.06	28.5
2174-53521-413	1.6	26	0.13	0.07	57.0
2174-53521-414	3.4	67	0.16	0.04	30.8
2174-53521-442	1.8	129	0.15	0.05	57.9
2174-53521-443	1.7	40	0.07	0.06	58.6
2174-53521-445	4.4	31	0.08	0.03	23.1
2174-53521-447	3.7	35	0.22	0.03	27.1
2174-53521-449	1.4	59	0.10	0.04	58.4
2174-53521-451	1.9	146	0.20	0.10	58.3
2174-53521-452	1.5	43	0.17	0.05	59.9
2174-53521-453	1.6	35	0.14	0.04	59.0

Continued on next page...

Table A.2 – Continued

spSpec name	$\sigma(\text{RV})$ (km s $^{-1}$)	$\sigma(\text{T}_{\text{eff}})$ (K)	$\sigma(\log g)$ (dex)	$\sigma(\text{[Fe/H]})$ (dex)	$\langle \text{S/N} \rangle$
2174-53521-455	1.3	41	0.14	0.06	58.6
2174-53521-456	2.9	31	0.16	0.03	32.0
2174-53521-457	1.3	40	0.15	0.03	59.8
2174-53521-458	1.7	63	0.20	0.07	60.4
2174-53521-459	1.3	25	0.15	0.06	59.6
2174-53521-460	1.4	60	0.17	0.09	61.7
2174-53521-461	2.9	29	0.17	0.02	29.8
2174-53521-462	1.5	42	0.14	0.04	59.7
2174-53521-463	1.8	46	0.15	0.06	55.6
2174-53521-464	1.8	166	0.11	0.00	58.2
2174-53521-470	1.5	59	0.16	0.06	61.6
2174-53521-471	1.9	46	0.13	0.05	48.5
2174-53521-472	1.6	81	0.15	0.04	59.5
2174-53521-474	4.0	44	0.26	0.04	27.3
2174-53521-475	1.3	159	0.44	0.04	61.1
2174-53521-476	2.0	32	0.14	0.11	53.6
2174-53521-477	1.5	39	0.14	0.03	59.6
2174-53521-478	1.6	44	0.11	0.04	58.1
2174-53521-480	2.5	18	0.16	0.02	39.3
2174-53521-481	5.3	34	0.22	0.05	20.4
2174-53521-483	1.3	35	0.16	0.03	59.7
2174-53521-484	1.3	50	0.14	0.01	59.8

Continued on next page...

Table A.2 – Continued

spSpec name	$\sigma(\text{RV})$ (km s $^{-1}$)	$\sigma(\text{T}_{\text{eff}})$ (K)	$\sigma(\log g)$ (dex)	$\sigma(\text{[Fe/H]})$ (dex)	$\langle \text{S/N} \rangle$
2174-53521-485	1.6	38	0.17	0.08	56.9
2174-53521-488	1.5	33	0.13	0.04	55.4
2174-53521-489	1.6	55	0.17	0.03	56.7
2174-53521-490	1.8	167	0.09	0.05	57.2
2174-53521-491	1.9	251	0.13	0.02	55.8
2174-53521-493	1.8	41	0.20	0.03	60.4
2174-53521-494	1.5	45	0.07	0.05	59.9
2174-53521-495	1.5	40	0.15	0.04	52.6
2174-53521-497	1.6	47	0.14	0.05	58.0
2174-53521-498	1.5	60	0.10	0.04	59.8
2174-53521-499	1.7	46	0.06	0.09	60.0
2174-53521-500	1.4	49	0.11	0.03	58.8
2174-53521-522	1.7	40	0.18	0.06	57.4
2174-53521-529	1.9	57	0.15	0.08	46.6
2174-53521-530	1.3	56	0.21	0.09	58.8
2174-53521-531	1.5	2	0.15	0.06	59.4
2174-53521-532	1.8	160	0.15	0.02	58.0
2174-53521-533	4.6	68	0.23	0.01	24.3
2174-53521-537	1.5	32	0.14	0.05	53.3
2174-53521-538	1.3	67	0.15	0.03	60.9
2174-53521-539	3.3	33	0.16	0.04	28.1
2174-53521-540	1.7	206	0.10	0.07	58.4

Continued on next page...

Table A.2 – Continued

spSpec name	$\sigma(\text{RV})$ (km s $^{-1}$)	$\sigma(\text{T}_{\text{eff}})$ (K)	$\sigma(\log g)$ (dex)	$\sigma(\text{[Fe/H]})$ (dex)	$\langle \text{S/N} \rangle$
2174-53521-542	1.4	61	0.18	0.03	58.7
2174-53521-554	1.6	49	0.13	0.04	54.0
2174-53521-560	3.6	36	0.19	0.03	30.2
2174-53521-563	1.9	32	0.20	0.07	44.0
2174-53521-565	4.5	75	0.20	0.03	23.5
2174-53521-573	5.3	59	0.14	0.04	22.9
2174-53521-576	3.6	49	0.14	0.06	28.3
2174-53521-577	4.0	45	0.12	0.05	24.3
2185-53532-106	8.2	96	0.33	0.03	13.1
2185-53532-111	4.9	46	0.26	0.02	25.2
2185-53532-113	11.7	82	0.39	0.02	10.9
2185-53532-116	8.0	107	0.29	0.06	16.5
2185-53532-120	6.3	52	0.10	0.04	18.4
2185-53532-141	4.0	52	0.38	0.03	31.4
2185-53532-143	5.0	27	0.03	0.03	27.9
2185-53532-146	10.9	43	0.49	0.09	11.5
2185-53532-148	5.8	45	0.29	0.03	21.6
2185-53532-150	5.5	46	0.29	0.04	24.6
2185-53532-151	7.0	42	0.38	0.03	16.1
2185-53532-152	5.5	49	0.47	0.01	24.6
2185-53532-153	2.8	21	0.12	0.02	40.7
2185-53532-154	9.4	140	0.38	0.01	13.6

Continued on next page...

Table A.2 – Continued

spSpec name	$\sigma(\text{RV})$ (km s $^{-1}$)	$\sigma(\text{T}_{\text{eff}})$ (K)	$\sigma(\log g)$ (dex)	$\sigma(\text{[Fe/H]})$ (dex)	$\langle \text{S/N} \rangle$
2185-53532-156	7.2	30	0.24	0.03	21.1
2185-53532-158	5.9	42	0.31	0.04	23.0
2185-53532-160	6.6	65	0.18	0.03	18.6
2185-53532-161	8.8	104	0.35	0.04	13.2
2185-53532-167	4.5	61	0.24	0.06	26.3
2185-53532-169	6.1	43	0.35	0.04	21.9
2185-53532-171	11.6	63	0.26	0.01	12.0
2185-53532-172	5.2	37	0.18	0.01	25.1
2185-53532-175	5.4	87	0.39	0.03	20.9
2185-53532-176	4.9	34	0.12	0.04	25.4
2185-53532-177	5.4	54	0.40	0.05	23.8
2185-53532-178	5.9	49	0.12	0.02	21.4
2185-53532-179	4.1	63	0.20	0.03	31.1
2185-53532-181	5.3	98	0.39	0.06	25.3
2185-53532-196	6.4	40	0.21	0.02	20.8
2185-53532-197	7.2	64	0.73	0.08	18.3
2185-53532-198	5.4	38	0.31	0.03	24.4
2185-53532-200	8.7	28	0.25	0.03	12.2
2185-53532-237	3.2	84	0.31	0.03	39.4
2185-53532-388	3.5	53	0.23	0.02	34.1
2185-53532-390	7.9	95	0.12	0.06	13.7
2185-53532-393	8.9	95	0.57	0.07	11.4

Continued on next page...

Table A.2 – Continued

spSpec name	$\sigma(\text{RV})$ (km s $^{-1}$)	$\sigma(\text{T}_{\text{eff}})$ (K)	$\sigma(\log g)$ (dex)	$\sigma(\text{[Fe/H]})$ (dex)	$\langle \text{S/N} \rangle$
2185-53532-423	5.2	80	0.28	0.06	24.7
2185-53532-424	4.7	55	0.41	0.06	25.6
2185-53532-425	3.3	32	0.20	0.05	36.1
2185-53532-426	2.7	26	0.07	0.03	41.7
2185-53532-427	2.7	30	0.14	0.05	42.6
2185-53532-428	5.8	32	0.22	0.06	19.8
2185-53532-430	8.5	66	0.32	0.05	14.0
2185-53532-431	9.4	63	0.21	0.05	12.4
2185-53532-433	9.4	44	0.20	0.09	12.4
2185-53532-435	5.7	46	0.25	0.01	22.1
2185-53532-439	2.7	58	0.15	0.04	40.1
2185-53532-440	9.0	68	0.32	0.05	13.1
2185-53532-461	3.6	41	0.21	0.03	34.0
2185-53532-462	2.7	40	0.17	0.04	38.6
2185-53532-464	8.7	34	0.26	0.03	16.9
2185-53532-466	5.2	49	0.13	0.04	23.1
2185-53532-469	5.8	50	0.01	0.08	20.0
2185-53532-473	6.2	40	0.26	0.03	19.6
2185-53532-475	4.1	44	0.22	0.05	30.2
2185-53532-476	5.8	69	0.21	0.07	22.1
2185-53532-477	7.2	25	0.28	0.04	15.2
2185-53532-478	5.3	62	0.20	0.02	24.0

Continued on next page...

Table A.2 – Continued

spSpec name	$\sigma(\text{RV})$ (km s $^{-1}$)	$\sigma(\text{T}_{\text{eff}})$ (K)	$\sigma(\log g)$ (dex)	$\sigma(\text{[Fe/H]})$ (dex)	$\langle \text{S/N} \rangle$
2185-53532-479	6.8	46	0.32	0.03	16.9
2185-53532-480	7.3	14	0.49	0.02	13.9
2185-53532-481	3.1	26	0.23	0.04	36.8
2185-53532-482	3.0	22	0.17	0.04	40.4
2185-53532-483	5.5	39	0.21	0.04	20.6
2185-53532-485	3.9	42	0.07	0.00	31.9
2185-53532-486	6.2	82	0.35	0.05	17.2
2185-53532-487	3.5	33	0.15	0.04	34.7
2185-53532-488	8.3	103	0.48	0.07	14.7
2185-53532-489	5.4	67	0.36	0.04	22.4
2185-53532-490	7.2	59	0.08	0.06	18.0
2185-53532-492	3.0	19	0.24	0.03	38.9
2185-53532-493	3.4	45	0.22	0.05	35.0
2185-53532-494	7.4	23	0.32	0.03	19.9
2185-53532-495	4.7	40	0.25	0.04	28.4
2185-53532-496	7.8	90	0.44	0.04	12.0
2185-53532-497	9.2	54	0.31	0.01	15.0
2185-53532-498	4.5	27	0.38	0.04	28.1
2185-53532-499	4.9	35	0.16	0.01	27.2
2185-53532-500	3.1	74	0.15	0.05	40.8
2185-53532-504	4.4	42	0.12	0.02	27.7
2185-53532-506	2.4	42	0.12	0.03	44.7

Continued on next page...

Table A.2 – Continued

spSpec name	$\sigma(\text{RV})$ (km s $^{-1}$)	$\sigma(\text{T}_{\text{eff}})$ (K)	$\sigma(\log g)$ (dex)	$\sigma(\text{[Fe/H]})$ (dex)	$\langle \text{S/N} \rangle$
2185-53532-507	5.5	34	0.15	0.01	20.9
2185-53532-508	4.5	164	0.14	0.05	23.6
2185-53532-511	7.2	106	0.07	0.06	16.4
2185-53532-512	3.4	35	0.16	0.02	37.8
2185-53532-513	4.8	37	0.25	0.03	25.6
2185-53532-514	5.1	49	0.37	0.05	21.0
2185-53532-515	5.2	63	0.20	0.03	24.4
2185-53532-516	9.3	68	0.26	0.06	12.6
2185-53532-517	9.6	171	0.17	0.09	12.2
2185-53532-519	5.0	48	0.11	0.05	25.6
2185-53532-520	3.3	34	0.31	0.03	34.9
2185-53532-534	4.3	48	0.17	0.05	29.9
2185-53532-537	4.9	38	0.20	0.03	27.0
2185-53532-539	6.8	63	0.25	0.04	16.0
2185-53532-540	6.8	59	0.26	0.05	19.2
2185-53532-541	11.4	34	0.32	0.04	12.2
2185-53532-542	6.9	89	0.08	0.07	17.5
2185-53532-543	3.4	52	0.24	0.02	36.7
2185-53532-544	5.2	28	0.24	0.04	24.0
2185-53532-545	5.7	51	0.14	0.07	21.3
2185-53532-546	8.9	4	0.27	0.06	13.1
2185-53532-547	8.6	121	0.70	0.10	12.4

Continued on next page...

Table A.2 – Continued

spSpec name	$\sigma(\text{RV})$ (km s $^{-1}$)	$\sigma(\text{T}_{\text{eff}})$ (K)	$\sigma(\log g)$ (dex)	$\sigma(\text{[Fe/H]})$ (dex)	$\langle \text{S/N} \rangle$
2185-53532-548	9.7	3	0.34	0.07	11.4
2185-53532-549	6.0	45	0.32	0.04	16.3
2185-53532-550	8.3	76	0.21	0.04	14.3
2185-53532-551	10.1	221	0.03	0.08	12.1
2185-53532-552	5.7	50	0.16	0.05	22.8
2185-53532-553	3.0	33	0.13	0.03	42.4
2185-53532-554	3.7	26	0.08	0.01	34.9
2185-53532-555	7.2	43	0.17	0.05	18.5
2185-53532-556	7.1	40	0.09	0.05	17.9
2185-53532-557	4.7	67	0.24	0.05	27.8
2185-53532-558	3.9	30	0.13	0.05	30.4
2185-53532-559	4.6	27	0.15	0.05	24.3
2185-53532-560	3.6	26	0.20	0.04	33.7
2185-53532-575	9.8	68	0.08	0.02	13.6
2185-53532-577	5.1	33	0.21	0.04	20.6
2185-53532-581	5.3	60	0.31	0.04	19.1
2185-53532-584	6.6	112	0.58	0.04	18.7
2185-53532-585	5.8	29	0.34	0.02	21.0
2185-53532-587	10.1	60	0.12	0.01	13.0
2185-53532-589	5.7	43	0.31	0.04	22.7
2185-53532-591	4.8	17	0.31	0.06	26.4
2185-53532-592	7.2	81	0.63	0.07	16.1

Continued on next page...

Table A.2 – Continued

spSpec name	$\sigma(\text{RV})$ (km s $^{-1}$)	$\sigma(\text{T}_{\text{eff}})$ (K)	$\sigma(\log g)$ (dex)	$\sigma(\text{[Fe/H]})$ (dex)	$\langle \text{S/N} \rangle$
2185-53532-593	4.9	51	0.35	0.02	24.2
2185-53532-594	8.3	42	0.32	0.09	15.5
2185-53532-596	8.5	196	0.35	0.09	12.5
2185-53532-598	7.6	64	0.16	0.06	16.8
2185-53532-599	6.3	61	0.27	0.06	17.0
2185-53532-600	8.5	108	0.23	0.05	12.3
2255-53565-103	5.4	52	0.16	0.03	22.1
2255-53565-112	4.1	93	0.12	0.05	20.6
2255-53565-114	3.0	40	0.08	0.05	37.2
2255-53565-115	4.7	33	0.17	0.02	24.5
2255-53565-116	1.8	61	0.13	0.03	52.2
2255-53565-120	1.7	60	0.14	0.02	61.8
2255-53565-143	3.2	52	0.08	0.06	57.5
2255-53565-144	1.6	33	0.17	0.04	60.4
2255-53565-147	1.7	191	0.13	0.22	61.3
2255-53565-148	1.7	44	0.05	0.05	58.9
2255-53565-153	1.5	53	0.10	0.05	60.0
2255-53565-157	1.5	58	0.12	0.02	65.9
2255-53565-171	1.4	48	0.14	0.05	63.7
2255-53565-173	4.1	83	0.14	0.05	28.3
2255-53565-174	1.7	132	0.12	0.06	58.6
2255-53565-175	1.7	38	0.11	0.03	57.4

Continued on next page...

Table A.2 – Continued

spSpec name	$\sigma(\text{RV})$ (km s $^{-1}$)	$\sigma(\text{T}_{\text{eff}})$ (K)	$\sigma(\log g)$ (dex)	$\sigma(\text{[Fe/H]})$ (dex)	$\langle \text{S/N} \rangle$
2255-53565-177	1.6	160	0.12	0.02	63.4
2255-53565-192	1.7	180	0.13	0.08	61.0
2255-53565-423	1.9	200	0.13	0.12	60.5
2255-53565-424	4.7	49	0.14	0.04	21.3
2255-53565-425	4.7	42	0.14	0.03	23.7
2255-53565-426	1.3	58	0.07	0.05	61.5
2255-53565-432	5.3	60	0.16	0.03	22.4
2255-53565-436	3.8	120	0.29	0.25	22.4
2255-53565-437	3.8	52	0.21	0.05	28.9
2255-53565-443	1.9	205	0.08	0.21	61.0
2255-53565-465	1.8	187	0.12	0.07	62.2
2255-53565-466	4.5	39	0.11	0.03	24.4
2255-53565-476	2.9	50	0.19	0.02	36.3
2255-53565-482	1.7	151	0.06	0.07	63.9
2255-53565-483	1.3	82	0.14	0.01	65.2
2255-53565-485	1.3	56	0.11	0.07	60.3
2255-53565-486	4.6	97	0.17	0.06	21.3
2255-53565-490	1.9	67	0.07	0.04	50.9
2255-53565-492	8.1	177	0.03	0.11	18.8
2255-53565-495	3.0	83	0.18	0.04	30.7
2255-53565-496	3.3	71	0.07	0.06	29.4
2255-53565-504	2.5	71	0.09	0.04	34.4

Continued on next page...

Table A.2 – Continued

spSpec name	$\sigma(\text{RV})$ (km s $^{-1}$)	$\sigma(\text{T}_{\text{eff}})$ (K)	$\sigma(\log g)$ (dex)	$\sigma(\text{[Fe/H]})$ (dex)	$\langle \text{S/N} \rangle$
2255-53565-510	1.6	70	0.13	0.05	59.7
2255-53565-512	4.3	90	0.06	0.05	22.2
2255-53565-515	1.4	77	0.09	0.13	58.6
2255-53565-518	3.1	69	0.22	0.04	27.9
2255-53565-520	3.7	87	0.16	0.07	26.5
2255-53565-542	1.3	77	0.08	0.06	62.4
2255-53565-543	1.3	85	0.17	0.06	62.1
2255-53565-544	4.5	88	0.13	0.06	23.5
2255-53565-545	1.4	66	0.12	0.03	61.6
2255-53565-548	1.5	93	0.21	0.05	63.4
2255-53565-550	1.6	70	0.13	0.02	59.5
2255-53565-551	1.4	89	0.14	0.02	65.3
2255-53565-552	2.6	65	0.12	0.02	34.5
2255-53565-553	1.5	58	0.12	0.05	64.2
2255-53565-556	2.9	63	0.10	0.05	36.8
2255-53565-557	3.2	105	0.13	0.08	26.3
2255-53565-559	3.2	87	0.15	0.06	33.1
2255-53565-586	3.1	90	0.15	0.02	32.2
2255-53565-589	1.4	80	0.14	0.05	64.7
2255-53565-597	1.9	56	0.09	0.03	49.2
M3					
2475-53845-105	2.9	26	0.27	0.07	34.6

Continued on next page...

Table A.2 – Continued

spSpec name	$\sigma(\text{RV})$ (km s $^{-1}$)	$\sigma(\text{T}_{\text{eff}})$ (K)	$\sigma(\log g)$ (dex)	$\sigma(\text{[Fe/H]})$ (dex)	$\langle \text{S/N} \rangle$
2475-53845-114	2.9	61	0.39	0.04	35.8
2475-53845-116	1.3	106	0.13	0.06	58.6
2475-53845-118	8.0	53	0.34	0.09	13.8
2475-53845-119	2.4	47	0.15	0.04	37.2
2475-53845-120	3.0	41	0.18	0.03	32.6
2475-53845-141	1.9	67	0.21	0.08	46.2
2475-53845-142	1.7	92	0.10	0.06	48.4
2475-53845-143	2.3	80	0.16	0.04	41.4
2475-53845-144	2.5	87	0.02	0.04	36.5
2475-53845-145	1.8	72	0.14	0.04	52.5
2475-53845-150	1.5	41	0.16	0.02	58.8
2475-53845-160	2.2	79	0.19	0.02	44.2
2475-53845-162	1.6	61	0.18	0.03	54.2
2475-53845-166	3.0	119	0.08	0.03	37.5
2475-53845-171	1.9	86	0.08	0.03	45.7
2475-53845-173	1.6	108	0.06	0.03	51.1
2475-53845-174	2.9	77	0.02	0.05	35.3
2475-53845-176	1.4	93	0.15	0.03	65.7
2475-53845-177	2.1	98	0.04	0.11	41.3
2475-53845-178	2.4	65	0.09	0.03	41.5
2475-53845-180	2.7	69	0.38	0.06	38.6
2475-53845-183	3.0	82	0.03	0.04	29.0

Continued on next page...

Table A.2 – Continued

spSpec name	$\sigma(\text{RV})$ (km s $^{-1}$)	$\sigma(\text{T}_{\text{eff}})$ (K)	$\sigma(\log g)$ (dex)	$\sigma(\text{[Fe/H]})$ (dex)	$\langle \text{S/N} \rangle$
2475-53845-185	5.4	89	0.22	0.10	17.1
2475-53845-186	1.8	78	0.07	0.06	52.3
2475-53845-187	3.9	66	0.10	0.06	36.7
2475-53845-190	3.0	59	0.15	0.04	38.8
2475-53845-192	4.9	72	0.16	0.04	20.9
2475-53845-193	3.2	83	0.22	0.05	38.9
2475-53845-194	3.6	94	0.28	0.02	34.5
2475-53845-196	1.9	76	0.11	0.04	47.9
2475-53845-198	1.5	104	0.11	0.07	58.2
2475-53845-199	1.7	70	0.10	0.03	58.1
2475-53845-200	5.4	134	0.38	0.03	17.9
2475-53845-421	1.1	79	0.12	0.06	68.4
2475-53845-430	5.8	95	0.11	0.04	17.2
2475-53845-436	1.2	101	0.11	0.05	62.6
2475-53845-440	1.3	73	0.11	0.10	60.3
2475-53845-461	1.6	46	0.13	0.04	50.6
2475-53845-462	2.4	91	0.35	0.04	40.6
2475-53845-463	1.7	72	0.02	0.06	56.5
2475-53845-466	1.8	59	0.12	0.05	52.6
2475-53845-469	3.0	56	0.07	0.04	27.8
2475-53845-471	1.5	97	0.03	0.04	55.8
2475-53845-473	1.2	74	0.14	0.06	63.1

Continued on next page...

Table A.2 – Continued

spSpec name	$\sigma(\text{RV})$ (km s $^{-1}$)	$\sigma(\text{T}_{\text{eff}})$ (K)	$\sigma(\log g)$ (dex)	$\sigma(\text{[Fe/H]})$ (dex)	$\langle \text{S/N} \rangle$
2475-53845-475	1.7	95	0.14	0.06	50.2
2475-53845-476	2.3	79	0.16	0.03	44.6
2475-53845-479	1.5	39	0.13	0.02	60.2
2475-53845-480	1.7	84	0.13	0.04	53.3
2475-53845-481	3.0	96	0.37	0.03	35.3
2475-53845-483	1.0	120	0.13	0.07	71.2
2475-53845-485	3.6	162	0.15	0.13	38.0
2475-53845-486	1.1	89	0.27	0.05	69.9
2475-53845-487	7.1	222	0.15	0.09	12.7
2475-53845-488	2.0	32	0.14	0.05	45.8
2475-53845-489	1.4	82	0.09	0.07	55.2
2475-53845-492	2.8	63	0.19	0.04	36.7
2475-53845-496	1.5	73	0.10	0.04	58.2
2475-53845-497	1.2	63	0.11	0.07	59.0
2475-53845-498	1.6	53	0.09	0.06	54.0
2475-53845-501	2.7	24	0.15	0.02	34.1
2475-53845-505	3.3	104	0.20	0.06	43.1
2475-53845-506	1.3	61	0.12	0.03	65.8
2475-53845-507	4.9	44	0.16	0.06	21.3
2475-53845-509	1.6	45	0.11	0.04	50.4
2475-53845-510	2.8	234	0.12	0.06	36.0
2475-53845-511	1.6	34	0.10	0.03	58.9

Continued on next page...

Table A.2 – Continued

spSpec name	$\sigma(\text{RV})$ (km s $^{-1}$)	$\sigma(\text{T}_{\text{eff}})$ (K)	$\sigma(\log g)$ (dex)	$\sigma(\text{[Fe/H]})$ (dex)	$\langle \text{S/N} \rangle$
2475-53845-514	2.3	43	0.21	0.03	37.1
2475-53845-515	1.6	62	0.09	0.05	54.6
2475-53845-518	1.1	64	0.14	0.03	62.3
2475-53845-519	1.9	34	0.11	0.00	41.6
2475-53845-520	2.2	19	0.13	0.06	38.0
2475-53845-550	7.2	123	0.21	0.00	13.8
2475-53845-551	1.4	71	0.16	0.05	55.7
2475-53845-557	3.3	31	0.22	0.05	27.4
2475-53845-558	2.1	42	0.06	0.03	40.8
2475-53845-559	1.7	53	0.11	0.04	47.6
M71					
2333-53682-077	0.8	186	0.21	0.05	79.6
2333-53682-105	1.1	98	0.20	0.03	63.3
2333-53682-144	1.3	116	0.10	0.08	84.5
2333-53682-153	2.5	181	0.29	0.05	29.8
2333-53682-167	1.2	58	0.16	0.05	65.8
2333-53682-176	1.2	65	0.10	0.05	66.0
2333-53682-178	1.3	114	0.18	0.05	64.1
2333-53682-183	1.0	128	0.15	0.05	84.6
2333-53682-191	1.5	132	0.11	0.01	62.3
2333-53682-193	1.4	112	0.08	0.05	60.8
2333-53682-198	1.6	83	0.07	0.02	52.0

Continued on next page...

Table A.2 – Continued

spSpec name	$\sigma(\text{RV})$ (km s $^{-1}$)	$\sigma(\text{T}_{\text{eff}})$ (K)	$\sigma(\log g)$ (dex)	$\sigma(\text{[Fe/H]})$ (dex)	$\langle \text{S/N} \rangle$
NGC 2420					
2333-53682-228	2.6	91	0.13	0.04	57.0
2333-53682-229	2.5	36	0.09	0.04	54.8
2338-53683-142	1.9	68	0.23	0.06	39.3
2338-53683-186	1.8	121	0.06	0.03	44.2
2338-53683-199	1.9	119	0.15	0.06	38.2
2338-53683-200	1.2	80	0.06	0.03	57.6

Continued on next page...

Table A.2 – Continued

spSpec name	$\sigma(\text{RV})$ (km s $^{-1}$)	$\sigma(\text{T}_{\text{eff}})$ (K)	$\sigma(\log g)$ (dex)	$\sigma(\text{[Fe/H]})$ (dex)	$\langle \text{S/N} \rangle$
2078-53378-165	2.9	4	0.05	0.01	19.8
2078-53378-166	1.4	31	0.08	0.03	56.3
2078-53378-167	1.6	54	0.04	0.04	37.4
2078-53378-168	1.4	41	0.12	0.01	55.0
2078-53378-169	1.1	19	0.11	0.01	66.8
2078-53378-170	2.4	95	0.03	0.01	17.2
2078-53378-171	2.0	33	0.05	0.03	30.6
2078-53378-172	1.7	62	0.07	0.01	31.6
2078-53378-173	2.9	96	0.17	0.05	18.2
2078-53378-174	2.1	1	0.03	0.04	21.3
2078-53378-175	2.6	42	0.04	0.06	20.5
2078-53378-176	1.2	28	0.14	0.02	63.4
2078-53378-177	2.1	53	0.03	0.06	25.9
2078-53378-178	2.4	35	0.04	0.05	21.0
2078-53378-179	1.2	19	0.12	0.05	61.6
2078-53378-182	1.4	8	0.08	0.04	63.5
2078-53378-186	1.3	55	0.09	0.04	61.5
2078-53378-192	1.8	65	0.06	0.04	34.7
2078-53378-194	2.7	57	0.06	0.05	26.9
2078-53378-195	1.3	24	0.11	0.02	58.2
2078-53378-197	1.9	44	0.07	0.03	33.3
2078-53378-199	1.4	38	0.10	0.03	53.3

Continued on next page...

Table A.2 – Continued

spSpec name	$\sigma(\text{RV})$ (km s $^{-1}$)	$\sigma(\text{T}_{\text{eff}})$ (K)	$\sigma(\log g)$ (dex)	$\sigma(\text{[Fe/H]})$ (dex)	$\langle \text{S/N} \rangle$
2078-53378-200	2.2	33	0.05	0.05	22.8
2078-53378-223	1.5	29	0.09	0.01	53.3
2078-53378-224	1.2	21	0.07	0.03	65.4
2078-53378-227	1.7	46	0.07	0.02	37.4
2078-53378-232	1.3	30	0.10	0.04	61.4
2078-53378-233	1.8	50	0.06	0.04	41.5
2078-53378-235	1.7	85	0.10	0.05	33.2
2078-53378-273	3.0	95	0.08	0.05	18.2
2078-53378-422	1.7	28	0.05	0.03	27.1
2078-53378-427	1.6	45	0.06	0.01	38.7
2078-53378-431	1.1	30	0.10	0.04	67.1
2078-53378-435	1.7	32	0.02	0.04	28.1
2078-53378-440	1.5	15	0.06	0.03	32.5
2078-53378-462	1.4	42	0.06	0.02	50.2
2078-53378-463	1.1	28	0.13	0.04	60.7
2078-53378-464	1.4	108	0.17	0.04	40.6
2078-53378-465	1.6	36	0.07	0.04	30.9
2078-53378-466	1.2	32	0.09	0.05	62.2
2078-53378-468	1.6	40	0.07	0.04	31.9
2078-53378-469	1.0	52	0.08	0.06	67.0
2078-53378-470	1.5	81	0.05	0.05	36.1
2078-53378-471	1.3	39	0.05	0.03	49.4

Continued on next page...

Table A.2 – Continued

spSpec name	$\sigma(\text{RV})$ (km s $^{-1}$)	$\sigma(\text{T}_{\text{eff}})$ (K)	$\sigma(\log g)$ (dex)	$\sigma(\text{[Fe/H]})$ (dex)	$\langle \text{S/N} \rangle$
2078-53378-472	1.1	39	0.10	0.04	67.3
2078-53378-473	1.4	32	0.06	0.02	46.4
2078-53378-475	1.9	55	0.08	0.04	22.6
2078-53378-476	1.6	37	0.07	0.06	26.4
2078-53378-477	1.4	60	0.10	0.06	37.8
2078-53378-478	1.5	31	0.08	0.05	30.1
2078-53378-480	1.5	68	0.09	0.05	35.6
2078-53378-481	1.8	44	0.01	0.04	51.4
2078-53378-485	1.3	60	0.07	0.03	41.7
2078-53378-491	1.1	49	0.09	0.07	64.9
2078-53378-492	1.4	36	0.05	0.02	40.4
2078-53378-493	1.7	43	0.11	0.05	27.7
2078-53378-496	1.5	51	0.07	0.03	39.5
2078-53378-499	1.5	56	0.07	0.08	35.8
2078-53378-503	1.1	51	0.08	0.05	67.0
2078-53378-510	1.5	42	0.08	0.02	40.2
2078-53378-511	1.3	24	0.09	0.04	62.4
2078-53378-512	1.2	33	0.07	0.06	58.2
2078-53378-513	1.3	37	0.06	0.02	47.2
2078-53378-514	1.5	46	0.07	0.02	40.7
2078-53378-515	1.4	36	0.07	0.02	45.2
2078-53378-516	1.3	31	0.09	0.01	51.1

Continued on next page...

Table A.2 – Continued

spSpec name	$\sigma(\text{RV})$ (km s $^{-1}$)	$\sigma(\text{T}_{\text{eff}})$ (K)	$\sigma(\log g)$ (dex)	$\sigma(\text{[Fe/H]})$ (dex)	$\langle \text{S/N} \rangle$
2078-53378-517	1.4	52	0.08	0.06	32.0
2078-53378-518	1.2	36	0.10	0.00	57.7
2078-53378-519	1.4	63	0.09	0.04	36.9
2078-53378-520	1.3	38	0.03	0.04	46.8
2078-53378-548	1.2	43	0.10	0.02	64.4
2078-53378-552	2.4	60	0.03	0.09	17.3
2078-53378-553	1.8	79	0.07	0.03	23.5
2078-53378-554	1.2	20	0.10	0.06	64.7
2078-53378-557	1.3	40	0.06	0.02	52.8
2078-53378-560	1.6	63	0.06	0.00	34.8
2079-53379-071	1.6	70	0.09	0.06	26.6
2079-53379-076	1.4	50	0.14	0.05	28.5
2079-53379-101	2.7	65	0.22	0.05	17.4
2079-53379-102	2.1	44	0.18	0.04	18.7
2079-53379-108	2.9	49	0.08	0.06	14.1
2079-53379-113	3.2	50	0.15	0.10	12.8
2079-53379-114	2.1	16	0.11	0.06	18.1
2079-53379-119	2.9	11	0.15	0.05	15.4
2079-53379-141	1.9	33	0.06	0.00	20.5
2079-53379-148	2.0	16	0.03	0.01	21.7
2079-53379-149	1.7	41	0.13	0.06	24.6
2079-53379-152	2.0	94	0.06	0.05	20.7

Continued on next page...

Table A.2 – Continued

spSpec name	$\sigma(\text{RV})$ (km s $^{-1}$)	$\sigma(\text{T}_{\text{eff}})$ (K)	$\sigma(\log g)$ (dex)	$\sigma(\text{[Fe/H]})$ (dex)	$\langle \text{S/N} \rangle$
2079-53379-153	2.4	37	0.04	0.05	16.4
2079-53379-156	1.5	49	0.10	0.06	28.0
2079-53379-157	2.0	51	0.03	0.04	18.1
2079-53379-158	2.0	41	0.18	0.01	18.8
2079-53379-159	1.9	3	0.04	0.04	20.1
2079-53379-160	1.7	102	0.04	0.01	22.5
2079-53379-161	2.9	52	0.15	0.06	12.9
2079-53379-162	1.4	88	0.12	0.04	28.2
2079-53379-163	2.4	13	0.16	0.05	17.9
2079-53379-164	1.9	91	0.12	0.08	22.7
2079-53379-165	2.3	35	0.22	0.06	16.5
2079-53379-166	1.4	68	0.10	0.04	27.7
2079-53379-167	3.4	68	0.44	0.08	12.5
2079-53379-168	2.5	12	0.21	0.12	14.6
2079-53379-169	1.7	88	0.12	0.04	23.5
2079-53379-178	1.6	101	0.07	0.04	25.9
2079-53379-181	1.0	20	0.06	0.02	79.6
2079-53379-182	1.9	38	0.13	0.02	19.4
2079-53379-185	3.2	68	0.04	0.19	11.8
2079-53379-191	2.1	121	0.13	0.03	20.0
2079-53379-192	1.5	71	0.08	0.03	26.2
2079-53379-194	1.4	68	0.10	0.04	29.7

Continued on next page...

Table A.2 – Continued

spSpec name	$\sigma(\text{RV})$ (km s $^{-1}$)	$\sigma(\text{T}_{\text{eff}})$ (K)	$\sigma(\log g)$ (dex)	$\sigma([\text{Fe}/\text{H}])$ (dex)	$\langle \text{S/N} \rangle$
2079-53379-195	1.7	88	0.13	0.06	23.7
2079-53379-196	2.3	51	0.02	0.07	16.3
2079-53379-198	1.6	62	0.04	0.01	29.3
2079-53379-199	2.3	37	0.23	0.04	15.9
2079-53379-200	1.8	70	0.10	0.03	21.9
2079-53379-234	2.0	20	0.02	0.06	18.6
2079-53379-237	1.8	28	0.14	0.03	21.1
2079-53379-238	1.7	51	0.08	0.07	24.8
2079-53379-270	1.7	49	0.09	0.07	23.9
2079-53379-431	1.3	86	0.10	0.01	26.5
2079-53379-434	1.6	62	0.08	0.02	25.2
2079-53379-440	2.1	32	0.04	0.04	17.7
2079-53379-463	3.1	111	0.06	0.11	12.3
2079-53379-466	2.1	95	0.16	0.04	18.3
2079-53379-467	1.5	76	0.10	0.06	24.2
2079-53379-474	2.3	45	0.02	0.06	18.6
2079-53379-476	2.5	1	0.23	0.06	15.4
2079-53379-477	1.5	87	0.11	0.05	25.2
2079-53379-480	1.5	21	0.05	0.01	24.1
2079-53379-482	2.1	34	0.02	0.09	19.2
2079-53379-483	1.0	41	0.10	0.03	82.4
2079-53379-487	2.0	77	0.15	0.04	19.7

Continued on next page...

Table A.2 – Continued

spSpec name	$\sigma(\text{RV})$ (km s $^{-1}$)	$\sigma(\text{T}_{\text{eff}})$ (K)	$\sigma(\log g)$ (dex)	$\sigma(\text{[Fe/H]})$ (dex)	$\langle \text{S/N} \rangle$
2079-53379-488	3.6	75	0.31	0.06	11.7
2079-53379-490	2.2	44	0.18	0.02	16.9
2079-53379-493	2.7	52	0.29	0.06	14.2
2079-53379-495	1.6	59	0.08	0.02	24.5
2079-53379-496	1.3	66	0.04	0.04	29.7
2079-53379-498	1.6	63	0.13	0.04	24.2
2079-53379-500	1.9	27	0.11	0.05	21.2
2079-53379-502	1.7	71	0.05	0.01	22.0
2079-53379-507	1.9	47	0.05	0.03	19.9
2079-53379-510	3.3	66	0.28	0.07	11.6
2079-53379-511	1.7	82	0.07	0.06	23.8
2079-53379-512	1.3	60	0.01	0.06	30.8
2079-53379-514	2.9	39	0.19	0.07	14.0
2079-53379-516	1.4	23	0.08	0.02	27.3
2079-53379-519	1.7	46	0.03	0.03	21.3
2079-53379-552	2.0	23	0.16	0.03	19.7
2079-53379-558	1.5	8	0.09	0.06	29.0
NGC 2158					
2887-54521-416	1.4	135	0.38	0.04	68.9
2887-54521-442	1.5	197	0.17	0.06	52.1
2887-54521-445	1.6	61	0.16	0.04	54.3
2887-54521-446	2.6	129	0.11	0.05	46.2

Continued on next page...

Table A.2 – Continued

spSpec name	$\sigma(\text{RV})$ (km s $^{-1}$)	$\sigma(\text{T}_{\text{eff}})$ (K)	$\sigma(\log g)$ (dex)	$\sigma(\text{[Fe/H]})$ (dex)	$\langle \text{S/N} \rangle$
2887-54521-447	0.9	104	0.30	0.02	68.0
2887-54521-451	1.6	81	0.26	0.04	54.5
2887-54521-452	1.6	99	0.27	0.02	53.8
2887-54521-460	2.1	85	0.36	0.07	48.6
2887-54521-511	1.7	64	0.38	0.06	51.6
2887-54521-531	0.8	174	0.39	0.04	70.0
2887-54521-532	0.8	112	0.32	0.01	72.2
2887-54521-547	0.8	110	0.30	0.04	72.5
2887-54521-552	0.8	79	0.30	0.02	68.7
2887-54521-559	0.9	67	0.19	0.04	66.1
2912-54499-409	2.9	225	0.18	0.05	49.5
2912-54499-416	2.1	139	0.28	0.03	49.5
2912-54499-417	2.7	67	0.10	0.03	39.0
2912-54499-442	1.8	174	0.18	0.07	55.7
2912-54499-444	1.7	125	0.20	0.03	52.5
2912-54499-445	1.8	144	0.26	0.08	51.4
2912-54499-446	3.0	221	0.10	0.04	32.9
2912-54499-450	1.6	87	0.18	0.03	62.7
2912-54499-453	2.6	198	0.09	0.04	48.7
2912-54499-458	1.8	72	0.14	0.05	55.5
2912-54499-459	3.8	49	0.09	0.02	34.8
2912-54499-461	2.7	241	0.15	0.02	40.8

Continued on next page...

Table A.2 – Continued

spSpec name	$\sigma(\text{RV})$ (km s $^{-1}$)	$\sigma(\text{T}_{\text{eff}})$ (K)	$\sigma(\log g)$ (dex)	$\sigma(\text{[Fe/H]})$ (dex)	$\langle \text{S/N} \rangle$
2912-54499-462	2.4	147	0.11	0.02	44.6
2912-54499-483	1.6	188	0.27	0.06	60.2
2912-54499-484	1.9	208	0.24	0.05	56.6
2912-54499-488	2.4	57	0.03	0.04	43.8
2912-54499-489	1.7	156	0.20	0.04	58.8
2912-54499-499	2.5	163	0.11	0.04	46.8
2912-54499-501	3.1	172	0.09	0.01	40.0
2912-54499-502	2.3	241	0.19	0.04	49.6
2912-54499-503	1.8	208	0.24	0.06	56.4
2912-54499-505	1.7	174	0.14	0.04	55.2
2912-54499-506	3.1	53	0.15	0.03	30.3
2912-54499-507	2.5	224	0.14	0.03	54.9
2912-54499-509	2.1	187	0.02	0.04	59.2
2912-54499-510	2.7	80	0.16	0.05	40.1
2912-54499-511	2.6	57	0.18	0.04	41.8
2912-54499-514	1.7	167	0.15	0.04	59.6
2912-54499-515	2.4	158	0.22	0.02	49.9
2912-54499-516	1.8	177	0.05	0.03	57.5
2912-54499-518	2.0	166	0.10	0.06	48.6
2912-54499-519	2.3	172	0.21	0.03	43.5
2912-54499-531	2.1	67	0.10	0.03	46.8
2912-54499-534	3.3	99	0.20	0.03	26.5

Continued on next page...

Table A.2 – Continued

spSpec name	$\sigma(\text{RV})$ (km s $^{-1}$)	$\sigma(\text{T}_{\text{eff}})$ (K)	$\sigma(\log g)$ (dex)	$\sigma(\text{[Fe/H]})$ (dex)	$\langle \text{S/N} \rangle$
2912-54499-539	3.1	207	0.02	0.01	37.5
2912-54499-540	2.7	255	0.14	0.04	35.7
2912-54499-542	1.4	58	0.06	0.04	67.9
2912-54499-543	2.4	200	0.14	0.01	44.3
2912-54499-544	3.6	123	0.16	0.02	29.2
2912-54499-545	1.7	188	0.15	0.07	56.6
2912-54499-547	2.6	200	0.09	0.05	38.6
2912-54499-549	1.8	188	0.10	0.04	56.8
2912-54499-552	1.6	155	0.18	0.05	62.0
2912-54499-553	3.3	196	0.14	0.03	44.8
2912-54499-556	1.7	171	0.03	0.03	63.1
2912-54499-558	1.6	161	0.20	0.06	57.5
2912-54499-559	2.7	197	0.13	0.01	36.8
2912-54499-560	2.3	77	0.16	0.02	39.3
M35					
2887-54521-528	1.1	79	0.09	0.09	72.7
2887-54521-534	1.1	344	0.15	0.01	76.9
2887-54521-561	1.2	247	0.15	0.04	75.6
2887-54521-562	1.2	181	0.10	0.03	77.2
2887-54521-566	1.2	217	0.11	0.03	74.6
2887-54521-571	1.2	37	0.03	0.01	73.3
2887-54521-574	1.1	72	0.14	0.01	69.1

Continued on next page...

Table A.2 – Continued

spSpec name	$\sigma(\text{RV})$ (km s $^{-1}$)	$\sigma(\text{T}_{\text{eff}})$ (K)	$\sigma(\log g)$ (dex)	$\sigma(\text{[Fe/H]})$ (dex)	$\langle \text{S/N} \rangle$
2887-54521-575	1.2	87	0.16	0.03	71.8
2887-54521-576	1.2	110	0.09	0.09	72.1
2887-54521-577	1.6	65	0.00	0.03	71.4
2887-54521-580	1.1	63	0.15	0.04	68.2
2887-54521-602	1.2	97	0.14	0.04	71.3
2887-54521-604	1.3	67	0.08	0.02	69.9
2887-54521-606	1.1	44	0.08	0.03	71.1
2887-54521-608	1.4	50	0.05	0.00	73.0
2887-54521-611	1.3	237	0.10	0.04	75.0
2887-54521-616	1.1	70	0.03	0.04	70.8
2887-54521-620	1.5	69	0.16	0.04	68.7
2912-54499-524	1.2	89	0.18	0.01	34.5
2912-54499-563	0.8	32	0.05	0.05	56.9
2912-54499-564	0.8	101	0.09	0.06	47.8
2912-54499-575	1.1	83	0.14	0.06	34.6
2912-54499-576	1.2	9	0.01	0.05	51.7
2912-54499-601	1.0	230	0.22	0.04	43.8
2912-54499-604	2.3	72	0.01	0.06	18.1
2912-54499-605	0.8	147	0.08	0.05	49.7
2912-54499-611	0.8	38	0.15	0.03	63.0
2912-54499-619	0.8	61	0.12	0.04	45.2
2912-54499-620	1.4	161	0.17	0.05	31.5

Continued on next page...

Table A.2 – Continued

spSpec name	$\sigma(\text{RV})$ (km s $^{-1}$)	$\sigma(\text{T}_{\text{eff}})$ (K)	$\sigma(\log g)$ (dex)	$\sigma(\text{[Fe/H]})$ (dex)	$\langle \text{S/N} \rangle$
M67					
2667-54142-361	0.8	54	0.06	0.06	60.9
2667-54142-363	0.8	34	0.06	0.05	60.1
2667-54142-364	0.9	44	0.05	0.03	63.7
2667-54142-372	0.9	61	0.06	0.05	57.6
2667-54142-378	0.8	115	0.11	0.00	51.0
2667-54142-379	0.9	45	0.06	0.04	62.9
2667-54142-402	0.9	25	0.05	0.04	59.5
2667-54142-404	0.8	45	0.05	0.05	61.2
2667-54142-406	0.9	34	0.06	0.03	63.7
2667-54142-407	0.9	46	0.04	0.01	63.9
2667-54142-408	0.9	36	0.06	0.03	63.3
2667-54142-409	0.8	40	0.05	0.06	59.7
2667-54142-410	0.9	40	0.05	0.04	60.1
2667-54142-411	0.9	44	0.06	0.04	60.0
2667-54142-412	0.9	37	0.06	0.04	62.3
2667-54142-413	0.8	61	0.06	0.03	64.1
2667-54142-414	0.9	36	0.09	0.05	49.1
2667-54142-415	0.8	36	0.06	0.04	62.6
2667-54142-417	0.8	36	0.06	0.04	60.9
2667-54142-418	0.9	28	0.05	0.01	62.4
2667-54142-419	1.0	44	0.04	0.05	62.5

Continued on next page...

Table A.2 – Continued

spSpec name	$\sigma(\text{RV})$ (km s $^{-1}$)	$\sigma(\text{T}_{\text{eff}})$ (K)	$\sigma(\log g)$ (dex)	$\sigma(\text{[Fe/H]})$ (dex)	$\langle \text{S/N} \rangle$
2667-54142-420	0.9	37	0.07	0.04	62.5
2667-54142-429	0.9	44	0.07	0.03	63.0
2667-54142-441	0.9	21	0.04	0.03	62.0
2667-54142-444	1.0	56	0.05	0.04	63.3
2667-54142-445	0.8	38	0.06	0.03	60.8
2667-54142-451	0.9	67	0.05	0.05	63.5
2667-54142-452	0.9	103	0.09	0.05	50.6
2667-54142-453	0.8	77	0.08	0.04	55.3
2667-54142-454	1.0	52	0.06	0.02	63.8
2667-54142-455	1.0	49	0.04	0.05	63.6
2667-54142-457	0.9	33	0.05	0.04	62.5
2667-54142-458	0.8	39	0.05	0.05	62.0
2667-54142-459	0.9	48	0.04	0.02	63.5
2667-54142-460	0.9	32	0.05	0.04	61.9
2667-54142-463	0.9	49	0.04	0.03	63.9
2667-54142-466	0.8	67	0.08	0.07	56.5
2667-54142-467	1.0	43	0.09	0.03	63.9
2667-54142-469	0.9	67	0.07	0.03	58.2
2667-54142-476	1.0	44	0.05	0.04	63.1
2667-54142-477	0.9	51	0.06	0.04	63.5
2667-54142-478	0.9	45	0.04	0.03	63.8
2667-54142-479	0.8	40	0.05	0.04	62.6

Continued on next page...

Table A.2 – Continued

spSpec name	$\sigma(\text{RV})$ (km s $^{-1}$)	$\sigma(\text{T}_{\text{eff}})$ (K)	$\sigma(\log g)$ (dex)	$\sigma(\text{[Fe/H]})$ (dex)	$\langle \text{S/N} \rangle$
2667-54142-481	0.9	33	0.05	0.03	62.1
2667-54142-485	0.8	49	0.06	0.04	60.6
2667-54142-486	0.8	63	0.07	0.05	58.6
2667-54142-487	0.9	40	0.05	0.05	64.2
2667-54142-491	0.9	40	0.05	0.02	64.0
2667-54142-492	1.0	37	0.05	0.04	63.2
2667-54142-496	0.9	34	0.05	0.06	62.0
2667-54142-500	1.1	75	0.05	0.04	57.8
2667-54142-504	0.9	43	0.06	0.05	63.6
2667-54142-505	0.9	35	0.06	0.03	61.7
2667-54142-507	0.8	46	0.06	0.05	61.5
2667-54142-508	0.8	48	0.07	0.02	58.8
2667-54142-516	0.7	26	0.04	0.04	60.1
2667-54142-517	0.8	49	0.06	0.05	59.2
2667-54142-518	0.9	29	0.05	0.03	62.1
2667-54142-522	1.1	37	0.05	0.03	63.2
2667-54142-531	0.9	9	0.06	0.03	63.4
2667-54142-533	0.9	60	0.08	0.06	57.7
2667-54142-537	0.9	52	0.05	0.03	63.5
2667-54142-538	0.8	94	0.10	0.00	53.9
2667-54142-539	1.0	58	0.10	0.06	55.9
2667-54142-540	0.8	57	0.07	0.03	58.9

Continued on next page...

Table A.2 – Continued

spSpec name	$\sigma(\text{RV})$ (km s $^{-1}$)	$\sigma(\text{T}_{\text{eff}})$ (K)	$\sigma(\log g)$ (dex)	$\sigma(\text{[Fe/H]})$ (dex)	$\langle \text{S/N} \rangle$
2667-54142-541	1.5	22	0.05	0.01	38.4
2667-54142-546	1.0	43	0.03	0.04	63.7
2667-54142-547	0.8	47	0.06	0.05	58.1
2667-54142-550	0.9	38	0.05	0.02	63.3
2667-54142-551	0.8	60	0.07	0.07	57.4
2667-54142-561	0.9	29	0.05	0.02	62.9
2667-54142-566	0.8	34	0.04	0.05	61.2
2667-54142-575	0.9	55	0.06	0.03	62.6
2667-54142-576	1.0	45	0.04	0.05	60.7
2667-54142-579	0.8	41	0.05	0.06	61.1
NGC 6791					
2800-54326-151	1.2	113	0.15	0.01	38.3
2800-54326-152	2.1	83	0.11	0.01	22.9
2800-54326-154	1.4	94	0.24	0.04	62.2
2800-54326-155	1.7	97	0.04	0.04	26.3
2800-54326-156	1.4	123	0.14	0.52	52.4
2800-54326-157	2.0	109	0.10	0.04	25.1
2800-54326-159	0.4	97	0.22	0.04	70.5
2800-54326-160	0.8	33	0.12	0.22	54.7
2800-54326-161	1.1	134	0.14	0.05	34.5
2800-54326-165	2.8	249	0.08	0.10	29.9
2800-54326-169	0.4	90	0.02	0.00	70.1

Continued on next page...

Table A.2 – Continued

spSpec name	$\sigma(\text{RV})$ (km s $^{-1}$)	$\sigma(\text{T}_{\text{eff}})$ (K)	$\sigma(\log g)$ (dex)	$\sigma(\text{[Fe/H]})$ (dex)	$\langle \text{S/N} \rangle$
2800-54326-171	1.8	53	0.07	0.06	24.5
2800-54326-172	1.6	80	0.04	0.26	31.8
2800-54326-173	1.1	86	0.07	0.02	34.0
2800-54326-174	0.5	80	0.27	0.04	71.1
2800-54326-175	0.6	113	0.01	0.04	73.3
2800-54326-176	1.1	58	0.05	0.06	40.7
2800-54326-178	0.5	124	0.16	0.04	71.3
2800-54326-180	0.6	99	0.01	0.01	70.3
2800-54326-181	0.4	86	0.23	0.08	68.5
2800-54326-182	2.3	210	0.04	0.07	28.7
2800-54326-183	0.6	96	0.21	0.04	69.8
2800-54326-184	1.8	7	0.13	0.04	29.9
2800-54326-185	0.6	101	0.28	0.04	68.6
2800-54326-186	0.8	25	0.12	0.21	53.6
2800-54326-189	0.9	3	0.12	0.02	43.7
2800-54326-190	1.0	135	0.17	0.04	57.7
2800-54326-194	1.5	194	0.20	0.06	31.5
2800-54326-197	1.3	63	0.03	0.12	53.4
2800-54326-199	1.5	88	0.03	0.04	70.2
2800-54326-424	1.6	74	0.08	0.09	28.1
2800-54326-462	1.5	48	0.11	0.08	33.7
2800-54326-464	1.2	56	0.07	0.04	40.6

Continued on next page...

Table A.2 – Continued

spSpec name	$\sigma(\text{RV})$ (km s $^{-1}$)	$\sigma(\text{T}_{\text{eff}})$ (K)	$\sigma(\log g)$ (dex)	$\sigma(\text{[Fe/H]})$ (dex)	$\langle \text{S/N} \rangle$
2800-54326-465	0.5	70	0.27	0.04	66.2
2800-54326-466	1.2	108	0.11	0.02	40.4
2800-54326-469	1.4	89	0.12	0.11	30.9
2800-54326-471	1.1	43	0.12	0.05	41.5
2800-54326-473	1.1	6	0.09	0.04	41.0
2800-54326-475	0.5	71	0.26	0.03	67.9
2800-54326-476	1.3	40	0.14	0.07	36.0
2800-54326-477	0.8	123	0.09	0.00	54.3
2800-54326-479	1.6	71	0.07	0.06	27.9
2800-54326-480	1.3	95	0.04	0.04	38.3
2800-54326-497	1.3	61	0.07	0.07	35.7
2821-54393-141	1.0	91	0.06	0.08	47.2
2821-54393-142	2.0	133	0.08	0.07	27.7
2821-54393-145	1.1	88	0.09	0.08	45.8
2821-54393-146	1.3	89	0.14	0.03	41.0
2821-54393-149	2.2	76	0.17	0.04	24.3
2821-54393-161	0.9	72	0.08	0.06	61.8
2821-54393-165	1.5	109	0.11	0.12	27.4
2821-54393-166	1.3	104	0.09	0.03	38.9
2821-54393-167	1.3	71	0.09	0.09	39.6
2821-54393-169	1.2	50	0.10	0.09	36.8
2821-54393-172	1.1	61	0.11	0.10	45.8

Continued on next page...

Table A.2 – Continued

spSpec name	$\sigma(\text{RV})$ (km s $^{-1}$)	$\sigma(\text{T}_{\text{eff}})$ (K)	$\sigma(\log g)$ (dex)	$\sigma(\text{[Fe/H]})$ (dex)	$\langle \text{S/N} \rangle$
2821-54393-173	1.2	44	0.07	0.09	39.4
2821-54393-174	1.2	127	0.12	0.05	37.1
2821-54393-176	1.3	146	0.18	0.06	28.7
2821-54393-177	1.1	1	0.05	0.01	39.9
2821-54393-178	1.2	83	0.09	0.09	35.4
2821-54393-179	0.9	60	0.07	0.07	67.3
2821-54393-182	1.1	76	0.13	0.06	47.4
2821-54393-183	0.9	66	0.08	0.08	57.6
2821-54393-184	1.6	84	0.08	0.04	28.7
2821-54393-185	1.0	6	0.09	0.03	42.2
2821-54393-187	1.0	44	0.10	0.06	60.4
2821-54393-188	1.6	57	0.11	0.02	27.0
2821-54393-190	2.6	121	0.19	0.03	19.6
2821-54393-191	1.2	68	0.07	0.09	40.8
2821-54393-192	1.8	107	0.10	0.09	23.0
2821-54393-193	1.8	24	0.13	0.06	34.8
2821-54393-194	1.0	79	0.07	0.03	48.3
2821-54393-195	1.4	99	0.09	0.03	27.5
2821-54393-196	1.0	64	0.08	0.07	47.3
2821-54393-197	1.0	53	0.08	0.05	56.7
2821-54393-199	1.9	67	0.16	0.03	24.9
2821-54393-235	1.1	56	0.09	0.10	63.0

Continued on next page...

Table A.2 – Continued

spSpec name	$\sigma(\text{RV})$ (km s $^{-1}$)	$\sigma(T_{\text{eff}})$ (K)	$\sigma(\log g)$ (dex)	$\sigma(\text{[Fe/H]})$ (dex)	$\langle \text{S/N} \rangle$
2821-54393-436	1.2	14	0.10	0.12	42.9
2821-54393-438	0.8	87	0.08	0.06	62.2
2821-54393-439	0.9	26	0.05	0.09	59.1
2821-54393-440	1.1	102	0.06	0.05	64.9
2821-54393-468	1.5	45	0.10	0.05	23.3
2821-54393-469	1.2	169	0.09	0.03	32.8
2821-54393-472	1.0	73	0.11	0.04	41.9
2821-54393-473	1.1	71	0.10	0.05	42.9
2821-54393-474	0.9	73	0.13	0.07	47.9
2821-54393-475	1.5	131	0.08	0.04	27.7
2821-54393-478	1.1	88	0.10	0.07	48.9
2821-54393-479	1.1	84	0.14	0.10	44.7
2821-54393-480	2.5	229	0.10	0.14	16.6

A.2 PHOTOMETRIC PARAMETERS DATA TABLE

Additionally, I have prepared the following table (Table A.3) of SDSS photometry for the adopted true members of the GCs and OCs in this sample and that of Lee et al. (2008b). Again, Column 1 lists the spSpec name, which identifies the star on the spectral plate in the form of spectroscopic plug-plate number (four digits), Modified Julian Date (five digits),

and fiber used (three digits). The final column indicates whether photometric values were drawn from “Best” photometry (B), the “Uber calibration” (U), the CASJOBS database (C), or the DAOPHOT crowded-field reduction (D).

Table A.3: Photometric Properties of Adopted True Member Stars

spSpec name	<i>u</i>	$\sigma(u)$	<i>g</i>	$\sigma(g)$	<i>r</i>	$\sigma(r)$	<i>i</i>	$\sigma(i)$	<i>z</i>	$\sigma(z)$	Tag
M92											
2247-54169-361	16.420	0.025	15.265	0.009	15.503	0.025	15.718	0.014	15.819	0.013	D
2247-54169-362	18.388	0.024	17.343	0.011	16.902	0.014	16.730	0.013	16.679	0.015	C
2247-54169-364	17.646	0.013	16.533	0.015	16.077	0.027	15.897	0.025	15.823	0.014	D
2247-54169-367	17.645	0.010	16.519	0.009	16.080	0.016	15.877	0.015	15.783	0.013	D
2247-54169-379	18.536	0.018	17.638	0.011	17.449	0.011	17.397	0.013	17.430	0.014	D
2247-54169-380	17.282	0.021	16.093	0.010	15.609	0.011	15.389	0.017	15.289	0.017	D
2247-54169-404	17.648	0.017	16.503	0.010	16.048	0.016	15.847	0.017	15.757	0.012	D
2247-54169-408	16.637	0.016	15.333	0.010	14.812	0.009	14.589	0.017	14.471	0.015	D
2247-54169-409	21.366	0.130	20.443	0.022	20.129	0.026	20.031	0.036	20.019	0.090	D
2247-54169-418	16.771	0.010	15.524	0.008	14.997	0.009	14.780	0.012	14.679	0.010	D
2247-54169-444	17.165	0.011	16.006	0.011	15.539	0.031	15.309	0.018	15.229	0.014	D
2247-54169-449	16.792	0.007	15.490	0.006	15.011	0.021	14.736	0.010	14.643	0.014	D
2247-54169-451	17.363	0.011	16.188	0.008	15.716	0.013	15.492	0.011	15.410	0.014	D
2247-54169-452	17.203	0.011	15.985	0.009	15.505	0.018	15.273	0.012	15.188	0.011	D
2247-54169-458	18.866	0.021	17.845	0.010	17.480	0.017	17.321	0.011	17.283	0.019	D
2247-54169-484	16.464	0.018	15.117	0.011	14.516	0.015	14.272	0.015	14.143	0.016	C
2247-54169-504	16.461	0.013	15.125	0.011	14.607	0.030	14.335	0.015	14.255	0.016	D
2247-54169-514	18.694	0.019	17.645	0.021	17.273	0.017	17.117	0.017	17.072	0.021	D

Continued on next page...

Table A.3 – Continued

spSpec name	<i>u</i>	$\sigma(u)$	<i>g</i>	$\sigma(g)$	<i>r</i>	$\sigma(r)$	<i>i</i>	$\sigma(i)$	<i>z</i>	$\sigma(z)$	Tag
2247-54169-516	18.847	0.022	17.860	0.016	17.497	0.013	17.346	0.014	17.323	0.021	D
2247-54169-519	18.793	0.025	17.809	0.018	17.430	0.014	17.257	0.017	17.205	0.018	D
2247-54169-529	18.246	0.018	17.182	0.008	16.742	0.019	16.560	0.016	16.491	0.013	D
2247-54169-531	17.650	0.010	16.488	0.007	16.045	0.005	15.842	0.007	15.730	0.007	D
2247-54169-538	18.888	0.023	17.966	0.007	17.660	0.007	17.518	0.008	17.453	0.014	D
2247-54169-541	18.758	0.032	17.691	0.009	17.304	0.013	17.146	0.016	17.124	0.023	D
2247-54169-546	18.187	0.015	17.107	0.007	16.699	0.010	16.512	0.010	16.439	0.012	D
2247-54169-561	17.658	0.014	16.490	0.010	16.011	0.009	15.812	0.014	15.726	0.016	D
2247-54169-563	16.759	0.016	15.492	0.007	14.959	0.013	14.754	0.015	14.623	0.011	D
2247-54169-573	17.098	0.010	16.016	0.013	15.569	0.009	15.375	0.010	15.290	0.011	D
2247-54169-575	18.868	0.023	17.882	0.006	17.522	0.006	17.372	0.005	17.298	0.012	D
2247-54169-581	17.578	0.018	16.373	0.007	15.916	0.012	15.704	0.010	15.607	0.014	D
2247-54169-582	16.251	0.009	15.061	0.004	15.119	0.005	15.186	0.004	15.205	0.005	D
2247-54169-584	18.768	0.021	17.789	0.006	17.422	0.006	17.251	0.006	17.155	0.015	D
2247-54169-589	18.123	0.027	17.007	0.010	16.550	0.014	16.371	0.011	16.279	0.020	D
2247-54169-608	16.631	0.007	15.383	0.003	14.852	0.006	14.612	0.004	14.483	0.007	D
2247-54169-610	16.497	0.006	15.198	0.004	14.660	0.005	14.405	0.004	14.272	0.006	D
2247-54169-616	18.879	0.026	17.890	0.008	17.524	0.005	17.369	0.008	17.293	0.012	D
2247-54169-620	18.511	0.019	17.503	0.005	17.098	0.005	16.918	0.006	16.834	0.012	D
2256-53859-411	19.329	0.034	18.413	0.012	18.173	0.015	18.119	0.015	18.131	0.023	C
2256-53859-455	19.483	0.044	18.576	0.014	18.371	0.012	18.312	0.011	18.346	0.032	D
2256-53859-485	19.940	0.051	19.103	0.018	18.912	0.018	18.874	0.016	18.855	0.042	D
2256-53859-489	19.707	0.040	18.749	0.011	18.567	0.013	18.514	0.015	18.567	0.030	D

Continued on next page...

Table A.3 – Continued

spSpec name	<i>u</i>	$\sigma(u)$	<i>g</i>	$\sigma(g)$	<i>r</i>	$\sigma(r)$	<i>i</i>	$\sigma(i)$	<i>z</i>	$\sigma(z)$	Tag
2256-53859-501	19.581	0.037	18.751	0.010	18.562	0.013	18.496	0.014	18.533	0.030	D
2256-53859-506	19.655	0.034	18.794	0.016	18.587	0.021	18.526	0.016	18.568	0.037	D
2256-53859-513	18.694	0.019	17.645	0.021	17.273	0.017	17.117	0.017	17.072	0.021	D
2256-53859-522	19.044	0.025	18.084	0.012	17.814	0.017	17.703	0.016	17.682	0.018	D
2256-53859-530	19.559	0.041	18.682	0.008	18.482	0.010	18.426	0.009	18.407	0.031	D
2256-53859-535	19.290	0.033	18.349	0.009	18.145	0.008	18.068	0.008	18.038	0.022	D
2256-53859-536	19.267	0.033	18.395	0.013	18.170	0.018	18.096	0.020	18.060	0.026	D
2256-53859-537	19.977	0.058	19.293	0.012	19.082	0.014	19.002	0.015	18.949	0.038	D
2256-53859-538	18.751	0.022	17.762	0.006	17.376	0.006	17.214	0.007	17.144	0.012	D
2256-53859-539	19.607	0.039	18.874	0.009	18.664	0.011	18.546	0.013	18.492	0.027	D
2256-53859-546	19.386	0.038	18.505	0.017	18.309	0.015	18.212	0.016	18.170	0.026	C
2256-53859-566	19.714	0.031	18.824	0.012	18.593	0.015	18.546	0.015	18.592	0.033	D
2256-53859-571	19.431	0.039	18.654	0.008	18.455	0.009	18.406	0.010	18.407	0.029	D
2256-53859-575	19.464	0.034	18.591	0.009	18.429	0.008	18.371	0.010	18.381	0.030	D
2256-53859-576	19.378	0.034	18.548	0.009	18.358	0.008	18.306	0.011	18.286	0.023	D
2256-53859-579	19.787	0.045	18.810	0.014	18.600	0.013	18.544	0.011	18.557	0.030	D
2256-53859-612	19.290	0.030	18.499	0.008	18.314	0.010	18.232	0.009	18.239	0.024	D
				M15							
1960-53289-401	17.228	0.019	16.078	0.008	15.593	0.008	15.374	0.012	15.268	0.012	D
1960-53289-402	16.719	0.015	15.391	0.008	14.839	0.010	14.584	0.011	14.469	0.015	D
1960-53289-406	16.692	0.013	15.393	0.007	14.841	0.006	14.594	0.007	14.490	0.015	D
1960-53289-413	16.892	0.012	15.687	0.007	15.179	0.008	14.945	0.009	14.839	0.016	D
1960-53289-419	16.707	0.016	15.433	0.008	14.891	0.011	14.646	0.008	14.537	0.013	D

Continued on next page...

Table A.3 – Continued

spSpec name	<i>u</i>	$\sigma(u)$	<i>g</i>	$\sigma(g)$	<i>r</i>	$\sigma(r)$	<i>i</i>	$\sigma(i)$	<i>z</i>	$\sigma(z)$	Tag
1960-53289-420	19.269	0.043	18.421	0.011	18.059	0.009	17.981	0.015	17.950	0.029	C
1960-53289-441	18.500	0.030	17.582	0.011	17.183	0.024	17.033	0.012	16.958	0.021	D
1960-53289-442	17.458	0.018	16.342	0.008	15.855	0.010	15.659	0.014	15.556	0.016	D
1960-53289-457	18.870	0.038	17.913	0.011	17.541	0.011	17.363	0.013	17.268	0.020	D
1960-53289-459	16.273	0.021	15.076	0.009	14.561	0.006	14.346	0.013	14.241	0.015	C
1960-53289-460	17.490	0.023	16.431	0.009	15.966	0.006	15.778	0.013	15.671	0.016	C
1960-53289-500	18.164	0.023	17.169	0.012	16.719	0.011	16.540	0.012	16.503	0.019	C
1960-53289-501	19.244	0.036	18.283	0.011	17.885	0.011	17.716	0.011	17.652	0.022	C
1960-53289-511	17.721	0.020	16.568	0.009	16.059	0.009	15.872	0.009	15.772	0.014	C
1960-53289-522	17.954	0.022	16.909	0.011	16.493	0.009	16.307	0.011	16.221	0.015	C
1960-53289-523	16.146	0.016	14.624	0.009	13.981	0.010	13.757	0.004	13.560	0.014	C
1960-53289-529	16.778	0.018	15.513	0.010	14.992	0.006	14.754	0.015	14.651	0.012	D
1960-53289-530	18.471	0.035	17.485	0.015	17.040	0.016	16.859	0.012	16.783	0.020	D
1962-53321-323	19.270	0.042	18.400	0.016	18.131	0.014	18.012	0.016	17.973	0.041	D
1962-53321-328	19.531	0.052	18.655	0.014	18.450	0.015	18.387	0.014	18.373	0.038	D
1962-53321-329	19.408	0.044	18.522	0.011	18.253	0.013	18.160	0.013	18.168	0.037	D
1962-53321-335	19.364	0.043	18.411	0.014	18.110	0.013	18.008	0.014	17.925	0.034	D
1962-53321-339	19.929	0.063	19.041	0.019	18.903	0.014	18.831	0.020	18.856	0.064	D
1962-53321-363	20.107	0.085	19.252	0.021	19.041	0.020	18.955	0.024	18.865	0.064	D
1962-53321-364	18.660	0.032	17.583	0.014	17.191	0.009	17.016	0.012	16.937	0.020	D
1962-53321-368	19.440	0.048	18.553	0.014	18.326	0.014	18.256	0.016	18.214	0.032	D
1962-53321-369	19.431	0.044	18.589	0.016	18.348	0.016	18.251	0.015	18.211	0.041	D
1962-53321-370	19.329	0.048	18.453	0.015	18.174	0.011	18.080	0.017	18.058	0.039	D

Continued on next page...

Table A.3 – Continued

spSpec name	<i>u</i>	$\sigma(u)$	<i>g</i>	$\sigma(g)$	<i>r</i>	$\sigma(r)$	<i>i</i>	$\sigma(i)$	<i>z</i>	$\sigma(z)$	Tag
1962-53321-371	19.446	0.043	18.507	0.017	18.253	0.013	18.136	0.016	18.084	0.028	D
1962-53321-372	19.296	0.046	18.371	0.012	18.086	0.011	17.956	0.012	17.927	0.032	D
1962-53321-375	18.807	0.036	17.758	0.008	17.365	0.010	17.208	0.011	17.149	0.022	D
1962-53321-376	18.521	0.029	17.515	0.009	17.119	0.012	16.938	0.010	16.858	0.020	D
1962-53321-378	19.945	0.057	19.052	0.016	18.861	0.019	18.800	0.021	18.830	0.049	D
1962-53321-399	19.711	0.060	18.831	0.017	18.635	0.019	18.648	0.020	18.559	0.044	C
1962-53321-402	18.870	0.038	17.913	0.011	17.541	0.011	17.363	0.013	17.268	0.020	D
1962-53321-403	18.913	0.038	17.887	0.011	17.504	0.011	17.343	0.012	17.277	0.023	D
1962-53321-406	18.929	0.038	17.944	0.014	17.561	0.010	17.405	0.012	17.339	0.023	D
1962-53321-407	19.343	0.053	18.444	0.013	18.218	0.015	18.122	0.018	18.106	0.038	D
1962-53321-409	20.065	0.072	19.145	0.015	18.991	0.018	18.995	0.026	18.863	0.064	D
1962-53321-412	19.790	0.060	18.872	0.016	18.698	0.016	18.639	0.018	18.588	0.046	D
1962-53321-413	18.649	0.032	17.556	0.011	17.172	0.012	16.966	0.023	16.902	0.020	D
1962-53321-414	19.336	0.049	18.472	0.017	18.197	0.015	18.084	0.019	18.055	0.041	D
1962-53321-415	18.443	0.020	17.419	0.014	17.025	0.010	16.879	0.013	16.788	0.016	D
1962-53321-416	19.987	0.068	19.081	0.018	18.921	0.020	18.868	0.024	18.803	0.053	D
1962-53321-419	20.169	0.107	19.268	0.017	19.087	0.018	19.005	0.025	19.220	0.075	D
1962-53321-421	19.266	0.051	18.371	0.015	18.033	0.011	17.891	0.015	17.848	0.033	D
1962-53321-422	19.850	0.066	19.094	0.021	18.866	0.023	18.836	0.025	18.764	0.052	C
1962-53321-423	19.203	0.039	18.205	0.013	17.842	0.011	17.684	0.013	17.599	0.024	C
1962-53321-424	19.619	0.056	18.952	0.018	18.782	0.019	18.783	0.021	18.854	0.055	C
1962-53321-427	18.649	0.029	17.643	0.013	17.249	0.010	17.089	0.012	16.993	0.020	C
1962-53321-428	19.856	0.061	18.951	0.015	18.786	0.014	18.695	0.018	18.695	0.047	C

Continued on next page...

Table A.3 – Continued

spSpec name	<i>u</i>	$\sigma(u)$	<i>g</i>	$\sigma(g)$	<i>r</i>	$\sigma(r)$	<i>i</i>	$\sigma(i)$	<i>z</i>	$\sigma(z)$	Tag
1962-53321-430	20.210	0.082	19.211	0.019	19.007	0.020	18.904	0.022	18.850	0.056	C
1962-53321-438	18.569	0.028	17.546	0.015	17.124	0.016	16.890	0.015	16.810	0.020	C
1962-53321-442	19.546	0.057	18.727	0.015	18.549	0.021	18.482	0.023	18.486	0.045	D
1962-53321-445	20.064	0.074	19.341	0.017	19.193	0.017	19.100	0.023	19.102	0.064	C
1962-53321-449	20.178	0.081	19.374	0.023	19.178	0.018	19.172	0.027	19.155	0.070	D
1962-53321-454	18.500	0.030	17.582	0.011	17.183	0.024	17.033	0.012	16.958	0.021	D
1962-53321-460	20.191	0.094	19.363	0.026	19.139	0.030	19.063	0.020	19.128	0.063	D
1962-53321-465	19.606	0.062	18.942	0.015	18.797	0.017	18.765	0.020	18.704	0.044	D
1962-53321-466	18.510	0.024	17.520	0.010	17.104	0.010	16.939	0.009	16.865	0.019	D
1962-53321-469	19.389	0.061	18.634	0.013	18.445	0.013	18.395	0.017	18.382	0.046	D
1962-53321-470	19.369	0.047	18.633	0.017	18.398	0.018	18.342	0.018	18.327	0.036	C
1962-53321-471	19.572	0.051	18.829	0.013	18.676	0.017	18.598	0.017	18.626	0.042	D
1962-53321-474	18.388	0.027	17.449	0.015	17.058	0.016	16.905	0.015	16.826	0.020	C
1962-53321-478	20.677	0.162	19.724	0.024	19.500	0.020	19.367	0.031	19.303	0.086	D
1962-53321-480	19.802	0.067	18.991	0.018	18.780	0.019	18.701	0.020	18.807	0.053	C
1962-53321-483	20.027	0.063	19.211	0.016	19.005	0.016	18.957	0.021	18.938	0.050	C
1962-53321-484	19.975	0.060	19.188	0.016	18.978	0.018	18.928	0.023	18.836	0.048	C
1962-53321-488	19.511	0.050	18.642	0.020	18.359	0.019	18.347	0.024	18.368	0.041	C
1962-53321-490	19.685	0.049	18.893	0.015	18.635	0.014	18.536	0.017	18.559	0.039	C
1962-53321-493	19.199	0.035	18.324	0.013	17.957	0.012	17.810	0.013	17.770	0.025	C
1962-53321-495	19.590	0.047	18.787	0.015	18.533	0.014	18.443	0.016	18.466	0.037	C
1962-53321-496	19.518	0.045	18.773	0.015	18.536	0.014	18.461	0.016	18.509	0.038	C
1962-53321-497	19.675	0.049	18.769	0.015	18.588	0.015	18.538	0.017	18.552	0.036	D

Continued on next page...

Table A.3 – Continued

spSpec name	<i>u</i>	$\sigma(u)$	<i>g</i>	$\sigma(g)$	<i>r</i>	$\sigma(r)$	<i>i</i>	$\sigma(i)$	<i>z</i>	$\sigma(z)$	Tag
1962-53321-500	19.216	0.036	18.396	0.013	18.140	0.012	18.047	0.014	18.060	0.029	C
1962-53321-503	19.756	0.050	18.961	0.014	18.764	0.014	18.721	0.017	18.765	0.044	C
1962-53321-505	20.398	0.112	19.488	0.016	19.327	0.021	19.290	0.026	19.316	0.076	D
1962-53321-506	18.395	0.029	17.378	0.009	16.962	0.009	16.758	0.014	16.667	0.013	D
1962-53321-509	19.962	0.057	19.260	0.015	19.006	0.015	18.974	0.019	18.948	0.051	C
1962-53321-510	19.520	0.043	18.529	0.012	18.238	0.011	18.144	0.013	18.102	0.028	C
1962-53321-512	20.338	0.077	19.508	0.017	19.260	0.017	19.248	0.023	19.225	0.063	C
1962-53321-515	18.529	0.026	17.568	0.010	17.125	0.010	16.929	0.010	16.839	0.016	C
1962-53321-516	19.244	0.036	18.283	0.011	17.885	0.011	17.716	0.011	17.652	0.022	C
1962-53321-518	19.113	0.039	18.253	0.011	17.892	0.008	17.763	0.015	17.724	0.025	C
1962-53321-519	19.883	0.059	19.058	0.016	18.896	0.016	18.858	0.022	18.841	0.054	D
1962-53321-520	19.482	0.042	18.619	0.013	18.343	0.083	18.261	0.014	18.219	0.030	C
1962-53321-522	19.946	0.067	19.128	0.016	18.973	0.015	18.953	0.021	18.868	0.053	C
1962-53321-532	18.485	0.027	17.487	0.012	17.105	0.010	16.935	0.012	16.828	0.017	C
1962-53321-533	19.484	0.053	18.638	0.012	18.363	0.010	18.317	0.017	18.369	0.038	C
1962-53321-539	19.750	0.061	18.815	0.013	18.621	0.011	18.574	0.018	18.508	0.040	C
1962-53321-540	20.279	0.091	19.401	0.016	19.207	0.016	19.165	0.024	19.160	0.069	C
1962-53321-543	19.782	0.059	18.916	0.013	18.642	0.012	18.612	0.018	18.695	0.049	C
1962-53321-545	19.868	0.065	19.107	0.014	18.808	0.012	18.815	0.019	18.836	0.053	C
1962-53321-549	19.235	0.037	18.326	0.028	18.030	0.026	17.878	0.010	17.778	0.026	D
1962-53321-550	19.269	0.043	18.421	0.011	18.059	0.009	17.981	0.015	17.950	0.029	C
1962-53321-554	20.191	0.083	19.385	0.016	19.211	0.015	19.149	0.023	19.090	0.064	C
1962-53321-555	20.361	0.090	19.532	0.017	19.274	0.016	19.276	0.025	19.398	0.083	C

Continued on next page...

Table A.3 – Continued

spSpec name	<i>u</i>	$\sigma(u)$	<i>g</i>	$\sigma(g)$	<i>r</i>	$\sigma(r)$	<i>i</i>	$\sigma(i)$	<i>z</i>	$\sigma(z)$	Tag
1962-53321-558	19.248	0.040	18.344	0.010	18.055	0.016	17.925	0.018	17.912	0.029	D
NGC 5053											
2476-53826-486	18.887	0.022	17.746	0.009	17.284	0.009	17.078	0.012	16.978	0.020	D
2476-53826-488	17.349	0.013	15.780	0.017	15.094	0.007	14.797	0.011	14.656	0.011	D
2476-53826-490	17.806	0.013	16.483	0.015	16.631	0.009	16.782	0.008	16.835	0.016	D
2476-53826-497	19.352	0.031	18.201	0.011	17.750	0.015	17.562	0.011	17.483	0.019	D
2476-53826-501	17.417	0.010	15.988	0.008	15.356	0.005	15.073	0.012	14.942	0.011	D
2476-53826-505	17.522	0.015	16.302	0.009	15.817	0.008	15.600	0.015	15.520	0.015	D
2476-53826-506	17.793	0.019	16.589	0.012	16.693	0.008	16.745	0.013	16.830	0.022	D
2476-53826-507	18.181	0.018	16.939	0.009	16.409	0.007	16.161	0.018	16.049	0.015	D
2476-53826-508	18.104	0.019	16.803	0.009	16.271	0.010	16.013	0.014	15.892	0.012	D
2476-53826-519	17.003	0.012	15.223	0.011	14.436	0.014	14.144	0.010	13.966	0.014	D
2476-53826-527	17.419	0.011	15.862	0.023	15.211	0.007	14.923	0.009	14.769	0.011	D
2476-53826-531	17.934	0.015	16.801	0.014	17.055	0.007	17.254	0.014	17.364	0.020	D
2476-53826-573	18.464	0.022	17.197	0.012	16.668	0.005	16.457	0.014	16.365	0.017	D
2476-53826-575	17.130	0.012	15.518	0.007	14.794	0.037	14.507	0.015	14.368	0.058	D
2476-53826-577	18.115	0.013	16.942	0.028	16.396	0.008	16.177	0.020	16.064	0.024	D
2476-53826-578	17.210	0.012	15.602	0.015	14.904	0.005	14.608	0.010	14.465	0.008	D
M53											
2476-53826-329	19.252	0.039	17.999	0.027	17.496	0.018	17.318	0.013	17.181	0.026	C
2476-53826-361	18.269	0.035	16.908	0.018	16.270	0.022	16.061	0.015	15.912	0.019	C
2476-53826-362	17.904	0.024	16.733	0.026	16.695	0.018	16.698	0.012	16.725	0.025	C
2476-53826-363	18.093	0.035	17.029	0.018	17.209	0.022	17.425	0.015	17.533	0.023	C

Continued on next page...

Table A.3 – Continued

spSpec name	<i>u</i>	$\sigma(u)$	<i>g</i>	$\sigma(g)$	<i>r</i>	$\sigma(r)$	<i>i</i>	$\sigma(i)$	<i>z</i>	$\sigma(z)$	Tag
2476-53826-369	18.084	0.035	17.048	0.018	17.257	0.022	17.455	0.015	17.564	0.024	C
2476-53826-372	18.082	0.034	16.868	0.018	16.322	0.022	16.152	0.015	16.021	0.019	C
2476-53826-375	18.504	0.037	17.094	0.018	16.550	0.022	16.344	0.015	16.190	0.019	C
2476-53826-376	18.136	0.035	17.234	0.018	17.489	0.022	17.732	0.016	17.827	0.026	C
2476-53826-378	17.589	0.033	16.225	0.018	15.607	0.022	15.377	0.015	15.249	0.019	C
2476-53826-379	18.129	0.025	17.160	0.025	17.445	0.018	17.642	0.025	17.799	0.024	C
2476-53826-401	18.768	0.028	17.438	0.017	16.907	0.012	16.670	0.015	16.570	0.020	C
2476-53826-404	17.501	0.033	15.836	0.018	15.087	0.022	14.831	0.015	14.665	0.018	C
2476-53826-405	19.218	0.033	18.055	0.017	17.561	0.013	17.344	0.015	17.259	0.022	C
2476-53826-408	18.090	0.024	16.925	0.016	17.108	0.012	17.269	0.015	17.410	0.023	C
2476-53826-409	18.679	0.027	17.321	0.017	16.813	0.012	16.586	0.015	16.466	0.020	C
2476-53826-413	19.025	0.030	17.791	0.017	17.256	0.012	17.034	0.015	16.942	0.021	C
2476-53826-418	19.327	0.034	18.063	0.017	17.559	0.013	17.344	0.015	17.272	0.022	C
2476-53826-451	18.175	0.029	16.775	0.019	16.173	0.021	15.932	0.017	15.786	0.022	C
2476-53826-452	18.600	0.026	17.369	0.017	16.866	0.012	16.626	0.015	16.463	0.020	C
M2											
1961-53299-124	17.533	0.014	16.087	0.020	15.489	0.009	15.219	0.040	15.106	0.019	D
1961-53299-125	17.543	0.014	15.997	0.006	15.405	0.008	15.160	0.016	15.041	0.007	D
1961-53299-131	18.042	0.016	16.680	0.008	16.125	0.009	15.911	0.008	15.804	0.021	D
1961-53299-134	16.957	0.018	15.105	0.015	14.404	0.012	14.100	0.017	13.935	0.027	D
1961-53299-136	18.214	0.017	16.913	0.011	16.384	0.012	16.180	0.030	16.060	0.010	D
1961-53299-140	18.555	0.019	17.276	0.019	16.805	0.015	16.574	0.024	16.519	0.017	D
1961-53299-144	18.300	0.015	16.940	0.008	16.470	0.013	16.235	0.014	16.155	0.016	D

Continued on next page...

Table A.3 – Continued

spSpec name	<i>u</i>	$\sigma(u)$	<i>g</i>	$\sigma(g)$	<i>r</i>	$\sigma(r)$	<i>i</i>	$\sigma(i)$	<i>z</i>	$\sigma(z)$	Tag
1961-53299-152	17.982	0.023	16.618	0.022	16.048	0.013	15.829	0.014	15.707	0.016	C
1961-53299-159	18.211	0.022	16.866	0.009	16.374	0.007	16.155	0.010	16.068	0.021	D
1961-53299-194	17.138	0.011	15.907	0.024	16.134	0.017	16.331	0.011	16.415	0.017	D
1961-53299-213	18.553	0.022	17.182	0.008	16.715	0.007	16.497	0.012	16.431	0.018	D
1961-53299-215	17.780	0.014	16.353	0.009	15.772	0.007	15.544	0.021	15.414	0.011	D
1963-54331-041	20.314	0.059	19.492	0.028	19.246	0.014	19.188	0.021	19.164	0.052	C
1963-54331-043	19.849	0.044	18.766	0.027	18.372	0.010	18.190	0.017	18.066	0.024	C
1963-54331-045	20.220	0.075	19.350	0.027	19.136	0.013	19.005	0.020	18.984	0.045	C
1963-54331-082	20.429	0.067	19.536	0.028	19.265	0.014	19.236	0.021	19.184	0.053	C
1963-54331-083	19.975	0.064	18.907	0.015	18.565	0.019	18.456	0.017	18.380	0.035	D
1963-54331-090	19.939	0.057	18.869	0.014	18.515	0.015	18.356	0.018	18.324	0.037	D
1963-54331-091	19.561	0.037	18.520	0.026	18.024	0.010	17.848	0.017	17.810	0.022	C
1963-54331-096	19.961	0.050	18.954	0.013	18.628	0.017	18.527	0.019	18.466	0.039	D
1963-54331-098	18.831	0.027	17.576	0.015	17.081	0.040	16.873	0.056	16.779	0.017	D
1963-54331-100	19.939	0.056	18.929	0.012	18.589	0.024	18.485	0.027	18.378	0.040	D
1963-54331-102	19.885	0.057	18.951	0.017	18.657	0.017	18.571	0.020	18.511	0.032	D
1963-54331-114	20.023	0.054	19.245	0.019	19.001	0.015	18.929	0.033	18.951	0.052	D
1963-54331-121	18.788	0.024	17.536	0.013	17.049	0.016	16.858	0.015	16.747	0.018	D
1963-54331-123	19.874	0.040	18.695	0.009	18.280	0.019	18.114	0.018	18.029	0.024	D
1963-54331-124	20.001	0.036	19.069	0.016	18.806	0.028	18.736	0.020	18.810	0.049	D
1963-54331-126	19.405	0.028	18.287	0.023	17.836	0.019	17.645	0.018	17.582	0.023	D
1963-54331-128	19.470	0.032	18.253	0.022	17.783	0.026	17.612	0.015	17.487	0.019	D
1963-54331-131	19.359	0.028	18.210	0.012	17.753	0.014	17.569	0.019	17.492	0.021	D

Continued on next page...

Table A.3 – Continued

spSpec name	<i>u</i>	$\sigma(u)$	<i>g</i>	$\sigma(g)$	<i>r</i>	$\sigma(r)$	<i>i</i>	$\sigma(i)$	<i>z</i>	$\sigma(z)$	Tag
1963-54331-137	19.067	0.024	17.895	0.008	17.420	0.019	17.236	0.016	17.177	0.018	D
1963-54331-139	19.056	0.029	17.919	0.008	17.436	0.013	17.254	0.015	17.163	0.018	D
1963-54331-143	19.885	0.055	18.808	0.016	18.456	0.018	18.302	0.018	18.266	0.028	D
1963-54331-144	18.892	0.023	17.663	0.016	17.192	0.019	17.008	0.019	16.878	0.017	D
1963-54331-145	19.866	0.047	18.911	0.015	18.536	0.014	18.394	0.018	18.276	0.035	D
1963-54331-146	20.231	0.077	19.186	0.013	18.955	0.019	18.876	0.025	18.850	0.054	D
1963-54331-147	20.105	0.069	19.252	0.017	19.041	0.018	18.992	0.024	18.934	0.053	D
1963-54331-148	19.890	0.064	18.896	0.014	18.516	0.016	18.373	0.020	18.355	0.045	D
1963-54331-150	19.881	0.046	18.980	0.015	18.678	0.016	18.574	0.015	18.492	0.041	D
1963-54331-154	20.492	0.082	19.588	0.023	19.364	0.024	19.316	0.028	19.313	0.083	D
1963-54331-156	20.465	0.096	19.443	0.020	19.232	0.019	19.189	0.034	19.218	0.065	D
1963-54331-162	20.546	0.080	19.585	0.022	19.385	0.028	19.291	0.022	19.255	0.058	D
1963-54331-164	19.624	0.050	18.434	0.022	18.000	0.018	17.845	0.016	17.738	0.025	D
1963-54331-169	20.482	0.073	19.599	0.018	19.366	0.043	19.286	0.030	19.315	0.072	D
1963-54331-170	20.430	0.064	19.483	0.017	19.317	0.020	19.244	0.022	19.261	0.055	D
1963-54331-178	19.588	0.038	18.477	0.016	18.054	0.014	17.891	0.015	17.836	0.023	D
1963-54331-179	20.041	0.058	19.219	0.016	18.985	0.019	18.919	0.019	18.931	0.057	D
1963-54331-180	19.789	0.047	18.721	0.013	18.306	0.021	18.182	0.016	18.023	0.023	D
1963-54331-181	20.111	0.061	19.174	0.015	18.973	0.023	18.885	0.025	18.866	0.054	D
1963-54331-184	19.721	0.041	18.640	0.012	18.226	0.014	18.052	0.020	17.979	0.017	D
1963-54331-185	20.309	0.062	19.507	0.018	19.306	0.024	19.239	0.029	19.220	0.064	D
1963-54331-186	20.556	0.087	19.654	0.022	19.466	0.020	19.370	0.029	19.376	0.060	D
1963-54331-189	20.213	0.061	19.273	0.017	19.058	0.017	18.997	0.023	19.116	0.056	D

Continued on next page...

Table A.3 – Continued

spSpec name	<i>u</i>	$\sigma(u)$	<i>g</i>	$\sigma(g)$	<i>r</i>	$\sigma(r)$	<i>i</i>	$\sigma(i)$	<i>z</i>	$\sigma(z)$	Tag
1963-54331-194	20.088	0.066	19.216	0.015	18.944	0.021	18.878	0.023	18.853	0.053	D
1963-54331-196	20.132	0.055	19.245	0.015	19.088	0.023	18.962	0.023	18.879	0.057	D
1963-54331-197	20.376	0.076	19.581	0.019	19.378	0.022	19.280	0.025	19.316	0.067	D
1963-54331-200	20.545	0.102	19.563	0.020	19.342	0.019	19.267	0.026	19.243	0.058	D
1963-54331-201	19.823	0.055	18.658	0.011	18.268	0.020	18.123	0.017	18.004	0.026	D
1963-54331-204	19.145	0.028	17.953	0.011	17.465	0.014	17.284	0.026	17.192	0.020	D
1963-54331-206	20.172	0.054	19.258	0.012	19.040	0.020	18.979	0.025	19.022	0.048	D
1963-54331-207	20.443	0.069	19.495	0.015	19.265	0.024	19.181	0.027	19.151	0.051	D
1963-54331-208	18.956	0.027	17.815	0.009	17.354	0.017	17.150	0.021	17.053	0.015	D
1963-54331-209	19.458	0.040	18.339	0.012	17.927	0.013	17.713	0.017	17.675	0.023	D
1963-54331-211	19.505	0.041	18.346	0.011	17.883	0.015	17.709	0.015	17.600	0.025	D
1963-54331-212	19.717	0.038	18.636	0.012	18.213	0.033	18.054	0.021	17.951	0.028	D
1963-54331-217	19.091	0.030	17.824	0.009	17.363	0.010	17.142	0.016	17.081	0.019	D
1963-54331-218	19.204	0.029	17.963	0.008	17.512	0.016	17.351	0.029	17.275	0.018	D
1963-54331-220	20.256	0.067	19.336	0.014	19.109	0.028	19.041	0.033	19.033	0.056	D
1963-54331-222	20.242	0.071	19.344	0.017	19.145	0.019	19.049	0.026	19.034	0.066	D
1963-54331-223	20.160	0.069	19.280	0.019	19.007	0.015	18.905	0.018	18.908	0.048	C
1963-54331-254	20.223	0.082	19.273	0.019	19.036	0.023	18.983	0.027	18.999	0.061	D
			M13								
2174-53521-054	18.978	0.029	17.814	0.014	17.391	0.020	17.237	0.020	17.185	0.020	C
2174-53521-082	16.905	0.017	15.424	0.013	14.845	0.020	14.627	0.019	14.505	0.017	C
2174-53521-087	18.441	0.022	17.258	0.016	16.796	0.018	16.619	0.019	16.547	0.021	C
2174-53521-093	16.672	0.009	15.225	0.012	14.589	0.036	14.342	0.020	14.208	0.032	D

Continued on next page...

Table A.3 – Continued

spSpec name	<i>u</i>	$\sigma(u)$	<i>g</i>	$\sigma(g)$	<i>r</i>	$\sigma(r)$	<i>i</i>	$\sigma(i)$	<i>z</i>	$\sigma(z)$	Tag
2174-53521-094	18.410	0.022	17.245	0.016	16.781	0.018	16.552	0.019	16.476	0.021	C
2174-53521-098	16.892	0.009	15.525	0.009	14.939	0.029	14.695	0.020	14.573	0.032	D
2174-53521-121	17.484	0.015	16.227	0.011	15.684	0.016	15.485	0.012	15.386	0.010	D
2174-53521-126	18.250	0.021	17.014	0.013	16.536	0.012	16.337	0.014	16.276	0.015	D
2174-53521-128	18.654	0.020	17.480	0.008	17.022	0.013	16.824	0.014	16.751	0.016	D
2174-53521-131	19.098	0.039	18.175	0.010	17.908	0.015	24.329	4.297	17.735	0.025	C
2174-53521-133	18.101	0.016	16.876	0.008	16.381	0.010	16.175	0.012	16.088	0.014	D
2174-53521-134	18.453	0.016	17.284	0.011	16.832	0.013	16.618	0.009	16.515	0.014	D
2174-53521-136	16.264	0.021	15.168	0.012	15.452	0.016	15.647	0.009	15.768	0.019	D
2174-53521-137	16.979	0.010	15.567	0.006	15.007	0.010	14.806	0.009	14.680	0.009	D
2174-53521-145	16.535	0.020	14.969	0.012	14.314	0.035	14.590	...	13.922	0.022	B
2174-53521-146	18.843	0.027	17.680	0.013	17.253	0.028	17.060	0.028	17.044	0.029	D
2174-53521-149	18.931	0.033	17.781	0.013	17.359	0.033	17.171	0.034	17.133	0.031	D
2174-53521-152	16.098	0.020	14.897	0.012	15.132	0.033	15.296	0.024	15.397	0.012	D
2174-53521-153	16.165	0.009	14.931	0.014	15.107	0.020	15.249	0.016	15.296	0.016	D
2174-53521-154	16.624	0.014	15.058	0.005	14.449	0.011	14.690	...	14.044	0.009	B
2174-53521-155	17.757	0.030	16.521	0.007	16.007	0.028	15.805	0.009	15.700	0.023	D
2174-53521-156	17.062	0.014	15.656	0.006	15.067	0.034	14.838	0.032	14.737	0.025	D
2174-53521-157	16.226	0.009	15.108	0.010	15.357	0.007	15.544	0.006	15.655	0.014	D
2174-53521-158	16.969	0.016	15.567	0.015	15.044	0.019	14.809	0.016	14.669	0.025	D
2174-53521-159	16.582	0.021	15.025	0.008	14.406	0.026	14.687	...	14.026	0.013	B
2174-53521-160	16.822	0.018	15.354	0.007	14.765	0.030	14.989	...	14.400	0.015	B
2174-53521-166	16.954	0.012	15.623	0.005	15.038	0.018	14.800	0.032	14.686	0.026	D

Continued on next page...

Table A.3 – Continued

spSpec name	<i>u</i>	$\sigma(u)$	<i>g</i>	$\sigma(g)$	<i>r</i>	$\sigma(r)$	<i>i</i>	$\sigma(i)$	<i>z</i>	$\sigma(z)$	Tag
2174-53521-167	16.408	0.008	14.817	0.010	14.191	0.008	14.483	...	13.789	0.018	B
2174-53521-168	16.750	0.008	15.244	0.012	14.665	0.009	14.941	...	14.276	0.018	B
2174-53521-171	16.478	0.015	14.958	0.011	14.298	0.015	14.566	...	13.909	0.018	B
2174-53521-172	16.745	0.012	15.298	0.010	14.689	0.012	14.915	...	14.319	0.021	B
2174-53521-174	18.875	0.034	17.904	0.017	17.478	0.018	17.357	0.016	17.304	0.022	C
2174-53521-175	16.066	0.022	14.865	0.010	15.062	0.014	15.224	0.009	15.309	0.019	D
2174-53521-176	17.115	0.020	15.730	0.005	15.165	0.027	14.930	0.013	14.818	0.015	D
2174-53521-215	16.780	0.019	15.346	0.016	14.782	0.018	14.561	0.025	14.440	0.017	C
2174-53521-368	18.661	0.024	17.507	0.016	17.046	0.010	16.865	0.025	16.787	0.020	C
2174-53521-376	17.124	0.017	15.783	0.015	15.212	0.009	14.987	0.025	14.935	0.017	C
2174-53521-402	18.904	0.032	17.810	0.009	17.398	0.012	17.219	0.018	17.087	0.020	D
2174-53521-403	18.946	0.032	17.981	0.010	17.608	0.009	17.443	0.012	17.377	0.019	D
2174-53521-406	18.971	0.036	17.893	0.008	17.487	0.011	17.308	0.012	17.248	0.028	D
2174-53521-407	17.806	0.023	16.612	0.009	16.094	0.008	15.894	0.012	15.771	0.012	D
2174-53521-410	16.775	0.012	15.329	0.008	14.694	0.012	15.007	...	14.341	0.021	B
2174-53521-412	18.602	0.024	17.467	0.016	16.961	0.009	16.800	0.025	16.748	0.019	C
2174-53521-413	16.976	0.009	15.535	0.012	14.964	0.006	14.720	0.011	14.599	0.012	D
2174-53521-414	18.604	0.024	17.456	0.016	16.909	0.009	16.782	0.025	16.711	0.019	C
2174-53521-442	16.067	0.014	14.867	0.015	15.037	0.005	15.205	0.014	15.269	0.014	D
2174-53521-443	16.817	0.009	15.333	0.015	14.746	0.009	14.962	...	14.387	0.026	B
2174-53521-445	18.970	0.032	17.893	0.011	17.490	0.010	17.316	0.011	17.262	0.018	D
2174-53521-447	18.742	0.021	17.683	0.011	17.240	0.009	17.050	0.010	17.008	0.019	D
2174-53521-449	16.818	0.009	15.349	0.014	14.765	0.006	15.020	...	14.364	0.024	B

Continued on next page...

Table A.3 – Continued

spSpec name	<i>u</i>	$\sigma(u)$	<i>g</i>	$\sigma(g)$	<i>r</i>	$\sigma(r)$	<i>i</i>	$\sigma(i)$	<i>z</i>	$\sigma(z)$	Tag
2174-53521-451	16.164	0.023	14.994	0.009	15.166	0.029	15.378	0.027	15.472	0.019	D
2174-53521-452	16.557	0.008	15.112	0.013	14.504	0.007	14.782	...	14.101	0.019	B
2174-53521-453	16.750	0.025	15.286	0.021	14.677	0.035	14.966	...	14.356	0.025	B
2174-53521-455	16.840	0.011	15.378	0.009	14.779	0.009	15.104	...	14.417	0.020	B
2174-53521-456	18.541	0.025	17.371	0.014	16.908	0.009	16.718	0.009	16.642	0.015	D
2174-53521-457	16.693	0.019	15.178	0.011	14.561	0.027	14.816	...	14.190	0.022	B
2174-53521-458	16.633	0.009	15.068	0.014	14.457	0.005	14.702	...	14.075	0.027	B
2174-53521-459	16.673	0.016	15.201	0.016	14.643	0.014	14.401	0.017	14.135	0.015	C
2174-53521-460	16.464	0.009	14.823	0.012	14.202	0.006	14.470	...	13.765	0.024	B
2174-53521-461	18.453	0.020	17.359	0.009	16.894	0.008	16.696	0.011	16.610	0.014	D
2174-53521-462	16.561	0.008	15.126	0.014	14.509	0.003	14.228	0.012	14.112	0.009	D
2174-53521-463	17.021	0.015	15.630	0.005	15.054	0.016	14.802	0.006	14.704	0.009	D
2174-53521-464	16.109	0.008	14.892	0.011	15.089	0.006	15.219	0.011	15.309	0.012	D
2174-53521-470	16.422	0.009	14.850	0.007	14.226	0.010	13.924	0.007	13.797	0.007	D
2174-53521-471	17.521	0.020	16.278	0.006	15.740	0.009	15.526	0.012	15.420	0.012	D
2174-53521-472	16.046	0.009	14.824	0.020	14.831	0.024	14.929	0.027	14.940	0.016	D
2174-53521-474	18.777	0.030	17.612	0.008	17.153	0.011	16.973	0.012	16.897	0.016	D
2174-53521-475	16.428	0.009	14.909	0.008	14.538	...	14.026	0.021	13.893	0.007	B
2174-53521-476	17.180	0.014	15.727	0.008	15.183	0.012	14.928	0.026	14.822	0.010	D
2174-53521-477	16.682	0.023	15.217	0.006	14.583	0.040	14.848	...	14.218	0.012	B
2174-53521-478	16.844	0.010	15.422	0.008	14.842	0.011	14.633	0.024	14.490	0.014	D
2174-53521-480	18.093	0.016	16.899	0.009	16.410	0.005	16.186	0.010	16.105	0.010	D
2174-53521-481	18.909	0.025	17.867	0.010	17.459	0.009	19.472	0.183	17.225	0.018	D

Continued on next page...

Table A.3 – Continued

spSpec name	<i>u</i>	$\sigma(u)$	<i>g</i>	$\sigma(g)$	<i>r</i>	$\sigma(r)$	<i>i</i>	$\sigma(i)$	<i>z</i>	$\sigma(z)$	Tag
2174-53521-483	16.623	0.013	15.141	0.013	14.532	0.024	14.261	0.021	14.156	0.019	D
2174-53521-484	16.656	0.012	15.187	0.015	14.558	0.026	14.295	0.026	14.175	0.012	D
2174-53521-485	16.911	0.015	15.489	0.016	14.940	0.024	14.684	0.028	14.588	0.014	D
2174-53521-488	17.079	0.012	15.725	0.013	15.152	0.016	14.906	0.018	14.783	0.008	D
2174-53521-489	16.996	0.013	15.576	0.009	14.972	0.010	14.737	0.016	14.599	0.010	D
2174-53521-490	16.199	0.007	15.009	0.016	15.220	0.024	15.372	0.025	15.466	0.014	D
2174-53521-491	16.202	0.012	15.140	0.013	15.392	0.016	15.596	0.021	15.712	0.017	D
2174-53521-493	16.592	0.010	15.088	0.024	14.484	0.021	14.205	0.022	14.081	0.013	D
2174-53521-494	16.646	0.012	15.143	0.019	14.523	0.014	14.264	0.026	14.133	0.008	D
2174-53521-495	17.303	0.014	15.998	0.015	15.425	0.016	15.189	0.019	15.082	0.007	D
2174-53521-497	16.883	0.014	15.410	0.009	14.782	0.015	14.543	0.011	14.394	0.012	D
2174-53521-498	16.579	0.015	15.122	0.006	14.522	0.012	14.244	0.011	14.131	0.013	D
2174-53521-499	16.605	0.013	15.089	0.014	14.482	0.014	14.206	0.010	14.088	0.015	D
2174-53521-500	16.701	0.012	15.302	0.011	14.700	0.009	14.438	0.026	14.329	0.010	D
2174-53521-522	16.957	0.012	15.503	0.010	14.919	0.014	14.665	0.014	14.557	0.011	D
2174-53521-529	17.703	0.020	16.474	0.020	15.954	0.019	15.746	0.019	15.664	0.017	C
2174-53521-530	16.818	0.007	15.287	0.004	14.667	0.010	14.416	0.008	14.261	0.036	D
2174-53521-531	16.624	0.012	15.229	0.006	14.614	0.009	14.349	0.010	14.230	0.016	D
2174-53521-532	16.147	0.010	14.970	0.009	15.172	0.007	15.325	0.012	15.428	0.013	D
2174-53521-533	18.853	0.025	17.797	0.009	17.360	0.013	17.165	0.011	17.125	0.017	D
2174-53521-537	17.275	0.012	15.965	0.007	15.433	0.009	15.188	0.010	15.082	0.009	D
2174-53521-538	16.543	0.013	15.042	0.003	14.412	0.009	14.148	0.013	14.020	0.012	D
2174-53521-539	18.758	0.022	17.657	0.007	17.184	0.015	16.983	0.010	16.884	0.032	D

Continued on next page...

Table A.3 – Continued

spSpec name	<i>u</i>	$\sigma(u)$	<i>g</i>	$\sigma(g)$	<i>r</i>	$\sigma(r)$	<i>i</i>	$\sigma(i)$	<i>z</i>	$\sigma(z)$	Tag
2174-53521-540	16.074	0.012	14.912	0.005	15.143	0.016	15.319	0.017	15.409	0.016	D
2174-53521-542	16.801	0.021	15.276	0.010	14.660	0.009	14.408	0.025	14.263	0.020	D
2174-53521-554	17.222	0.034	15.843	0.009	15.281	0.010	15.041	0.013	14.925	0.012	D
2174-53521-560	18.717	0.047	17.547	0.008	17.019	0.009	16.860	0.009	16.754	0.019	D
2174-53521-563	17.661	0.023	16.408	0.015	15.892	0.015	15.685	0.014	15.581	0.021	C
2174-53521-565	18.935	0.028	17.915	0.008	17.493	0.017	17.340	0.009	17.264	0.013	D
2174-53521-573	19.056	0.030	17.961	0.014	17.592	0.020	17.451	0.020	17.392	0.021	C
2174-53521-576	18.891	0.030	17.672	0.007	17.223	0.009	17.022	0.011	16.938	0.021	D
2174-53521-577	18.986	0.028	17.902	0.009	17.481	0.019	17.313	0.013	17.236	0.021	D
2185-53532-106	20.558	0.077	19.687	0.019	19.412	0.025	19.274	0.027	19.372	0.065	C
2185-53532-111	19.485	0.037	18.572	0.016	18.330	0.035	18.315	0.053	18.373	0.036	C
2185-53532-113	20.677	0.084	19.812	0.020	19.479	0.026	19.379	0.028	19.368	0.064	C
2185-53532-116	20.333	0.065	19.363	0.018	19.105	0.023	19.022	0.025	18.984	0.048	C
2185-53532-120	20.041	0.053	19.189	0.018	18.907	0.023	18.805	0.024	18.682	0.038	C
2185-53532-141	19.285	0.033	18.392	0.019	18.165	0.018	18.102	0.022	18.078	0.032	D
2185-53532-143	19.452	0.033	18.517	0.018	18.272	0.019	18.207	0.030	18.204	0.028	D
2185-53532-146	20.841	0.080	19.753	0.021	19.459	0.018	19.346	0.025	19.376	0.096	D
2185-53532-148	19.860	0.044	18.997	0.016	18.746	0.021	18.663	0.035	18.687	0.050	D
2185-53532-150	19.791	0.041	18.782	0.021	18.544	0.024	18.485	0.032	18.446	0.049	D
2185-53532-151	20.399	0.061	19.422	0.018	19.143	0.024	19.070	0.021	19.063	0.036	D
2185-53532-152	19.722	0.037	18.796	0.016	18.580	0.023	18.488	0.020	18.459	0.044	D
2185-53532-153	19.077	0.033	18.098	0.015	17.719	0.013	17.586	0.014	17.506	0.023	D
2185-53532-154	20.629	0.083	19.689	0.020	19.422	0.034	19.295	0.023	19.337	0.072	D

Continued on next page...

Table A.3 – Continued

spSpec name	<i>u</i>	$\sigma(u)$	<i>g</i>	$\sigma(g)$	<i>r</i>	$\sigma(r)$	<i>i</i>	$\sigma(i)$	<i>z</i>	$\sigma(z)$	Tag
2185-53532-156	19.901	0.054	19.033	0.012	18.766	0.030	18.706	0.020	18.695	0.045	D
2185-53532-158	19.910	0.051	18.930	0.013	18.678	0.016	18.608	0.021	18.563	0.042	D
2185-53532-160	20.032	0.050	19.196	0.014	18.960	0.020	18.884	0.021	18.841	0.050	D
2185-53532-161	20.534	0.070	19.647	0.015	19.387	0.024	19.343	0.033	19.196	0.066	D
2185-53532-167	19.725	0.046	18.742	0.015	18.518	0.028	18.425	0.029	18.406	0.038	D
2185-53532-169	20.005	0.057	19.007	0.016	18.756	0.031	18.659	0.034	18.676	0.051	D
2185-53532-171	20.841	0.094	19.837	0.015	19.544	0.020	19.417	0.020	19.377	0.079	D
2185-53532-172	19.674	0.037	18.769	0.018	18.531	0.019	18.458	0.017	18.414	0.043	D
2185-53532-175	19.752	0.050	18.804	0.011	18.617	0.020	18.502	0.016	18.521	0.053	D
2185-53532-176	19.784	0.048	18.810	0.011	18.570	0.015	18.466	0.017	18.414	0.045	D
2185-53532-177	19.736	0.038	18.859	0.010	18.642	0.014	18.523	0.015	18.576	0.045	D
2185-53532-178	19.951	0.047	19.076	0.017	18.826	0.019	18.747	0.020	18.732	0.054	D
2185-53532-179	19.259	0.033	18.436	0.018	18.207	0.015	18.121	0.017	18.144	0.035	D
2185-53532-181	19.601	0.048	18.742	0.018	18.506	0.019	18.446	0.018	18.385	0.037	C
2185-53532-196	19.854	0.054	19.028	0.018	18.758	0.020	18.698	0.019	18.748	0.047	C
2185-53532-197	20.078	0.064	19.108	0.019	18.849	0.020	18.802	0.028	18.838	0.051	C
2185-53532-198	19.566	0.044	18.883	0.018	18.621	0.020	18.527	0.027	18.534	0.041	C
2185-53532-200	20.629	0.098	19.754	0.022	19.468	0.024	19.360	0.032	19.243	0.074	C
2185-53532-237	19.066	0.034	18.063	0.017	17.777	0.018	17.644	0.026	17.631	0.025	C
2185-53532-388	19.200	0.030	18.283	0.016	18.043	0.010	17.934	0.025	17.899	0.027	C
2185-53532-390	20.230	0.055	19.372	0.018	19.109	0.014	19.014	0.027	19.001	0.054	C
2185-53532-393	20.768	0.083	19.913	0.025	19.538	0.019	19.445	0.026	19.498	0.078	C
2185-53532-423	19.827	0.043	18.879	0.017	18.636	0.012	18.560	0.026	18.582	0.040	C

Continued on next page...

Table A.3 – Continued

spSpec name	<i>u</i>	$\sigma(u)$	<i>g</i>	$\sigma(g)$	<i>r</i>	$\sigma(r)$	<i>i</i>	$\sigma(i)$	<i>z</i>	$\sigma(z)$	Tag
2185-53532-424	19.981	0.103	19.227	0.106	18.962	0.098	18.796	0.092	19.014	0.161	C
2185-53532-425	19.222	0.031	18.304	0.022	18.042	0.014	17.978	0.021	17.945	0.028	C
2185-53532-426	19.046	0.028	18.012	0.016	17.676	0.010	17.535	0.025	17.504	0.023	C
2185-53532-427	19.039	0.028	18.001	0.016	17.651	0.010	17.513	0.025	17.502	0.023	C
2185-53532-428	20.088	0.052	19.180	0.018	18.904	0.013	18.803	0.027	18.857	0.049	C
2185-53532-430	20.498	0.069	19.686	0.020	19.390	0.015	19.260	0.029	19.261	0.065	C
2185-53532-431	20.878	0.089	19.867	0.018	19.579	0.029	19.476	0.031	19.338	0.096	D
2185-53532-433	20.554	0.097	19.927	0.023	19.551	0.025	19.440	0.035	19.383	0.082	C
2185-53532-435	19.844	0.049	19.031	0.011	18.786	0.020	18.722	0.019	18.740	0.046	D
2185-53532-439	19.071	0.029	18.125	0.016	17.847	0.010	17.698	0.025	17.728	0.025	C
2185-53532-440	20.627	0.077	19.727	0.015	19.447	0.031	19.343	0.028	19.339	0.072	D
2185-53532-461	19.297	0.046	18.368	0.010	18.134	0.011	18.035	0.016	18.070	0.035	D
2185-53532-462	19.099	0.035	18.194	0.018	17.921	0.019	17.836	0.015	17.858	0.025	C
2185-53532-464	20.450	0.092	19.434	0.018	19.158	0.017	19.129	0.028	19.060	0.063	D
2185-53532-466	19.695	0.047	18.790	0.019	18.593	0.020	18.451	0.017	18.533	0.036	C
2185-53532-469	19.871	0.052	18.983	0.010	18.750	0.012	18.639	0.015	18.611	0.044	D
2185-53532-473	20.229	0.066	19.259	0.015	18.993	0.024	18.923	0.032	18.988	0.078	D
2185-53532-475	19.458	0.035	18.585	0.017	18.293	0.011	18.234	0.026	18.309	0.034	C
2185-53532-476	19.946	0.045	19.062	0.018	18.738	0.014	18.688	0.039	18.636	0.049	C
2185-53532-477	20.596	0.074	19.570	0.019	19.259	0.015	19.181	0.028	19.354	0.072	C
2185-53532-478	19.860	0.062	19.009	0.019	18.698	0.023	18.600	0.017	18.588	0.041	D
2185-53532-479	20.310	0.067	19.447	0.018	19.116	0.032	19.055	0.023	18.990	0.073	D
2185-53532-480	20.524	0.070	19.678	0.020	19.378	0.015	19.245	0.029	19.438	0.077	C

Continued on next page...

Table A.3 – Continued

spSpec name	<i>u</i>	$\sigma(u)$	<i>g</i>	$\sigma(g)$	<i>r</i>	$\sigma(r)$	<i>i</i>	$\sigma(i)$	<i>z</i>	$\sigma(z)$	Tag
2185-53532-481	19.163	0.042	18.195	0.008	17.925	0.012	17.799	0.011	17.754	0.030	D
2185-53532-482	19.078	0.031	18.100	0.008	17.789	0.010	17.664	0.009	17.626	0.022	D
2185-53532-483	20.044	0.057	19.130	0.014	18.865	0.013	18.788	0.019	18.737	0.044	D
2185-53532-485	19.273	0.037	18.446	0.011	18.216	0.009	18.074	0.012	18.103	0.027	D
2185-53532-486	20.186	0.068	19.404	0.018	19.172	0.013	19.062	0.023	18.997	0.045	D
2185-53532-487	19.234	0.029	18.319	0.010	18.048	0.009	17.979	0.014	17.950	0.028	D
2185-53532-488	20.203	0.066	19.547	0.019	19.277	0.018	19.123	0.021	19.159	0.052	D
2185-53532-489	19.918	0.068	19.029	0.013	18.812	0.013	18.694	0.016	18.595	0.033	D
2185-53532-490	20.221	0.059	19.343	0.016	19.073	0.013	18.976	0.019	18.996	0.052	D
2185-53532-492	19.045	0.024	18.167	0.015	17.882	0.011	17.768	0.009	17.794	0.024	D
2185-53532-493	19.312	0.036	18.347	0.013	18.128	0.010	18.017	0.014	18.041	0.032	D
2185-53532-494	20.174	0.065	19.210	0.013	18.923	0.014	18.859	0.019	18.894	0.052	D
2185-53532-495	19.455	0.047	18.657	0.012	18.427	0.012	18.324	0.015	18.313	0.031	D
2185-53532-496	20.863	0.109	19.899	0.020	19.567	0.017	19.450	0.028	19.535	0.088	D
2185-53532-497	20.532	0.080	19.585	0.025	19.265	0.015	19.172	0.022	19.103	0.063	D
2185-53532-498	19.446	0.039	18.689	0.010	18.422	0.012	18.329	0.014	18.354	0.028	D
2185-53532-499	19.546	0.036	18.733	0.015	18.504	0.011	18.394	0.015	18.389	0.040	D
2185-53532-500	19.902	0.061	19.108	0.027	18.914	0.019	18.767	0.022	18.750	0.053	D
2185-53532-504	19.554	0.034	18.726	0.021	18.501	0.020	18.412	0.021	18.440	0.031	C
2185-53532-506	19.015	0.028	18.036	0.012	17.664	0.008	17.523	0.012	17.466	0.024	D
2185-53532-507	20.066	0.052	19.165	0.015	18.864	0.016	18.787	0.018	18.753	0.054	D
2185-53532-508	19.964	0.068	18.999	0.014	18.832	0.027	18.655	0.020	18.641	0.040	D
2185-53532-511	20.737	0.090	19.856	0.022	19.564	0.019	19.425	0.023	19.289	0.062	D

Continued on next page...

Table A.3 – Continued

spSpec name	<i>u</i>	$\sigma(u)$	<i>g</i>	$\sigma(g)$	<i>r</i>	$\sigma(r)$	<i>i</i>	$\sigma(i)$	<i>z</i>	$\sigma(z)$	Tag
2185-53532-512	19.188	0.025	18.258	0.010	18.006	0.012	17.889	0.009	17.891	0.022	D
2185-53532-513	19.772	0.044	18.920	0.012	18.648	0.015	18.591	0.012	18.575	0.042	D
2185-53532-514	20.241	0.072	19.263	0.016	19.009	0.013	18.924	0.017	18.878	0.037	D
2185-53532-515	19.793	0.041	18.936	0.013	18.700	0.015	18.619	0.016	18.663	0.038	D
2185-53532-516	20.761	0.093	19.869	0.017	19.571	0.020	19.407	0.025	19.355	0.070	D
2185-53532-517	20.828	0.104	19.904	0.019	19.589	0.022	19.427	0.023	19.427	0.071	D
2185-53532-519	19.811	0.046	18.973	0.012	18.742	0.016	18.625	0.012	18.631	0.039	D
2185-53532-520	19.377	0.030	18.398	0.013	18.137	0.016	18.066	0.012	18.042	0.025	D
2185-53532-534	19.461	0.040	18.601	0.019	18.320	0.019	18.258	0.016	18.246	0.031	C
2185-53532-537	19.586	0.035	18.767	0.016	18.509	0.017	18.452	0.019	18.420	0.030	C
2185-53532-539	20.379	0.077	19.508	0.021	19.230	0.022	19.115	0.022	19.159	0.057	C
2185-53532-540	19.990	0.057	19.204	0.020	18.951	0.021	18.848	0.020	18.930	0.047	C
2185-53532-541	20.773	0.072	19.867	0.024	19.544	0.023	19.389	0.026	19.418	0.058	C
2185-53532-542	20.383	0.063	19.432	0.017	19.120	0.013	18.998	0.018	19.031	0.048	D
2185-53532-543	19.206	0.034	18.284	0.010	18.018	0.009	17.916	0.009	17.883	0.032	D
2185-53532-544	19.889	0.056	18.847	0.011	18.604	0.011	18.524	0.012	18.525	0.047	D
2185-53532-545	19.959	0.042	19.061	0.021	18.769	0.021	18.692	0.022	18.698	0.035	C
2185-53532-546	20.690	0.084	19.915	0.017	19.595	0.021	19.414	0.025	19.522	0.054	D
2185-53532-547	20.703	0.069	19.909	0.024	19.549	0.023	19.443	0.026	19.483	0.062	C
2185-53532-548	20.863	0.104	19.959	0.023	19.598	0.020	19.508	0.036	19.689	0.077	D
2185-53532-549	20.358	0.070	19.507	0.018	19.125	0.018	18.983	0.018	19.018	0.053	D
2185-53532-550	20.535	0.083	19.738	0.019	19.452	0.022	19.298	0.021	19.271	0.073	D
2185-53532-551	20.801	0.088	19.909	0.022	19.599	0.024	19.432	0.023	19.459	0.078	D

Continued on next page...

Table A.3 – Continued

spSpec name	<i>u</i>	$\sigma(u)$	<i>g</i>	$\sigma(g)$	<i>r</i>	$\sigma(r)$	<i>i</i>	$\sigma(i)$	<i>z</i>	$\sigma(z)$	Tag
2185-53532-552	19.709	0.046	18.899	0.012	18.648	0.016	18.577	0.014	18.586	0.032	D
2185-53532-553	18.992	0.023	18.065	0.011	17.731	0.026	17.574	0.017	17.546	0.027	D
2185-53532-554	19.214	0.027	18.347	0.012	18.078	0.012	17.980	0.010	17.943	0.026	D
2185-53532-555	20.206	0.061	19.342	0.019	19.039	0.020	18.928	0.017	18.870	0.037	D
2185-53532-556	20.239	0.061	19.376	0.018	19.095	0.026	18.999	0.022	18.989	0.054	D
2185-53532-557	19.594	0.041	18.690	0.014	18.424	0.022	18.341	0.014	18.371	0.036	D
2185-53532-558	19.441	0.038	18.577	0.009	18.313	0.014	18.211	0.012	18.238	0.035	D
2185-53532-559	19.829	0.049	18.915	0.011	18.661	0.012	18.552	0.012	18.572	0.037	D
2185-53532-560	19.275	0.032	18.421	0.013	18.160	0.017	18.084	0.011	18.069	0.033	D
2185-53532-575	20.664	0.066	19.769	0.024	19.420	0.023	19.330	0.025	19.194	0.049	C
2185-53532-577	20.035	0.043	19.163	0.017	18.903	0.018	18.808	0.020	18.856	0.039	C
2185-53532-581	20.194	0.051	19.299	0.018	19.003	0.017	18.911	0.019	18.871	0.041	C
2185-53532-584	20.045	0.054	19.257	0.014	19.058	0.022	18.904	0.015	18.910	0.042	D
2185-53532-585	20.130	0.050	19.137	0.014	18.847	0.015	18.771	0.015	18.751	0.045	D
2185-53532-587	20.730	0.084	19.806	0.023	19.513	0.019	19.384	0.028	19.325	0.070	D
2185-53532-589	19.926	0.059	18.974	0.012	18.733	0.027	18.636	0.026	18.609	0.045	D
2185-53532-591	19.683	0.049	18.773	0.013	18.545	0.021	18.450	0.025	18.401	0.036	D
2185-53532-592	20.429	0.072	19.454	0.015	19.207	0.034	19.055	0.029	19.097	0.065	D
2185-53532-593	19.744	0.043	18.893	0.012	18.664	0.023	18.595	0.019	18.602	0.035	D
2185-53532-594	20.327	0.053	19.523	0.023	19.230	0.022	19.155	0.024	19.155	0.048	C
2185-53532-596	20.792	0.102	19.876	0.020	19.519	0.022	19.398	0.028	19.449	0.078	D
2185-53532-598	20.290	0.061	19.415	0.020	19.153	0.024	19.029	0.030	19.116	0.057	D
2185-53532-599	20.251	0.060	19.391	0.017	19.128	0.016	19.020	0.021	19.036	0.052	D

Continued on next page...

Table A.3 – Continued

spSpec name	<i>u</i>	$\sigma(u)$	<i>g</i>	$\sigma(g)$	<i>r</i>	$\sigma(r)$	<i>i</i>	$\sigma(i)$	<i>z</i>	$\sigma(z)$	Tag
2185-53532-600	20.705	0.080	19.845	0.019	19.542	0.029	19.409	0.035	19.320	0.052	D
2255-53565-103	19.032	0.029	17.974	0.014	17.591	0.020	17.473	0.020	17.406	0.021	C
2255-53565-112	16.672	0.009	15.225	0.012	14.589	0.036	14.342	0.020	14.208	0.032	D
2255-53565-114	18.277	0.017	17.080	0.012	16.614	0.012	16.406	0.012	16.316	0.014	D
2255-53565-115	18.997	0.023	17.934	0.014	17.540	0.021	17.371	0.015	17.320	0.024	D
2255-53565-116	17.536	0.016	16.291	0.009	15.751	0.011	15.525	0.012	15.420	0.014	D
2255-53565-120	16.892	0.009	15.525	0.009	14.939	0.029	14.695	0.020	14.572	0.032	D
2255-53565-143	17.321	0.016	15.959	0.011	15.415	0.011	15.186	0.015	15.077	0.018	D
2255-53565-144	16.969	0.016	15.567	0.015	15.044	0.019	14.809	0.016	14.669	0.025	D
2255-53565-147	16.226	0.009	15.108	0.010	15.357	0.007	15.544	0.006	15.655	0.014	D
2255-53565-148	17.218	0.012	15.819	0.007	15.262	0.011	15.023	0.011	14.927	0.013	D
2255-53565-153	17.099	0.019	15.684	0.008	15.120	0.024	14.896	0.015	14.768	0.013	D
2255-53565-157	16.562	0.015	15.107	0.007	14.484	0.025	19.375	...	14.080	0.017	B
2255-53565-171	16.822	0.018	15.354	0.007	14.765	0.030	14.297	...	14.400	0.015	B
2255-53565-173	18.744	0.022	17.636	0.012	17.183	0.014	16.985	0.026	16.908	0.020	D
2255-53565-174	16.116	0.017	14.916	0.008	15.092	0.016	15.243	0.046	15.344	0.016	D
2255-53565-175	17.115	0.020	15.730	0.005	15.165	0.027	14.930	0.013	14.818	0.015	D
2255-53565-177	16.066	0.022	14.865	0.010	15.062	0.014	15.224	0.009	15.309	0.019	D
2255-53565-192	16.190	0.018	15.083	0.016	15.300	0.018	15.476	0.025	15.599	0.018	C
2255-53565-423	16.206	0.015	15.114	0.015	15.316	0.009	15.523	0.025	15.658	0.018	C
2255-53565-424	18.874	0.023	17.789	0.011	17.365	0.009	17.186	0.022	17.126	0.032	D
2255-53565-425	18.971	0.034	17.915	0.010	17.519	0.012	17.339	0.013	17.268	0.024	D
2255-53565-426	16.976	0.009	15.535	0.012	14.964	0.006	14.720	0.011	14.599	0.012	D

Continued on next page...

Table A.3 – Continued

spSpec name	<i>u</i>	$\sigma(u)$	<i>g</i>	$\sigma(g)$	<i>r</i>	$\sigma(r)$	<i>i</i>	$\sigma(i)$	<i>z</i>	$\sigma(z)$	Tag
2255-53565-432	19.060	0.024	17.981	0.011	17.592	0.015	17.432	0.017	17.360	0.034	D
2255-53565-436	21.007	0.108	20.193	0.022	19.824	0.025	19.688	0.046	19.560	0.095	B
2255-53565-437	18.666	0.027	17.471	0.009	17.017	0.008	16.851	0.009	16.763	0.018	D
2255-53565-443	16.212	0.022	15.040	0.017	15.278	0.018	15.428	0.013	15.560	0.018	C
2255-53565-465	16.131	0.008	14.989	0.019	15.222	0.026	15.385	0.028	15.478	0.014	D
2255-53565-466	18.922	0.029	17.856	0.020	17.465	0.019	17.279	0.016	17.194	0.022	C
2255-53565-476	18.358	0.017	17.172	0.009	16.703	0.009	16.499	0.009	16.399	0.015	D
2255-53565-482	16.067	0.014	14.867	0.015	15.037	0.005	15.205	0.014	15.269	0.014	D
2255-53565-483	16.561	0.008	15.126	0.014	14.509	0.003	14.228	0.012	14.112	0.009	D
2255-53565-485	17.004	0.008	15.581	0.009	15.020	0.007	14.752	0.007	14.648	0.012	D
2255-53565-486	16.710	0.014	15.229	0.004	14.626	0.007	14.349	0.012	14.225	0.009	D
2255-53565-490	17.559	0.012	16.279	0.007	15.765	0.004	15.528	0.011	15.444	0.010	D
2255-53565-492	16.109	0.008	14.892	0.011	15.089	0.006	15.219	0.011	15.309	0.012	D
2255-53565-495	16.279	0.007	14.660	0.022	14.030	0.021	13.682	0.007	13.512	0.013	D
2255-53565-496	16.422	0.009	14.850	0.007	14.226	0.010	13.924	0.007	13.797	0.007	D
2255-53565-504	16.133	0.012	14.477	0.005	13.840	0.014	13.466	0.006	13.336	0.009	D
2255-53565-510	17.021	0.015	15.630	0.005	15.054	0.016	14.802	0.006	14.704	0.009	D
2255-53565-512	16.579	0.015	15.122	0.006	14.522	0.012	14.244	0.011	14.131	0.013	D
2255-53565-515	17.180	0.014	15.727	0.008	15.183	0.012	14.928	0.026	14.822	0.010	D
2255-53565-518	21.616	0.186	20.561	0.035	20.105	0.039	19.949	0.044	20.205	0.144	B
2255-53565-520	16.509	0.009	14.930	0.015	14.328	0.026	14.102	0.020	13.952	0.011	D
2255-53565-542	16.957	0.012	15.503	0.010	14.919	0.014	14.665	0.014	14.557	0.011	D
2255-53565-543	16.996	0.013	15.576	0.009	14.972	0.010	14.737	0.016	14.599	0.010	D

Continued on next page...

Table A.3 – Continued

spSpec name	<i>u</i>	$\sigma(u)$	<i>g</i>	$\sigma(g)$	<i>r</i>	$\sigma(r)$	<i>i</i>	$\sigma(i)$	<i>z</i>	$\sigma(z)$	Tag
2255-53565-544	16.595	0.013	15.131	0.015	14.525	0.019	14.250	0.026	14.123	0.021	D
2255-53565-545	16.919	0.014	15.473	0.007	14.882	0.018	14.643	0.009	14.520	0.011	D
2255-53565-548	16.883	0.014	15.410	0.009	14.782	0.015	14.543	0.011	14.394	0.012	D
2255-53565-550	17.079	0.012	15.725	0.013	15.152	0.016	14.906	0.018	14.783	0.008	D
2255-53565-551	16.624	0.012	15.229	0.006	14.614	0.009	14.349	0.010	14.230	0.016	D
2255-53565-552	16.214	0.011	14.555	0.005	13.916	0.034	13.597	0.012	13.457	0.013	D
2255-53565-553	16.817	0.014	15.382	0.007	14.797	0.025	14.546	0.016	14.440	0.027	D
2255-53565-556	18.408	0.019	17.253	0.007	16.789	0.013	16.590	0.012	16.510	0.022	D
2255-53565-557	16.543	0.013	15.042	0.003	14.412	0.009	14.148	0.013	14.020	0.012	D
2255-53565-559	16.340	0.011	14.741	0.014	14.097	0.034	13.791	0.026	13.653	0.012	D
2255-53565-586	15.981	0.009	14.521	0.009	13.885	0.025	13.713	0.014	13.600	0.008	D
2255-53565-589	16.818	0.007	15.287	0.004	14.667	0.010	14.416	0.008	14.261	0.036	D
2255-53565-597	17.690	0.021	16.411	0.006	15.888	0.019	15.665	0.009	15.560	0.012	D
M3											
2475-53845-105	16.941	0.011	15.834	0.008	15.555	0.004	15.473	0.008	15.438	0.009	D
2475-53845-114	16.871	0.009	15.706	0.008	15.275	0.018	15.116	0.005	15.055	0.009	D
2475-53845-116	16.909	0.022	15.109	0.014	14.395	0.012	14.112	0.012	13.967	0.018	C
2475-53845-118	18.722	0.028	17.492	0.015	17.007	0.012	16.807	0.013	16.735	0.020	C
2475-53845-119	17.405	0.012	16.003	0.004	15.395	0.003	15.160	0.006	15.043	0.009	D
2475-53845-120	17.560	0.012	16.254	0.005	15.679	0.005	15.472	0.008	15.341	0.008	D
2475-53845-141	17.085	0.019	15.471	0.022	14.795	0.017	14.531	0.017	14.411	0.016	C
2475-53845-142	17.014	0.011	15.427	0.014	14.755	0.004	14.479	0.005	14.348	0.009	D
2475-53845-143	17.070	0.009	15.621	0.010	14.990	0.008	14.713	0.012	14.621	0.009	D

Continued on next page...

Table A.3 – Continued

spSpec name	<i>u</i>	$\sigma(u)$	<i>g</i>	$\sigma(g)$	<i>r</i>	$\sigma(r)$	<i>i</i>	$\sigma(i)$	<i>z</i>	$\sigma(z)$	Tag
2475-53845-144	17.386	0.013	15.915	0.005	15.291	0.007	15.040	0.007	14.913	0.009	D
2475-53845-145	16.531	0.010	15.116	0.006	14.549	0.005	14.308	0.008	14.204	0.009	D
2475-53845-150	16.452	0.014	14.933	0.006	14.298	0.003	14.058	0.010	13.930	0.008	D
2475-53845-160	17.112	0.028	15.631	0.020	15.029	0.011	14.769	0.011	14.635	0.022	C
2475-53845-162	16.693	0.019	15.176	0.022	14.586	0.017	14.345	0.017	14.233	0.016	C
2475-53845-166	16.986	0.010	15.846	0.014	15.633	0.009	15.641	0.014	15.715	0.014	D
2475-53845-171	17.042	0.010	15.421	0.005	14.737	0.005	14.474	0.005	14.337	0.008	D
2475-53845-173	16.585	0.010	15.115	0.007	14.479	0.005	14.219	0.005	14.116	0.008	D
2475-53845-174	16.852	0.009	15.699	0.013	15.324	0.004	15.184	0.007	15.147	0.008	D
2475-53845-176	16.472	0.014	14.720	0.013	13.980	0.004	14.301	...	13.522	0.010	B
2475-53845-177	17.343	0.014	15.806	0.005	15.210	0.005	14.950	0.008	14.837	0.012	D
2475-53845-178	17.115	0.009	15.715	0.013	15.091	0.006	14.839	0.006	14.709	0.012	D
2475-53845-180	16.839	0.008	15.728	0.007	15.390	0.008	15.276	0.007	15.250	0.012	D
2475-53845-183	17.767	0.011	16.382	0.011	15.807	0.008	15.581	0.011	15.466	0.009	D
2475-53845-185	18.421	0.019	17.131	0.011	16.623	0.007	16.412	0.007	16.319	0.011	D
2475-53845-186	16.933	0.009	15.265	0.006	14.577	0.004	14.294	0.006	14.161	0.010	D
2475-53845-187	16.807	0.017	15.646	0.024	15.741	0.013	15.894	0.014	15.984	0.016	C
2475-53845-190	16.975	0.008	15.764	0.007	15.310	0.014	15.134	0.015	15.062	0.008	D
2475-53845-192	18.129	0.021	16.891	0.024	16.317	0.013	16.108	0.014	16.026	0.016	C
2475-53845-193	16.857	0.007	15.703	0.008	15.333	0.008	15.175	0.009	15.125	0.010	D
2475-53845-194	17.115	0.011	16.016	0.014	15.804	0.007	15.753	0.006	15.746	0.010	D
2475-53845-196	17.034	0.009	15.513	0.011	14.868	0.005	14.599	0.005	14.491	0.011	D
2475-53845-198	16.816	0.009	15.040	0.016	14.329	0.005	14.048	0.008	13.892	0.010	D

Continued on next page...

Table A.3 – Continued

spSpec name	<i>u</i>	$\sigma(u)$	<i>g</i>	$\sigma(g)$	<i>r</i>	$\sigma(r)$	<i>i</i>	$\sigma(i)$	<i>z</i>	$\sigma(z)$	Tag
2475-53845-199	16.500	0.006	14.936	0.010	14.303	0.008	14.049	0.006	13.943	0.011	D
2475-53845-200	18.499	0.018	17.238	0.009	16.730	0.008	16.527	0.010	16.440	0.011	D
2475-53845-421	16.575	0.014	14.656	0.014	13.901	0.018	13.575	0.001	13.403	0.014	C
2475-53845-430	18.656	0.024	17.342	0.024	16.819	0.020	16.612	0.010	16.518	0.019	C
2475-53845-436	16.803	0.007	14.956	0.011	14.232	0.007	13.924	0.008	13.762	0.009	D
2475-53845-440	16.833	0.011	15.039	0.010	14.353	0.011	14.061	0.006	13.886	0.010	D
2475-53845-461	16.962	0.008	15.477	0.009	14.836	0.012	14.561	0.029	14.444	0.011	D
2475-53845-462	16.742	0.008	15.592	0.004	15.366	0.009	15.322	0.008	15.290	0.009	D
2475-53845-463	16.565	0.007	15.139	0.008	14.561	0.009	14.323	0.004	14.219	0.010	D
2475-53845-466	16.875	0.009	15.360	0.012	14.710	0.013	14.443	0.005	14.314	0.007	D
2475-53845-469	17.969	0.012	16.634	0.007	16.106	0.007	15.877	0.007	15.779	0.009	D
2475-53845-471	16.601	0.008	15.103	0.005	14.527	0.014	14.294	0.014	14.189	0.006	D
2475-53845-473	16.792	0.010	14.981	0.005	14.300	0.013	14.542	...	13.824	0.013	B
2475-53845-475	17.107	0.010	15.547	0.004	14.911	0.007	14.653	0.007	14.527	0.007	D
2475-53845-476	16.900	0.008	15.664	0.005	15.211	0.005	15.020	0.008	14.953	0.005	D
2475-53845-479	16.440	0.010	14.984	0.012	14.381	0.012	14.129	0.012	14.013	0.009	D
2475-53845-480	17.009	0.010	15.350	0.007	14.712	0.009	14.433	0.011	14.296	0.010	D
2475-53845-481	17.059	0.010	15.886	0.006	15.567	0.016	15.462	0.011	15.440	0.007	D
2475-53845-483	16.500	0.011	14.470	0.010	13.717	0.015	13.971	...	13.138	0.012	B
2475-53845-485	16.821	0.010	15.558	0.011	15.740	0.004	15.886	0.010	15.991	0.013	D
2475-53845-486	16.463	0.014	14.507	0.014	13.938	0.001	13.383	0.001	13.216	0.014	C
2475-53845-487	18.982	0.020	17.760	0.006	17.274	0.008	17.077	0.010	16.984	0.018	D
2475-53845-488	17.130	0.008	15.680	0.005	15.078	0.010	14.826	0.004	14.720	0.013	D

Continued on next page...

Table A.3 – Continued

spSpec name	<i>u</i>	$\sigma(u)$	<i>g</i>	$\sigma(g)$	<i>r</i>	$\sigma(r)$	<i>i</i>	$\sigma(i)$	<i>z</i>	$\sigma(z)$	Tag
2475-53845-489	16.958	0.012	15.342	0.011	14.657	0.007	14.376	0.007	14.233	0.013	D
2475-53845-492	16.921	0.010	15.767	0.004	15.418	0.005	15.295	0.005	15.249	0.016	D
2475-53845-496	16.796	0.009	15.134	0.005	14.457	0.008	14.700	...	14.043	0.013	B
2475-53845-497	16.784	0.019	15.078	0.013	14.401	0.014	15.218	0.024	14.085	0.016	C
2475-53845-498	17.069	0.009	15.368	0.005	14.701	0.012	14.445	0.011	14.316	0.010	D
2475-53845-501	17.749	0.009	16.335	0.007	15.785	0.006	15.552	0.007	15.456	0.010	D
2475-53845-505	16.722	0.006	15.475	0.007	15.572	0.008	15.657	0.007	15.746	0.009	D
2475-53845-506	16.492	0.011	14.816	0.005	14.158	0.007	13.856	0.031	13.760	0.012	D
2475-53845-507	18.251	0.014	17.033	0.005	16.542	0.005	16.323	0.005	16.254	0.010	D
2475-53845-509	17.169	0.008	15.615	0.006	14.975	0.007	14.723	0.004	14.592	0.010	D
2475-53845-510	16.542	0.009	15.309	0.007	15.306	0.007	15.360	0.007	15.410	0.008	D
2475-53845-511	16.628	0.006	15.134	0.005	14.521	0.006	14.274	0.012	14.178	0.007	D
2475-53845-514	17.545	0.009	16.109	0.005	15.539	0.008	15.313	0.008	15.190	0.006	D
2475-53845-515	17.098	0.008	15.384	0.005	14.735	0.006	14.444	0.008	14.318	0.007	D
2475-53845-518	16.915	0.009	15.058	0.004	14.330	0.004	14.012	0.014	13.866	0.009	D
2475-53845-519	17.416	0.010	15.947	0.007	15.343	0.009	15.097	0.006	14.992	0.008	D
2475-53845-520	17.607	0.009	16.177	0.008	15.578	0.028	15.361	0.011	15.239	0.016	D
2475-53845-550	18.834	0.029	17.683	0.017	17.222	0.016	17.006	0.012	16.909	0.019	C
2475-53845-551	16.951	0.008	15.296	0.007	14.610	0.007	14.330	0.010	14.200	0.009	D
2475-53845-557	18.087	0.019	16.703	0.006	16.158	0.005	15.932	0.007	15.834	0.012	D
2475-53845-558	17.560	0.010	16.075	0.004	15.473	0.004	15.227	0.006	15.114	0.009	D
2475-53845-559	17.278	0.009	15.713	0.006	15.086	0.005	14.835	0.008	14.713	0.007	D

M71

Continued on next page...

Table A.3 – Continued

spSpec name	<i>u</i>	$\sigma(u)$	<i>g</i>	$\sigma(g)$	<i>r</i>	$\sigma(r)$	<i>i</i>	$\sigma(i)$	<i>z</i>	$\sigma(z)$	Tag
2333-53682-077	15.381	...	13.164	...	12.379	...	12.079	...	11.943	...	U
2333-53682-105	15.202	...	13.707	...	13.165	...	12.984	...	12.935	...	U
2333-53682-144	12.320	...	11.746	...	10.977	...	11.174	...	11.341	...	U
2333-53682-153	15.310	...	14.052	...	13.608	...	13.498	...	13.497	...	U
2333-53682-167	13.241	...	12.889	...	12.343	...	12.541	...	12.708	...	U
2333-53682-176	13.180	...	12.829	...	12.282	...	12.479	...	12.646	...	U
2333-53682-178	15.328	...	13.874	...	13.329	...	13.164	...	13.121	...	U
2333-53682-183	12.561	...	11.842	...	10.928	...	11.125	...	11.292	...	U
2333-53682-191	16.326	0.017	14.282	0.007	13.512	0.007	13.135	0.008	13.016	0.012	D
2333-53682-193	15.844	0.012	14.170	0.006	13.556	0.007	13.301	0.007	13.234	0.009	D
2333-53682-198	16.303	0.014	14.494	0.006	13.850	0.008	13.579	0.010	13.505	0.014	D
2333-53682-228	16.190	0.014	14.357	0.007	13.699	0.013	13.446	0.007	13.381	0.012	D
2333-53682-229	16.287	0.013	14.488	0.004	13.831	0.007	13.576	0.011	13.512	0.011	D
2338-53683-142	17.103	...	15.298	...	14.693	...	14.557	...	14.591	...	U
2338-53683-186	16.876	0.016	15.236	0.005	14.608	0.010	14.350	0.013	14.289	0.013	D
2338-53683-199	17.108	0.014	15.533	0.005	14.905	0.008	14.614	0.010	14.567	0.010	D
2338-53683-200	16.294	0.012	14.561	0.013	13.912	0.008	13.646	0.008	13.577	0.010	D

NGC 2420

2078-53378-111	18.285	0.014	17.058	0.006	16.656	0.010	16.547	0.007	16.502	0.012	D
2078-53378-114	17.894	0.016	16.719	0.005	16.382	0.009	16.282	0.009	16.278	0.009	D
2078-53378-116	19.954	0.047	18.342	0.009	17.712	0.011	17.518	0.010	17.369	0.019	D
2078-53378-118	19.602	0.034	18.035	0.008	17.469	0.011	17.296	0.008	17.193	0.015	D
2078-53378-142	18.476	0.015	17.193	0.006	16.778	0.015	16.654	0.010	16.618	0.012	D

Continued on next page...

Table A.3 – Continued

spSpec name	<i>u</i>	$\sigma(u)$	<i>g</i>	$\sigma(g)$	<i>r</i>	$\sigma(r)$	<i>i</i>	$\sigma(i)$	<i>z</i>	$\sigma(z)$	Tag
2078-53378-149	16.072	0.008	15.001	0.004	14.822	0.006	14.801	0.006	14.834	0.009	D
2078-53378-150	18.113	0.020	16.954	0.004	16.564	0.005	16.436	0.011	16.367	0.011	D
2078-53378-151	17.820	0.017	16.667	0.007	16.332	0.007	16.240	0.007	16.238	0.011	D
2078-53378-152	19.670	0.037	18.089	0.007	17.462	0.011	17.239	0.008	17.115	0.018	D
2078-53378-154	19.401	0.028	17.901	0.006	17.369	0.014	17.197	0.010	17.100	0.016	D
2078-53378-156	17.881	0.011	16.746	0.006	16.401	0.011	16.294	0.008	16.282	0.010	D
2078-53378-157	18.285	0.017	17.055	0.005	16.670	0.009	16.568	0.007	16.528	0.012	D
2078-53378-158	19.477	0.029	17.957	0.007	17.353	0.013	17.132	0.010	17.039	0.015	D
2078-53378-159	16.291	0.008	15.227	0.005	15.048	0.010	15.019	0.005	15.054	0.008	D
2078-53378-161	16.078	0.013	14.986	0.004	14.784	0.006	14.753	0.005	14.792	0.008	D
2078-53378-165	19.862	0.044	18.232	0.009	17.645	0.011	17.452	0.009	17.386	0.021	D
2078-53378-166	16.719	0.009	15.652	0.004	15.424	0.007	15.369	0.007	15.392	0.008	D
2078-53378-167	18.119	0.014	16.953	0.005	16.578	0.008	16.461	0.009	16.446	0.011	D
2078-53378-168	16.792	0.017	15.747	0.005	15.514	0.018	15.467	0.009	15.509	0.012	D
2078-53378-169	15.538	0.016	14.487	0.012	14.284	0.008	14.258	0.009	14.328	0.015	C
2078-53378-170	20.146	0.047	18.464	0.008	17.825	0.009	17.603	0.009	17.471	0.020	D
2078-53378-171	18.767	0.025	17.451	0.009	17.006	0.008	16.852	0.009	16.798	0.012	D
2078-53378-172	18.631	0.020	17.336	0.006	16.895	0.009	16.754	0.008	16.736	0.011	D
2078-53378-173	20.033	0.053	18.364	0.009	17.713	0.010	17.504	0.015	17.421	0.020	D
2078-53378-174	19.384	0.030	17.904	0.007	17.369	0.008	17.183	0.010	17.131	0.019	D
2078-53378-175	19.477	0.031	17.928	0.009	17.376	0.008	17.210	0.012	17.140	0.014	D
2078-53378-176	15.988	0.007	14.933	0.006	14.746	0.011	14.713	0.006	14.769	0.010	D
2078-53378-177	19.205	0.023	17.765	0.010	17.263	0.008	17.113	0.015	17.051	0.015	D

Continued on next page...

Table A.3 – Continued

spSpec name	<i>u</i>	$\sigma(u)$	<i>g</i>	$\sigma(g)$	<i>r</i>	$\sigma(r)$	<i>i</i>	$\sigma(i)$	<i>z</i>	$\sigma(z)$	Tag
2078-53378-178	19.721	0.030	18.145	0.009	17.552	0.012	17.358	0.011	17.292	0.022	D
2078-53378-179	16.244	0.005	15.179	0.017	15.001	0.004	14.969	0.021	15.015	0.029	D
2078-53378-182	15.898	0.009	14.824	0.004	14.654	0.016	14.639	0.007	14.679	0.007	D
2078-53378-186	16.134	0.017	15.137	0.006	14.988	0.006	14.951	0.019	14.962	0.012	D
2078-53378-192	18.291	0.019	17.111	0.006	16.727	0.007	16.612	0.018	16.558	0.015	D
2078-53378-194	19.010	0.029	17.654	0.006	17.178	0.011	17.019	0.014	16.946	0.014	D
2078-53378-195	16.446	0.021	15.411	0.006	15.235	0.011	15.195	0.028	15.211	0.012	D
2078-53378-197	18.304	0.013	17.124	0.012	16.711	0.006	16.590	0.025	16.564	0.011	D
2078-53378-199	16.988	0.010	15.905	0.012	15.658	0.018	15.591	0.008	15.601	0.013	D
2078-53378-200	19.574	0.047	17.997	0.006	17.446	0.006	17.220	0.011	17.123	0.018	D
2078-53378-223	16.951	0.019	15.876	0.007	15.636	0.023	15.544	0.040	15.581	0.016	D
2078-53378-224	15.774	0.016	14.716	0.003	14.560	0.012	14.518	0.009	14.546	0.014	D
2078-53378-227	18.129	0.029	16.910	0.008	16.555	0.023	16.436	0.039	16.405	0.018	D
2078-53378-232	16.210	0.010	15.171	0.015	15.008	0.057	14.957	0.037	15.005	0.026	D
2078-53378-233	17.864	0.018	16.699	0.008	16.367	0.021	16.241	0.042	16.244	0.019	D
2078-53378-235	18.448	0.020	17.230	0.005	16.825	0.008	16.670	0.015	16.630	0.017	D
2078-53378-273	17.996	0.022	16.812	0.010	16.446	0.007	16.360	0.018	16.318	0.017	C
2078-53378-422	19.200	0.034	17.742	0.007	17.270	0.007	17.078	0.011	17.028	0.014	D
2078-53378-427	18.177	0.022	16.962	0.013	16.597	0.009	16.451	0.011	16.488	0.023	C
2078-53378-431	15.731	0.006	14.641	0.012	14.468	0.011	14.448	0.026	14.450	0.012	D
2078-53378-435	19.165	0.022	17.731	0.006	17.246	0.006	17.067	0.012	17.011	0.018	D
2078-53378-440	18.726	0.020	17.465	0.006	17.027	0.006	16.879	0.016	16.844	0.014	D
2078-53378-462	17.379	0.010	16.297	0.007	16.007	0.005	15.912	0.007	15.908	0.021	D

Continued on next page...

Table A.3 – Continued

spSpec name	<i>u</i>	$\sigma(u)$	<i>g</i>	$\sigma(g)$	<i>r</i>	$\sigma(r)$	<i>i</i>	$\sigma(i)$	<i>z</i>	$\sigma(z)$	Tag
2078-53378-463	16.519	0.007	15.459	0.006	15.248	0.004	15.205	0.009	15.222	0.015	D
2078-53378-464	18.041	0.020	16.870	0.011	16.502	0.008	16.381	0.011	16.378	0.016	C
2078-53378-465	18.867	0.027	17.525	0.008	17.046	0.008	16.866	0.014	16.825	0.019	D
2078-53378-466	16.199	0.023	15.113	0.008	14.922	0.005	14.874	0.019	14.895	0.010	D
2078-53378-468	18.748	0.020	17.467	0.010	17.006	0.011	16.877	0.016	16.816	0.011	D
2078-53378-469	15.552	0.008	14.454	0.014	14.234	0.010	14.196	0.029	14.224	0.007	D
2078-53378-470	18.506	0.016	17.224	0.006	16.797	0.009	16.668	0.010	16.619	0.017	D
2078-53378-471	17.394	0.010	16.330	0.013	16.044	0.007	15.972	0.031	15.981	0.013	D
2078-53378-472	15.683	0.006	14.620	0.012	14.441	0.011	14.418	0.016	14.455	0.007	D
2078-53378-473	17.624	0.012	16.522	0.012	16.206	0.007	16.131	0.021	16.122	0.011	D
2078-53378-475	19.854	0.040	18.217	0.014	17.606	0.013	17.410	0.022	17.290	0.020	D
2078-53378-476	19.354	0.025	17.913	0.018	17.377	0.011	17.228	0.021	17.120	0.016	D
2078-53378-477	18.352	0.015	17.128	0.010	16.709	0.012	16.597	0.024	16.547	0.014	D
2078-53378-478	19.046	0.024	17.636	0.012	17.157	0.009	17.012	0.017	16.945	0.018	D
2078-53378-480	18.496	0.018	17.263	0.008	16.837	0.011	16.706	0.013	16.670	0.017	D
2078-53378-481	17.208	0.009	16.128	0.005	15.840	0.010	15.770	0.010	15.793	0.013	D
2078-53378-485	17.972	0.012	16.804	0.007	16.415	0.006	16.313	0.009	16.280	0.014	D
2078-53378-491	15.909	0.005	14.848	0.007	14.636	0.011	14.586	0.007	14.625	0.007	D
2078-53378-492	18.044	0.014	16.881	0.009	16.501	0.007	16.404	0.012	16.372	0.016	D
2078-53378-493	19.249	0.022	17.777	0.009	17.256	0.011	17.108	0.024	17.030	0.023	D
2078-53378-496	18.088	0.014	16.899	0.009	16.520	0.012	16.410	0.019	16.373	0.014	D
2078-53378-499	18.403	0.017	17.177	0.007	16.766	0.008	16.651	0.015	16.615	0.017	D
2078-53378-503	15.718	0.026	14.633	0.008	14.447	0.009	14.424	0.023	14.464	0.009	D

Continued on next page...

Table A.3 – Continued

spSpec name	<i>u</i>	$\sigma(u)$	<i>g</i>	$\sigma(g)$	<i>r</i>	$\sigma(r)$	<i>i</i>	$\sigma(i)$	<i>z</i>	$\sigma(z)$	Tag
2078-53378-510	18.154	0.017	16.959	0.007	16.543	0.009	16.402	0.014	16.374	0.016	D
2078-53378-511	16.249	0.006	15.197	0.007	15.014	0.010	14.990	0.008	15.030	0.012	D
2078-53378-512	16.658	0.010	15.613	0.006	15.391	0.005	15.350	0.008	15.365	0.018	D
2078-53378-513	17.649	0.010	16.556	0.004	16.230	0.010	16.144	0.008	16.129	0.018	D
2078-53378-514	17.970	0.013	16.826	0.005	16.470	0.010	16.378	0.009	16.332	0.011	D
2078-53378-515	17.690	0.012	16.601	0.006	16.260	0.006	16.186	0.012	16.178	0.015	D
2078-53378-516	17.284	0.010	16.206	0.007	15.930	0.008	15.872	0.008	15.877	0.016	D
2078-53378-517	18.803	0.024	17.503	0.007	17.018	0.007	16.888	0.015	16.853	0.015	D
2078-53378-518	16.676	0.018	15.646	0.012	15.428	0.011	15.386	0.020	15.418	0.008	D
2078-53378-519	18.410	0.021	17.195	0.008	16.740	0.010	16.603	0.011	16.551	0.015	D
2078-53378-520	17.598	0.011	16.516	0.011	16.182	0.009	16.094	0.010	16.110	0.017	D
2078-53378-548	15.872	0.029	14.795	0.009	14.640	0.013	14.597	0.037	14.667	0.011	D
2078-53378-552	20.133	0.058	18.385	0.010	17.765	0.011	17.553	0.009	17.485	0.018	D
2078-53378-553	19.647	0.041	18.024	0.011	17.449	0.009	17.281	0.017	17.206	0.015	D
2078-53378-554	15.887	0.026	14.846	0.005	14.671	0.008	14.655	0.023	14.703	0.017	D
2078-53378-557	17.041	0.010	15.961	0.005	15.704	0.007	15.645	0.009	15.662	0.012	D
2078-53378-560	18.421	0.013	17.180	0.005	16.775	0.007	16.656	0.010	16.631	0.017	D
2079-53379-071	20.474	0.079	18.720	0.011	18.023	0.008	17.804	0.014	17.697	0.021	C
2079-53379-076	20.400	0.069	18.538	0.009	17.890	0.009	17.653	0.010	17.604	0.022	D
2079-53379-101	22.055	0.287	19.568	0.019	18.651	0.013	18.325	0.014	18.117	0.025	D
2079-53379-102	21.751	0.236	19.528	0.023	18.559	0.017	18.264	0.015	18.142	0.026	C
2079-53379-108	21.995	0.322	19.996	0.019	18.920	0.016	18.552	0.017	18.318	0.033	D
2079-53379-113	21.762	0.278	20.121	0.026	19.046	0.016	18.658	0.015	18.463	0.036	D

Continued on next page...

Table A.3 – Continued

spSpec name	<i>u</i>	$\sigma(u)$	<i>g</i>	$\sigma(g)$	<i>r</i>	$\sigma(r)$	<i>i</i>	$\sigma(i)$	<i>z</i>	$\sigma(z)$	Tag
2079-53379-114	21.304	0.158	19.352	0.014	18.539	0.010	18.248	0.015	18.087	0.025	C
2079-53379-119	21.975	0.252	19.827	0.021	18.801	0.017	18.416	0.013	18.221	0.034	D
2079-53379-141	21.723	0.223	19.287	0.012	18.432	0.012	18.127	0.012	17.978	0.030	D
2079-53379-148	21.201	0.120	19.189	0.014	18.354	0.015	18.069	0.014	17.906	0.029	D
2079-53379-149	20.913	0.094	18.897	0.012	18.158	0.013	17.920	0.014	17.772	0.027	D
2079-53379-152	21.228	0.151	19.230	0.012	18.378	0.012	18.106	0.013	17.931	0.030	D
2079-53379-153	22.148	0.247	19.706	0.018	18.718	0.016	18.363	0.017	18.157	0.030	D
2079-53379-156	20.567	0.060	18.689	0.009	18.005	0.013	17.767	0.011	17.664	0.023	D
2079-53379-157	21.765	0.213	19.586	0.018	18.619	0.015	18.309	0.014	18.137	0.026	D
2079-53379-158	21.441	0.172	19.448	0.015	18.560	0.014	18.262	0.013	18.097	0.029	D
2079-53379-159	21.293	0.115	19.313	0.012	18.458	0.011	18.160	0.012	17.942	0.033	D
2079-53379-160	21.188	0.121	19.128	0.015	18.318	0.009	18.033	0.014	17.888	0.031	D
2079-53379-161	22.006	0.278	19.789	0.018	18.788	0.012	18.437	0.012	18.316	0.038	D
2079-53379-162	20.433	0.052	18.675	0.010	17.956	0.009	17.754	0.009	17.658	0.026	D
2079-53379-163	21.454	0.175	19.244	0.012	18.413	0.015	18.102	0.012	17.901	0.025	D
2079-53379-164	20.852	0.101	18.993	0.011	18.233	0.008	17.935	0.014	17.764	0.022	D
2079-53379-165	22.042	0.289	19.688	0.019	18.725	0.013	18.335	0.012	18.203	0.036	D
2079-53379-166	20.572	0.103	18.659	0.008	17.982	0.009	17.727	0.009	17.618	0.019	D
2079-53379-167	22.146	0.307	20.160	0.024	19.042	0.017	18.649	0.015	18.463	0.044	D
2079-53379-168	22.278	0.240	19.706	0.018	18.748	0.011	18.436	0.015	18.214	0.036	D
2079-53379-169	20.879	0.106	18.811	0.011	18.113	0.008	17.852	0.010	17.711	0.019	D
2079-53379-178	20.491	0.076	18.672	0.012	17.993	0.013	17.749	0.010	17.640	0.019	D
2079-53379-181	15.898	0.009	14.824	0.004	14.654	0.016	14.639	0.007	14.679	0.007	D

Continued on next page...

Table A.3 – Continued

spSpec name	<i>u</i>	$\sigma(u)$	<i>g</i>	$\sigma(g)$	<i>r</i>	$\sigma(r)$	<i>i</i>	$\sigma(i)$	<i>z</i>	$\sigma(z)$	Tag
2079-53379-182	21.060	0.115	19.132	0.016	18.339	0.011	18.046	0.011	17.872	0.024	C
2079-53379-185	22.199	0.376	20.251	0.023	19.079	0.024	18.676	0.016	18.410	0.042	D
2079-53379-191	21.245	0.153	19.149	0.011	18.370	0.010	18.051	0.015	17.942	0.028	D
2079-53379-192	20.564	0.068	18.734	0.010	18.005	0.019	17.784	0.011	17.687	0.023	D
2079-53379-194	20.283	0.062	18.536	0.011	17.878	0.023	17.637	0.010	17.553	0.022	D
2079-53379-195	20.808	0.095	18.905	0.013	18.162	0.020	17.907	0.012	17.721	0.027	D
2079-53379-196	21.896	0.258	19.651	0.017	18.691	0.012	18.370	0.014	18.210	0.033	D
2079-53379-198	20.236	0.053	18.581	0.008	17.927	0.008	17.687	0.011	17.575	0.022	D
2079-53379-199	22.046	0.259	19.754	0.019	18.760	0.012	18.419	0.019	18.171	0.029	D
2079-53379-200	20.892	0.111	19.068	0.011	18.285	0.010	18.002	0.015	17.865	0.023	D
2079-53379-234	21.922	0.264	19.413	0.012	18.533	0.013	18.198	0.014	18.049	0.031	D
2079-53379-237	21.110	0.119	19.177	0.013	18.376	0.015	18.063	0.026	17.904	0.024	D
2079-53379-238	20.833	0.089	18.801	0.011	18.099	0.014	17.857	0.026	17.692	0.020	D
2079-53379-270	20.739	0.075	18.861	0.024	18.079	0.053	17.780	0.040	17.648	0.037	D
2079-53379-431	20.622	0.095	18.836	0.013	18.068	0.009	17.784	0.019	17.711	0.024	C
2079-53379-434	20.945	0.108	18.933	0.012	18.152	0.011	17.825	0.013	17.722	0.024	D
2079-53379-440	22.059	0.323	19.483	0.016	18.569	0.011	18.217	0.019	18.094	0.030	C
2079-53379-463	23.338	0.904	20.209	0.025	19.099	0.016	18.687	0.016	18.448	0.039	C
2079-53379-466	21.983	0.296	19.497	0.015	18.587	0.014	18.292	0.028	18.160	0.029	D
2079-53379-467	21.096	0.152	18.954	0.010	18.182	0.011	17.875	0.023	17.732	0.026	D
2079-53379-474	21.679	0.151	19.677	0.022	18.687	0.015	18.304	0.019	18.047	0.027	D
2079-53379-476	21.927	0.232	19.769	0.026	18.800	0.015	18.444	0.019	18.290	0.032	D
2079-53379-477	21.096	0.105	18.939	0.012	18.171	0.011	17.937	0.020	17.791	0.025	D

Continued on next page...

Table A.3 – Continued

spSpec name	<i>u</i>	$\sigma(u)$	<i>g</i>	$\sigma(g)$	<i>r</i>	$\sigma(r)$	<i>i</i>	$\sigma(i)$	<i>z</i>	$\sigma(z)$	Tag
2079-53379-480	21.208	0.104	19.076	0.017	18.272	0.009	17.965	0.019	17.813	0.021	D
2079-53379-482	21.370	0.141	19.429	0.015	18.500	0.013	18.124	0.012	17.907	0.022	D
2079-53379-483	15.683	0.006	14.620	0.012	14.441	0.011	14.418	0.016	14.455	0.007	D
2079-53379-487	21.607	0.163	19.438	0.013	18.509	0.013	18.209	0.015	18.048	0.027	D
2079-53379-488	22.407	0.294	20.287	0.031	19.151	0.015	18.763	0.017	18.476	0.038	D
2079-53379-490	22.384	0.333	19.758	0.020	18.755	0.011	18.431	0.014	18.236	0.030	D
2079-53379-493	22.119	0.235	19.970	0.020	18.919	0.016	18.551	0.021	18.329	0.030	D
2079-53379-495	20.975	0.084	18.914	0.011	18.176	0.011	17.931	0.021	17.810	0.021	D
2079-53379-496	20.457	0.069	18.674	0.013	17.945	0.024	17.748	0.018	17.651	0.022	D
2079-53379-498	20.891	0.093	18.977	0.013	18.219	0.012	17.963	0.010	17.800	0.022	D
2079-53379-500	21.368	0.145	19.214	0.014	18.393	0.012	18.110	0.019	17.931	0.033	D
2079-53379-502	21.184	0.115	19.101	0.015	18.299	0.010	18.017	0.020	17.873	0.024	D
2079-53379-507	21.398	0.142	19.348	0.014	18.486	0.013	18.170	0.017	18.107	0.031	D
2079-53379-510	22.837	0.525	20.376	0.024	19.191	0.014	18.802	0.027	18.555	0.037	D
2079-53379-511	20.814	0.101	18.978	0.013	18.211	0.011	17.933	0.021	17.829	0.025	D
2079-53379-512	20.161	0.062	18.507	0.010	17.850	0.011	17.631	0.019	17.525	0.015	D
2079-53379-514	22.047	0.232	19.953	0.021	18.930	0.017	18.538	0.016	18.330	0.032	D
2079-53379-516	20.717	0.074	18.760	0.012	18.042	0.010	17.759	0.032	17.697	0.022	D
2079-53379-519	21.190	0.112	19.198	0.013	18.381	0.010	18.082	0.021	17.932	0.023	D
2079-53379-552	21.393	0.154	19.407	0.015	18.530	0.013	18.234	0.014	18.085	0.029	D
2079-53379-558	20.244	0.058	18.566	0.017	17.884	0.014	17.668	0.031	17.589	0.025	D

NGC 2158

2887-54521-416 16.282 0.024 14.296 0.012 13.506 0.008 13.156 0.007 13.056 0.015 C

Continued on next page...

Table A.3 – Continued

spSpec name	<i>u</i>	$\sigma(u)$	<i>g</i>	$\sigma(g)$	<i>r</i>	$\sigma(r)$	<i>i</i>	$\sigma(i)$	<i>z</i>	$\sigma(z)$	Tag
2887-54521-442	16.025	0.020	15.023	0.005	14.648	0.007	14.572	0.007	14.568	0.012	C
2887-54521-445	15.721	...	15.321	...	14.909	...	15.702	...	15.969	...	B
2887-54521-446	16.164	0.025	15.135	0.007	14.979	0.010	14.916	0.009	14.951	0.016	C
2887-54521-447	15.997	0.020	14.192	0.019	13.437	0.016	15.498	0.089	13.071	0.015	C
2887-54521-451	15.782	0.019	14.809	0.005	14.602	0.007	14.616	0.007	14.658	0.012	C
2887-54521-452	16.017	0.023	15.098	0.008	14.668	0.007	14.609	0.007	14.623	0.013	C
2887-54521-460	16.112	...	15.711	...	15.420	...	16.213	...	16.480	...	B
2887-54521-511	15.952	...	15.551	...	15.030	...	15.823	...	16.090	...	B
2887-54521-531	15.761	0.023	13.912	0.007	13.318	0.008	13.069	0.006	12.978	0.015	C
2887-54521-532	15.808	0.019	13.818	0.005	13.033	0.007	15.253	0.010	12.656	0.012	C
2887-54521-547	15.667	0.019	14.036	0.005	13.279	0.007	15.157	0.009	12.933	0.012	C
2887-54521-552	16.300	0.022	14.450	0.005	13.636	0.007	15.007	0.009	13.235	0.012	C
2887-54521-559	16.438	0.023	14.711	0.005	13.861	0.007	14.448	0.011	13.452	0.012	C
2912-54499-409	17.219	0.033	16.096	0.008	15.818	0.008	15.730	0.006	15.755	0.016	C
2912-54499-416	17.231	0.034	16.068	0.016	15.912	0.019	15.847	0.007	15.883	0.017	C
2912-54499-417	17.411	0.036	16.393	0.008	16.183	0.008	16.096	0.007	16.176	0.017	C
2912-54499-442	16.790	0.027	15.875	0.013	15.620	0.030	15.648	0.082	15.700	0.015	C
2912-54499-444	16.719	0.026	15.777	0.007	15.692	0.008	15.724	0.009	15.810	0.016	C
2912-54499-445	16.825	0.029	15.852	0.007	15.754	0.008	15.732	0.006	15.795	0.016	C
2912-54499-446	17.804	0.046	16.870	0.009	16.608	0.008	16.586	0.008	16.649	0.018	C
2912-54499-450	16.321	0.025	15.327	0.007	15.234	0.008	15.193	0.006	15.264	0.015	C
2912-54499-453	17.123	...	16.722	...	16.400	...	17.192	...	17.460	...	B
2912-54499-458	16.725	0.026	15.716	0.006	15.580	0.007	15.578	0.007	15.651	0.013	C

Continued on next page...

Table A.3 – Continued

spSpec name	<i>u</i>	$\sigma(u)$	<i>g</i>	$\sigma(g)$	<i>r</i>	$\sigma(r)$	<i>i</i>	$\sigma(i)$	<i>z</i>	$\sigma(z)$	Tag
2912-54499-459	18.930	0.237	16.882	0.010	16.710	0.012	16.542	0.011	16.494	0.018	C
2912-54499-461	17.674	0.051	16.613	0.027	16.241	0.025	16.143	0.026	16.150	0.028	C
2912-54499-462	17.603	...	17.202	...	16.710	...	17.503	...	17.769	...	B
2912-54499-483	16.563	...	16.162	...	15.810	...	16.603	...	16.869	...	B
2912-54499-484	16.710	...	16.310	...	15.959	...	16.752	...	17.019	...	B
2912-54499-488	17.353	0.034	16.269	0.013	15.983	0.009	15.820	0.008	15.896	0.017	C
2912-54499-489	16.779	...	16.379	...	15.998	...	16.791	...	17.058	...	B
2912-54499-499	17.341	...	16.941	...	16.479	...	17.272	...	17.539	...	B
2912-54499-501	17.793	...	17.392	...	17.040	...	17.833	...	18.100	...	B
2912-54499-502	17.143	...	16.742	...	16.471	...	17.264	...	17.531	...	B
2912-54499-503	16.810	...	16.409	...	16.089	...	16.881	...	17.149	...	B
2912-54499-505	16.861	...	16.461	...	16.199	...	16.992	...	17.259	...	B
2912-54499-506	18.350	...	17.950	...	17.549	...	18.341	...	18.609	...	B
2912-54499-507	16.863	...	16.462	...	16.189	...	16.982	...	17.248	...	B
2912-54499-509	16.821	...	16.420	...	16.069	...	16.863	...	17.130	...	B
2912-54499-510	17.751	...	17.351	...	16.889	...	17.682	...	17.949	...	B
2912-54499-511	17.669	...	17.269	...	16.768	...	17.561	...	17.828	...	B
2912-54499-514	16.733	...	16.331	...	15.950	...	16.743	...	17.010	...	B
2912-54499-515	17.174	...	16.772	...	16.420	...	17.213	...	17.479	...	B
2912-54499-516	16.831	...	16.431	...	16.059	...	16.852	...	17.119	...	B
2912-54499-518	17.250	...	16.850	...	16.509	...	17.302	...	17.569	...	B
2912-54499-519	17.595	...	17.193	...	16.851	...	17.644	...	17.910	...	B
2912-54499-531	17.091	0.031	16.252	0.007	16.068	0.008	16.101	0.008	16.185	0.016	C

Continued on next page...

Table A.3 – Continued

spSpec name	<i>u</i>	$\sigma(u)$	<i>g</i>	$\sigma(g)$	<i>r</i>	$\sigma(r)$	<i>i</i>	$\sigma(i)$	<i>z</i>	$\sigma(z)$	Tag
2912-54499-534	18.393	0.072	17.488	0.010	17.107	0.009	17.031	0.009	17.058	0.021	C
2912-54499-539	17.653	0.043	16.770	0.008	16.530	0.008	16.525	0.008	16.570	0.017	C
2912-54499-540	17.803	0.048	16.963	0.008	16.669	0.010	16.636	0.012	16.709	0.022	C
2912-54499-542	16.305	0.022	15.386	0.016	15.098	0.020	15.060	0.007	15.074	0.013	C
2912-54499-543	17.404	...	17.003	...	16.620	...	17.412	...	17.679	...	B
2912-54499-544	18.191	...	17.790	...	17.339	...	18.132	...	18.399	...	B
2912-54499-545	16.690	...	16.290	...	16.019	...	16.812	...	17.079	...	B
2912-54499-547	17.780	...	17.380	...	16.999	...	17.792	...	18.060	...	B
2912-54499-549	16.893	...	16.492	...	16.180	...	16.972	...	17.239	...	B
2912-54499-552	16.443	...	16.042	...	15.730	...	16.522	...	16.789	...	B
2912-54499-553	17.423	...	17.021	...	16.670	...	17.462	...	17.729	...	B
2912-54499-556	16.560	...	16.160	...	15.839	...	16.632	...	16.900	...	B
2912-54499-558	16.741	0.026	15.915	0.006	15.600	0.007	15.591	0.007	15.652	0.014	C
2912-54499-559	17.750	0.045	16.870	0.008	16.545	0.008	16.497	0.008	16.517	0.017	C
2912-54499-560	17.742	...	17.341	...	16.870	...	17.662	...	17.929	...	B
M35											
2887-54521-528	15.182	0.014	14.084	0.008	13.603	0.001	13.548	0.008	13.533	0.012	C
2887-54521-534	13.998	0.013	13.012	0.008	12.769	0.002	12.762	0.001	12.873	0.012	C
2887-54521-561	14.391	0.013	13.412	0.008	13.043	0.001	13.049	0.008	13.094	0.012	C
2887-54521-562	14.114	0.014	13.069	0.008	12.840	0.001	12.807	0.001	12.889	0.014	C
2887-54521-566	14.710	0.014	13.612	0.008	13.191	0.001	13.148	0.008	13.157	0.012	C
2887-54521-571	14.659	0.012	13.647	0.010	13.362	0.011	15.795	0.010	13.318	0.010	C
2887-54521-574	15.553	0.013	14.400	0.010	13.999	0.011	13.836	0.001	13.872	0.011	C

Continued on next page...

Table A.3 – Continued

spSpec name	<i>u</i>	$\sigma(u)$	<i>g</i>	$\sigma(g)$	<i>r</i>	$\sigma(r)$	<i>i</i>	$\sigma(i)$	<i>z</i>	$\sigma(z)$	Tag
2887-54521-575	15.085	0.013	13.977	0.010	13.621	0.011	15.741	0.025	13.501	0.011	C
2887-54521-576	14.787	0.012	13.770	0.010	13.466	0.011	16.380	0.014	13.413	0.010	C
2887-54521-577	14.785	0.219	13.682	0.014	13.379	0.010	15.369	0.178	13.366	0.118	C
2887-54521-580	15.594	0.013	14.412	0.010	14.006	0.011	16.271	0.088	13.842	0.011	C
2887-54521-602	15.126	0.013	14.009	0.010	13.680	0.011	16.041	0.014	13.574	0.010	C
2887-54521-604	15.425	0.014	14.271	0.009	13.874	0.006	16.108	0.015	13.751	0.013	C
2887-54521-606	15.303	0.014	14.134	0.009	13.802	0.006	16.146	0.017	13.669	0.013	C
2887-54521-608	14.904	0.013	13.800	0.010	13.517	0.011	15.227	0.010	13.461	0.010	C
2887-54521-611	14.520	0.013	13.452	0.009	13.163	0.001	13.111	0.001	13.178	0.013	C
2887-54521-616	15.370	0.013	14.226	0.010	13.856	0.011	15.514	0.016	13.729	0.011	C
2887-54521-620	15.638	0.014	14.414	0.009	14.006	0.006	15.972	0.021	13.824	0.013	C
2912-54499-524	20.207	0.094	17.847	0.011	16.717	0.006	16.306	0.010	16.061	0.016	C
2912-54499-563	19.271	0.056	17.114	0.123	16.199	0.162	15.899	0.141	15.983	0.209	C
2912-54499-564	19.953	0.077	17.492	0.013	16.364	0.010	15.970	0.012	15.728	0.015	C
2912-54499-575	20.797	0.189	17.994	0.009	16.848	0.007	16.429	0.008	16.218	0.012	C
2912-54499-576	18.894	0.036	16.985	0.009	16.133	0.007	15.759	0.010	15.617	0.015	C
2912-54499-601	19.290	0.048	17.370	0.010	16.411	0.008	16.028	0.010	15.876	0.015	C
2912-54499-604	20.451	1.916	18.978	0.014	17.578	0.010	17.018	0.010	16.693	0.015	D
2912-54499-605	19.114	0.064	16.940	0.008	16.002	0.009	15.655	0.007	15.428	0.010	D
2912-54499-611	18.502	0.029	16.452	0.008	15.559	0.005	15.259	0.005	15.098	0.012	D
2912-54499-619	19.207	0.049	16.977	0.009	16.026	0.006	15.718	0.009	15.546	0.013	D
2912-54499-620	20.183	0.094	17.863	0.015	16.776	0.007	16.347	0.009	16.078	0.019	C

M67

Continued on next page...

Table A.3 – Continued

spSpec name	<i>u</i>	$\sigma(u)$	<i>g</i>	$\sigma(g)$	<i>r</i>	$\sigma(r)$	<i>i</i>	$\sigma(i)$	<i>z</i>	$\sigma(z)$	Tag
2667-54142-361	16.832	0.009	15.218	0.004	14.655	0.008	14.442	0.008	14.354	0.013	D
2667-54142-363	16.776	0.022	15.270	0.014	14.749	0.016	14.567	0.011	14.565	0.013	C
2667-54142-364	15.551	0.021	14.316	0.014	13.926	0.016	13.774	0.011	13.786	0.013	C
2667-54142-372	17.164	0.011	15.549	0.005	14.963	0.007	14.804	0.010	14.756	0.015	D
2667-54142-378	18.069	0.026	16.114	0.005	15.397	0.039	15.181	0.008	15.087	0.027	D
2667-54142-379	15.947	0.012	14.663	0.017	14.227	0.011	14.128	0.016	14.083	0.016	C
2667-54142-402	16.821	0.022	15.304	0.014	14.788	0.016	14.581	0.011	14.528	0.013	C
2667-54142-404	16.397	0.006	14.959	0.008	14.480	0.006	14.356	0.006	14.306	0.008	D
2667-54142-406	15.433	0.021	14.199	0.006	13.820	0.034	13.718	0.010	13.725	0.025	D
2667-54142-407	15.463	0.004	14.216	0.008	13.848	0.010	13.749	0.005	13.745	0.009	D
2667-54142-408	15.646	0.012	14.363	0.007	13.974	0.003	13.848	0.004	13.809	0.007	D
2667-54142-409	16.769	0.007	15.246	0.007	14.732	0.005	14.587	0.007	14.526	0.007	D
2667-54142-410	16.603	0.010	15.149	0.002	14.642	0.006	14.495	0.006	14.456	0.011	D
2667-54142-411	16.901	0.016	15.346	0.009	14.811	0.008	14.632	0.010	14.545	0.026	D
2667-54142-412	16.177	0.007	14.804	0.005	14.356	0.008	14.226	0.005	14.201	0.007	D
2667-54142-413	15.460	0.009	14.232	0.022	13.766	0.008	13.598	0.012	13.601	0.008	C
2667-54142-414	18.984	0.023	16.814	0.007	15.939	0.005	15.672	0.021	15.507	0.027	D
2667-54142-415	16.042	0.009	14.687	0.005	14.244	0.006	14.116	0.009	14.081	0.010	D
2667-54142-417	16.634	0.009	15.122	0.004	14.607	0.007	14.455	0.006	14.403	0.010	D
2667-54142-418	16.152	0.011	14.777	0.005	14.347	0.018	14.218	0.007	14.191	0.020	D
2667-54142-419	15.951	0.006	14.639	0.004	14.221	0.005	14.092	0.004	14.074	0.006	D
2667-54142-420	16.023	0.007	14.703	0.009	14.266	0.010	14.130	0.006	14.091	0.010	D
2667-54142-429	15.760	0.014	14.484	0.018	14.134	0.013	13.964	0.016	13.967	0.014	C

Continued on next page...

Table A.3 – Continued

spSpec name	<i>u</i>	$\sigma(u)$	<i>g</i>	$\sigma(g)$	<i>r</i>	$\sigma(r)$	<i>i</i>	$\sigma(i)$	<i>z</i>	$\sigma(z)$	Tag
2667-54142-441	15.887	0.006	14.581	0.003	14.166	0.015	14.030	0.011	14.015	0.009	D
2667-54142-444	15.495	0.012	14.225	0.006	13.854	0.011	13.741	0.012	13.758	0.008	D
2667-54142-445	16.341	0.008	14.920	0.002	14.449	0.013	14.305	0.011	14.278	0.010	D
2667-54142-451	15.531	0.004	14.269	0.004	13.885	0.013	13.768	0.009	13.768	0.005	D
2667-54142-452	18.454	0.024	16.433	0.016	15.656	0.015	15.441	0.014	15.317	0.021	C
2667-54142-453	17.862	0.023	16.006	0.007	15.310	0.012	15.085	0.020	14.932	0.020	D
2667-54142-454	15.426	0.006	14.182	0.007	13.777	0.008	13.679	0.026	13.612	0.008	D
2667-54142-455	15.368	0.004	14.148	0.004	13.768	0.008	13.666	0.009	13.656	0.006	D
2667-54142-457	15.884	0.011	14.554	0.005	14.131	0.007	14.032	0.010	14.004	0.010	D
2667-54142-458	15.896	0.017	14.566	0.022	14.119	0.011	14.002	0.017	13.995	0.015	C
2667-54142-459	15.470	0.009	14.276	0.022	13.886	0.008	13.759	0.012	13.770	0.008	C
2667-54142-460	16.016	0.007	14.692	0.002	14.265	0.013	14.138	0.010	14.124	0.006	D
2667-54142-463	15.575	0.014	14.317	0.018	13.914	0.013	13.818	0.016	13.802	0.014	C
2667-54142-466	17.693	0.028	15.902	0.015	15.245	0.016	15.048	0.015	14.973	0.014	C
2667-54142-467	15.518	0.018	14.292	0.019	13.944	0.001	13.831	0.019	13.840	0.015	C
2667-54142-469	17.370	0.014	15.708	0.017	15.100	0.011	14.879	0.016	14.831	0.017	C
2667-54142-476	15.916	0.020	14.650	0.018	14.220	0.001	14.109	0.019	14.070	0.017	C
2667-54142-477	15.956	0.011	14.582	0.004	14.117	0.005	13.953	0.017	13.917	0.011	D
2667-54142-478	15.548	0.014	14.277	0.008	13.896	0.013	13.780	0.022	13.808	0.018	D
2667-54142-479	16.138	0.010	14.793	0.004	14.357	0.005	14.220	0.019	14.208	0.013	D
2667-54142-481	16.198	0.014	14.834	0.004	14.386	0.020	14.242	0.015	14.215	0.008	D
2667-54142-485	16.658	0.007	15.177	0.006	14.670	0.006	14.512	0.010	14.488	0.012	D
2667-54142-486	17.253	0.021	15.622	0.006	15.033	0.009	14.847	0.010	14.786	0.008	D

Continued on next page...

Table A.3 – Continued

spSpec name	<i>u</i>	$\sigma(u)$	<i>g</i>	$\sigma(g)$	<i>r</i>	$\sigma(r)$	<i>i</i>	$\sigma(i)$	<i>z</i>	$\sigma(z)$	Tag
2667-54142-487	15.582	0.008	14.219	0.007	13.763	0.013	13.620	0.010	13.600	0.007	D
2667-54142-491	15.446	0.016	14.262	0.012	13.916	0.001	13.812	0.013	13.791	0.012	C
2667-54142-492	15.916	0.016	14.625	0.012	14.208	0.001	14.111	0.013	14.076	0.012	C
2667-54142-496	16.399	0.014	14.978	0.013	14.510	0.001	14.375	0.015	14.359	0.017	C
2667-54142-500	17.746	0.018	15.936	0.005	15.220	0.011	14.964	0.008	14.844	0.009	D
2667-54142-504	15.624	0.014	14.221	0.013	13.741	0.001	13.611	0.015	13.563	0.017	C
2667-54142-505	15.655	0.009	14.345	0.007	13.911	0.006	13.765	0.007	13.743	0.009	D
2667-54142-507	16.371	0.012	14.930	0.005	14.423	0.008	14.227	0.007	14.148	0.011	D
2667-54142-508	17.057	0.011	15.468	0.008	14.919	0.007	14.750	0.011	14.694	0.009	D
2667-54142-516	16.629	0.013	15.149	0.010	14.689	0.001	14.471	0.008	14.423	0.011	C
2667-54142-517	16.797	0.014	15.341	0.026	14.788	0.014	16.922	0.163	14.601	0.016	C
2667-54142-518	16.081	0.016	14.723	0.014	14.297	0.020	14.176	0.001	14.159	0.014	C
2667-54142-522	15.808	0.008	14.486	0.005	14.069	0.004	13.951	0.007	13.947	0.006	D
2667-54142-531	15.810	0.008	14.526	0.004	14.117	0.004	14.009	0.009	13.998	0.013	D
2667-54142-533	17.646	0.011	15.849	0.005	15.211	0.005	15.006	0.008	14.931	0.010	D
2667-54142-537	15.755	0.005	14.480	0.007	14.049	0.007	13.901	0.006	13.872	0.010	D
2667-54142-538	18.114	0.015	16.185	0.006	15.461	0.008	15.244	0.008	15.141	0.013	D
2667-54142-539	17.842	0.015	15.989	0.012	15.327	0.008	15.112	0.007	15.002	0.007	D
2667-54142-540	17.157	0.007	15.515	0.005	14.941	0.007	14.770	0.008	14.697	0.013	D
2667-54142-541	15.488	0.013	14.232	0.019	13.860	0.001	13.858	0.001	13.760	0.015	C
2667-54142-546	15.379	0.011	14.160	0.008	13.790	0.009	13.693	0.004	13.703	0.006	D
2667-54142-547	17.022	0.012	15.458	0.015	14.913	0.014	14.739	0.013	14.702	0.011	C
2667-54142-550	15.646	0.013	14.373	0.019	13.979	0.001	13.988	0.001	13.843	0.015	C

Continued on next page...

Table A.3 – Continued

spSpec name	<i>u</i>	$\sigma(u)$	<i>g</i>	$\sigma(g)$	<i>r</i>	$\sigma(r)$	<i>i</i>	$\sigma(i)$	<i>z</i>	$\sigma(z)$	Tag
2667-54142-551	17.628	0.015	15.807	0.004	15.105	0.005	14.833	0.011	14.658	0.012	D
2667-54142-561	15.536	0.016	14.275	0.017	13.928	0.015	13.807	0.019	13.779	0.015	C
2667-54142-566	16.563	0.017	15.085	0.017	14.569	0.015	14.431	0.019	14.359	0.015	C
2667-54142-575	15.930	0.007	14.640	0.012	14.217	0.009	14.104	0.005	14.084	0.008	D
2667-54142-576	16.596	0.007	15.122	0.012	14.599	0.012	14.420	0.005	14.353	0.009	D
2667-54142-579	16.694	0.010	15.206	0.009	14.701	0.011	14.535	0.007	14.493	0.006	D
NGC 6791											
2800-54326-151	19.588	0.061	17.289	0.008	16.520	0.005	16.313	0.010	16.197	0.014	D
2800-54326-152	19.716	0.075	18.013	0.009	17.483	0.011	17.356	0.013	17.289	0.019	D
2800-54326-154	18.600	0.030	15.888	0.011	14.939	0.005	14.643	0.006	14.471	0.020	D
2800-54326-155	19.410	0.055	17.773	0.007	17.270	0.009	17.171	0.010	17.154	0.018	D
2800-54326-156	19.129	0.056	16.572	0.007	15.690	0.005	15.436	0.011	15.280	0.010	D
2800-54326-157	19.585	0.055	17.941	0.009	17.405	0.010	17.294	0.015	17.308	0.021	D
2800-54326-159	17.176	0.016	14.589	0.007	13.631	0.005	13.324	0.014	13.180	0.006	D
2800-54326-160	18.966	0.046	16.378	0.009	15.531	0.013	15.280	0.017	15.149	0.021	D
2800-54326-161	19.560	0.057	17.443	0.012	16.706	0.009	16.512	0.009	16.451	0.019	D
2800-54326-165	19.106	0.050	17.508	0.013	16.979	0.008	16.865	0.009	16.837	0.023	D
2800-54326-169	17.480	0.021	14.708	0.007	13.711	0.007	13.393	0.016	13.248	0.005	D
2800-54326-171	19.375	0.052	17.833	0.007	17.286	0.010	17.165	0.013	17.139	0.015	D
2800-54326-172	19.260	0.054	17.466	0.011	16.890	0.007	16.772	0.011	16.712	0.020	D
2800-54326-173	19.822	0.078	17.472	0.007	16.659	0.007	16.419	0.014	16.325	0.011	D
2800-54326-174	17.608	0.022	14.678	0.005	13.643	0.005	13.316	0.022	13.136	0.004	D
2800-54326-175	17.502	0.018	14.689	0.005	13.682	0.005	13.378	0.019	13.203	0.005	D

Continued on next page...

Table A.3 – Continued

spSpec name	<i>u</i>	$\sigma(u)$	<i>g</i>	$\sigma(g)$	<i>r</i>	$\sigma(r)$	<i>i</i>	$\sigma(i)$	<i>z</i>	$\sigma(z)$	Tag
2800-54326-176	18.561	0.029	16.868	0.006	16.317	0.009	16.189	0.018	16.155	0.009	D
2800-54326-178	17.057	0.018	14.279	0.004	13.334	0.003	13.031	0.025	12.901	0.007	D
2800-54326-180	17.349	0.017	14.653	0.011	13.690	0.006	13.402	0.009	13.239	0.022	D
2800-54326-181	17.959	0.023	15.062	0.012	14.009	0.006	13.667	0.007	13.490	0.017	D
2800-54326-182	19.171	0.049	17.534	0.008	17.027	0.012	16.925	0.010	16.903	0.016	D
2800-54326-183	17.508	0.018	14.700	0.005	13.715	0.006	13.421	0.014	13.240	0.008	D
2800-54326-184	19.026	0.044	17.432	0.006	16.936	0.009	16.818	0.011	16.807	0.016	D
2800-54326-185	17.712	0.021	14.929	0.004	13.950	0.005	13.670	0.014	13.514	0.009	D
2800-54326-186	18.932	0.036	16.425	0.009	15.570	0.007	15.339	0.009	15.230	0.014	D
2800-54326-189	19.403	0.057	16.992	0.008	16.165	0.007	15.932	0.010	15.808	0.017	D
2800-54326-190	18.788	0.038	16.170	0.005	15.268	0.006	14.997	0.012	14.855	0.009	D
2800-54326-194	19.100	0.053	17.390	0.013	16.880	0.007	16.775	0.007	16.795	0.022	D
2800-54326-197	18.901	0.039	16.433	0.011	15.570	0.008	15.322	0.010	15.203	0.019	D
2800-54326-199	17.828	0.024	14.796	0.005	13.668	0.004	13.284	0.009	13.039	0.013	D
2800-54326-424	19.743	0.086	18.025	0.017	17.451	0.014	17.283	0.007	17.223	0.020	D
2800-54326-462	19.160	0.044	17.610	0.009	17.122	0.010	17.029	0.007	16.999	0.021	D
2800-54326-464	18.942	0.039	17.296	0.016	16.749	0.010	16.654	0.014	16.638	0.017	D
2800-54326-465	18.283	0.029	15.529	0.012	14.548	0.004	14.218	0.014	14.033	0.008	D
2800-54326-466	19.549	0.062	17.443	0.014	16.709	0.011	16.539	0.012	16.455	0.023	D
2800-54326-469	19.349	0.047	17.760	0.012	17.217	0.007	17.126	0.009	17.121	0.020	D
2800-54326-471	18.860	0.033	17.227	0.010	16.662	0.008	16.551	0.011	16.514	0.014	D
2800-54326-473	18.871	0.031	17.240	0.015	16.646	0.007	16.529	0.014	16.513	0.021	D
2800-54326-475	18.116	0.027	15.317	0.004	14.348	0.010	14.038	0.010	13.844	0.007	D

Continued on next page...

Table A.3 – Continued

spSpec name	<i>u</i>	$\sigma(u)$	<i>g</i>	$\sigma(g)$	<i>r</i>	$\sigma(r)$	<i>i</i>	$\sigma(i)$	<i>z</i>	$\sigma(z)$	Tag
2800-54326-476	18.942	0.037	17.306	0.005	16.840	0.006	16.727	0.008	16.712	0.012	D
2800-54326-477	19.005	0.045	16.586	0.014	15.718	0.006	15.486	0.011	15.364	0.022	D
2800-54326-479	19.581	0.054	18.005	0.014	17.433	0.011	17.317	0.010	17.297	0.020	D
2800-54326-480	19.096	0.040	17.424	0.007	16.824	0.007	16.646	0.007	16.594	0.013	D
2800-54326-497	19.042	0.031	17.517	0.010	16.987	0.010	16.882	0.011	16.865	0.017	D
2821-54393-141	19.825	0.083	18.072	0.010	17.535	0.013	17.413	0.012	17.426	0.020	D
2821-54393-142	20.729	0.190	18.957	0.012	18.334	0.013	18.146	0.014	18.112	0.036	D
2821-54393-145	19.869	0.086	18.099	0.010	17.561	0.009	17.447	0.009	17.420	0.024	D
2821-54393-146	20.285	0.119	18.329	0.010	17.783	0.009	17.658	0.012	17.620	0.026	D
2821-54393-149	19.260	0.056	17.657	0.011	17.191	0.010	17.071	0.018	17.076	0.019	D
2821-54393-161	19.306	0.057	17.635	0.014	17.130	0.011	17.021	0.011	17.026	0.026	D
2821-54393-165	21.185	0.299	18.973	0.018	18.322	0.012	18.149	0.013	18.092	0.036	D
2821-54393-166	20.728	0.194	18.723	0.017	18.125	0.009	17.960	0.011	17.877	0.031	D
2821-54393-167	20.543	0.126	18.574	0.012	17.962	0.013	17.800	0.017	17.832	0.025	D
2821-54393-169	20.667	0.153	18.605	0.013	17.982	0.009	17.825	0.013	17.760	0.037	D
2821-54393-172	20.074	0.094	18.359	0.013	17.775	0.011	17.659	0.010	17.621	0.028	D
2821-54393-173	19.884	0.090	18.208	0.010	17.656	0.013	17.535	0.019	17.525	0.021	D
2821-54393-174	20.300	0.124	18.441	0.014	17.885	0.013	17.742	0.012	17.733	0.032	D
2821-54393-176	21.092	0.256	19.293	0.017	18.564	0.014	18.384	0.014	18.338	0.045	D
2821-54393-177	20.204	0.109	18.520	0.014	17.921	0.010	17.779	0.009	17.751	0.025	D
2821-54393-178	20.754	0.160	18.669	0.012	18.040	0.011	17.877	0.015	17.801	0.026	D
2821-54393-179	19.190	0.054	17.556	0.014	17.031	0.007	16.913	0.007	16.886	0.026	D
2821-54393-182	19.926	0.088	18.170	0.013	17.616	0.007	17.494	0.009	17.465	0.023	D

Continued on next page...

Table A.3 – Continued

spSpec name	<i>u</i>	$\sigma(u)$	<i>g</i>	$\sigma(g)$	<i>r</i>	$\sigma(r)$	<i>i</i>	$\sigma(i)$	<i>z</i>	$\sigma(z)$	Tag
2821-54393-183	19.416	0.058	17.838	0.011	17.333	0.010	17.229	0.009	17.239	0.022	D
2821-54393-184	21.085	0.285	19.030	0.017	18.342	0.013	18.176	0.018	18.003	0.032	D
2821-54393-185	20.033	0.104	18.345	0.009	17.755	0.011	17.625	0.013	17.561	0.021	D
2821-54393-187	19.404	0.052	17.728	0.012	17.240	0.008	17.114	0.007	17.136	0.022	D
2821-54393-188	20.780	0.164	19.049	0.016	18.334	0.010	18.160	0.014	18.113	0.030	D
2821-54393-190	20.372	0.287	19.594	0.023	18.796	0.015	18.592	0.015	18.565	0.051	D
2821-54393-191	20.257	0.131	18.431	0.012	17.824	0.009	17.716	0.010	17.689	0.026	D
2821-54393-192	20.348	0.231	19.289	0.016	18.544	0.011	18.309	0.014	18.198	0.033	D
2821-54393-193	20.833	0.188	18.714	0.010	18.062	0.009	17.911	0.010	17.903	0.029	D
2821-54393-194	19.960	0.104	18.218	0.012	17.640	0.009	17.508	0.012	17.462	0.026	D
2821-54393-195	21.249	0.232	19.101	0.018	18.420	0.012	18.243	0.015	18.162	0.033	D
2821-54393-196	19.907	0.089	18.197	0.011	17.638	0.010	17.527	0.013	17.511	0.033	D
2821-54393-197	19.492	0.062	17.833	0.007	17.329	0.006	17.208	0.009	17.198	0.019	D
2821-54393-199	20.517	0.225	19.162	0.017	18.474	0.014	18.325	0.012	18.261	0.036	D
2821-54393-235	19.348	0.047	17.648	0.007	17.120	0.009	17.012	0.011	17.011	0.022	D
2821-54393-436	20.484	0.139	18.557	0.016	17.927	0.013	17.732	0.009	17.650	0.020	D
2821-54393-438	19.623	0.078	17.927	0.016	17.334	0.018	17.185	0.006	17.121	0.017	D
2821-54393-439	19.364	0.062	17.692	0.008	17.159	0.014	17.045	0.010	17.024	0.015	D
2821-54393-440	19.651	0.065	17.798	0.009	17.165	0.009	16.959	0.012	16.896	0.016	D
2821-54393-468	21.425	0.296	19.449	0.020	18.625	0.015	18.434	0.020	18.438	0.043	D
2821-54393-469	21.200	0.236	18.990	0.024	18.310	0.015	18.141	0.020	18.127	0.034	D
2821-54393-472	20.296	0.107	18.564	0.015	17.963	0.010	17.830	0.016	17.749	0.033	D
2821-54393-473	20.299	0.105	18.535	0.013	17.918	0.012	17.787	0.014	17.741	0.027	D

Continued on next page...

Table A.3 – Continued

spSpec name	<i>u</i>	$\sigma(u)$	<i>g</i>	$\sigma(g)$	<i>r</i>	$\sigma(r)$	<i>i</i>	$\sigma(i)$	<i>z</i>	$\sigma(z)$	Tag
2821-54393-474	19.818	0.074	18.064	0.036	17.597	0.009	17.486	0.012	17.486	0.026	D
2821-54393-475	21.165	0.260	19.129	0.017	18.436	0.012	18.325	0.013	18.226	0.035	D
2821-54393-478	19.933	0.067	18.175	0.012	17.606	0.010	17.493	0.013	17.493	0.029	D
2821-54393-479	20.541	0.147	18.509	0.015	17.775	0.011	17.615	0.010	17.550	0.019	D
2821-54393-480	20.482	0.122	18.827	0.014	18.173	0.011	18.047	0.013	17.981	0.029	D

APPENDIX B: CN, δ CN, AND CH LINE INDICES OF TRUE MEMBER STARS

B.1 SPECTROSCOPIC LINE INDICES DATA TABLE

Having measured the S(3839) and CH(4300) line indices for all member stars in the eight GCs in this sample, I have tabulated the quantities below in Tables B.1 and B.2. Column 1 lists the spSpec name, which identifies the star on the spectral plate in the form of spectroscopic plug-plate number (four digits), Modified Julian Date (five digits), and fiber used (three digits), while (in Table B.1) Columns 2 and 3 list the $(g - r)_0$ and g_0 photometry. Column 4 lists the raw S(3839) CN index, which for AGB, RGB, and SGB stars was calculated using the definition from Norris et al. (1981) and for MS stars was calculated using the definition from Harbeck et al. (2003a), and column 5 gives the temperature-corrected CN index. Finally, column 6 lists the CH indices. Column 7 indicates the luminosity class. Table B.2 lists the uncertainties for the measured parameters.

Table B.1: Line Indices of Adopted True Member Stars

spSpec name (1)	$(g - r)_0$ (2)	g_0 (3)	S(3839) (4)	δ S(3839) (5)	CH(4300) (6)	Type (7)
--------------------	--------------------	--------------	----------------	-------------------------	-----------------	-------------

Table B.1 – Continued

spSpec name	$(g - r)_0$	g_0	S(3839)	$\delta S(3839)$	CH(4300)	Type
(1)	(2)	(3)	(4)	(5)	(6)	(7)
2247-54169-362	0.441	17.343	-0.172	0.022	-0.489	RGB
2247-54169-364	0.456	16.533	-0.196	-0.020	-0.466	RGB
2247-54169-367	0.439	16.519	-0.169	0.006	-0.460	RGB
2247-54169-380	0.484	16.093	-0.187	-0.021	-0.450	RGB
2247-54169-404	0.455	16.503	-0.165	0.010	-0.504	RGB
2247-54169-444	0.467	16.006	-0.184	-0.020	-0.453	RGB
2247-54169-451	0.472	16.188	-0.133	0.035	-0.479	RGB
2247-54169-452	0.480	15.985	-0.142	0.021	-0.497	RGB
2247-54169-529	0.440	17.182	-0.176	0.015	-0.483	RGB
2247-54169-531	0.443	16.488	-0.170	0.005	-0.459	RGB
2247-54169-546	0.408	17.107	-0.076	0.113	-0.492	RGB
2247-54169-561	0.479	16.490	-0.194	-0.020	-0.456	RGB
2247-54169-573	0.447	16.016	-0.189	-0.025	-0.441	RGB
2247-54169-581	0.457	16.373	-0.178	-0.006	-0.490	RGB
2247-54169-589	0.457	17.007	-0.200	-0.014	-0.478	RGB
2247-54169-620	0.405	17.503	-0.179	0.019	-0.494	RGB
2247-54169-408	0.521	15.333	-0.132	0.016	-0.473	RGB
2247-54169-418	0.527	15.524	-0.199	-0.046	-0.428	RGB
2247-54169-449	0.479	15.490	-0.111	0.040	-0.478	RGB
2247-54169-484	0.601	15.117	-0.117	0.026	-0.428	RGB
2247-54169-504	0.518	15.125	-0.134	0.009	-0.452	RGB
2247-54169-563	0.533	15.492	-0.148	0.003	-0.436	RGB

Continued on next page...

Table B.1 – Continued

spSpec name	$(g - r)_0$	g_0	S(3839)	$\delta S(3839)$	CH(4300)	Type
(1)	(2)	(3)	(4)	(5)	(6)	(7)
2247-54169-608	0.531	15.383	-0.215	-0.066	-0.421	RGB
2247-54169-610	0.538	15.198	-0.143	0.002	-0.417	RGB
2247-54169-379	0.189	17.638	-0.254	-0.053	-0.511	SGB
2247-54169-458	0.365	17.845	-0.209	-0.003	-0.494	SGB
2247-54169-514	0.372	17.645	-0.073	0.128	-0.507	SGB
2247-54169-516	0.363	17.860	-0.165	0.041	-0.523	SGB
2247-54169-519	0.379	17.809	-0.164	0.040	-0.465	SGB
2247-54169-538	0.306	17.966	-0.135	0.074	-0.521	SGB
2247-54169-541	0.387	17.691	-0.121	0.081	-0.514	SGB
2247-54169-575	0.360	17.882	-0.248	-0.042	-0.496	SGB
2247-54169-584	0.367	17.789	-0.275	-0.071	-0.529	SGB
2247-54169-616	0.366	17.890	-0.263	-0.057	-0.521	SGB
2256-53859-513	0.372	17.645	-0.142	0.059	-0.517	SGB
2256-53859-522	0.270	18.084	-0.228	-0.017	-0.550	SGB
2256-53859-535	0.204	18.349	-0.270	-0.053	-0.549	SGB
2256-53859-536	0.225	18.395	-0.255	-0.036	-0.531	SGB
2256-53859-538	0.386	17.762	-0.187	0.017	-0.490	SGB
2247-54169-409	0.314	20.443	-0.282	-0.016	-0.561	MS
2256-53859-411	0.240	18.413	-0.285	-0.066	-0.534	MS
2256-53859-455	0.205	18.576	-0.245	-0.022	-0.564	MS
2256-53859-485	0.191	19.103	-0.253	-0.018	-0.544	MS
2256-53859-489	0.182	18.749	-0.310	-0.084	-0.544	MS

Continued on next page...

Table B.1 – Continued

spSpec name	$(g - r)_0$	g_0	S(3839)	$\delta S(3839)$	CH(4300)	Type
(1)	(2)	(3)	(4)	(5)	(6)	(7)
2256-53859-501	0.189	18.751	-0.329	-0.102	-0.523	MS
2256-53859-506	0.207	18.794	-0.230	-0.003	-0.565	MS
2256-53859-530	0.200	18.682	-0.180	0.045	-0.518	MS
2256-53859-537	0.211	19.293	-0.277	-0.038	-0.563	MS
2256-53859-539	0.210	18.874	-0.174	0.056	-0.511	MS
2256-53859-546	0.196	18.505	-0.229	-0.008	-0.528	MS
2256-53859-566	0.231	18.824	-0.249	-0.021	-0.522	MS
2256-53859-571	0.199	18.654	-0.271	-0.047	-0.506	MS
2256-53859-575	0.162	18.591	-0.246	-0.023	-0.570	MS
2256-53859-576	0.190	18.548	-0.196	0.026	-0.557	MS
2256-53859-579	0.210	18.810	-0.303	-0.075	-0.532	MS
2256-53859-612	0.185	18.499	-0.242	-0.022	-0.528	MS
			M15			
1960-53289-441	0.399	17.582	-0.203	-0.009	-0.465	RGB
1960-53289-457	0.372	17.913	-0.206	-0.009	-0.472	RGB
1960-53289-500	0.450	17.169	-0.093	0.097	-0.481	RGB
1960-53289-522	0.416	16.909	-0.228	-0.041	-0.494	RGB
1960-53289-530	0.445	17.485	-0.211	-0.018	-0.393	RGB
1962-53321-364	0.392	17.583	-0.167	0.027	-0.489	RGB
1962-53321-375	0.393	17.758	-0.193	0.003	-0.497	RGB
1962-53321-376	0.396	17.515	-0.221	-0.027	-0.473	RGB
1962-53321-402	0.372	17.913	-0.264	-0.067	-0.481	RGB

Continued on next page...

Table B.1 – Continued

spSpec name	$(g - r)_0$	g_0	S(3839)	$\delta S(3839)$	CH(4300)	Type
(1)	(2)	(3)	(4)	(5)	(6)	(7)
1962-53321-403	0.383	17.887	-0.184	0.013	-0.488	RGB
1962-53321-406	0.383	17.944	-0.210	-0.012	-0.523	RGB
1962-53321-413	0.384	17.556	-0.183	0.010	-0.489	RGB
1962-53321-415	0.394	17.419	-0.155	0.038	-0.511	RGB
1962-53321-427	0.394	17.643	-0.179	0.016	-0.484	RGB
1962-53321-438	0.422	17.546	-0.186	0.008	-0.483	RGB
1962-53321-454	0.399	17.582	-0.196	-0.001	-0.485	RGB
1962-53321-466	0.416	17.520	-0.198	-0.005	-0.480	RGB
1962-53321-474	0.391	17.449	-0.194	-0.002	-0.485	RGB
1962-53321-506	0.416	17.378	-0.207	-0.015	-0.448	RGB
1962-53321-515	0.443	17.568	-0.219	-0.025	-0.474	RGB
1962-53321-532	0.382	17.487	-0.191	0.002	-0.510	RGB
1960-53289-401	0.485	16.078	-0.207	-0.028	-0.442	RGB
1960-53289-402	0.552	15.391	-0.113	0.059	-0.411	RGB
1960-53289-406	0.552	15.393	-0.153	0.020	-0.446	RGB
1960-53289-413	0.508	15.687	-0.186	-0.011	-0.464	RGB
1960-53289-419	0.542	15.433	-0.208	-0.035	-0.434	RGB
1960-53289-442	0.487	16.342	-0.238	-0.056	-0.437	RGB
1960-53289-459	0.515	15.076	-0.208	-0.039	-0.515	RGB
1960-53289-460	0.465	16.431	-0.221	-0.038	-0.471	RGB
1960-53289-511	0.509	16.568	-0.189	-0.005	-0.505	RGB
1960-53289-523	0.643	14.624	-0.159	0.005	-0.426	RGB

Continued on next page...

Table B.1 – Continued

spSpec name	$(g - r)_0$	g_0	S(3839)	$\delta S(3839)$	CH(4300)	Type
(1)	(2)	(3)	(4)	(5)	(6)	(7)
1960-53289-529	0.521	15.513	-0.130	0.043	-0.483	RGB
1960-53289-420	0.362	18.421	-0.201	0.002	-0.525	SGB
1960-53289-501	0.398	18.283	-0.215	-0.013	-0.553	SGB
1962-53321-323	0.269	18.400	-0.272	-0.070	-0.523	SGB
1962-53321-328	0.205	18.655	-0.271	-0.067	-0.530	SGB
1962-53321-329	0.269	18.522	-0.250	-0.047	-0.551	SGB
1962-53321-335	0.301	18.411	-0.274	-0.072	-0.516	SGB
1962-53321-368	0.227	18.553	-0.247	-0.043	-0.515	SGB
1962-53321-369	0.241	18.589	-0.300	-0.096	-0.543	SGB
1962-53321-370	0.279	18.453	-0.274	-0.071	-0.542	SGB
1962-53321-371	0.254	18.507	-0.234	-0.031	-0.522	SGB
1962-53321-372	0.285	18.371	-0.229	-0.027	-0.511	SGB
1962-53321-407	0.226	18.444	-0.260	-0.057	-0.526	SGB
1962-53321-414	0.275	18.472	-0.287	-0.084	-0.519	SGB
1962-53321-421	0.338	18.371	-0.266	-0.064	-0.473	SGB
1962-53321-423	0.363	18.205	-0.125	0.076	-0.466	SGB
1962-53321-442	0.178	18.727	-0.226	-0.020	-0.550	SGB
1962-53321-469	0.189	18.634	-0.258	-0.054	-0.531	SGB
1962-53321-470	0.235	18.633	-0.248	-0.044	-0.536	SGB
1962-53321-488	0.283	18.642	-0.256	-0.051	-0.530	SGB
1962-53321-493	0.367	18.324	-0.218	-0.016	-0.517	SGB
1962-53321-495	0.254	18.787	-0.300	-0.094	-0.523	SGB

Continued on next page...

Table B.1 – Continued

spSpec name	$(g - r)_0$	g_0	S(3839)	$\delta S(3839)$	CH(4300)	Type
(1)	(2)	(3)	(4)	(5)	(6)	(7)
1962-53321-496	0.237	18.773	-0.258	-0.052	-0.512	SGB
1962-53321-497	0.181	18.769	-0.248	-0.042	-0.539	SGB
1962-53321-500	0.256	18.396	-0.253	-0.051	-0.525	SGB
1962-53321-510	0.291	18.529	-0.246	-0.042	-0.522	SGB
1962-53321-516	0.398	18.283	-0.253	-0.052	-0.526	SGB
1962-53321-518	0.361	18.253	-0.239	-0.039	-0.504	SGB
1962-53321-520	0.276	18.619	-0.282	-0.077	-0.530	SGB
1962-53321-533	0.275	18.638	-0.279	-0.074	-0.517	SGB
1962-53321-549	0.296	18.326	-0.285	-0.083	-0.528	SGB
1962-53321-550	0.362	18.421	-0.282	-0.079	-0.530	SGB
1962-53321-558	0.289	18.344	-0.257	-0.056	-0.530	SGB
1962-53321-339	0.138	19.041	-0.330	-0.122	-0.550	MS
1962-53321-363	0.211	19.252	-0.204	0.007	-0.505	MS
1962-53321-378	0.191	19.052	-0.242	-0.033	-0.539	MS
1962-53321-399	0.196	18.831	-0.307	-0.100	-0.537	MS
1962-53321-409	0.154	19.145	-0.340	-0.130	-0.536	MS
1962-53321-412	0.174	18.872	-0.315	-0.108	-0.514	MS
1962-53321-416	0.160	19.081	-0.279	-0.070	-0.498	MS
1962-53321-419	0.181	19.268	-0.288	-0.077	-0.540	MS
1962-53321-422	0.228	19.094	-0.212	-0.003	-0.522	MS
1962-53321-424	0.170	18.952	-0.348	-0.140	-0.515	MS
1962-53321-428	0.165	18.951	-0.285	-0.077	-0.542	MS

Continued on next page...

Table B.1 – Continued

spSpec name	$(g - r)_0$	g_0	S(3839)	$\delta S(3839)$	CH(4300)	Type
(1)	(2)	(3)	(4)	(5)	(6)	(7)
1962-53321-430	0.204	19.211	-0.279	-0.068	-0.521	MS
1962-53321-445	0.148	19.341	-0.201	0.011	-0.534	MS
1962-53321-449	0.196	19.374	-0.315	-0.103	-0.518	MS
1962-53321-460	0.224	19.363	-0.281	-0.069	-0.510	MS
1962-53321-465	0.145	18.942	-0.273	-0.066	-0.527	MS
1962-53321-471	0.153	18.829	-0.303	-0.096	-0.535	MS
1962-53321-478	0.224	19.724	-0.265	-0.049	-0.497	MS
1962-53321-480	0.211	18.991	-0.234	-0.026	-0.520	MS
1962-53321-483	0.206	19.211	-0.297	-0.086	-0.515	MS
1962-53321-484	0.210	19.188	-0.270	-0.060	-0.507	MS
1962-53321-490	0.258	18.893	-0.257	-0.050	-0.520	MS
1962-53321-503	0.197	18.961	-0.246	-0.038	-0.547	MS
1962-53321-505	0.161	19.488	-0.240	-0.027	-0.520	MS
1962-53321-509	0.254	19.260	-0.228	-0.017	-0.504	MS
1962-53321-512	0.248	19.508	-0.322	-0.108	-0.493	MS
1962-53321-519	0.162	19.058	-0.261	-0.052	-0.548	MS
1962-53321-522	0.155	19.128	-0.209	0.001	-0.568	MS
1962-53321-539	0.194	18.815	-0.289	-0.082	-0.516	MS
1962-53321-540	0.194	19.401	-0.281	-0.068	-0.520	MS
1962-53321-543	0.274	18.916	-0.216	-0.009	-0.532	MS
1962-53321-545	0.299	19.107	-0.332	-0.122	-0.530	MS
1962-53321-554	0.174	19.385	-0.236	-0.024	-0.482	MS

Continued on next page...

Table B.1 – Continued

spSpec name	$(g - r)_0$	g_0	S(3839)	$\delta S(3839)$	CH(4300)	Type
	(1)	(2)	(3)	(4)	(5)	(7)
1962-53321-555	0.258	19.532	-0.334	-0.120	-0.519	MS
NGC 5053						
2476-53826-486	0.462	17.746	-0.126	0.058	-0.429	RGB
2476-53826-497	0.451	18.201	-0.098	0.098	-0.442	RGB
2476-53826-488	0.686	15.780	-0.119	0.017	-0.432	RGB
2476-53826-501	0.632	15.988	-0.182	-0.042	-0.443	RGB
2476-53826-505	0.485	16.302	-0.221	-0.072	-0.523	RGB
2476-53826-507	0.530	16.939	-0.101	0.063	-0.450	RGB
2476-53826-508	0.532	16.803	-0.131	0.030	-0.447	RGB
2476-53826-519	0.787	15.223	-0.104	0.018	-0.450	RGB
2476-53826-527	0.651	15.862	-0.115	0.023	-0.467	RGB
2476-53826-573	0.529	17.197	-0.169	0.002	-0.447	RGB
2476-53826-575	0.724	15.518	-0.160	-0.031	-0.432	RGB
2476-53826-577	0.546	16.942	-0.214	-0.050	-0.428	RGB
2476-53826-578	0.698	15.602	-0.111	0.020	-0.450	RGB
M53						
2476-53826-329	0.503	17.999	-0.258	-0.036	-0.429	RGB
2476-53826-405	0.494	18.055	-0.049	0.175	-0.377	RGB
2476-53826-413	0.535	17.791	-0.188	0.029	-0.444	RGB
2476-53826-418	0.504	18.063	-0.032	0.192	-0.465	RGB
2476-53826-361	0.638	16.908	-0.166	0.026	-0.359	RGB
2476-53826-372	0.546	16.868	-0.209	-0.017	-0.450	RGB

Continued on next page...

Table B.1 – Continued

spSpec name	$(g - r)_0$	g_0	S(3839)	$\delta S(3839)$	CH(4300)	Type
(1)	(2)	(3)	(4)	(5)	(6)	(7)
2476-53826-375	0.544	17.094	0.041	0.239	-0.435	RGB
2476-53826-378	0.618	16.225	-0.159	0.016	-0.457	RGB
2476-53826-401	0.531	17.438	-0.154	0.053	-0.369	RGB
2476-53826-404	0.749	15.836	-0.011	0.153	-0.431	RGB
2476-53826-409	0.508	17.321	-0.052	0.152	-0.419	RGB
2476-53826-451	0.602	16.775	-0.257	-0.068	-0.367	RGB
2476-53826-452	0.503	17.369	-0.192	0.013	-0.387	RGB
M2						
1961-53299-140	0.471	17.276	-0.037	0.207	-0.462	RGB
1961-53299-213	0.467	17.182	-0.032	0.206	-0.463	RGB
1963-54331-098	0.495	17.576	-0.065	0.199	-0.438	RGB
1963-54331-121	0.487	17.536	0.018	0.280	-0.453	RGB
1963-54331-126	0.451	18.287	-0.063	0.247	-0.449	RGB
1963-54331-128	0.470	18.253	-0.006	0.302	-0.422	RGB
1963-54331-131	0.457	18.210	-0.011	0.294	-0.441	RGB
1963-54331-137	0.475	17.895	-0.172	0.113	-0.413	RGB
1963-54331-139	0.483	17.919	-0.147	0.139	-0.414	RGB
1963-54331-144	0.471	17.663	-0.211	0.059	-0.393	RGB
1963-54331-164	0.434	18.434	-0.178	0.142	-0.432	RGB
1963-54331-178	0.423	18.477	-0.164	0.158	-0.408	RGB
1963-54331-204	0.488	17.953	-0.255	0.033	-0.394	RGB
1963-54331-208	0.461	17.815	-0.245	0.034	-0.418	RGB

Continued on next page...

Table B.1 – Continued

spSpec name	$(g - r)_0$	g_0	S(3839)	$\delta S(3839)$	CH(4300)	Type
(1)	(2)	(3)	(4)	(5)	(6)	(7)
1963-54331-209	0.412	18.339	-0.106	0.207	-0.450	RGB
1963-54331-211	0.463	18.346	-0.116	0.198	-0.430	RGB
1963-54331-217	0.461	17.824	-0.059	0.221	-0.456	RGB
1963-54331-218	0.451	17.963	-0.158	0.131	-0.444	RGB
1961-53299-124	0.598	16.087	-0.184	-0.017	-0.358	RGB
1961-53299-125	0.592	15.997	0.175	0.336	-0.378	RGB
1961-53299-131	0.555	16.680	-0.219	-0.014	-0.372	RGB
1961-53299-134	0.701	15.105	0.174	0.277	-0.397	RGB
1961-53299-136	0.529	16.913	-0.243	-0.022	-0.378	RGB
1961-53299-144	0.470	16.940	-0.003	0.219	-0.464	RGB
1961-53299-152	0.570	16.618	-0.037	0.164	-0.415	RGB
1961-53299-159	0.492	16.866	-0.028	0.189	-0.452	RGB
1961-53299-215	0.581	16.353	0.026	0.211	-0.392	RGB
1963-54331-043	0.394	18.766	-0.128	0.213	-0.496	SGB
1963-54331-083	0.342	18.907	-0.204	0.147	-0.514	SGB
1963-54331-090	0.354	18.869	-0.167	0.181	-0.466	SGB
1963-54331-091	0.496	18.520	-0.287	0.038	-0.422	SGB
1963-54331-096	0.326	18.954	-0.087	0.267	-0.504	SGB
1963-54331-100	0.340	18.929	-0.286	0.065	-0.441	SGB
1963-54331-102	0.294	18.951	-0.190	0.163	-0.506	SGB
1963-54331-114	0.244	19.245	-0.195	0.177	-0.543	SGB
1963-54331-123	0.415	18.695	-0.132	0.205	-0.452	SGB

Continued on next page...

Table B.1 – Continued

spSpec name	$(g - r)_0$	g_0	S(3839)	$\delta S(3839)$	CH(4300)	Type
(1)	(2)	(3)	(4)	(5)	(6)	(7)
1963-54331-124	0.263	19.069	-0.280	0.081	-0.571	SGB
1963-54331-143	0.352	18.808	-0.182	0.162	-0.473	SGB
1963-54331-145	0.375	18.911	-0.200	0.150	-0.453	SGB
1963-54331-146	0.231	19.186	-0.241	0.127	-0.518	SGB
1963-54331-147	0.211	19.252	-0.225	0.147	-0.516	SGB
1963-54331-148	0.380	18.896	-0.122	0.228	-0.459	SGB
1963-54331-150	0.302	18.980	-0.222	0.133	-0.555	SGB
1963-54331-179	0.234	19.219	-0.167	0.203	-0.494	SGB
1963-54331-180	0.415	18.721	-0.144	0.195	-0.490	SGB
1963-54331-181	0.201	19.174	-0.329	0.039	-0.511	SGB
1963-54331-184	0.414	18.640	-0.185	0.148	-0.478	SGB
1963-54331-189	0.215	19.273	-0.243	0.131	-0.535	SGB
1963-54331-194	0.272	19.216	-0.207	0.164	-0.552	SGB
1963-54331-196	0.157	19.245	-0.283	0.089	-0.528	SGB
1963-54331-201	0.390	18.658	-0.116	0.218	-0.481	SGB
1963-54331-206	0.218	19.258	-0.329	0.044	-0.523	SGB
1963-54331-212	0.423	18.636	-0.315	0.018	-0.441	SGB
1963-54331-223	0.273	19.280	-0.263	0.112	-0.508	SGB
1963-54331-254	0.237	19.273	-0.362	0.012	-0.536	SGB
1963-54331-041	0.246	19.492	-0.258	-0.126	-0.514	MS
1963-54331-045	0.214	19.350	-0.144	-0.022	-0.562	MS
1963-54331-082	0.271	19.536	-0.156	-0.022	-0.485	MS

Continued on next page...

Table B.1 – Continued

spSpec name	$(g - r)_0$	g_0	S(3839)	$\delta S(3839)$	CH(4300)	Type
(1)	(2)	(3)	(4)	(5)	(6)	(7)
1963-54331-154	0.224	19.588	-0.226	-0.088	-0.554	MS
1963-54331-156	0.211	19.443	-0.239	-0.111	-0.564	MS
1963-54331-162	0.200	19.585	-0.161	-0.023	-0.537	MS
1963-54331-169	0.233	19.599	-0.181	-0.043	-0.558	MS
1963-54331-170	0.166	19.483	-0.252	-0.121	-0.563	MS
1963-54331-185	0.201	19.507	-0.329	-0.197	-0.527	MS
1963-54331-186	0.188	19.654	-0.238	-0.096	-0.509	MS
1963-54331-197	0.203	19.581	-0.183	-0.046	-0.553	MS
1963-54331-200	0.221	19.563	-0.274	-0.138	-0.537	MS
1963-54331-207	0.230	19.495	-0.187	-0.055	-0.558	MS
1963-54331-220	0.227	19.336	-0.287	-0.166	-0.506	MS
1963-54331-222	0.199	19.344	-0.233	-0.111	-0.508	MS
M13						
2174-53521-087	0.462	17.258	-0.117	0.100	-0.431	RGB
2174-53521-094	0.464	17.245	-0.270	-0.053	-0.409	RGB
2174-53521-121	0.543	16.227	-0.031	0.167	-0.437	RGB
2174-53521-126	0.478	17.014	-0.048	0.164	-0.487	RGB
2174-53521-128	0.458	17.480	0.181	0.402	-0.445	RGB
2174-53521-133	0.495	16.876	-0.075	0.135	-0.424	RGB
2174-53521-134	0.452	17.284	-0.190	0.028	-0.422	RGB
2174-53521-155	0.514	16.521	-0.008	0.196	-0.431	RGB
2174-53521-407	0.518	16.612	-0.215	-0.010	-0.394	RGB

Continued on next page...

Table B.1 – Continued

spSpec name	$(g - r)_0$	g_0	S(3839)	$\delta S(3839)$	CH(4300)	Type
(1)	(2)	(3)	(4)	(5)	(6)	(7)
2174-53521-412	0.506	17.467	-0.051	0.169	-0.489	RGB
2174-53521-414	0.547	17.456	-0.091	0.129	-0.442	RGB
2174-53521-456	0.463	17.371	-0.075	0.144	-0.473	RGB
2174-53521-461	0.465	17.359	-0.216	0.003	-0.408	RGB
2174-53521-471	0.538	16.278	-0.113	0.086	-0.406	RGB
2174-53521-480	0.489	16.899	-0.124	0.086	-0.415	RGB
2174-53521-529	0.520	16.474	-0.216	-0.013	-0.381	RGB
2174-53521-563	0.516	16.408	-0.119	0.083	-0.397	RGB
2255-53565-114	0.466	17.080	-0.097	0.117	-0.467	RGB
2255-53565-116	0.540	16.291	-0.132	0.068	-0.396	RGB
2255-53565-437	0.454	17.471	-0.122	0.099	-0.467	RGB
2255-53565-476	0.469	17.172	-0.082	0.133	-0.426	RGB
2255-53565-490	0.514	16.279	-0.049	0.151	-0.429	RGB
2255-53565-556	0.464	17.253	-0.076	0.141	-0.462	RGB
2255-53565-597	0.523	16.411	-0.133	0.069	-0.391	RGB
2174-53521-082	0.579	15.424	0.066	0.250	-0.387	RGB
2174-53521-093	0.636	15.225	-0.167	0.014	-0.352	RGB
2174-53521-098	0.586	15.525	-0.191	-0.005	-0.372	RGB
2174-53521-137	0.560	15.567	0.054	0.241	-0.438	RGB
2174-53521-145	0.655	14.969	-0.011	0.165	-0.361	RGB
2174-53521-154	0.609	15.058	0.121	0.299	-0.386	RGB
2174-53521-156	0.589	15.656	0.029	0.217	-0.399	RGB

Continued on next page...

Table B.1 – Continued

spSpec name	$(g - r)_0$	g_0	S(3839)	$\delta S(3839)$	CH(4300)	Type
(1)	(2)	(3)	(4)	(5)	(6)	(7)
2174-53521-158	0.523	15.567	0.041	0.228	-0.395	RGB
2174-53521-159	0.619	15.025	0.132	0.309	-0.438	RGB
2174-53521-160	0.589	15.354	0.073	0.256	-0.434	RGB
2174-53521-166	0.585	15.623	-0.185	0.003	-0.361	RGB
2174-53521-167	0.626	14.817	0.144	0.317	-0.427	RGB
2174-53521-168	0.579	15.244	0.120	0.301	-0.420	RGB
2174-53521-171	0.660	14.958	-0.041	0.135	-0.353	RGB
2174-53521-172	0.609	15.298	0.088	0.269	-0.371	RGB
2174-53521-176	0.565	15.730	-0.079	0.110	-0.359	RGB
2174-53521-215	0.564	15.346	-0.059	0.124	-0.377	RGB
2174-53521-376	0.571	15.783	0.007	0.198	-0.429	RGB
2174-53521-410	0.635	15.329	0.053	0.235	-0.384	RGB
2174-53521-413	0.571	15.535	0.051	0.237	-0.452	RGB
2174-53521-443	0.587	15.333	0.087	0.269	-0.438	RGB
2174-53521-449	0.584	15.349	0.081	0.264	-0.406	RGB
2174-53521-452	0.608	15.112	-0.193	-0.015	-0.358	RGB
2174-53521-453	0.609	15.286	-0.155	0.027	-0.372	RGB
2174-53521-455	0.599	15.378	0.086	0.270	-0.388	RGB
2174-53521-457	0.617	15.178	0.065	0.245	-0.390	RGB
2174-53521-458	0.611	15.068	0.130	0.307	-0.414	RGB
2174-53521-459	0.558	15.201	0.047	0.227	-0.363	RGB
2174-53521-460	0.621	14.823	0.138	0.311	-0.443	RGB

Continued on next page...

Table B.1 – Continued

spSpec name	$(g - r)_0$	g_0	S(3839)	$\delta S(3839)$	CH(4300)	Type
(1)	(2)	(3)	(4)	(5)	(6)	(7)
2174-53521-462	0.617	15.126	-0.194	-0.016	-0.351	RGB
2174-53521-463	0.576	15.630	0.076	0.264	-0.420	RGB
2174-53521-470	0.624	14.850	0.138	0.312	-0.403	RGB
2174-53521-476	0.544	15.727	0.334	0.523	-0.367	RGB
2174-53521-477	0.634	15.217	-0.153	0.027	-0.352	RGB
2174-53521-478	0.580	15.422	0.069	0.253	-0.430	RGB
2174-53521-483	0.609	15.141	0.077	0.256	-0.382	RGB
2174-53521-484	0.629	15.187	-0.018	0.162	-0.365	RGB
2174-53521-485	0.549	15.489	0.044	0.229	-0.449	RGB
2174-53521-488	0.573	15.725	-0.060	0.129	-0.373	RGB
2174-53521-489	0.604	15.576	0.083	0.270	-0.435	RGB
2174-53521-493	0.604	15.088	0.042	0.220	-0.407	RGB
2174-53521-494	0.620	15.143	0.092	0.271	-0.435	RGB
2174-53521-495	0.573	15.998	-0.110	0.085	-0.396	RGB
2174-53521-497	0.628	15.410	0.100	0.283	-0.422	RGB
2174-53521-498	0.600	15.122	0.023	0.202	-0.376	RGB
2174-53521-499	0.607	15.089	0.135	0.313	-0.416	RGB
2174-53521-500	0.602	15.302	-0.169	0.013	-0.365	RGB
2174-53521-522	0.584	15.503	0.083	0.269	-0.417	RGB
2174-53521-530	0.620	15.287	0.112	0.294	-0.393	RGB
2174-53521-531	0.615	15.229	-0.196	-0.016	-0.354	RGB
2174-53521-537	0.532	15.965	-0.033	0.161	-0.396	RGB

Continued on next page...

Table B.1 – Continued

spSpec name	$(g - r)_0$	g_0	S(3839)	$\delta S(3839)$	CH(4300)	Type
(1)	(2)	(3)	(4)	(5)	(6)	(7)
2174-53521-538	0.630	15.042	0.079	0.256	-0.382	RGB
2174-53521-542	0.616	15.276	0.092	0.273	-0.383	RGB
2174-53521-554	0.562	15.843	-0.022	0.169	-0.409	RGB
2255-53565-112	0.636	15.225	-0.184	-0.003	-0.347	RGB
2255-53565-120	0.586	15.525	-0.175	0.010	-0.374	RGB
2255-53565-143	0.544	15.959	0.006	0.199	-0.415	RGB
2255-53565-144	0.523	15.567	0.019	0.206	-0.397	RGB
2255-53565-148	0.557	15.819	0.096	0.287	-0.412	RGB
2255-53565-153	0.564	15.684	0.050	0.238	-0.415	RGB
2255-53565-157	0.623	15.107	-0.188	-0.010	-0.347	RGB
2255-53565-171	0.589	15.354	0.074	0.257	-0.439	RGB
2255-53565-175	0.565	15.730	-0.065	0.124	-0.370	RGB
2255-53565-426	0.571	15.535	0.071	0.257	-0.444	RGB
2255-53565-483	0.617	15.126	-0.188	-0.010	-0.349	RGB
2255-53565-485	0.561	15.581	0.060	0.247	-0.430	RGB
2255-53565-486	0.603	15.229	0.104	0.284	-0.358	RGB
2255-53565-495	0.630	14.660	-0.160	0.010	-0.352	RGB
2255-53565-496	0.624	14.850	0.091	0.265	-0.400	RGB
2255-53565-504	0.637	14.477	-0.011	0.156	-0.378	RGB
2255-53565-510	0.576	15.630	0.065	0.253	-0.415	RGB
2255-53565-512	0.600	15.122	0.060	0.238	-0.382	RGB
2255-53565-515	0.544	15.727	0.314	0.504	-0.350	RGB

Continued on next page...

Table B.1 – Continued

spSpec name	$(g - r)_0$	g_0	S(3839)	$\delta S(3839)$	CH(4300)	Type
(1)	(2)	(3)	(4)	(5)	(6)	(7)
2255-53565-520	0.602	14.930	0.019	0.194	-0.454	RGB
2255-53565-542	0.584	15.503	0.084	0.269	-0.418	RGB
2255-53565-543	0.604	15.576	0.069	0.256	-0.427	RGB
2255-53565-544	0.606	15.131	0.048	0.227	-0.427	RGB
2255-53565-545	0.591	15.473	0.073	0.258	-0.442	RGB
2255-53565-548	0.628	15.410	0.099	0.283	-0.421	RGB
2255-53565-550	0.573	15.725	-0.074	0.116	-0.372	RGB
2255-53565-551	0.615	15.229	-0.197	-0.016	-0.346	RGB
2255-53565-552	0.639	14.555	0.155	0.323	-0.412	RGB
2255-53565-553	0.585	15.382	0.091	0.274	-0.430	RGB
2255-53565-557	0.630	15.042	0.091	0.268	-0.389	RGB
2255-53565-559	0.644	14.741	0.037	0.209	-0.427	RGB
2255-53565-586	0.636	14.521	-0.173	-0.005	-0.453	RGB
2255-53565-589	0.620	15.287	0.104	0.286	-0.395	RGB
2174-53521-054	0.423	17.814	-0.249	-0.022	-0.515	SGB
2174-53521-131	0.267	18.175	-0.219	0.015	-0.347	SGB
2174-53521-146	0.427	17.680	-0.144	0.080	-0.479	SGB
2174-53521-149	0.422	17.781	-0.159	0.067	-0.466	SGB
2174-53521-174	0.426	17.904	-0.001	0.228	-0.474	SGB
2174-53521-368	0.461	17.507	-0.230	-0.009	-0.433	SGB
2174-53521-402	0.412	17.810	-0.193	0.034	-0.441	SGB
2174-53521-403	0.373	17.981	-0.142	0.088	-0.492	SGB

Continued on next page...

Table B.1 – Continued

spSpec name	$(g - r)_0$	g_0	S(3839)	$\delta S(3839)$	CH(4300)	Type
(1)	(2)	(3)	(4)	(5)	(6)	(7)
2174-53521-406	0.406	17.893	-0.157	0.072	-0.465	SGB
2174-53521-445	0.403	17.893	-0.131	0.098	-0.500	SGB
2174-53521-447	0.443	17.683	-0.123	0.101	-0.477	SGB
2174-53521-474	0.459	17.612	-0.128	0.096	-0.452	SGB
2174-53521-481	0.408	17.867	-0.129	0.099	-0.462	SGB
2174-53521-533	0.437	17.797	-0.181	0.046	-0.465	SGB
2174-53521-539	0.473	17.657	-0.203	0.022	-0.399	SGB
2174-53521-560	0.528	17.547	-0.150	0.072	-0.445	SGB
2174-53521-565	0.422	17.915	-0.255	-0.026	-0.451	SGB
2174-53521-573	0.369	17.961	-0.254	-0.025	-0.427	SGB
2174-53521-576	0.449	17.672	-0.120	0.105	-0.428	SGB
2174-53521-577	0.421	17.902	-0.172	0.056	-0.447	SGB
2185-53532-141	0.227	18.392	-0.249	-0.012	-0.525	SGB
2185-53532-153	0.379	18.098	-0.241	-0.009	-0.494	SGB
2185-53532-237	0.286	18.063	-0.243	-0.011	-0.523	SGB
2185-53532-388	0.240	18.283	-0.270	-0.035	-0.524	SGB
2185-53532-425	0.262	18.304	-0.241	-0.005	-0.539	SGB
2185-53532-426	0.336	18.012	-0.192	0.038	-0.509	SGB
2185-53532-427	0.350	18.001	-0.178	0.052	-0.522	SGB
2185-53532-439	0.278	18.125	-0.232	0.001	-0.520	SGB
2185-53532-461	0.234	18.368	-0.241	-0.005	-0.546	SGB
2185-53532-462	0.273	18.194	-0.232	0.001	-0.519	SGB

Continued on next page...

Table B.1 – Continued

spSpec name	$(g - r)_0$	g_0	S(3839)	$\delta S(3839)$	CH(4300)	Type
(1)	(2)	(3)	(4)	(5)	(6)	(7)
2185-53532-481	0.270	18.195	-0.262	-0.028	-0.523	SGB
2185-53532-482	0.311	18.100	-0.236	-0.004	-0.514	SGB
2185-53532-487	0.271	18.319	-0.255	-0.019	-0.529	SGB
2185-53532-492	0.285	18.167	-0.263	-0.030	-0.520	SGB
2185-53532-493	0.219	18.347	-0.248	-0.011	-0.522	SGB
2185-53532-506	0.372	18.036	-0.184	0.047	-0.502	SGB
2185-53532-512	0.252	18.258	-0.254	-0.019	-0.515	SGB
2185-53532-520	0.261	18.398	-0.254	-0.016	-0.528	SGB
2185-53532-543	0.266	18.284	-0.216	0.020	-0.527	SGB
2185-53532-553	0.334	18.065	-0.214	0.018	-0.486	SGB
2185-53532-554	0.269	18.347	-0.249	-0.012	-0.533	SGB
2255-53565-103	0.383	17.974	-0.155	0.075	-0.509	SGB
2255-53565-115	0.394	17.934	-0.169	0.060	-0.506	SGB
2255-53565-173	0.453	17.636	-0.131	0.093	-0.428	SGB
2255-53565-424	0.424	17.789	-0.130	0.096	-0.429	SGB
2255-53565-425	0.396	17.915	-0.152	0.077	-0.433	SGB
2255-53565-432	0.389	17.981	-0.190	0.040	-0.451	SGB
2255-53565-466	0.391	17.856	-0.142	0.085	-0.482	SGB
2185-53532-106	0.275	19.687	-0.197	0.064	-0.494	MS
2185-53532-111	0.242	18.572	-0.259	-0.018	-0.541	MS
2185-53532-113	0.333	19.812	-0.193	0.070	-0.569	MS
2185-53532-116	0.258	19.363	-0.252	0.003	-0.506	MS

Continued on next page...

Table B.1 – Continued

spSpec name	$(g - r)_0$	g_0	S(3839)	$\delta S(3839)$	CH(4300)	Type
(1)	(2)	(3)	(4)	(5)	(6)	(7)
2185-53532-120	0.282	19.189	-0.280	-0.028	-0.534	MS
2185-53532-143	0.245	18.517	-0.186	0.053	-0.520	MS
2185-53532-146	0.294	19.753	-0.386	-0.124	-0.544	MS
2185-53532-148	0.251	18.997	-0.262	-0.013	-0.538	MS
2185-53532-150	0.238	18.782	-0.260	-0.015	-0.537	MS
2185-53532-151	0.279	19.422	-0.158	0.098	-0.535	MS
2185-53532-152	0.216	18.796	-0.268	-0.023	-0.542	MS
2185-53532-154	0.267	19.689	-0.238	0.023	-0.510	MS
2185-53532-156	0.267	19.033	-0.250	-0.001	-0.527	MS
2185-53532-158	0.252	18.930	-0.257	-0.010	-0.558	MS
2185-53532-160	0.236	19.196	-0.259	-0.007	-0.545	MS
2185-53532-161	0.260	19.647	-0.286	-0.026	-0.471	MS
2185-53532-167	0.224	18.742	-0.251	-0.008	-0.531	MS
2185-53532-169	0.251	19.007	-0.305	-0.056	-0.541	MS
2185-53532-171	0.293	19.837	-0.017	0.246	-0.516	MS
2185-53532-172	0.238	18.769	-0.278	-0.034	-0.522	MS
2185-53532-175	0.187	18.804	-0.277	-0.032	-0.529	MS
2185-53532-176	0.240	18.810	-0.300	-0.055	-0.514	MS
2185-53532-177	0.217	18.859	-0.294	-0.048	-0.522	MS
2185-53532-178	0.250	19.076	-0.268	-0.019	-0.547	MS
2185-53532-179	0.229	18.436	-0.262	-0.024	-0.527	MS
2185-53532-181	0.236	18.742	-0.324	-0.080	-0.520	MS

Continued on next page...

Table B.1 – Continued

spSpec name	$(g - r)_0$	g_0	S(3839)	$\delta S(3839)$	CH(4300)	Type
(1)	(2)	(3)	(4)	(5)	(6)	(7)
2185-53532-196	0.270	19.028	-0.258	-0.009	-0.522	MS
2185-53532-197	0.259	19.108	-0.282	-0.032	-0.534	MS
2185-53532-198	0.262	18.883	-0.276	-0.029	-0.523	MS
2185-53532-200	0.286	19.754	-0.174	0.088	-0.535	MS
2185-53532-390	0.263	19.372	-0.263	-0.008	-0.517	MS
2185-53532-393	0.375	19.913	-0.256	0.009	-0.514	MS
2185-53532-423	0.243	18.879	-0.278	-0.032	-0.534	MS
2185-53532-424	0.265	19.227	-0.259	-0.006	-0.540	MS
2185-53532-428	0.276	19.180	-0.235	0.016	-0.513	MS
2185-53532-430	0.296	19.686	-0.279	-0.019	-0.513	MS
2185-53532-431	0.288	19.867	-0.244	0.020	-0.505	MS
2185-53532-433	0.376	19.927	-0.260	0.005	-0.483	MS
2185-53532-435	0.245	19.031	-0.242	0.007	-0.519	MS
2185-53532-440	0.280	19.727	-0.269	-0.008	-0.507	MS
2185-53532-464	0.276	19.434	-0.261	-0.005	-0.523	MS
2185-53532-466	0.197	18.790	-0.219	0.025	-0.528	MS
2185-53532-469	0.233	18.983	-0.283	-0.035	-0.523	MS
2185-53532-473	0.266	19.259	-0.238	0.015	-0.535	MS
2185-53532-475	0.292	18.585	-0.257	-0.016	-0.515	MS
2185-53532-476	0.324	19.062	-0.210	0.040	-0.527	MS
2185-53532-477	0.311	19.570	-0.203	0.056	-0.503	MS
2185-53532-478	0.311	19.009	-0.193	0.056	-0.522	MS

Continued on next page...

Table B.1 – Continued

spSpec name	$(g - r)_0$	g_0	S(3839)	$\delta S(3839)$	CH(4300)	Type
(1)	(2)	(3)	(4)	(5)	(6)	(7)
2185-53532-479	0.331	19.447	-0.259	-0.003	-0.535	MS
2185-53532-480	0.300	19.678	-0.170	0.091	-0.500	MS
2185-53532-483	0.265	19.130	-0.226	0.025	-0.526	MS
2185-53532-485	0.230	18.446	-0.284	-0.046	-0.528	MS
2185-53532-486	0.232	19.404	-0.242	0.013	-0.521	MS
2185-53532-488	0.270	19.547	-0.214	0.044	-0.535	MS
2185-53532-489	0.217	19.029	-0.214	0.034	-0.497	MS
2185-53532-490	0.270	19.343	-0.202	0.053	-0.520	MS
2185-53532-494	0.287	19.210	-0.247	0.005	-0.521	MS
2185-53532-495	0.230	18.657	-0.261	-0.019	-0.534	MS
2185-53532-496	0.332	19.899	-0.254	0.010	-0.485	MS
2185-53532-497	0.320	19.585	-0.193	0.066	-0.486	MS
2185-53532-498	0.267	18.689	-0.257	-0.015	-0.537	MS
2185-53532-499	0.229	18.733	-0.253	-0.009	-0.540	MS
2185-53532-500	0.194	19.108	-0.252	-0.002	-0.518	MS
2185-53532-504	0.225	18.726	-0.258	-0.014	-0.508	MS
2185-53532-507	0.301	19.165	-0.170	0.082	-0.533	MS
2185-53532-508	0.167	18.999	-0.190	0.058	-0.522	MS
2185-53532-511	0.292	19.856	-0.243	0.021	-0.456	MS
2185-53532-513	0.272	18.920	-0.252	-0.005	-0.508	MS
2185-53532-514	0.254	19.263	-0.250	0.003	-0.521	MS
2185-53532-515	0.236	18.936	-0.250	-0.003	-0.540	MS

Continued on next page...

Table B.1 – Continued

spSpec name	$(g - r)_0$	g_0	S(3839)	$\delta S(3839)$	CH(4300)	Type
(1)	(2)	(3)	(4)	(5)	(6)	(7)
2185-53532-516	0.298	19.869	-0.226	0.038	-0.491	MS
2185-53532-517	0.315	19.904	-0.187	0.078	-0.469	MS
2185-53532-519	0.231	18.973	-0.203	0.045	-0.536	MS
2185-53532-534	0.281	18.601	-0.241	0.000	-0.525	MS
2185-53532-537	0.258	18.767	-0.228	0.016	-0.533	MS
2185-53532-539	0.278	19.508	-0.217	0.040	-0.494	MS
2185-53532-540	0.253	19.204	-0.257	-0.005	-0.518	MS
2185-53532-541	0.323	19.867	-0.196	0.068	-0.530	MS
2185-53532-542	0.312	19.432	-0.263	-0.007	-0.530	MS
2185-53532-544	0.243	18.847	-0.249	-0.003	-0.526	MS
2185-53532-545	0.292	19.061	-0.230	0.019	-0.513	MS
2185-53532-546	0.320	19.915	-0.247	0.018	-0.464	MS
2185-53532-547	0.360	19.909	-0.259	0.006	-0.483	MS
2185-53532-548	0.361	19.959	-0.124	0.142	-0.545	MS
2185-53532-549	0.382	19.507	-0.276	-0.018	-0.460	MS
2185-53532-550	0.286	19.738	-0.189	0.073	-0.486	MS
2185-53532-551	0.310	19.909	-0.143	0.122	-0.465	MS
2185-53532-552	0.251	18.899	-0.252	-0.005	-0.522	MS
2185-53532-555	0.303	19.342	-0.224	0.031	-0.515	MS
2185-53532-556	0.281	19.376	-0.238	0.017	-0.547	MS
2185-53532-557	0.266	18.690	-0.291	-0.048	-0.529	MS
2185-53532-558	0.264	18.577	-0.262	-0.022	-0.516	MS

Continued on next page...

Table B.1 – Continued

spSpec name	$(g - r)_0$	g_0	S(3839)	$\delta S(3839)$	CH(4300)	Type
(1)	(2)	(3)	(4)	(5)	(6)	(7)
2185-53532-559	0.254	18.915	-0.277	-0.030	-0.518	MS
2185-53532-560	0.261	18.421	-0.256	-0.018	-0.535	MS
2185-53532-575	0.349	19.769	-0.209	0.053	-0.542	MS
2185-53532-577	0.260	19.163	-0.253	-0.002	-0.515	MS
2185-53532-581	0.296	19.299	-0.228	0.026	-0.515	MS
2185-53532-584	0.199	19.257	-0.196	0.057	-0.522	MS
2185-53532-585	0.290	19.137	-0.245	0.006	-0.501	MS
2185-53532-587	0.293	19.806	-0.163	0.100	-0.498	MS
2185-53532-589	0.241	18.974	-0.238	0.010	-0.529	MS
2185-53532-591	0.228	18.773	-0.245	-0.001	-0.526	MS
2185-53532-592	0.247	19.454	-0.284	-0.028	-0.515	MS
2185-53532-593	0.229	18.893	-0.248	-0.001	-0.525	MS
2185-53532-594	0.293	19.523	-0.188	0.070	-0.517	MS
2185-53532-596	0.357	19.876	-0.301	-0.036	-0.494	MS
2185-53532-598	0.262	19.415	-0.201	0.055	-0.528	MS
2185-53532-599	0.263	19.391	-0.180	0.075	-0.508	MS
2185-53532-600	0.303	19.845	-0.234	0.030	-0.471	MS
2255-53565-436	0.369	20.193	-0.018	0.251	-0.423	MS
2255-53565-518	0.456	20.561	-0.159	0.117	-0.370	MS
			M3			
2475-53845-145	0.567	15.116	-0.096	-0.032	-0.468	AGB
2475-53845-150	0.635	14.933	-0.156	-0.115	-0.425	AGB

Continued on next page...

Table B.1 – Continued

spSpec name	$(g - r)_0$	g_0	S(3839)	$\delta S(3839)$	CH(4300)	Type
(1)	(2)	(3)	(4)	(5)	(6)	(7)
2475-53845-162	0.590	15.176	-0.113	-0.042	-0.425	AGB
2475-53845-173	0.636	15.115	-0.125	-0.061	-0.409	AGB
2475-53845-199	0.633	14.936	-0.024	0.017	-0.434	AGB
2475-53845-463	0.578	15.139	-0.150	-0.083	-0.455	AGB
2475-53845-471	0.576	15.103	-0.071	-0.009	-0.471	AGB
2475-53845-479	0.603	14.984	-0.138	-0.091	-0.439	AGB
2475-53845-486	0.569	14.507	0.168	0.155	-0.349	AGB
2475-53845-506	0.658	14.816	-0.082	-0.056	-0.398	AGB
2475-53845-511	0.613	15.134	-0.136	-0.069	-0.408	AGB
2475-53845-118	0.485	17.492	-0.229	0.134	-0.443	RGB
2475-53845-183	0.575	16.382	-0.244	-0.021	-0.371	RGB
2475-53845-185	0.508	17.131	-0.101	0.217	-0.398	RGB
2475-53845-192	0.574	16.891	-0.162	0.126	-0.394	RGB
2475-53845-200	0.508	17.238	0.034	0.365	-0.385	RGB
2475-53845-430	0.523	17.342	0.003	0.347	-0.443	RGB
2475-53845-469	0.528	16.634	-0.017	0.238	-0.387	RGB
2475-53845-487	0.486	17.760	-0.256	0.141	-0.438	RGB
2475-53845-501	0.550	16.335	-0.063	0.154	-0.375	RGB
2475-53845-507	0.491	17.033	-0.129	0.177	-0.401	RGB
2475-53845-550	0.461	17.683	-0.163	0.224	-0.395	RGB
2475-53845-557	0.545	16.703	0.077	0.340	-0.397	RGB
2475-53845-116	0.714	15.109	-0.014	0.049	-0.331	RGB

Continued on next page...

Table B.1 – Continued

spSpec name	$(g - r)_0$	g_0	S(3839)	$\delta S(3839)$	CH(4300)	Type
(1)	(2)	(3)	(4)	(5)	(6)	(7)
2475-53845-119	0.608	16.003	-0.177	-0.002	-0.350	RGB
2475-53845-120	0.575	16.254	-0.221	-0.013	-0.361	RGB
2475-53845-141	0.676	15.471	-0.099	0.009	-0.332	RGB
2475-53845-142	0.672	15.427	-0.058	0.045	-0.335	RGB
2475-53845-143	0.631	15.621	-0.166	-0.038	-0.336	RGB
2475-53845-144	0.624	15.915	-0.169	-0.004	-0.339	RGB
2475-53845-160	0.602	15.631	-0.200	-0.071	-0.349	RGB
2475-53845-171	0.684	15.421	-0.076	0.027	-0.331	RGB
2475-53845-176	0.740	14.720	-0.089	-0.075	-0.353	RGB
2475-53845-177	0.596	15.806	0.129	0.280	-0.338	RGB
2475-53845-178	0.624	15.715	-0.191	-0.052	-0.347	RGB
2475-53845-186	0.688	15.265	-0.108	-0.025	-0.331	RGB
2475-53845-196	0.645	15.513	-0.125	-0.011	-0.342	RGB
2475-53845-198	0.711	15.040	0.270	0.324	-0.389	RGB
2475-53845-421	0.755	14.656	0.007	0.013	-0.348	RGB
2475-53845-436	0.724	14.956	0.314	0.357	-0.346	RGB
2475-53845-440	0.686	15.039	0.245	0.299	-0.380	RGB
2475-53845-461	0.641	15.477	-0.147	-0.037	-0.373	RGB
2475-53845-466	0.650	15.360	-0.127	-0.033	-0.379	RGB
2475-53845-473	0.681	14.981	0.202	0.249	-0.373	RGB
2475-53845-475	0.636	15.547	-0.085	0.033	-0.374	RGB
2475-53845-480	0.638	15.350	0.204	0.297	-0.393	RGB

Continued on next page...

Table B.1 – Continued

spSpec name	$(g - r)_0$	g_0	S(3839)	$\delta S(3839)$	CH(4300)	Type
(1)	(2)	(3)	(4)	(5)	(6)	(7)
2475-53845-483	0.753	14.470	0.300	0.282	-0.389	RGB
2475-53845-488	0.602	15.680	-0.138	-0.003	-0.360	RGB
2475-53845-489	0.685	15.342	0.274	0.366	-0.368	RGB
2475-53845-496	0.677	15.134	-0.075	-0.009	-0.362	RGB
2475-53845-497	0.677	15.078	-0.043	0.016	-0.345	RGB
2475-53845-498	0.667	15.368	0.178	0.273	-0.377	RGB
2475-53845-509	0.640	15.615	-0.119	0.008	-0.345	RGB
2475-53845-514	0.570	16.109	0.017	0.206	-0.350	RGB
2475-53845-515	0.649	15.384	0.216	0.313	-0.394	RGB
2475-53845-518	0.728	15.058	0.020	0.076	-0.334	RGB
2475-53845-519	0.604	15.947	-0.186	-0.017	-0.354	RGB
2475-53845-520	0.599	16.177	-0.184	0.014	-0.344	RGB
2475-53845-551	0.686	15.296	-0.082	0.005	-0.351	RGB
2475-53845-558	0.602	16.075	-0.155	0.030	-0.368	RGB
2475-53845-559	0.627	15.713	-0.128	0.011	-0.353	RGB
			M71			
2338-53683-186	0.628	15.236	-0.206	-0.018	-0.307	RGB
2338-53683-199	0.628	15.533	-0.062	0.191	-0.312	RGB
2333-53682-191	0.770	14.282	-0.046	-0.067	-0.302	RGB
2333-53682-193	0.614	14.170	0.198	0.152	-0.380	RGB
2333-53682-198	0.644	14.494	0.376	0.401	-0.334	RGB
2333-53682-228	0.658	14.357	0.200	0.196	-0.354	RGB

Continued on next page...

Table B.1 – Continued

spSpec name	$(g - r)_0$	g_0	S(3839)	$\delta S(3839)$	CH(4300)	Type
(1)	(2)	(3)	(4)	(5)	(6)	(7)
2333-53682-229	0.657	14.488	0.160	0.184	-0.338	RGB
2338-53683-200	0.649	14.561	-0.003	0.037	-0.319	RGB

Table B.2: Line Index Uncertainties of Adopted True Member Stars

spSpec name	$\sigma(g)$	$\sigma(S(3839))$	$\sigma(CH(4300))$
(1)	(2)	(3)	(4)
M92			
2247-54169-362	0.011	0.031	0.013
2247-54169-364	0.015	0.015	0.008
2247-54169-367	0.009	0.018	0.008
2247-54169-380	0.010	0.016	0.008
2247-54169-404	0.010	0.016	0.009
2247-54169-444	0.011	0.010	0.006
2247-54169-451	0.008	0.013	0.007
2247-54169-452	0.009	0.014	0.006
2247-54169-529	0.008	0.028	0.010
2247-54169-531	0.007	0.019	0.008
2247-54169-546	0.007	0.025	0.011

Continued on next page...

Table B.2 – Continued

spSpec name	$\sigma(g)$	$\sigma(\text{S}(3839))$	$\sigma(\text{CH}(4300))$
(1)	(2)	(3)	(4)
2247-54169-561	0.010	0.020	0.007
2247-54169-573	0.013	0.012	0.006
2247-54169-581	0.007	0.018	0.009
2247-54169-589	0.010	0.025	0.012
2247-54169-620	0.005	0.033	0.013
2247-54169-408	0.010	0.009	0.005
2247-54169-418	0.008	0.009	0.004
2247-54169-449	0.006	0.010	0.006
2247-54169-484	0.011	0.008	0.005
2247-54169-504	0.011	0.010	0.005
2247-54169-563	0.007	0.009	0.005
2247-54169-608	0.003	0.011	0.006
2247-54169-610	0.004	0.009	0.005
2247-54169-379	0.011	0.033	0.013
2247-54169-458	0.010	0.035	0.016
2247-54169-514	0.021	0.029	0.013
2247-54169-516	0.016	0.033	0.015
2247-54169-519	0.018	0.043	0.018
2247-54169-538	0.007	0.044	0.021
2247-54169-541	0.009	0.035	0.016
2247-54169-575	0.006	0.047	0.021
2247-54169-584	0.006	0.043	0.016

Continued on next page...

Table B.2 – Continued

spSpec name	$\sigma(g)$	$\sigma(\text{S}(3839))$	$\sigma(\text{CH}(4300))$
(1)	(2)	(3)	(4)
2247-54169-616	0.008	0.040	0.016
2256-53859-513	0.021	0.021	0.011
2256-53859-522	0.012	0.031	0.014
2256-53859-535	0.009	0.032	0.014
2256-53859-536	0.013	0.027	0.015
2256-53859-538	0.006	0.022	0.011
2247-54169-409	0.022	0.045	0.022
2256-53859-411	0.012	0.037	0.016
2256-53859-455	0.014	0.033	0.017
2256-53859-485	0.018	0.057	0.023
2256-53859-489	0.011	0.059	0.026
2256-53859-501	0.010	0.042	0.016
2256-53859-506	0.016	0.044	0.020
2256-53859-530	0.008	0.039	0.020
2256-53859-537	0.012	0.043	0.021
2256-53859-539	0.009	0.041	0.019
2256-53859-546	0.017	0.042	0.019
2256-53859-566	0.012	0.045	0.021
2256-53859-571	0.008	0.037	0.015
2256-53859-575	0.009	0.041	0.019
2256-53859-576	0.009	0.033	0.016
2256-53859-579	0.014	0.040	0.020

Continued on next page...

Table B.2 – Continued

spSpec name	$\sigma(g)$	$\sigma(\text{S}(3839))$	$\sigma(\text{CH}(4300))$
(1)	(2)	(3)	(4)
2256-53859-612	0.008	0.041	0.019
M15			
1960-53289-441	0.011	0.033	0.013
1960-53289-457	0.011	0.034	0.013
1960-53289-500	0.012	0.017	0.008
1960-53289-522	0.011	0.022	0.012
1960-53289-530	0.015	0.025	0.010
1962-53321-364	0.014	0.014	0.007
1962-53321-375	0.008	0.016	0.007
1962-53321-376	0.009	0.014	0.007
1962-53321-402	0.011	0.021	0.008
1962-53321-403	0.011	0.022	0.009
1962-53321-406	0.014	0.018	0.009
1962-53321-413	0.011	0.015	0.007
1962-53321-415	0.014	0.012	0.006
1962-53321-427	0.013	0.014	0.007
1962-53321-438	0.015	0.014	0.006
1962-53321-454	0.011	0.016	0.007
1962-53321-466	0.010	0.014	0.005
1962-53321-474	0.015	0.014	0.006
1962-53321-506	0.009	0.011	0.006
1962-53321-515	0.010	0.014	0.006

Continued on next page...

Table B.2 – Continued

spSpec name	$\sigma(g)$	$\sigma(\text{S}(3839))$	$\sigma(\text{CH}(4300))$
(1)	(2)	(3)	(4)
1962-53321-532	0.012	0.013	0.005
1960-53289-401	0.008	0.009	0.005
1960-53289-402	0.008	0.008	0.004
1960-53289-406	0.007	0.007	0.004
1960-53289-413	0.007	0.009	0.005
1960-53289-419	0.008	0.007	0.004
1960-53289-442	0.008	0.015	0.006
1960-53289-459	0.009	0.006	0.003
1960-53289-460	0.009	0.012	0.007
1960-53289-511	0.009	0.014	0.007
1960-53289-523	0.009	0.008	0.004
1960-53289-529	0.010	0.007	0.004
1960-53289-420	0.011	0.040	0.017
1960-53289-501	0.011	0.039	0.016
1962-53321-323	0.016	0.023	0.009
1962-53321-328	0.014	0.026	0.013
1962-53321-329	0.011	0.025	0.012
1962-53321-335	0.014	0.024	0.009
1962-53321-368	0.014	0.026	0.012
1962-53321-369	0.016	0.031	0.012
1962-53321-370	0.015	0.022	0.011
1962-53321-371	0.017	0.029	0.012

Continued on next page...

Table B.2 – Continued

spSpec name	$\sigma(g)$	$\sigma(\text{S}(3839))$	$\sigma(\text{CH}(4300))$
(1)	(2)	(3)	(4)
1962-53321-372	0.012	0.022	0.011
1962-53321-407	0.013	0.029	0.013
1962-53321-414	0.017	0.025	0.011
1962-53321-421	0.015	0.027	0.012
1962-53321-423	0.013	0.022	0.009
1962-53321-442	0.015	0.034	0.013
1962-53321-469	0.013	0.024	0.012
1962-53321-470	0.017	0.022	0.011
1962-53321-488	0.020	0.029	0.012
1962-53321-493	0.013	0.020	0.009
1962-53321-495	0.015	0.030	0.011
1962-53321-496	0.015	0.026	0.014
1962-53321-497	0.015	0.030	0.013
1962-53321-500	0.013	0.020	0.009
1962-53321-510	0.012	0.023	0.010
1962-53321-516	0.011	0.022	0.009
1962-53321-518	0.011	0.019	0.008
1962-53321-520	0.013	0.023	0.010
1962-53321-533	0.012	0.023	0.010
1962-53321-549	0.028	0.022	0.010
1962-53321-550	0.011	0.021	0.009
1962-53321-558	0.010	0.020	0.009

Continued on next page...

Table B.2 – Continued

spSpec name	$\sigma(g)$	$\sigma(\text{S}(3839))$	$\sigma(\text{CH}(4300))$
(1)	(2)	(3)	(4)
1962-53321-339	0.019	0.036	0.015
1962-53321-363	0.021	0.048	0.020
1962-53321-378	0.016	0.038	0.016
1962-53321-399	0.017	0.032	0.014
1962-53321-409	0.015	0.043	0.020
1962-53321-412	0.016	0.044	0.017
1962-53321-416	0.018	0.043	0.017
1962-53321-419	0.017	0.048	0.022
1962-53321-422	0.021	0.043	0.017
1962-53321-424	0.018	0.034	0.017
1962-53321-428	0.015	0.035	0.017
1962-53321-430	0.019	0.042	0.020
1962-53321-445	0.017	0.048	0.023
1962-53321-449	0.023	0.056	0.022
1962-53321-460	0.026	0.043	0.022
1962-53321-465	0.015	0.032	0.015
1962-53321-471	0.013	0.026	0.013
1962-53321-478	0.024	0.067	0.025
1962-53321-480	0.018	0.031	0.014
1962-53321-483	0.016	0.050	0.021
1962-53321-484	0.016	0.035	0.016
1962-53321-490	0.015	0.030	0.012

Continued on next page...

Table B.2 – Continued

spSpec name	$\sigma(g)$	$\sigma(\text{S}(3839))$	$\sigma(\text{CH}(4300))$
(1)	(2)	(3)	(4)
1962-53321-503	0.014	0.032	0.014
1962-53321-505	0.016	0.047	0.020
1962-53321-509	0.015	0.042	0.018
1962-53321-512	0.017	0.051	0.021
1962-53321-519	0.016	0.034	0.015
1962-53321-522	0.016	0.051	0.020
1962-53321-539	0.013	0.028	0.010
1962-53321-540	0.016	0.040	0.018
1962-53321-543	0.013	0.031	0.013
1962-53321-545	0.014	0.032	0.014
1962-53321-554	0.016	0.037	0.018
1962-53321-555	0.017	0.052	0.020
NGC 5053			
2476-53826-486	0.009	0.043	0.019
2476-53826-497	0.011	0.064	0.025
2476-53826-488	0.017	0.015	0.006
2476-53826-501	0.008	0.012	0.006
2476-53826-505	0.009	0.016	0.007
2476-53826-507	0.009	0.020	0.009
2476-53826-508	0.009	0.022	0.010
2476-53826-519	0.011	0.010	0.005
2476-53826-527	0.023	0.013	0.007

Continued on next page...

Table B.2 – Continued

spSpec name	$\sigma(g)$	$\sigma(\text{S}(3839))$	$\sigma(\text{CH}(4300))$
(1)	(2)	(3)	(4)
2476-53826-573	0.012	0.024	0.011
2476-53826-575	0.007	0.013	0.006
2476-53826-577	0.028	0.023	0.010
2476-53826-578	0.015	0.012	0.006
	M53		
2476-53826-329	0.027	0.068	0.025
2476-53826-405	0.017	0.078	0.032
2476-53826-413	0.017	0.062	0.019
2476-53826-418	0.017	0.079	0.028
2476-53826-361	0.018	0.037	0.014
2476-53826-372	0.018	0.025	0.013
2476-53826-375	0.018	0.041	0.014
2476-53826-378	0.018	0.018	0.006
2476-53826-401	0.017	0.039	0.017
2476-53826-404	0.018	0.018	0.007
2476-53826-409	0.017	0.044	0.017
2476-53826-451	0.019	0.029	0.014
2476-53826-452	0.017	0.042	0.017
	M2		
1961-53299-140	0.019	0.020	0.008
1961-53299-213	0.008	0.019	0.008
1963-54331-098	0.015	0.021	0.007

Continued on next page...

Table B.2 – Continued

spSpec name	$\sigma(g)$	$\sigma(\text{S}(3839))$	$\sigma(\text{CH}(4300))$
(1)	(2)	(3)	(4)
1963-54331-121	0.013	0.018	0.006
1963-54331-126	0.023	0.033	0.013
1963-54331-128	0.022	0.032	0.012
1963-54331-131	0.012	0.032	0.011
1963-54331-137	0.008	0.022	0.010
1963-54331-139	0.008	0.025	0.010
1963-54331-144	0.016	0.020	0.008
1963-54331-164	0.022	0.029	0.013
1963-54331-178	0.016	0.037	0.014
1963-54331-204	0.011	0.023	0.009
1963-54331-208	0.009	0.022	0.009
1963-54331-209	0.012	0.027	0.012
1963-54331-211	0.011	0.028	0.011
1963-54331-217	0.009	0.019	0.010
1963-54331-218	0.008	0.023	0.011
1961-53299-124	0.020	0.013	0.005
1961-53299-125	0.006	0.011	0.005
1961-53299-131	0.008	0.013	0.008
1961-53299-134	0.015	0.008	0.004
1961-53299-136	0.011	0.019	0.008
1961-53299-144	0.008	0.017	0.008
1961-53299-152	0.022	0.014	0.006

Continued on next page...

Table B.2 – Continued

spSpec name	$\sigma(g)$	$\sigma(\text{S}(3839))$	$\sigma(\text{CH}(4300))$
(1)	(2)	(3)	(4)
1961-53299-159	0.009	0.018	0.007
1961-53299-215	0.009	0.013	0.005
1963-54331-043	0.027	0.043	0.015
1963-54331-083	0.015	0.041	0.019
1963-54331-090	0.014	0.035	0.016
1963-54331-091	0.026	0.040	0.014
1963-54331-096	0.013	0.040	0.017
1963-54331-100	0.012	0.044	0.015
1963-54331-102	0.017	0.052	0.017
1963-54331-114	0.019	0.054	0.018
1963-54331-123	0.009	0.043	0.018
1963-54331-124	0.016	0.049	0.017
1963-54331-143	0.016	0.040	0.017
1963-54331-145	0.015	0.047	0.018
1963-54331-146	0.013	0.053	0.020
1963-54331-147	0.017	0.049	0.020
1963-54331-148	0.014	0.046	0.020
1963-54331-150	0.015	0.068	0.029
1963-54331-179	0.016	0.050	0.018
1963-54331-180	0.013	0.037	0.013
1963-54331-181	0.015	0.038	0.016
1963-54331-184	0.012	0.037	0.013

Continued on next page...

Table B.2 – Continued

spSpec name	$\sigma(g)$	$\sigma(\text{S}(3839))$	$\sigma(\text{CH}(4300))$
(1)	(2)	(3)	(4)
1963-54331-189	0.017	0.047	0.018
1963-54331-194	0.015	0.047	0.019
1963-54331-196	0.015	0.046	0.020
1963-54331-201	0.011	0.033	0.015
1963-54331-206	0.012	0.048	0.023
1963-54331-212	0.012	0.038	0.013
1963-54331-223	0.019	0.045	0.022
1963-54331-254	0.019	0.055	0.021
1963-54331-041	0.028	0.070	0.024
1963-54331-045	0.027	0.055	0.019
1963-54331-082	0.028	0.067	0.023
1963-54331-154	0.023	0.067	0.025
1963-54331-156	0.020	0.059	0.024
1963-54331-162	0.022	0.069	0.025
1963-54331-169	0.018	0.061	0.024
1963-54331-170	0.017	0.059	0.022
1963-54331-185	0.018	0.059	0.022
1963-54331-186	0.022	0.061	0.024
1963-54331-197	0.019	0.061	0.022
1963-54331-200	0.020	0.056	0.025
1963-54331-207	0.015	0.067	0.022
1963-54331-220	0.014	0.048	0.018

Continued on next page...

Table B.2 – Continued

spSpec name	$\sigma(g)$	$\sigma(\text{S}(3839))$	$\sigma(\text{CH}(4300))$
(1)	(2)	(3)	(4)
1963-54331-222	0.017	0.049	0.021
M13			
2174-53521-087	0.016	0.026	0.010
2174-53521-094	0.016	0.022	0.008
2174-53521-121	0.011	0.013	0.006
2174-53521-126	0.013	0.019	0.009
2174-53521-128	0.008	0.041	0.013
2174-53521-133	0.008	0.017	0.007
2174-53521-134	0.011	0.019	0.010
2174-53521-155	0.007	0.016	0.007
2174-53521-407	0.009	0.011	0.006
2174-53521-412	0.016	0.023	0.009
2174-53521-414	0.016	0.018	0.009
2174-53521-456	0.014	0.019	0.008
2174-53521-461	0.009	0.020	0.010
2174-53521-471	0.006	0.011	0.006
2174-53521-480	0.009	0.016	0.007
2174-53521-529	0.020	0.011	0.006
2174-53521-563	0.015	0.013	0.006
2255-53565-114	0.012	0.019	0.009
2255-53565-116	0.009	0.013	0.005
2255-53565-437	0.009	0.025	0.010

Continued on next page...

Table B.2 – Continued

spSpec name	$\sigma(g)$	$\sigma(\text{S}(3839))$	$\sigma(\text{CH}(4300))$
(1)	(2)	(3)	(4)
2255-53565-476	0.009	0.021	0.009
2255-53565-490	0.007	0.009	0.005
2255-53565-556	0.007	0.018	0.007
2255-53565-597	0.006	0.011	0.006
2174-53521-082	0.013	0.010	0.004
2174-53521-093	0.012	0.008	0.004
2174-53521-098	0.009	0.008	0.004
2174-53521-137	0.006	0.009	0.004
2174-53521-145	0.012	0.007	0.004
2174-53521-154	0.005	0.009	0.004
2174-53521-156	0.006	0.010	0.005
2174-53521-158	0.015	0.010	0.006
2174-53521-159	0.008	0.008	0.004
2174-53521-160	0.007	0.008	0.004
2174-53521-166	0.005	0.009	0.005
2174-53521-167	0.010	0.008	0.005
2174-53521-168	0.012	0.009	0.005
2174-53521-171	0.011	0.007	0.004
2174-53521-172	0.010	0.009	0.004
2174-53521-176	0.005	0.011	0.005
2174-53521-215	0.016	0.008	0.005
2174-53521-376	0.015	0.008	0.004

Continued on next page...

Table B.2 – Continued

spSpec name	$\sigma(g)$	$\sigma(\text{S}(3839))$	$\sigma(\text{CH}(4300))$
(1)	(2)	(3)	(4)
2174-53521-410	0.008	0.007	0.005
2174-53521-413	0.012	0.008	0.005
2174-53521-443	0.015	0.007	0.004
2174-53521-449	0.014	0.007	0.004
2174-53521-452	0.013	0.007	0.003
2174-53521-453	0.021	0.007	0.004
2174-53521-455	0.009	0.007	0.005
2174-53521-457	0.011	0.006	0.004
2174-53521-458	0.014	0.006	0.004
2174-53521-459	0.016	0.007	0.004
2174-53521-460	0.012	0.006	0.004
2174-53521-462	0.014	0.006	0.004
2174-53521-463	0.005	0.010	0.004
2174-53521-470	0.007	0.006	0.004
2174-53521-476	0.008	0.008	0.005
2174-53521-477	0.006	0.008	0.005
2174-53521-478	0.008	0.008	0.005
2174-53521-483	0.013	0.007	0.004
2174-53521-484	0.015	0.007	0.004
2174-53521-485	0.016	0.007	0.004
2174-53521-488	0.013	0.008	0.005
2174-53521-489	0.009	0.009	0.004

Continued on next page...

Table B.2 – Continued

spSpec name	$\sigma(g)$	$\sigma(\text{S}(3839))$	$\sigma(\text{CH}(4300))$
(1)	(2)	(3)	(4)
2174-53521-493	0.024	0.006	0.003
2174-53521-494	0.019	0.007	0.004
2174-53521-495	0.015	0.009	0.005
2174-53521-497	0.009	0.008	0.004
2174-53521-498	0.006	0.007	0.004
2174-53521-499	0.014	0.007	0.004
2174-53521-500	0.011	0.006	0.004
2174-53521-522	0.010	0.008	0.004
2174-53521-530	0.004	0.007	0.004
2174-53521-531	0.006	0.008	0.004
2174-53521-537	0.007	0.007	0.004
2174-53521-538	0.003	0.006	0.005
2174-53521-542	0.010	0.007	0.004
2174-53521-554	0.009	0.008	0.004
2255-53565-112	0.012	0.045	0.021
2255-53565-120	0.009	0.008	0.005
2255-53565-143	0.011	0.010	0.005
2255-53565-144	0.015	0.009	0.004
2255-53565-148	0.007	0.010	0.005
2255-53565-153	0.008	0.010	0.004
2255-53565-157	0.007	0.007	0.003
2255-53565-171	0.007	0.007	0.004

Continued on next page...

Table B.2 – Continued

spSpec name	$\sigma(g)$	$\sigma(\text{S}(3839))$	$\sigma(\text{CH}(4300))$
(1)	(2)	(3)	(4)
2255-53565-175	0.005	0.009	0.005
2255-53565-426	0.012	0.007	0.004
2255-53565-483	0.014	0.007	0.004
2255-53565-485	0.009	0.010	0.005
2255-53565-486	0.004	0.056	0.018
2255-53565-495	0.022	0.039	0.012
2255-53565-496	0.007	0.034	0.011
2255-53565-504	0.005	0.036	0.011
2255-53565-510	0.005	0.008	0.005
2255-53565-512	0.006	0.046	0.017
2255-53565-515	0.008	0.011	0.004
2255-53565-520	0.015	0.042	0.014
2255-53565-542	0.010	0.007	0.004
2255-53565-543	0.009	0.008	0.004
2255-53565-544	0.015	0.044	0.017
2255-53565-545	0.007	0.008	0.004
2255-53565-548	0.009	0.008	0.005
2255-53565-550	0.013	0.007	0.004
2255-53565-551	0.006	0.007	0.004
2255-53565-552	0.005	0.034	0.010
2255-53565-553	0.007	0.006	0.003
2255-53565-557	0.003	0.039	0.016

Continued on next page...

Table B.2 – Continued

spSpec name	$\sigma(g)$	$\sigma(\text{S}(3839))$	$\sigma(\text{CH}(4300))$
(1)	(2)	(3)	(4)
2255-53565-559	0.014	0.028	0.009
2255-53565-586	0.009	0.025	0.011
2255-53565-589	0.004	0.007	0.004
2174-53521-054	0.014	0.031	0.012
2174-53521-131	0.010	0.008	0.004
2174-53521-146	0.013	0.033	0.012
2174-53521-149	0.013	0.035	0.015
2174-53521-174	0.017	0.039	0.016
2174-53521-368	0.016	0.023	0.011
2174-53521-402	0.009	0.027	0.012
2174-53521-403	0.010	0.028	0.012
2174-53521-406	0.008	0.022	0.012
2174-53521-445	0.011	0.026	0.011
2174-53521-447	0.011	0.025	0.011
2174-53521-474	0.008	0.022	0.010
2174-53521-481	0.010	0.039	0.014
2174-53521-533	0.009	0.030	0.012
2174-53521-539	0.007	0.021	0.012
2174-53521-560	0.008	0.019	0.009
2174-53521-565	0.008	0.020	0.013
2174-53521-573	0.014	0.026	0.012
2174-53521-576	0.007	0.022	0.011

Continued on next page...

Table B.2 – Continued

spSpec name	$\sigma(g)$	$\sigma(\text{S}(3839))$	$\sigma(\text{CH}(4300))$
(1)	(2)	(3)	(4)
2174-53521-577	0.009	0.024	0.012
2185-53532-141	0.019	0.020	0.008
2185-53532-153	0.015	0.015	0.006
2185-53532-237	0.017	0.018	0.007
2185-53532-388	0.016	0.015	0.007
2185-53532-425	0.022	0.014	0.007
2185-53532-426	0.016	0.013	0.006
2185-53532-427	0.016	0.013	0.006
2185-53532-439	0.016	0.012	0.006
2185-53532-461	0.010	0.014	0.006
2185-53532-462	0.018	0.014	0.006
2185-53532-481	0.008	0.014	0.006
2185-53532-482	0.008	0.015	0.007
2185-53532-487	0.010	0.016	0.007
2185-53532-492	0.015	0.011	0.006
2185-53532-493	0.013	0.013	0.007
2185-53532-506	0.012	0.012	0.006
2185-53532-512	0.010	0.012	0.006
2185-53532-520	0.013	0.013	0.007
2185-53532-543	0.010	0.014	0.007
2185-53532-553	0.011	0.012	0.006
2185-53532-554	0.012	0.015	0.006

Continued on next page...

Table B.2 – Continued

spSpec name	$\sigma(g)$	$\sigma(\text{S}(3839))$	$\sigma(\text{CH}(4300))$
(1)	(2)	(3)	(4)
2255-53565-103	0.014	0.030	0.013
2255-53565-115	0.014	0.030	0.012
2255-53565-173	0.012	0.041	0.016
2255-53565-424	0.011	0.032	0.015
2255-53565-425	0.010	0.030	0.012
2255-53565-432	0.011	0.032	0.014
2255-53565-466	0.020	0.027	0.013
2185-53532-106	0.019	0.048	0.020
2185-53532-111	0.016	0.028	0.011
2185-53532-113	0.020	0.072	0.027
2185-53532-116	0.018	0.041	0.016
2185-53532-120	0.018	0.036	0.015
2185-53532-143	0.018	0.022	0.010
2185-53532-146	0.021	0.051	0.021
2185-53532-148	0.016	0.024	0.011
2185-53532-150	0.021	0.025	0.010
2185-53532-151	0.018	0.038	0.016
2185-53532-152	0.016	0.024	0.011
2185-53532-154	0.020	0.052	0.018
2185-53532-156	0.012	0.027	0.011
2185-53532-158	0.013	0.024	0.012
2185-53532-160	0.014	0.032	0.013

Continued on next page...

Table B.2 – Continued

spSpec name	$\sigma(g)$	$\sigma(\text{S}(3839))$	$\sigma(\text{CH}(4300))$
(1)	(2)	(3)	(4)
2185-53532-161	0.015	0.048	0.024
2185-53532-167	0.015	0.022	0.011
2185-53532-169	0.016	0.027	0.012
2185-53532-171	0.015	0.055	0.020
2185-53532-172	0.018	0.021	0.011
2185-53532-175	0.011	0.026	0.010
2185-53532-176	0.011	0.024	0.009
2185-53532-177	0.010	0.024	0.010
2185-53532-178	0.017	0.028	0.010
2185-53532-179	0.018	0.018	0.008
2185-53532-181	0.018	0.024	0.012
2185-53532-196	0.018	0.033	0.013
2185-53532-197	0.019	0.035	0.015
2185-53532-198	0.018	0.025	0.009
2185-53532-200	0.022	0.047	0.024
2185-53532-390	0.018	0.045	0.019
2185-53532-393	0.025	0.057	0.023
2185-53532-423	0.017	0.018	0.010
2185-53532-424	0.106	0.022	0.009
2185-53532-428	0.018	0.028	0.011
2185-53532-430	0.020	0.047	0.020
2185-53532-431	0.018	0.052	0.020

Continued on next page...

Table B.2 – Continued

spSpec name	$\sigma(g)$	$\sigma(\text{S}(3839))$	$\sigma(\text{CH}(4300))$
(1)	(2)	(3)	(4)
2185-53532-433	0.023	0.050	0.023
2185-53532-435	0.011	0.027	0.013
2185-53532-440	0.015	0.045	0.018
2185-53532-464	0.018	0.036	0.015
2185-53532-466	0.019	0.025	0.010
2185-53532-469	0.010	0.031	0.014
2185-53532-473	0.015	0.030	0.012
2185-53532-475	0.017	0.020	0.008
2185-53532-476	0.018	0.026	0.012
2185-53532-477	0.019	0.043	0.016
2185-53532-478	0.019	0.024	0.010
2185-53532-479	0.018	0.037	0.014
2185-53532-480	0.020	0.041	0.018
2185-53532-483	0.014	0.030	0.012
2185-53532-485	0.011	0.012	0.007
2185-53532-486	0.018	0.035	0.014
2185-53532-488	0.019	0.040	0.017
2185-53532-489	0.013	0.025	0.011
2185-53532-490	0.016	0.029	0.015
2185-53532-494	0.013	0.025	0.011
2185-53532-495	0.012	0.018	0.009
2185-53532-496	0.020	0.049	0.020

Continued on next page...

Table B.2 – Continued

spSpec name	$\sigma(g)$	$\sigma(\text{S}(3839))$	$\sigma(\text{CH}(4300))$
(1)	(2)	(3)	(4)
2185-53532-497	0.025	0.037	0.017
2185-53532-498	0.010	0.017	0.008
2185-53532-499	0.015	0.021	0.009
2185-53532-500	0.027	0.012	0.007
2185-53532-504	0.021	0.017	0.008
2185-53532-507	0.015	0.024	0.011
2185-53532-508	0.014	0.022	0.010
2185-53532-511	0.022	0.040	0.015
2185-53532-513	0.012	0.020	0.010
2185-53532-514	0.016	0.026	0.012
2185-53532-515	0.013	0.021	0.011
2185-53532-516	0.017	0.051	0.022
2185-53532-517	0.019	0.043	0.020
2185-53532-519	0.012	0.019	0.011
2185-53532-534	0.019	0.015	0.008
2185-53532-537	0.016	0.019	0.010
2185-53532-539	0.021	0.038	0.014
2185-53532-540	0.020	0.030	0.014
2185-53532-541	0.024	0.051	0.019
2185-53532-542	0.017	0.034	0.013
2185-53532-544	0.011	0.022	0.010
2185-53532-545	0.021	0.023	0.010

Continued on next page...

Table B.2 – Continued

spSpec name	$\sigma(g)$	$\sigma(\text{S}(3839))$	$\sigma(\text{CH}(4300))$
(1)	(2)	(3)	(4)
2185-53532-546	0.017	0.043	0.021
2185-53532-547	0.024	0.042	0.015
2185-53532-548	0.023	0.044	0.025
2185-53532-549	0.018	0.034	0.017
2185-53532-550	0.019	0.042	0.017
2185-53532-551	0.022	0.045	0.020
2185-53532-552	0.012	0.024	0.011
2185-53532-555	0.019	0.029	0.012
2185-53532-556	0.018	0.029	0.013
2185-53532-557	0.014	0.018	0.009
2185-53532-558	0.009	0.016	0.008
2185-53532-559	0.011	0.024	0.009
2185-53532-560	0.013	0.014	0.007
2185-53532-575	0.024	0.050	0.018
2185-53532-577	0.017	0.023	0.011
2185-53532-581	0.018	0.030	0.012
2185-53532-584	0.014	0.029	0.012
2185-53532-585	0.014	0.026	0.012
2185-53532-587	0.023	0.051	0.021
2185-53532-589	0.012	0.022	0.012
2185-53532-591	0.013	0.020	0.010
2185-53532-592	0.015	0.032	0.016

Continued on next page...

Table B.2 – Continued

spSpec name	$\sigma(g)$	$\sigma(\text{S}(3839))$	$\sigma(\text{CH}(4300))$
(1)	(2)	(3)	(4)
2185-53532-593	0.012	0.023	0.009
2185-53532-594	0.023	0.033	0.017
2185-53532-596	0.020	0.042	0.022
2185-53532-598	0.020	0.032	0.016
2185-53532-599	0.017	0.036	0.015
2185-53532-600	0.019	0.051	0.019
2255-53565-436	0.022	0.050	0.016
2255-53565-518	0.035	0.038	0.014
M3			
2475-53845-145	0.006	0.015	0.006
2475-53845-150	0.006	0.013	0.005
2475-53845-162	0.022	0.016	0.007
2475-53845-173	0.007	0.014	0.005
2475-53845-199	0.010	0.015	0.006
2475-53845-463	0.008	0.012	0.006
2475-53845-471	0.005	0.012	0.005
2475-53845-479	0.012	0.010	0.005
2475-53845-486	0.014	0.011	0.004
2475-53845-506	0.005	0.008	0.004
2475-53845-511	0.005	0.012	0.005
2475-53845-118	0.015	0.092	0.030
2475-53845-183	0.011	0.032	0.013

Continued on next page...

Table B.2 – Continued

spSpec name	$\sigma(g)$	$\sigma(\text{S}(3839))$	$\sigma(\text{CH}(4300))$
(1)	(2)	(3)	(4)
2475-53845-185	0.011	0.067	0.023
2475-53845-192	0.024	0.052	0.021
2475-53845-200	0.009	0.069	0.021
2475-53845-430	0.024	0.071	0.021
2475-53845-469	0.007	0.032	0.013
2475-53845-487	0.006	0.098	0.030
2475-53845-501	0.007	0.028	0.010
2475-53845-507	0.005	0.052	0.018
2475-53845-550	0.017	0.076	0.026
2475-53845-557	0.006	0.042	0.012
2475-53845-116	0.014	0.015	0.006
2475-53845-119	0.004	0.031	0.009
2475-53845-120	0.005	0.033	0.011
2475-53845-141	0.022	0.028	0.010
2475-53845-142	0.014	0.022	0.009
2475-53845-143	0.010	0.024	0.009
2475-53845-144	0.005	0.030	0.011
2475-53845-160	0.020	0.022	0.009
2475-53845-171	0.005	0.028	0.010
2475-53845-176	0.013	0.013	0.006
2475-53845-177	0.005	0.027	0.009
2475-53845-178	0.013	0.025	0.009

Continued on next page...

Table B.2 – Continued

spSpec name	$\sigma(g)$	$\sigma(\text{S}(3839))$	$\sigma(\text{CH}(4300))$
(1)	(2)	(3)	(4)
2475-53845-186	0.006	0.021	0.008
2475-53845-196	0.011	0.019	0.007
2475-53845-198	0.016	0.016	0.006
2475-53845-421	0.014	0.012	0.005
2475-53845-436	0.011	0.018	0.007
2475-53845-440	0.010	0.018	0.006
2475-53845-461	0.009	0.018	0.007
2475-53845-466	0.012	0.018	0.006
2475-53845-473	0.005	0.013	0.005
2475-53845-475	0.004	0.016	0.006
2475-53845-480	0.007	0.020	0.006
2475-53845-483	0.010	0.013	0.005
2475-53845-488	0.005	0.020	0.009
2475-53845-489	0.011	0.018	0.006
2475-53845-496	0.005	0.015	0.005
2475-53845-497	0.013	0.014	0.006
2475-53845-498	0.005	0.018	0.006
2475-53845-509	0.006	0.015	0.007
2475-53845-514	0.005	0.025	0.009
2475-53845-515	0.005	0.020	0.006
2475-53845-518	0.004	0.015	0.005
2475-53845-519	0.007	0.019	0.009

Continued on next page...

Table B.2 – Continued

spSpec name	$\sigma(g)$	$\sigma(\text{S}(3839))$	$\sigma(\text{CH}(4300))$
(1)	(2)	(3)	(4)
2475-53845-520	0.008	0.024	0.009
2475-53845-551	0.007	0.016	0.006
2475-53845-558	0.004	0.024	0.008
2475-53845-559	0.006	0.018	0.007
M71			
2338-53683-186	0.005	0.024	0.010
2338-53683-199	0.005	0.040	0.012
2333-53682-191	0.007	0.030	0.007
2333-53682-193	0.006	0.020	0.006
2333-53682-198	0.006	0.035	0.009
2333-53682-228	0.007	0.025	0.007
2333-53682-229	0.004	0.023	0.007
2338-53683-200	0.013	0.019	0.006

BIBLIOGRAPHY

BIBLIOGRAPHY

- Abazajian, K. N., et al. 2009, ApJS, 182, 543
—. 2004, AJ, 128, 502
—. 2005, AJ, 129, 1755
—. 2003, AJ, 126, 2081
- Adelman-McCarthy, J. K., et al. 2008, ApJS, 175, 297
—. 2007, ApJS, 172, 634
—. 2006, ApJS, 162, 38
- Aihara, H., et al. 2011, ApJS, 193, 29
- Allende Prieto, C., et al. 2008, AJ, 136, 2070
- Alves-Brito, A., Schiavon, R. P., Castilho, B., & Barbuy, B. 2008, A&A, 486, 941
- An, D., et al. 2008, ApJS, 179, 326
—. 2009, ApJ, 700, 523
- Arp, H. C., & Johnson, H. L. 1955, ApJ, 122, 171
- Ashman, K. M., Bird, C. M., & Zepf, S. E. 1994, AJ, 108, 2348
- Barrado y Navascués, D., Deliyannis, C. P., & Stauffer, J. R. 2001, ApJ, 549, 452
- Bedin, L. R., Piotto, G., Anderson, J., King, I. R., Cassisi, S., & Momany, Y. 2004, Memorie della Societa Astronomica Italiana Supplementi, 5, 105
- Bellman, S., Briley, M. M., Smith, G. H., & Claver, C. F. 2001, PASP, 113, 326
- Binney, J., & Tremaine, S. 1987, Galactic dynamics, ed. Binney, J. & Tremaine, S.
- Boesgaard, A. M., Jensen, E. E. C., & Deliyannis, C. P. 2009, AJ, 137, 4949
- Boesgaard, A. M., King, J. R., Cody, A. M., Stephens, A., & Deliyannis, C. P. 2005, ApJ, 629, 832
- Bragaglia, A., Carretta, E., Gratton, R., D’Orazi, V., Cassisi, S., & Lucatello, S. 2010, A&A, 519, A60+
- Briley, M. M., & Cohen, J. G. 2001, AJ, 122, 242
- Briley, M. M., Cohen, J. G., & Stetson, P. B. 2002, ApJ, 579, L17

- . 2004, AJ, 127, 1579
- Briley, M. M., & Smith, G. H. 1993, PASP, 105, 1260
- Butler, D., Dickens, R. J., & Epps, E. 1978, ApJ, 225, 148
- Campbell, S. W., Yong, D., Wylie-de Boer, E. C., Stancliffe, R. J., Lattanzio, J. C., Angelou, G. C., Grundahl, F., & Sneden, C. 2010, Mem. Soc. Astron. Italiana, 81, 1004
- Cannon, R. D., Croke, B. F. W., Bell, R. A., Hesser, J. E., & Stathakis, R. A. 1998, MNRAS, 298, 601
- Carbon, D. F., Romanishin, W., Langer, G. E., Butler, D., Kemper, E., Trefzger, C. F., Kraft, R. P., & Suntzeff, N. B. 1982, ApJS, 49, 207
- Carraro, G., Girardi, L., & Marigo, P. 2002, MNRAS, 332, 705
- Carretta, E., Bragaglia, A., D’Orazi, V., Lucatello, S., & Gratton, R. G. 2010a, A&A, 519, A71+
- Carretta, E., Bragaglia, A., Gratton, R., D’Orazi, V., & Lucatello, S. 2009a, A&A, 508, 695
- Carretta, E., Bragaglia, A., Gratton, R., & Lucatello, S. 2009b, A&A, 505, 139
- Carretta, E., et al. 2010b, A&A, 520, A95+
- . 2010c, ApJ, 714, L7
- . 2009c, A&A, 505, 117
- Carretta, E., Gratton, R. G., Lucatello, S., Bragaglia, A., & Bonifacio, P. 2005, A&A, 433, 597
- Carretta, E., et al. 2010d, ApJ, 722, L1
- Carroll, B. W., & Ostlie, D. A. 1996, An Introduction to Modern Astrophysics, ed. Carroll, B. W. & Ostlie, D. A.
- Cassisi, S., Salaris, M., Pietrinferni, A., Piotto, G., Milone, A. P., Bedin, L. R., & Anderson, J. 2008, ApJ, 672, L115
- Cavallo, R. M., & Nagar, N. M. 2000, AJ, 120, 1364
- Charbonnel, C. 1994, A&A, 282, 811
- Chernoff, D. F., & Weinberg, M. D. 1990, ApJ, 351, 121
- Cohen, J. G. 1978, ApJ, 223, 487
- . 1999a, AJ, 117, 2428
- . 1999b, AJ, 117, 2434

- Cohen, J. G., Behr, B. B., & Briley, M. M. 2001, AJ, 122, 1420
- Cohen, J. G., Briley, M. M., & Stetson, P. B. 2002, AJ, 123, 2525
- . 2005a, AJ, 130, 1177
- . 2005b, AJ, 130, 1177
- Cohen, J. G., Kirby, E. N., Simon, J. D., & Geha, M. 2010, ApJ, 725, 288
- Cohen, J. G., & Meléndez, J. 2005, AJ, 129, 303
- Conroy, C., & Spergel, D. N. 2011, ApJ, 726, 36
- D'Antona, F., Gratton, R., & Chieffi, A. 1983, Mem. Soc. Astron. Italiana, 54, 173
- Decressin, T., Baumgardt, H., Charbonnel, C., & Kroupa, P. 2010, A&A, 516, A73+
- Decressin, T., Charbonnel, C., & Meynet, G. 2007a, A&A, 475, 859
- Decressin, T., Charbonnel, C., Siess, L., Palacios, A., Meynet, G., & Georgy, C. 2009, A&A, 505, 727
- Decressin, T., Meynet, G., Charbonnel, C., Prantzos, N., & Ekström, S. 2007b, A&A, 464, 1029
- Dékány, I., & Kovács, G. 2009, A&A, 507, 803
- Denissenkov, P. A., & VandenBerg, D. A. 2003, ApJ, 593, 509
- D'Ercole, A., Vesperini, E., D'Antona, F., McMillan, S. L. W., & Recchi, S. 2008, MNRAS, 391, 825
- Dias, W. S., Alessi, B. S., Moitinho, A., & Lépine, J. R. D. 2002, A&A, 389, 871
- Djorgovski, S. G., & Meylan, G., eds. 1993, Astronomical Society of the Pacific Conference Series, Vol. 50, Structure and dynamics of globular clusters
- Drukier, G. A., Cohn, H. N., Lugger, P. M., Slavin, S. D., Berrington, R. C., & Murphy, B. W. 2007, AJ, 133, 1041
- Freeman, K. C., & Rodgers, A. W. 1975, ApJ, 201, L71+
- Fukugita, M., Ichikawa, T., Gunn, J. E., Doi, M., Shimasaku, K., & Schneider, D. P. 1996, AJ, 111, 1748
- Fukushige, T., & Heggie, D. C. 1995, MNRAS, 276, 206
- Fusi Pecci, F., Ferraro, F. R., Crocker, D. A., Rood, R. T., & Buonanno, R. 1990, A&A, 238, 95

- Geller, A. M., Mathieu, R. D., Braden, E. K., Meibom, S., Platais, I., & Dolan, C. J. 2010, AJ, 139, 1383
- Girardi, L., Bressan, A., Bertelli, G., & Chiosi, C. 2000, A&AS, 141, 371
- Goldsbury, R., Richer, H. B., Anderson, J., Dotter, A., Sarajedini, A., & Woodley, K. 2010, AJ, 140, 1830
- Goodwin, S. P. 1996, in Astronomical Society of the Pacific Conference Series, Vol. 92, Formation of the Galactic Halo...Inside and Out, ed. H. L. Morrison & A. Sarajedini, 495–+
- Gratton, R., Bragaglia, A., Carretta, E., & Tosi, M. 2006, ApJ, 642, 462
- Gratton, R., Sneden, C., & Carretta, E. 2004, ARA&A, 42, 385
- Gratton, R. G., Sneden, C., Carretta, E., & Bragaglia, A. 2000, A&A, 354, 169
- Grillmair, C. J., Freeman, K. C., Irwin, M., & Quinn, P. J. 1995, AJ, 109, 2553
- Grundahl, F., Stetson, P. B., & Andersen, M. I. 2002, A&A, 395, 481
- Gunn, J. E., et al. 1998, AJ, 116, 3040
- . 2006, AJ, 131, 2332
- Harbeck, D., Smith, G. H., & Grebel, E. K. 2003a, AJ, 125, 197
- . 2003b, A&A, 409, 553
- Harris, W. E. 1996, AJ, 112, 1487
- Hunter, I., et al. 2008, ApJ, 676, L29
- Iben, Jr., I. 1964, ApJ, 140, 1630
- . 1968, ApJ, 154, 581
- Jacobson, H. R., Friel, E. D., & Pilachowski, C. A. 2008, AJ, 135, 2341
- . 2009, AJ, 137, 4753
- Kalirai, J. S., Fahlman, G. G., Richer, H. B., & Ventura, P. 2003, AJ, 126, 1402
- Kayser, A., Hilker, M., Grebel, E. K., & Willemse, P. G. 2008, A&A, 486, 437
- King, J. R., Stephens, A., Boesgaard, A. M., & Deliyannis, C. 1998, AJ, 115, 666
- Kraft, R. P., & Ivans, I. I. 2003, PASP, 115, 143
- Kravtsov, V., Alcaíno, G., Marconi, G., & Alvarado, F. 2010a, A&A, 512, L6+
- . 2010b, A&A, 516, A23+

- Kravtsov, V., Alcaino, G., Marconi, G., & Alvarado, F. 2011, ArXiv e-prints
- Lane, R. R., Kiss, L. L., Lewis, G. F., Ibata, R. A., Siebert, A., Bedding, T. R., & Székely, P. 2009, MNRAS, 400, 917
- . 2010, MNRAS, 401, 2521
- Langer, G. E. 1985, PASP, 97, 382
- Langer, G. E., Kraft, R. P., Carbon, D. F., Friel, E., & Oke, J. B. 1986, PASP, 98, 473
- Langer, G. E., Suntzeff, N. B., & Kraft, R. P. 1992, PASP, 104, 523
- Lardo, C., Bellazzini, M., Pancino, E., Carretta, E., Bragaglia, A., & Dalessandro, E. 2011, A&A, 525, A114+
- Lee, S. 1999, AJ, 118, 920
- . 2005, Journal of Korean Astronomical Society, 38, 23
- Lee, S. G. 2000, Journal of Korean Astronomical Society, 33, 137
- Lee, Y. S., et al. 2008a, AJ, 136, 2022
- . 2008b, AJ, 136, 2050
- Lupton, R., Gunn, J. E., Ivezić, Z., Knapp, G. R., & Kent, S. 2001, in Astronomical Society of the Pacific Conference Series, Vol. 238, Astronomical Data Analysis Software and Systems X, ed. F. R. Harnden Jr., F. A. Primini, & H. E. Payne, 269–+
- Maeder, A., & Meynet, G. 2006, A&A, 448, L37
- Mallia, E. A. 1978, A&A, 70, 115
- Mandushev, G., Staneva, A., & Spasova, N. 1991, A&A, 252, 94
- Marino, A. F., Villanova, S., Piotto, G., Milone, A. P., Momany, Y., Bedin, L. R., & Medling, A. M. 2008a, A&A, 490, 625
- . 2008b, A&A, 490, 625
- Martell, S. L., & Grebel, E. K. 2010, A&A, 519, A14+
- Martell, S. L., & Smith, G. H. 2009, PASP, 121, 577
- Martell, S. L., Smith, G. H., & Briley, M. M. 2008a, PASP, 120, 839
- . 2008b, PASP, 120, 7
- . 2008c, AJ, 136, 2522
- McClure, R. D. 1979, Mem. Soc. Astron. Italiana, 50, 15

- McLaughlin, D. E., & van der Marel, R. P. 2005, ApJS, 161, 304
- Meylan, G., & Heggie, D. C. 1997, A&A Rev., 8, 1
- Meynet, G., Ekström, S., & Maeder, A. 2006, A&A, 447, 623
- Milone, A. P., Piotto, G., Bedin, L. R., Bellini, A., Marino, A. F., & Momany, Y. 2010, in SF2A-2010: Proceedings of the Annual meeting of the French Society of Astronomy and Astrophysics, ed. S. Boissier, M. Heydari-Malayeri, R. Samadi, & D. Valls-Gabaud , 319–+
- Norris, J. 1987, ApJ, 313, L65
- Norris, J., Cottrell, P. L., Freeman, K. C., & Da Costa, G. S. 1981, ApJ, 244, 205
- Norris, J., & Freeman, K. C. 1979, ApJ, 230, L179
- Norris, J., & Smith, G. H. 1984, ApJ, 287, 255
- Norris, J. E., & Da Costa, G. S. 1995, ApJ, 447, 680
- Origlia, L., Valenti, E., Rich, R. M., & Ferraro, F. R. 2006, ApJ, 646, 499
- Osborn, W. 1971, The Observatory, 91, 223
- Pancino, E., Rejkuba, M., Zoccali, M., & Carrera, R. 2010, A&A, 524, A44+
- Pancino, E., Seleznev, A., Ferraro, F. R., Bellazzini, M., & Piotto, G. 2003, MNRAS, 345, 683
- Peterson, R. C. 1980, ApJ, 237, L87
- Pier, J. R., Munn, J. A., Hindsley, R. B., Hennessy, G. S., Kent, S. M., Lupton, R. H., & Ivezić, Ž. 2003, AJ, 125, 1559
- Pilachowski, C. A., Bothun, G. D., Olszewski, E. W., & Odell, A. 1983, ApJ, 273, 187
- Piotto, G., et al. 2007, ApJ, 661, L53
- Ramírez, S. V., Cohen, J. G., Buss, J., & Briley, M. M. 2001, AJ, 122, 1429
- Schlegel, D. J., Finkbeiner, D. P., & Davis, M. 1998, ApJ, 500, 525
- Scott, J. E., Friel, E. D., & Janes, K. A. 1995, AJ, 109, 1706
- Shetrone, M., Martell, S. L., Wilkerson, R., Adams, J., Siegel, M. H., Smith, G. H., & Bond, H. E. 2010, AJ, 140, 1119
- Shetrone, M. D. 2003, ApJ, 585, L45
- Smith, G. H., & Mateo, M. 1990, ApJ, 353, 533

- Smith, G. H., & Norris, J. 1982, ApJ, 254, 149
- Smith, G. H., Shetrone, M. D., Bell, R. A., Churchill, C. W., & Briley, M. M. 1996, AJ, 112, 1511
- Smolinski, J. P., et al. 2011a, AJ, 141, 89
- Smolinski, J. P., Martell, S. L., Beers, T. C., & Lee, Y. S. 2011b, ArXiv e-prints
- Sneden, C., Kraft, R. P., Guhathakurta, P., Peterson, R. C., & Fulbright, J. P. 2004, AJ, 127, 2162
- Sollima, A., Ferraro, F. R., Bellazzini, M., Origlia, L., Straniero, O., & Pancino, E. 2007, ApJ, 654, 915
- Spitzer, L. 1987, Dynamical evolution of globular clusters, ed. Spitzer, L.
- Stetson, P. B. 1987, PASP, 99, 191
- . 1994, PASP, 106, 250
- Stoughton, C., et al. 2002, AJ, 123, 485
- Suntzeff, N. B. 1981, ApJS, 47, 1
- Sweigart, A. V., & Mengel, J. G. 1979, ApJ, 229, 624
- Thomas, H. 1967, ZAp, 67, 420
- Trefzger, D. V., Langer, G. E., Carbon, D. F., Suntzeff, N. B., & Kraft, R. P. 1983, ApJ, 266, 144
- Twarog, B. A., Ashman, K. M., & Anthony-Twarog, B. J. 1997, AJ, 114, 2556
- VandenBerg, D. A., Bergbusch, P. A., & Dowler, P. D. 2006, ApJS, 162, 375
- Ventura, P., & D'Antona, F. 2008, MNRAS, 385, 2034
- Ventura, P., D'Antona, F., Mazzitelli, I., & Gratton, R. 2001, ApJ, 550, L65
- Villanova, S., et al. 2007, ApJ, 663, 296
- Worthey, G., & Jowett, K. J. 2003, PASP, 115, 96
- Yanny, B., et al. 2009, AJ, 137, 4377
- Yi, S., Demarque, P., Kim, Y.-C., Lee, Y.-W., Ree, C. H., Lejeune, T., & Barnes, S. 2001, ApJS, 136, 417
- York, D. G., et al. 2000, AJ, 120, 1579